

Human homologues to hypothalamic autonomic control centers identified in rat and monkey, a chemoarchitectonic and developmental study

Author:

Koutcherov, Yuri G

Publication Date:

2000

DOI:

<https://doi.org/10.26190/unsworks/6376>

License:

<https://creativecommons.org/licenses/by-nc-nd/3.0/au/>

Link to license to see what you are allowed to do with this resource.

Downloaded from <http://hdl.handle.net/1959.4/59070> in <https://unsworks.unsw.edu.au> on 2024-05-05

**HUMAN HOMOLOGUES TO HYPOTHALAMIC AUTONOMIC
CONTROL CENTERS IDENTIFIED IN RAT AND MONKEY:
A CHEMOARCHITECTONIC AND DEVELOPMENTAL STUDY**

by

Yuri G. Koutcherov

This thesis is submitted in partial fulfillment of the requirement for the degree of
Doctor of Philosophy

School of Psychology, The University of New South Wales.

April, 2000

CERTIFICATE OF ORIGINALITY

I hereby declare that this submission is my own work and to the best of my knowledge it contains no materials previously published or written by another person, nor material which to a substantial extent has been accepted for the award of any other degree or diploma at UNSW or any other educational institution, except where due acknowledgement is made in the thesis. Any contribution made to the research by others, with whom I have worked at UNSW or elsewhere, is explicitly acknowledged in the thesis.

I also declare that the intellectual content of this thesis is the product of my own work, except to the extent that assistance from others in the project's design and conception or in style, presentation and linguistic expression is acknowledged.

PUBLICATIONS DERIVED (TOTALLY OR SUBSTANTIALLY) FROM WORK
REPORTED IN THIS THESIS

Article in Refereed Journal

Koutcherov Y., K.W.A. Ashwell, J.K. Mai, and G. Paxinos (2000) Organization of the human paraventricular hypothalamic nucleus. *J. Comp. Neurol.* 423 (2): 299-318

Koutcherov Y., K.W.A. Ashwell and G. Paxinos (2000) The Distribution of the Neurokinin B Receptor in the Human and Rat Hypothalamus. *NeuroReport* 11(14)

Koutcherov Y., J.K. Mai, K.W.A. Ashwell, and G. Paxinos. Human hypothalamus in fetal and perinatal periods. *To be submitted shortly*

Abstracts

Koutcherov I. and G. Paxinos. Distribution of the neurokinin B receptors in the human hypothalamus. (1998) *Proc. Austr. Neurosc. Soc. Abstr. Vol. 9, p. 131*

Koutcherov, I., K. Ashwell and G. Paxinos (1998) Parcellation of the human paraventricular hypothalamic nucleus. *Soc. Neurosci. Abstr., Vol. 24, Part 1, p. 119*

Koutcherov I., J.K. Mai, K.W. Ashwell, and G. Paxinos. Fetal development of the human hypothalamus (1999) *Proc. Austr. Neurosc. Soc. Abstr. Vol. 10, p. 107*

Koutcherov I., J.K. Mai, K.W.A. Ashwell, and G. Paxinos (1999) Human hypothalamus in fetal and perinatal periods *Soc. Neurosci. Abstr., Vol. 25, Part p. 1018*

Koutcherov I., J.K. Mai, K.W.S. Ashwell, and G. Paxinos (2000) Hypothalamic autonomic control centers in the human, monkey and rat *Proc. Austr. Neurosc. Soc. Abstr. Vol 11, p.135*

Koutcherov I., J.K. Mai, K.W.S. Ashwell, and G. Paxinos (2000) Human hypothalamic autonomic control centers in ontogeny and phylogeny *European Journal of Neuroscience* 12:159

ACKNOWLEDGMENTS

I warmly acknowledge my supervisor George Paxinos and my co-supervisor Ken Ashwell for their tolerance, help and encouragement during the course of this thesis. I am also greatly indebted to Jorgen Mai for the fetal tissue he provided for this study but also for helpful discussions, encouragement, guidance and help I received from him during my visits to his laboratory in Düsseldorf and also back here in Sydney.

I thank my parents Koutcherova Nelly Vasilievna and Koutcherov Georgy Borisovich and my brother Koutcherov Anton Georgievich for their precious support and encouragement which made my work possible.

I am deeply indebted to Ms. Sabina Lensing-Höhn for histology and histochemistry of the fetal tissue used in this study. I greatly appreciate Mr. Paul Halasz, Mr. Tomas Voß and Mr. Tobias Kalensch for their invaluable assistance with 3-dimensional reconstruction, computations and morphometric analysis.

I am grateful to Dr. Rauto Shegemoto for providing me with the antibody against NK3 receptors. I also thank Hongqin Wang for her great help she gave me with photography. I thank The Forensic Institute of New South Wales for providing me with adult tissue used in this study.

CONTENTS

Title	1
Declaration	2
Publications	3
Acknowledgments	4
Contents	5
Abstract	7
Abbreviations	9
CHAPTER 1	
General Introduction	11
CHAPTER 2	
The Organization of the Human Paraventricular Hypothalamic Nucleus	24
Introduction	24
Materials and Methods	28
Results	31
Discussion	38
Conclusions	46
CHAPTER 3	
Distribution of the Neurokinin B Receptor in the Human and Rat Hypothalamus	47
Introduction	47
Materials and Methods	50
Results	53
Discussion	57

CHAPTER 4

Chemoarchitectonic Study of the Human and Monkey Medial Preoptic Nucleus	61
Introduction	61
Materials and Methods	64
Results	66
Discussion	69

CHAPTER 5

Topography of the Human and Monkey Dorsomedial Hypothalamic Nucleus	74
Introduction	74
Materials and Methods	77
Results	78
Discussion	80

CHAPTER 6

Human Hypothalamus in Fetal and Perinatal Periods	83
Introduction	83
Materials and Methods	87
Results	89
Discussion	100
Conclusion	119

CHAPTER 7

General Discussion/Conclusions	123
--------------------------------	-----

LITERATURE CITED	127
------------------	-----

ABSTRACT

The purpose of this thesis was to establish the human hypothalamic homologues of nuclei known to be involved in autonomic regulation in rats. Homologies were established on the basis of similarities in cytoarchitecture, chemoarchitecture and development. Serial sections from 8 adult human brains, 3 monkey brains, 3 rat brains and 31 fetal human brains were processed immunohistochemically, enzymatically or for the demonstration of Nissl substance.

Plots of the human paraventricular nucleus (Pa) neurons containing pituitary hormones and other neuroactive substances were reconstructed in three dimensions. The reconstruction revealed four subnuclei which are homologous to subnuclei of the rat. The human parvicellular Pa is homologous to the medial and ventral parvicellular Pa of the rat; the magnocellular Pa is homologous to the lateral magnocellular Pa of the rat; the dorsal Pa is homologous to the medial magnocellular Pa of the rat; and the posterior Pa is homologous to posterior subnuclei of the rat. The Pa subnuclei were characterized by individual patterns of fetal differentiation. The parvicellular Pa and the perifornical nucleus were distinguished by the presence of neurons immunoreactive for neurokinin B receptors in both the adult human and rat. The medial preoptic nucleus (MPO) of the human, monkey and rat featured medial and lateral subnuclei distinguishable by complimentary distribution of acetylcholinesterase, and antibody to a neurofilament protein (SMI32) and calbindin. The present study revealed the entire extent of the dorsomedial hypothalamic nucleus (DM), a nucleus featuring strikingly similar AChE staining pattern in the human and monkey. The differentiation pattern of the human fetal hypothalamus was similar to that of the rat with a clear presence of three longitudinal zones each associated with specific nuclei.

In conclusion, chemoarchitecture especially in conjunction with development, is a useful paradigm for revealing the human homologues to nuclei involved in autonomic control in

the rat. This thesis revealed that the human hypothalamus bears a greater similarity to that of monkey and rat than hitherto believed. The findings reported herein may assist in the formulation of hypotheses about the human central autonomic nervous system and in the cross-fertilization of ideas between research in humans and experimental animals.

Abbreviations

3V	third ventricle
ac	anterior commissure
AChE	acetylcholinesterase
Arc	arcuate nucleus
AVP	arginin vasopressin
AVPV	anteroventral periventricular nucleus
Cb	calbindin
Cr	calretinin
DM	dorsomedial hypothalamic nucleus
DMC	dorsomedial hypothalamic nucleus, compact part
f	fornix
FAL	3-fucosyl-N-acetyl-lactosamine-epitop
GAP43	Growth associated protein
hs	hypothalamic sulcus
INAH	interstitial nucleus of the anterior hypothalamus
InM	intermediate (sexually dimorphic) nucleus
LH	lateral hypothalamic area
LTu	lateral tuberal hypothalamic nucleus
MbL	mammillary body, lateral part
MbM	mammillary body, medial part
MEE	median eminence, external
MEI	medial eminence, internal
MPA	medial preoptic area
MPO	medial preoptic nucleus
MPOC	medial preoptic nucleus, central subnucleus
MPOL	medial preoptic nucleus, medial subnucleus
MPOM	medial preoptic nucleus, lateral subnucleus
mt	mammillo-thalamic tract
ne	neuronal epithelium
NK3	neurkinin B receptor
NKB	neurokinin B

NPH	neurophysin
NPY	neuropeptide Y
opt	optic tract
ox	optic chiasm
OXY	oxytocin
PaAP	paraventricular hypothalamic nucleus, anterior parvicellular subnucleus
PaD	paraventricular hypothalamic nucleus, dorsal subnucleus
PaM	paraventricular hypothalamic nucleus, magnocellular subnucleus
PaP	paraventricular hypothalamic nucleus, parvicellular subnucleus
PaPo	paraventricular hypothalamic nucleus, posterior subnucleus
PeF	perifornical hypothalamic nucleus
PH	posterior hypothalamic area
Pv	parvalbumin
SCh	suprachiasmatic nucleus
SMI32	Sternberger Monoclonal Inc. non-phosphorylated epitopes in neurofilament B
SO	supraoptic nucleus
SUM	supramammillary nucleus
SYN	synaptophysin
Un	uncinate nucleus
VMH	ventromedial hypothalamic nucleus
VMHDM	ventromedial hypothalamic nucleus, dorsomedial subnucleus
VMHVL	ventromedial hypothalamic nucleus, ventrolateral subnucleus
VTM	ventral tuberomammillary hypothalamic nucleus

CHAPTER 1

General Introduction

Functional and neuroanatomical investigations in experimental animals have revealed the hypothalamic regions most intimately involved in regulation of the autonomic nervous system. Extrapolations to humans of the conclusions obtained from studies on experimental animals have been based on the rationale that homologous structures have analogous function across mammals. However, in many instances, homologies between the rat and the human hypothalamic nuclei and subnuclei involved in autonomic control have not as yet been established conclusively. The purpose of this thesis is to establish comprehensively the human hypothalamic homologues to nuclei that have been shown to be involved in autonomic regulation in the rat hypothalamus so as to facilitate the formulation of hypotheses on the central human hypothalamic autonomic system and the cross-referencing of findings between experimental animal studies and clinical observations. The rat is chosen for comparison because most of our knowledge of central autonomic control structures is derived from functional and connectivity studies done in this species. The monkey is chosen because its brain is structurally very similar to that of humans, but the tissue can be obtained under more optimal conditions.

Functionally, animal experiments have demonstrated a major role for various hypothalamic cell groups in the regulation of the autonomic nervous system. Thus, hypothalamic nuclei have been shown to affect metabolism, stress, thermoregulation, cardiovascular functions, sleep, immune responses and water and electrolyte balance (Saper, 1995; Swanson et al., 1983). Information from other brain regions, bodily organs and the external environment reaches hypothalamic neurons by many means of which neural afferents and humoral signaling molecules are most frequently studied. The effector pathways from the

hypothalamus are equally diverse and include neural efferents which directly or via other relays regulate the activity of postganglionic autonomic motor neurons. However, purely autonomic responses are rare. As the principal component of the neuronal circuitry regulating homeostasis, hypothalamic autonomic regulatory circuitry is closely integrated with the endocrine and behavioral pathways (see Simerly, 1995 and Saper, 1990). This integration grants hypothalamic neural relays the means for a robust and diverse influence over reproductive and survival responses.

For a century the human hypothalamus has been known to play an important role in the regulation of homeostasis. At the beginning of the 20th century, Babinski (1900) and Frohlich (1901) described the syndrome of obesity and genital dystrophy in patients with tumors of the pituitary gland. Soon, Cushing (1906) and Erdheim (1904) made an important observation that the obesity in the syndrome is due not to the damage of the pituitary but to the involvement of the structures of the floor of the third ventricle. The importance of the hypothalamus in thermoregulation was suggested by Ott (1891), and more prominently by Isenschmid and Krehl (1912) and by Ranson, Fisher and Ingham (1937) who established that lesions of the hypothalamus in the monkey and particularly of the posterior hypothalamus affect thermoregulation. Similar findings were also documented in humans with lesions at posterior hypothalamic levels (Ratner, 1925; Davidson and Selby, 1935).

A direct link between the regulation of the autonomic nervous system and the human hypothalamus was first described by Penfield (1929) in a syndrome of diencephalic autonomic epilepsy in a patient with a pearly tumor "cholesteatoma" of the third ventricle. The attacks of diencephalic autonomic epilepsy, which lasted about 7-8 minutes, were characterized by vasodilation of the skin vessels supplied by cervical sympathetic nerves, a rise in blood pressure, lacrimation, diaphoresis, salivation, dilatation or contraction of the pupils, protrusion of the

eyes, increased heart rate, slowing of respiratory rate. Similar observations were also documented in more recent reports (Carmel, 1980; Ropper, 1993). As a focal point in the regulation of homeostasis and autonomic nervous system, the hypothalamus is reportedly implicated in obesity, type II diabetes mellitus, hereditary diabetes insipidus, Prader-Willi syndrome, Kallmann's syndrome, depression, AIDS, Sudden Infant Death syndrome, disturbances in sleep and temperature regulation (Braverman et al., 1965; Carmel, 1980; Reichlin, 1985; Saper and German, 1987; Bergeron et al., 1991; Purba, 1993; Ropper, 1993; Swaab et al., 1993; Guldenaar and Swaab, 1995; Purba et al., 1996; Swaab, 1997; Gabreels et al., 1998, Bernstein et al., 1998).

Anatomically, the past century has seen comprehensive cytoarchitectonic and comparative studies, which have provided plans for the structural organization of the human hypothalamus (Malone, 1910; Monakow, 1927; Greving, 1928; LeGros Clark, 1938; Brockhause, 1942; Christ, 1951; Kahle, 1956; Wahren, 1959; Diepen, 1962; Nauta and Haymaker, 1969; Lang, 1985; Saper, 1990; Braak and Braak, 1992). However, apart from the work Saper (1990) and Braak and Braak (1992), these studies relied on cytoarchitecture and myeloarchitecture for their delineations. Cytoarchitecture when used as a single comparative criterion has shortcomings because the cell groups in the adult human hypothalamus are somewhat dispersed and certainly less obvious with respect to their subnuclear boundaries than in the rat. As a possible consequence of ineffectual comparative investigations there is confusion in the terminology of the human hypothalamic cell groups including those implicated in autonomic control.

The basic organizational plan of the hypothalamus is thought to be well preserved throughout the mammalian lineage (Nauta and Haymaker, 1969; Saper, 1990). It is thus necessary that the human and rat hypothalami be studied in parallel using the same criteria for

the establishment of homologues from which the unified nomenclature can be derived. The criteria for establishing a homology in the present thesis will be morphological and involve cytoarchitecture, chemoarchitecture, topography, subnuclear organization and pattern of development.

Chemoarchitecture as a Criterion for Establishing a Homologies

Connectivity and functional studies are virtually unachievable in humans, and for this reason the human homologues to the rat hypothalamic nuclei will be inferred on the basis of chemoarchitecture. Previous work has shown a high degree of conservation in the chemical identity of brainstem neurons from rat to monkey and human (Geula et al, 1993). Cell groups such as the A1 and C1 catecholamine neurons, which are crucially involved in autonomic control, are strikingly similar in rat and human (Halliday et al, 1988). The present thesis aims at establishing the correspondences between the hypothalamic autonomic control system of the rat, monkey and human. In doing so it will also reveal the distribution in the relevant nuclei of some of the neurotransmitters, receptors and enzymes of importance in neural computations. Each chemical substance examined offers a different window to the organization of the central autonomic system, with successive stains betraying more of the areas of interest. There can of course be species differences and any given substance may have inconsistent distributions in otherwise homologous nuclei.

Substances were chosen for investigation on the basis of how well they reveal the organization of the hypothalamic nuclei. For example, neuroactive substances that distinguish prominent rat hypothalamic nuclei include arginin-vasopressin (AVP), neuropeptide Y (NPY), oxytocin (OXY), tyrosine hydroxylase (TH) and corticotropin releasing factor (CRF). These substances are also present in the human hypothalamus (Dierickx and Vandesande, 1977;

Pelletier et al., 1983; Spencer et al., 1985; Schwanzel-Fukuda et al., 1989; Swaab, 1993) and will be examined in parallel in the rat and human in the present thesis. Additional substances chosen for examination include the ubiquitous AChE, calbindin-D28k (Cb), parvalbumin (Pv), calretinin (Cb), and a non-phosphorylated neurofilament protein (SMI32). The distribution of SMI32 was examined in the human hypothalamus for the first time and found instructive for establishing homologues.

In mammals, the tachykinins including Neurokinin B (NKB) are involved in a variety of physiological functions including central cardiovascular, autonomic and neuroendocrine regulation (Jensen, 1991; Marksteiner et al., 1992; Culman, 1995; Nalivaiko et al., 1997; Danzer et al, 1999). The physiological effects of tachykinins are mediated via a specific G-protein-coupled family of receptors that includes the NK3 receptor, selective for NKB (Helke et al., 1990; Nakanishi, 1991; Maggi, 1995). It has been shown, that the hypertensive effect of intracerebroventricular injection of the NKB peptide is mediated by NK3 in the rat hypothalamus (Polidori et al., 1989, Takano et al., 1990; Ding et al., 1999). However, the presence of NK3 in the human hypothalamus is disputed (Dietl and Palacios, 1991). The present study used a novel antibody (Ding et al., 1996) to reveal the regional distribution of NK3 in the human hypothalamus and to compare it with the distribution of the receptor in the rat hypothalamus, where the structure/function associations are better studied.

Fetal Development and the Search for Homologues

The adult human hypothalamus looks puzzlingly simpler (less differentiated) than that of the rat. Le Gross Clark (1936; 1938), who was the first to describe various hypothalamic nuclei in humans, relied on studies of the human fetus where cell groups are better defined. Subsequently, a number of cytoarchitectonic studies described human developmental material

(Gilbert, 1935; Diepen, 1948; Spatz, 1949; Kahle, 1956; Kühlenbek, 1959; Diepen, 1962; Richter, 1965) but these were more concerned with general principles of diencephalic development rather than with the differentiation of particular nuclei. In the rat, developmental studies contributed greatly to the understanding of hypothalamic nuclear organization (Ströer, 1956; Coggeshall, 1964; Hyypä, 1969; Ifft, 1972; Altman and Bayer, 1986; also see Swanson, 1987).

Chemoarchitecture is also applicable to the fetal hypothalamic tissue. Thus, more recent chemoarchitectonic studies of the human fetal hypothalamus reported on the development of the hypophyseal portal plasma system (Trandafir et al., 1988), CRF containing circuitry (Bugnon et al., 1982), growth hormone releasing hormone (GRH) neurons (Bloch et al., 1984), somatostatin (Ackland et al., 1983), oxytocin and vasopressin (Burford and Robinson, 1982) and neurophysin (Mai et al., 1997). By combining the developmental approach with chemoarchitecture in the human the present study is aiming to reveal hypothalamic homologues with the adult or developing rat. The developmental analysis of the present thesis used as markers of hypothalamic nuclei antibodies to calbindin (Cb), calretinin (Cr), parvalbumin (Pv), neuropeptide Y (NPY), neurophysin (NPH), as well as substances that exposed some aspects of the synaptogenesis such as GAP43 and SYN. In addition, an antibody directed against a cell surface membrane glycoconjugate, 3-fucosyl-N-acetyl-lactosamine (FAL or CD15) was used because of its capacity to revealing general topography of the fetal hypothalamus and glial cells including radial glia.

In this thesis the term differentiation is used with respect to the fetal hypothalamic nuclei to indicate the acquisition of chemoarchitecture, cytoarchitecture, topography and subcompartmental organization by which this nucleus is defined in the adult or in other mammals.

Hypothalamic Nuclei of Interest

In the forthcoming pages, the specific issues related to nuclei of interest will be dealt with briefly. A more extensive consideration is given in introductions to the individual chapters.

The Paraventricular Nucleus (Pa) The Pa is the major autonomic and endocrine motor relay in the hypothalamus. Its role has been demonstrated by many physiological, tracing and pharmacological studies in the rat and mouse and its endocrine function has been demonstrated elegantly in the human (Morton, 1969; Swanson, 1991; Armstrong, 1995). However, no conclusive plan of its organization has yet been proposed. The rat paraventricular subnuclei are reasonably well chemically coded and some project directly to the parasympathetic and sympathetic preganglionic neurons of the medulla and spinal cord. Swanson and Sawchenko (1983) have shown that the subcompartments of the rat Pa can be differentiated on the basis of their chemical profiles. The present thesis investigates in a comprehensive fashion the organization of this important autonomic control nucleus and reveals correspondences with the rat. In the rat, different subdivisions of Pa develop at different gestational ages (Altman and Bayer, 1986). This fact is used in this thesis to advantage in revealing the subnuclei of the human Pa in fetal development.

Dorsomedial Hypothalamic Nucleus (DM) Experimental evidence from lesion and stimulation studies in the rat suggests that DM plays an important role in the regulation of the autonomic nervous system (Soltis & Dimicco, 1990; 1992). Neuroanatomical evidence has shown potent projections from the DM to the dorsal motor nucleus of vagus, the principal parasympathetic nucleus of the brain (Saper et al., 1976; Ter Horst and Luiten, 1986). Surprisingly little is known about the DM in human. Even the boundaries of the nucleus are currently in dispute (Braak and Braak, 1992). Dai et al (1998) used DiI in postmortem human

tissue to trace a projection from the DM to the paraventricular nucleus. Their greatest shortcoming was that they did not know exactly where the human DM was. The DM has recently been well delineated in the monkey on the basis of AChE and various receptors (Paxinos et al., 2000). The present thesis explores AChE as a chemical marker for the human DM boundaries and compares the topography of the human DM to that of the monkey and rat.

Medial Preoptic Nucleus (MPO) In the rat, the medial preoptic nucleus and medial preoptic area have been shown to be in receipt of projections from the solitary nucleus, the parabrachial nuclei and C1 cells and to project to autonomic regions of the brainstem (Simerly & Swanson, 1986; Verberne, Waite and Sartor, 2000; also see Simerly, 1995). The preoptic region is involved in cardiovascular control, thermoregulation, fluid homeostasis and maternal and sexual behaviour (Saper & Levisohn, 1983). The medial preoptic nucleus is well described in the rat (and recently in the monkey, Paxinos et al, 2000), but only vaguely acknowledged as a cytoarchitectonic domain in the human (Brockhaus, 1942). In the present thesis the medial preoptic nucleus is examined chemoarchitectonically in adult human and developmental tissue to establish its subcompartmental borders and their putative homologies.

Other Hypothalamic Areas Considered in this Thesis

Neurons surrounding the fornix at tuberal levels project directly to the sympathetic preganglionic column (Cechetto & Saper, '88; Saper et al, '76). In a functional study, Allen and Cechetto ('92) established pressor and depressor sites in the rat hypothalamus whose stimulation results in dramatic changes in blood pressure. The areas that yielded the most striking results were the perifornical nucleus (PeF), magnocellular lateral hypothalamic nucleus (MCLH) and lateral hypothalamic area (LH). Brockhaus (1942) identified five subcompartments to the human

PeF. Little else is known about this nucleus in the human. In the monkey, the PeF is divisible into medial and lateral components (Paxinos et al, 2000). This thesis investigates the organization of the human PeF using chemoarchitecture and development.

The lateral hypothalamic area (LH) has never been well delineated in spite of its crucial role in feeding, drinking, cardiovascular function and aggression (Allen & Cechetto, 1992; Bandler and Flynn, 1972; Spencer et al, 1988). Its connections with the parabrachial nuclei and the spinal cord are also suggestive of a crucial involvement in autonomic control (Cechetto & Saper, 1988). Interest in organisation of lateral hypothalamus has been recently reiterated with a discovery of a new lateral hypothalamic neurotransmitter orexin (or hypocretin) directly implicated in feeding and energy expenditure (Sakurai et al., 1998). Shortly after the discovery it has been reported that orexin- and melanin-concentrating hormone-expressing cells form distinct populations in the rodent lateral hypothalamus (Broberger et al., 1998). Concurrent study used chemoarchitecture to define the orexin containing projections from the mediobasal hypothalamus and the lateral hypothalamic area in human and rats (Elias et al., 1998). It must be acknowledged that orexin is not unique in its functional role in food intake and that other hypothalamic hormones and neurotransmitters including leptin, neuropeptide Y and agouti-related protein have also been strongly implicated in hypothalamic control of feeding. On the other hand recent review discussed strong relationship of orexin and melanin-concentrating hormone containing cells in the lateral hypothalamus to the neuropeptide Y and agouti gene-related protein systems (Elmqvist and Saper, 1999). Thus functionally orexin containing neurons probably take an important place among numerous hypothalamic networks regulating feeding. With respect to neuroanatomy, distinct distribution of orexin and melanin-concentrating hormone containing cells in the lateral hypothalamus of the rat and human (Broberger et al., 1998; Elias et al., 1998) reiterate practical incentives for comprehensive structural delineation of

the LH in the rat and in the human. On the basis of Nissl and chemoarchitectonic stains, the present study will compare the organization and development of the human LH with its rat homologue (Altman and Bayer, 1986).

The human lateral tuberal nucleus (LTu) has been implicated in energy metabolism (Kremer, 1992). It is critical to know more about this area considering current work on metabolism in mice. In the rat, Paxinos and Watson (1986) identified the terete nucleus on the basis of Timm's stained preparations. Saper (1990) suggested that the human LTu may be homologous to the rat terete nucleus. The early fetal position of the human LTu resembles that assumed by the Te in the adult rat, but later the human nucleus migrates ventrally to form the tuber cinereum, thus concealing the homology. The present study establishes the chemoarchitecture of the LTu during fetal development in the human and compares it with that of the adult rat and monkey so as to infer the degree of homology.

The VMH is critically involved in energy metabolism and the subjacent arcuate nucleus in endocrine control (for review see Saper, 1995; Simerly, 1995). As in the case for other hypothalamic nuclei, the VMH of the adult human appears subdued in Nissl preparations (Saper, 1990).

The arcuate nucleus (Arc) is known to provide major projections to the median eminence where they form a pivotal component of the tubero-infundibular system which, in turn,, regulates output from the anterior pituitary (Lechlan, et al., 1982). Other important projections from the Arc were traced to the Pa, to the ventromedial hypothalamic nucleus, parabrachial nucleus and spinal cord, suggesting that Arc plays significant role in regulation of the autonomic function (Swanson and Kuypers, 1980; Cechetto and Saper, 1988; Moga et al., 1990, also see Saper, 1995). Chemoarchitectonically Arc is arguably the most diverse cell group in the brain with respect to neuroactive substances in the rat (Simerly, 1995). In the adult human, Christ

(1951) made a profound observation of the close relationship between the cerebrospinal fluid in 3V and the Arc. He revealed that Arc as well as the infundibulum itself lack the inner layer of glial fibers which separate ependyma from the neurons of the hypothalamus and, thus, formed an anatomical basis for the idea of diffusion exchange of molecules between the neurohypophysis and the brain. Examples of molecules using this pathway may include the *obese* gene product leptin (Stephens, et al, 1995). Further on this point, most recent interest in the chemoarchitecture of Arc has been fueled by demonstration of prominent pathway from Arc to orexin containing neurons in the lateral hypothalamus and to the Pa. Two populations of Arc neurons with opposite effect on feeding have been shown to send these projections in the rat as well as in the human (Saper and Elmquist, 1999). One population contains NPY, agouti-related peptide and leptin receptors (Broberger et al., 1998; Elias et al., 1998; Huang et al, 1996) and the other contains pro-opiomelanocortins and CART (cocaine and amphetamine regulated transcript). Other neuroactive substances found in the rat Arc include neurokinin B, somatostatin, neurotensin, luteinizing hormone-releasing hormone (LHRH) and catecholamines were also reported in the human Arc (Spencer et al., 1985; Schwanzel-Fukuda et al., 1989; Swaab, 1993; Chawla, et al.,1997). Both Arc and VMH will be studied immunohistochemically in the adult and the fetus and the subcompartments that correspond to those of the rat will be specified.

The focus of this thesis is the nuclei involved in the autonomic control. However, in description of fetal hypothalamic development note is made of some hypothalamic nuclei which have not yet been linked to autonomic control (supramammillary, intermediate nucleus, mammillary body). The reason for inclusion of these incidental observations in the thesis is that these nuclei can form landmarks for identification of the nuclei of immediate interest to this project or their development illustrates general principals of hypothalamic development.

Ethical considerations

My experiments with human and monkey brains formed a part of the project “Chemoarchitecture of the Human and Monkey Brain Cardiovascular Control Centers” Committee on Experimental Procedures Involving Human Subjects CEPIHS approval number 96053. All adult human tissue was procured from the forensic institute of NSW. The aborted fetuses were collected and examined by the departments of Pathology and Neuropathology, H. Heine University, Düsseldorf, between 1989 –1998, in accordance with the local Ethical Committee protocols. Procedures for collecting the fetal tissue strictly conformed to the ethical guidelines of the Helsinki Declaration regarding informed consent (British Medical Council, 1964). (Human Experimentation. Code of ethics of the World Medical Association and statement on responsibility in investigations on human subjects. Br. Med. J. 2: 177-180). The techniques used in my research require the use of poisonous and toxic chemicals. The safety precautions employed in my research strictly complied with the safety regulations of the School of Psychology, UNSW.

General Aim

The present thesis aims to identify the human homologues to the hypothalamic autonomic control centers that have been established experimentally in the rat and monkey. Connectivity and functional studies are virtually unachievable in humans, and for this reason the human homologues of the relevant brain regions of experimental animals will be inferred on the basis of correspondence in cyto-, chemoarchitecture and development in the adult human and fetus. Specific aims for each of the five studies reported in this thesis are described in relevant introductions.

Hypotheses:

1) Most nuclei of the adult primate hypothalamic autonomic control system display a unique chemical “signature” which, while not identical, is unmistakably similar to that of the well studied rat.

2) Unlike the adult human hypothalamus, the fetal human hypothalamus bears great resemblance to that of the adult rat. A corollary of this hypothesis is that studying the chemoarchitecture of nuclei during fetal development will prove more powerful than any technique currently available for establishing homologies.

CHAPTER 2

The Organization of the Human Paraventricular Hypothalamic Nucleus

The paraventricular nucleus of the hypothalamus (Pa) is a complex motor relay, integrating essential endocrine and autonomic responses that sustain homeostasis. First depicted by Marie and Leri (1905), the nucleus was termed paraventricular by Malone (1910), while also referred to as “nucleus filiformis” by Gurjian (1927), Krieg, (1932) and Crouch (1934), and as “nucleus magnocellularis hypothalami” by Papez and Aronson (1934). In the rat and other animals, this nucleus is comprised of several subnuclei that are substantially distinct morphologically and neurochemically (Gurjian, 1927; Rioch, 1929; Krieg, 1932; Hatton et al., 1976; Armstrong et al., 1980; Swanson and Sawchenko, 1983 also see Swanson, 1991 and Armstrong, 1995). Several studies have shown that Pa subdivisions also differ with respect to their affiliations and function. For example, in the rat, neurons of the anterior and medial magnocellular Pa contain oxytocin (OXY), the cells of the lateral magnocellular Pa contain vasopressin (AVP); all three of these cell groups issue projections to the posterior pituitary where OXY and AVP are released into the bloodstream (Schrarrer and Schrarrer, 1940; Vandesande and Dierickx, 1975; Swanson and Kuypers, 1980; Armstrong, 1995). The neurons from the dorsal, ventral, and posterior parvocellular subnuclei, on the other hand, project to the autonomic centers in the brainstem and spinal cord, enabling these cell groups to influence directly the activity of the autonomic nervous system (Saper et al., 1976; Swanson and Kuypers, 1980; Luiten et al., 1985). The dorsal, ventral, and posterior parvocellular subnuclei feature neurons containing dopamine, somatostatin, enkephalin, corticotropin-releasing factor (CRF), neurotensin, angiotensin and AVP or OXY (Swanson, 1977; Swanson et al., 1981; Sawchenko

and Swanson, 1983; Cechetto and Saper, 1988). Finally, the neurons of the medial parvicellular Pa that contain somatostatin (Sawchenko and Swanson, 1982), CRF (Swanson et al., 1983) and other releasing hormones (Brownstein et al., 1982) send axons to the neurohaemal zone of the median eminence, where they regulate the hormonal output from the anterior pituitary (Vandesande et al., 1977; Swanson et al., 1980; Brownstein et al., 1982; Antoni et al., 1983). The organization of the rat Pa as a conglomerate of functionally and neurochemically distinct subcompartments may prove important for the effective integration and execution of the information and functions of this nucleus. The 10 structural subdivisions of the Pa in the rat are conventionally identified by cyto- and chemoarchitectonic criteria and topography (Paxinos and Watson, 1986).

The human Pa is also involved in the regulation of pituitary output and the autonomic nervous system. For example, a reduction in the number of magnocellular neurons in the Pa has been found in human patients after hypophysectomy (Morton, 1969). Notable alterations in the cyto- and chemoarchitecture of the Pa were also reported in patients with conditions accompanied by altered homeostatic control, such as Prader-Willi syndrome, depression and AIDS (Saper and German, 1987; Purba, 1993; Swaab et al., 1993; Guldenaar and Swaab, 1995; Purba et al., 1996; Swaab, 1997; Gabreels et al., 1998, Bernstein et al., 1998). Depletion in number of neurons in Pa has been found in cases of hereditary diabetes insipidus (Braverman et al., 1965; Bergeron et al., 1991) and lesions in the area of the Pa were reported to be accompanied by hyperactivity of the autonomic nervous system (Carmel, 1980; Ropper, 1993). Neuroactive substances including AVP, OXY, TH, thyrotropin-releasing hormone, dynorphin and CRF, that are found in the rat, are also present in the human Pa (Dierickx and Vandesande, 1977; Pelletier et al., 1983; Spencer et al., 1985; Borson-Chazot et al., 1986; Abe et al., 1988;

Fliers et al., 1994). Nevertheless, evidence on the compartmental subdivision of the human Pa remains inconclusive.

The general topography of the human Pa has been known for a while (Greving, 1925; Grünthal, 1930; Ingram, 1940). The first tentative suggestion of the subdivision in the human Pa by Roussy and Mossinger (1935) was received apathetically, as at the time it held no apparent significance. Brockhaus (1942) subdivided the human Pa into rostral, magnocellular, parvicellular, and caudal subcompartments on the basis of cytoarchitectonics while Wahren (1959) described an “influx of small cells” within the Pa, from the side of the ventricle, and a shift in a concentration of large neurons along the rostro-caudal extent of the nucleus from the ventrolateral through the mixed area to the dorsal. Some subsequent chemoarchitectonic studies, based on single immunohistochemical markers, largely failed to support these findings, suggesting that, unlike the rat, there is no topographic subdivision in the human Pa (Sofroniew, 1985; Raadsheer et al., 1993; Harding et al., 1995). In contrast, other researchers noted some differences in the distribution of neuroactive substances including AVP, OXY, growth hormone-releasing hormone and somatostatin in the human Pa (Saper, 1990; Bloch et al., 1984; Bouras et al., 1987). The principal aim of the later workers was to establish the presence of certain neurochemicals in the Pa and not to determine the existence of Pa subdivisions, let alone the homologies with the rat. Elucidating the intrinsic chemical organization of the human Pa would help to extrapolate the organization of the central homeostatic control mechanism from experimental animals to humans.

The aim of the present study was to determine the intrinsic organization of the human Pa using chemoarchitectonic and cytoarchitectonic criteria. This was achieved by comparing the topographic distribution of a series of chemical markers (AChE, tyrosine hydroxylase - TH, calbindin - Cb, neurokinin B receptor - NK3, corticotropin releasing factor – CRF and non-

phosphorylated neurofilament protein - SMI32) as well as neuronal types and density in cresyl violet stained sections in the nucleus using adjacent sections from the same hypothalamus. To avoid technical limitations that may have hindered previous attempts to reveal compartmental organization of the human Pa, we have used only brains obtained after short postmortem delay in conjunction with free-floating immunohistochemical staining techniques for better penetration. The resulting organizational plan of the Pa was verified in respect to distributions of AVP, OXY and neurophysin-NPH in adjacent sections from different humans. We have presented the results as a three dimensional model of the human Pa in stereotaxic coordinates to illustrate the chemical topography of the nuclear subcompartments. Some of the results from this study have been previously presented in abstract form (Koutcherov et al., 1998).

MATERIALS AND METHODS

Procurement of brains and ethical considerations

Eight human brains (five males and three female) with ages ranging from 15 - 76 years and postmortem delays varying from 3 to 11 hours were obtained at autopsy from the City of Sydney Morgue (n=5) or from Departments of Pathology and Neuropathology of the University of Duesseldorf (n=3). All procedures had been approved by the Committee on Experimental Procedures Involving Human Subjects of the University of New South Wales. Clinical histories and postmortem examination showed no signs of cerebral disease. The cause of death was a myocardial infarction in four cases, aneurysm of inferior vena cava in one case, cardiac failure in two cases and a traffic accident in one case. The hypothalami were dissected at necropsy and fixed by immersion in 4% paraformaldehyde in 0.1 M phosphate buffer at pH 7.4 for 3 days and cryoprotected in 25% buffered sucrose for 10 days.

Enzyme- and immuno-histochemistry

Blocks of the human hypothalamus were frozen at -70°C and sectioned in the frontal plane, perpendicular to the intercommissural line, with the aid of a cryostat, at a thickness of $50\mu\text{m}$. Alternate sections from three brains were stained immunohistochemically for AVP, OXY and NPH. The OXY stained sections were counterstained for Nissl substance to create a common denominator with other brains for the identification of the Pa subcompartments. For another five brains, alternate sections were stained for the demonstration of Nissl substance, reacted for acetylcholinesterase according to the protocol used by Paxinos and Watson (1986), or processed immunohistochemically for six different neuroactive substances (see below). Free-floating sections for immunohistochemistry were incubated with primary antibody in PBH [normal horse serum (2%), Triton X-100 (0.2%) and bovine serum albumin (0.1%, Sigma B-8894) in PB]. The incubation was done on an orbital mixer at 4°C for 32 hours. The specificity

of the anti-NK3 antibody was originally tested by preadsorption with an excess amount of trpE-NK3 fusion protein, and by replacing the primary antibody with normal IgG (Ding et al., 1996). The homology between the rat and human NK3 molecules has also been established (Buell et al., 1992). Present study also tested the specificity of the antibody by replacing it with normal IgG. Other antibodies, used in the present study are widely used in mammals including human. The antibodies and dilutions were: anti-calbindin D28k (Mouse monoclonal IgG1, SWant), 1:20,000 (Sanghera, et al., 1995); anti-CRF (Mouse monoclonal, Vector), 1: 20 000 (Mouri et al., 1984); anti-Neuromedin K3 Receptor [Rabbit IgG, Ding et al., (1996)], 1: 10,000; SMI32 (Mouse monoclonal IgG1 directed against non-phosphorylated epitopes in neurofilament B), Sternberger Monoclonal Inc, 1: 32,000 (Hof et al., 1995); anti-tyrosine hydroxylase (Mouse monoclonal IgG1, Incstar), 1: 16,000 (Li et al., 1988), anti-neurophysin (Rabbit polyclonal, M. Sofroniew), 1:300 (Mai et al., 1991), anti-arginin-vasopressin (Rabbit polyclonal Camon, M. Safroniew), 1:400 (Mai et al., 1991), anti-oxytocin (Rabbit polyclonal, M. Sofroniew), 1:400 (Mai et al., 1991). The antibodies and dilutions for secondary antibodies were: anti-mouse IgG, (Goat Biotin-SP-conjugated AffiniPure, Jackson ImmunoResearch Laboratories), 1: 200; anti-rabbit IgG (Goat Biotin-SP-conjugated AffiniPure, Jackson ImmunoResearch Laboratories), 1: 200. Sections were incubated in ExtrAvidin (Sigma E-2886) 1:1,000 in scintillation glass vials on an orbital mixer at room temperature for 1 hour, and washed in 0.1M Tris buffer (pH 7.4) containing 0.004% nickel ammonium sulfate. The final DAB (3'-3 diaminobenzidine) reaction was nickel-enhanced and used a glucose oxidase reaction to generate peroxide.

Three-dimensional model of the human Pa

A microscope driven by an IBM compatible computer with the DOS based application of the Magellan 3.1 software (Halasz and Tork, 1989) was used for the plotting of cellular distributions for each of the six chemical markers and corresponding reconstructions of the Pa.

The image of the specimen in the microscope and that on the computer screen were superimposed using a camera lucida. The outlines of the section and the cells of the Pa were plotted as data in individual files for each section. Only somata with visible proximal dendrites were plotted. The outlines of labeled somata were measured automatically by the Magellan 3.1 software. On completion of data collection, these files were displayed in a sequential mode to create six 3-dimensional views of the Pa each on the basis of a histochemical marker. The three-dimensional images were then rotated to achieve the most informative angle of view (Fig. 10).

The reconstruction of the human Pa (Fig. 11) was derived from the combined analysis of the six plots of the different histochemical markers used in the present study. The individual files for each section from all histochemical markers were displayed in a sequential mode to create one three-dimensional view of the Pa based on all six chemical markers. Correct alignment of the sections was obtained by reference to outlines of the sections. This resulted in a series of thirteen two-dimensional images, each representing a 300 μm thick coronal slab of the Pa, containing information about the distribution of the six chemical markers. The stereotaxic grid (Mai et al., 1997) was aligned in according to the position of anatomical landmarks including fornix, anterior commissure, hypothalamic sulcus and the wall of the third ventricle (Fig. 11). The subnuclear boundaries revealed by the markers were averaged. The final series was then exported and recompiled using Adobe Illustrator 8.0 for three-dimensional reconstruction. Rotation of the image was performed in order to determine the best angle (45° to the sagittal axis of midline in the rostro-lateral direction) from which to view the macro- and microtopography of the Pa. To test the validity and accuracy of the three dimensional Pa reconstruction results obtained from other brains using antibodies to the widely studied substances AVP, OXY and NPH were analyzed within the model using staining for Nissl substance and anatomical landmarks.

RESULTS

General topography of the human Pa

In terms of general topography, the human Pa appears as a vertically elongated structure, which is immediately adjacent to the wall of the third ventricle and indented laterally and dorsally by the descending fornix (Figs. 1 and 11). Ventral to the fornix, the main body of the Pa rises vertically along the wall of the third ventricle throughout the preoptic and tuberal regions of the hypothalamus. At more posterior levels, the Pa curves behind the fornix and skirts lateral to the hypothalamic sulcus. Finally, a small element of the Pa dorsal to the fornix protrudes anteriorly along the hypothalamic sulcus. The distribution of the chemical substances used in this study is initially presented without reference to subnuclei. Subnuclei of the Pa are then described on the basis of the distribution of these chemical markers and cytoarchitecture.

Acetylcholinesterase histochemistry. The AChE staining labeled three types of neurons that could be distinguished according to their somatic morphology. Most of the AChE-labeled cells in the Pa were large to medium-sized ($22.3 \pm 3.4 \mu\text{m}$ diameter, $N=100$) spindle-shaped neurons showing various intensities of staining (Fig. 6b). Posterior to the fornix, these neurons were darkly to moderately stained and abundantly distributed throughout the nucleus (Fig. 4C). Above the fornix, these cells were also darkly stained and segregated in the lateral part, avoiding the periventricular area (Fig. 3B). Ventrally these neurons were darkly stained and were found primarily in the ventrolateral quadrant (Fig. 2B), although some poorly stained isolated cells were present in the dorsolateral quadrant and in the proximity of the ventricular wall. The AChE reactivity also revealed a population of large ($23.7 \pm 4.0 \mu\text{m}$ diameter, $N=100$), darkly stained multipolar neurons (Fig. 6a). Some of these neurons were scattered throughout the dorsolateral quadrant of the Pa while most of these cells formed a compact group in the ventrolateral

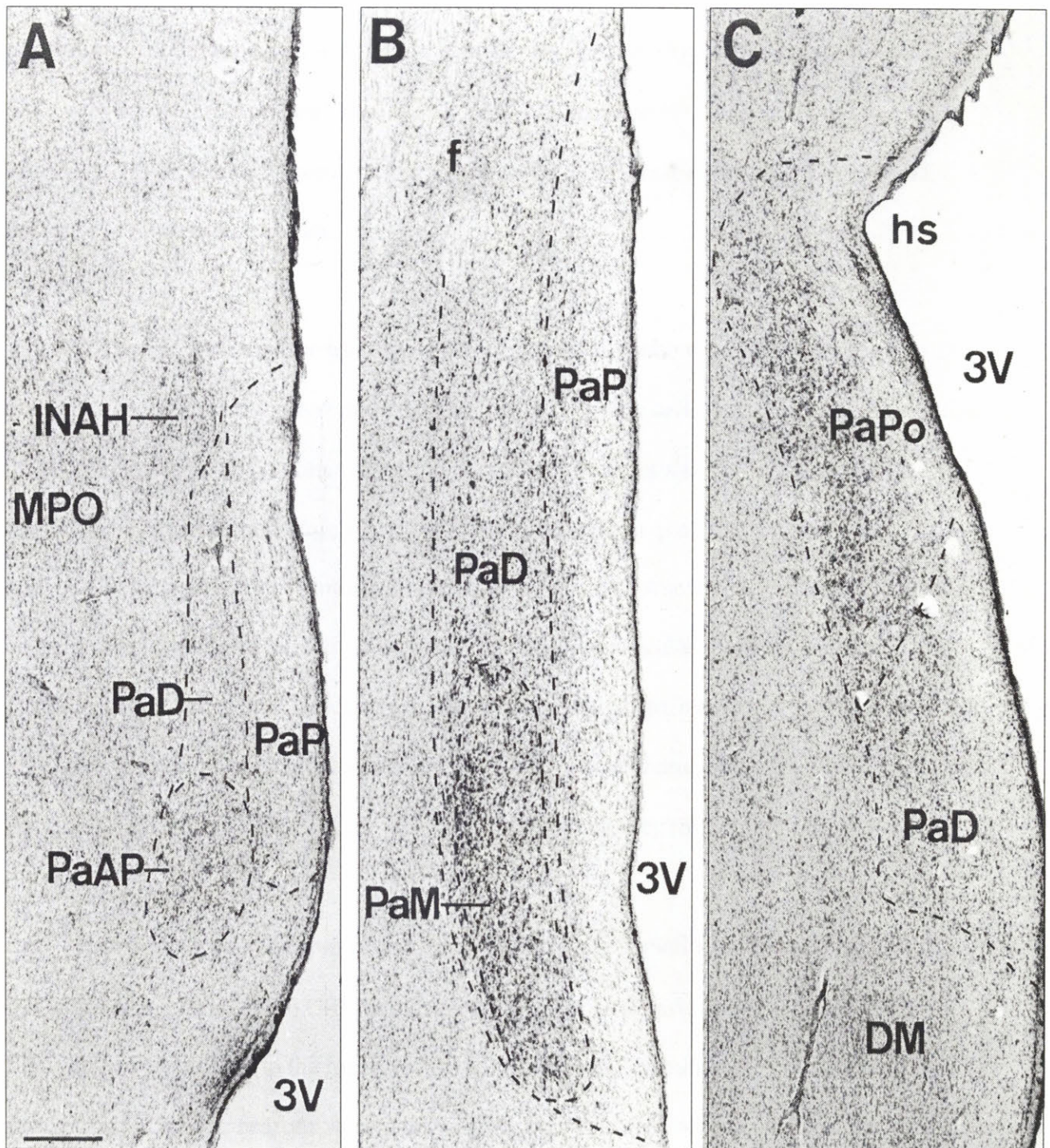


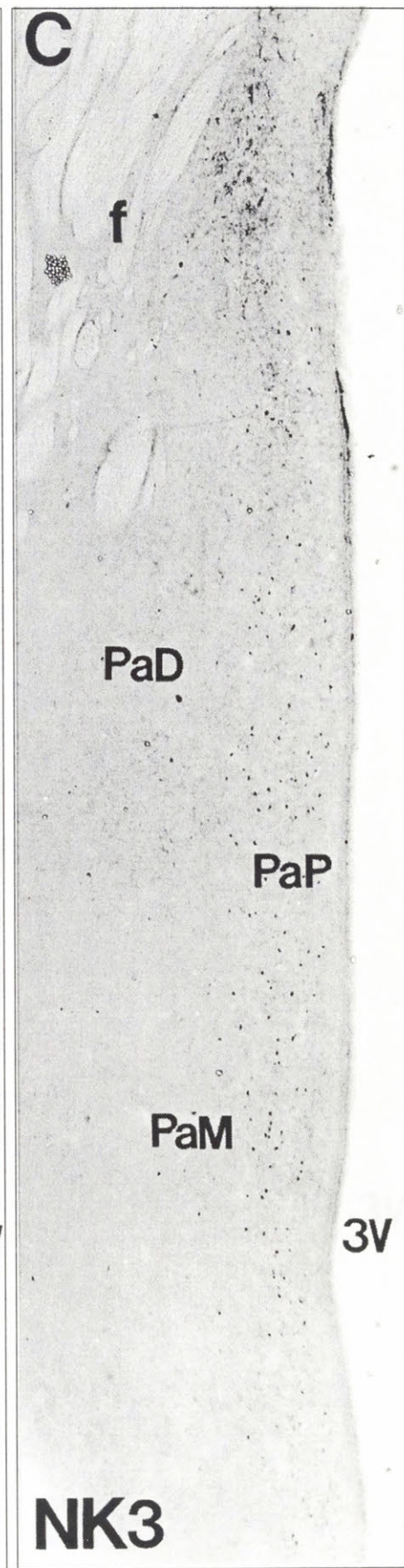
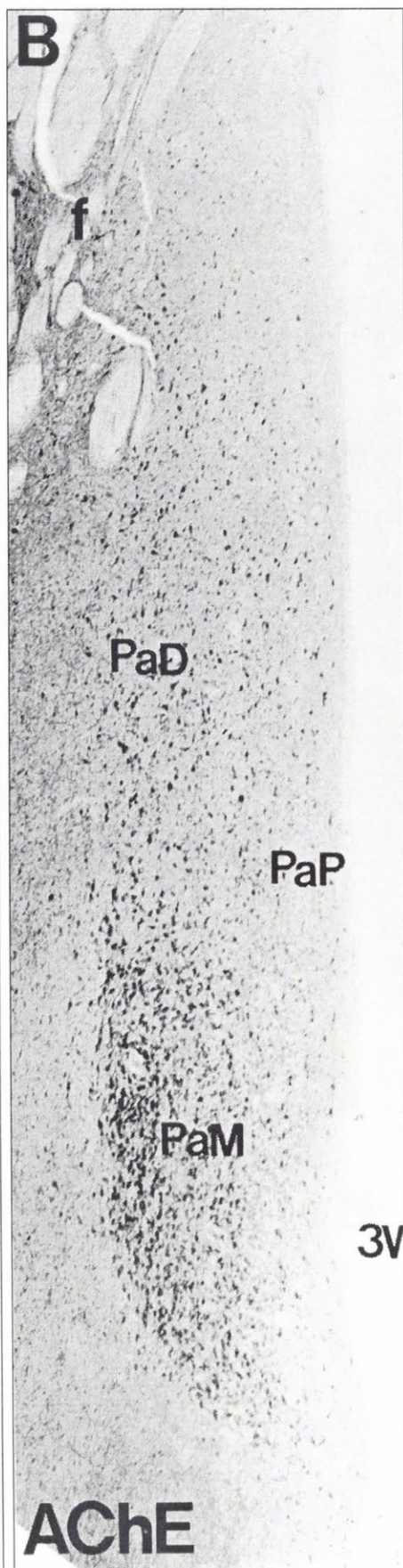
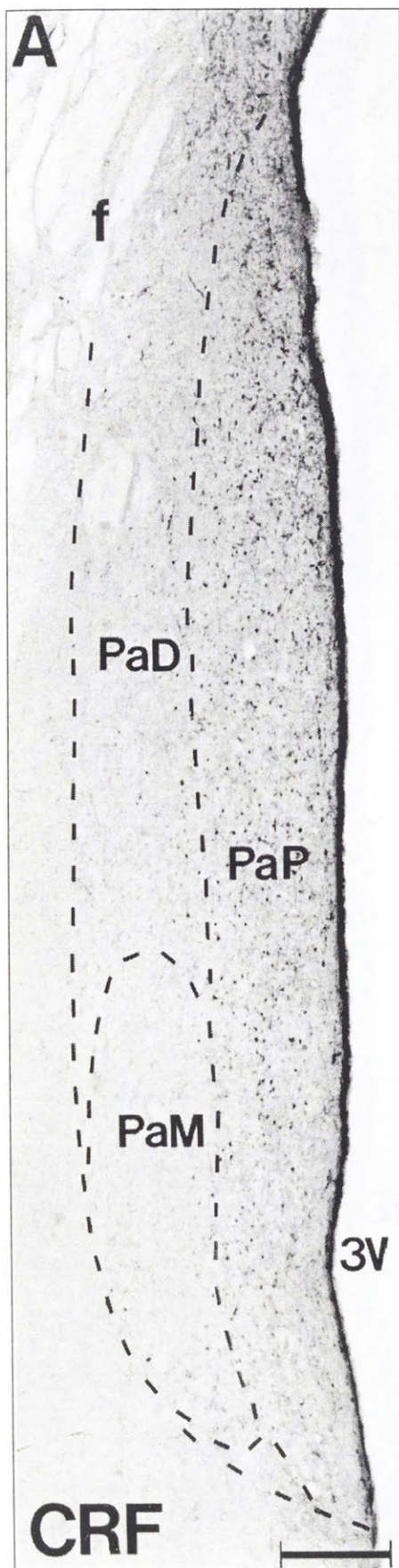
Figure 1. Photomicrographs of cresyl violet stained sections from three rostro-caudal levels of the human Pa (A, B and C) showing the variations in cell concentration, shape and topographical position between different subnuclei of the human Pa. Scale bar indicates 1 mm for all photomicrographs.

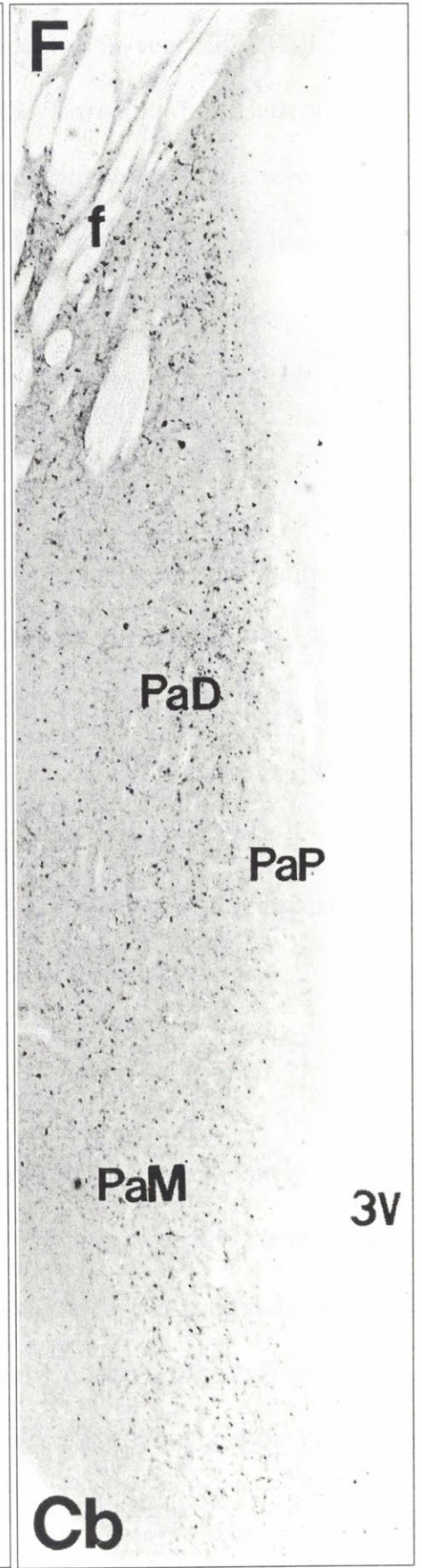
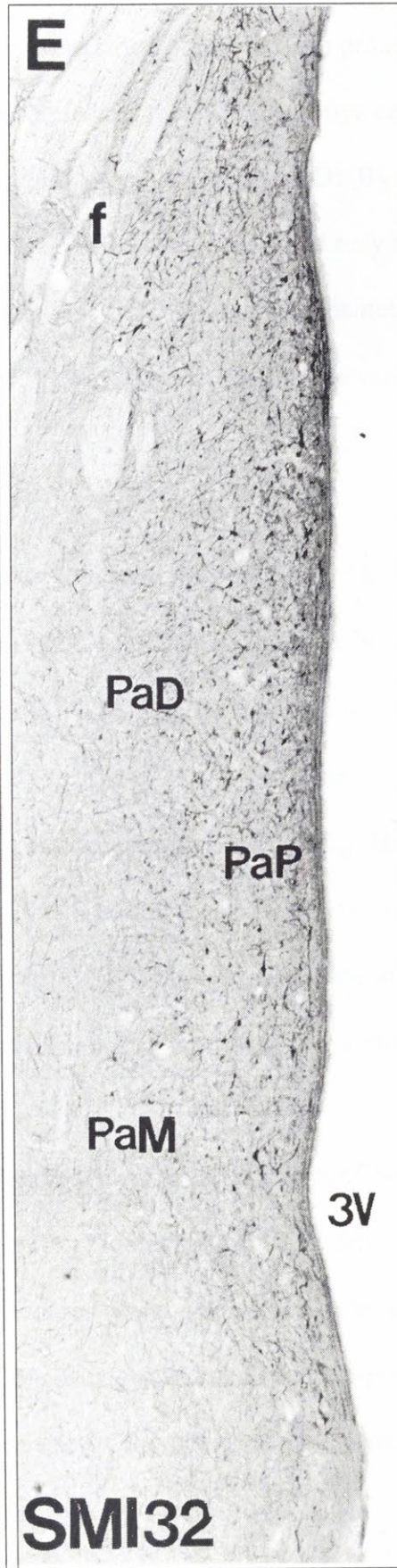
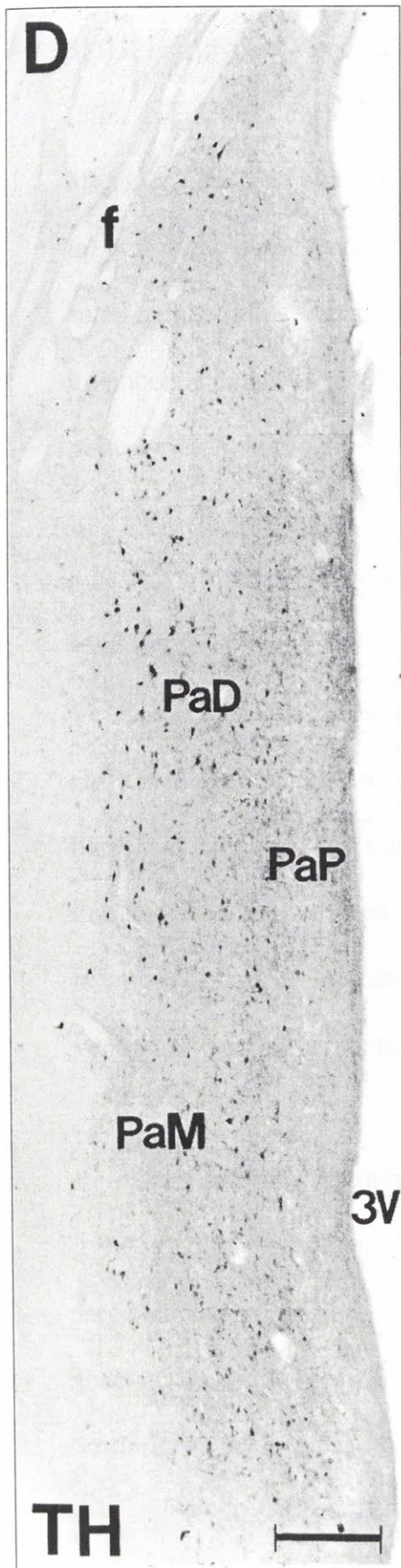
quadrant of the nucleus (Fig. 2B). Just rostrally to this magnocellular neuronal cluster, a population of small (about $17.1 \pm 2.9 \mu\text{m}$ diameter somata, $N=30$) darkly-stained cells with processes was seen. Numerous small ($14.9 \pm 4.2 \mu\text{m}$ diameter, $N=100$) faintly to moderately stained AChE-labeled cells were present in proximity to the ventricular wall (Fig. 6c) and posterior to the fornix in the Pa.

Tyrosine hydroxylase immunoreactivity. All TH-positive neurons were large to medium sized ($22.7 \pm 6.1 \mu\text{m}$ somal diameter, $N=100$) bipolar cells (Fig. 5e). The distribution of TH-immunoreactive neurons varied considerably throughout the Pa. In the ventral parts of the Pa, these neurons were largely confined to the dorsolateral quadrant, avoiding the periventricular area and the ventrolateral quadrant (Fig. 2D). Above the fornix, the TH-positive neurons were segregated laterally, also avoiding the periventricular area (Fig. 3D), while posterior to the fornix the TH-positive neurons were evenly distributed though the nucleus (Fig. 4B). A prominent population of small (about $16.2 \pm 4.9 \mu\text{m}$ diameter somata, $N=30$) TH-positive cells with visible processes was also present in the very rostral tip of the Pa.

Corticotropin-releasing factor immunoreactivity. Small to medium sized ($17.9 \pm 3.9 \mu\text{m}$ somal diameter, $N=100$) CRF-immunoreactive neurons (Fig. 5c) were distributed evenly through the Pa posterior to the fornix (Fig. 4A). In contrast, ventrally (Fig. 2A) and above the fornix (Fig. 3C) these neurons were clearly segregated in immediate proximity of the ventricular wall while the more lateral areas showed no reactivity for the peptide. No CRF-immunoreactive neurons were present in the small most antero-ventral tip of the Pa.

Neurofilament protein SMI32 immunoreactivity. Immunostaining with the SMI32 antibody revealed a population of small to medium sized ($19.8 \pm 6.3 \mu\text{m}$ diameter, $N=100$)





bipolar neurons (Fig. 5h) and a large number of fibers in the Pa. Ventrally and above the fornix, SMI32-positive cells and fibers were strictly segregated in proximity to the ventricular wall (Figs. 2E and 3E). Posterior to the fornix, the SMI32 positive cells were somewhat smaller (Fig. 5f) and evenly distributed throughout the nucleus (Fig. 4D). By contrast, the most antero-ventral tip of the Pa did not contain any SMI32-positive cells and only a few immunoreactive fibers. A small number of particularly large ($31.8 \pm 3.7 \mu\text{m}$ somal diameter, N=20) SMI32-immunoreactive neurons (Fig. 5g) was detected close to the ventricular wall in the nucleus posterior to the fornix.

Neuromedin K receptor-like immunoreactivity. All cells labeled with NK3 antibody were small (approximately $16.7 \pm 3.3 \mu\text{m}$ diameter somata, N=100) bipolar neurons (Fig. 5a). Ventrally and above the fornix the NK3-like immunoreactive cells were segregated medially, close to the ventricular wall (Figs. 2C and 3A); while posterior to the fornical column the NK3-like positive neurons were dispersed throughout the Pa (Fig. 4E). There was no NK3-like immunoreactivity observed in the most antero-ventral tip of the Pa. Individual medium sized neurons ($21.8 \pm 3.3 \mu\text{m}$ diameter, N=20) (Fig. 5b) were seen in close proximity of the ventricular wall in the nucleus posterior to the descending column of the fornix.

Calbindin immunoreactivity. All cells labeled for Cb were small (approximately $13.5 \pm 4.9 \mu\text{m}$ diameter somata; N=100) bipolar neurons (Fig. 5d). Ventral and dorsal to the fornix a large number of Cb-positive neurons was segregated laterally avoiding the periventricular area that was devoid not only of Cb-positive cells but also of Cb-positive neuropil (Figs. 2F and 3F). Posterior to the fornical column, few Cb-positive neurons were dispersed throughout the Pa

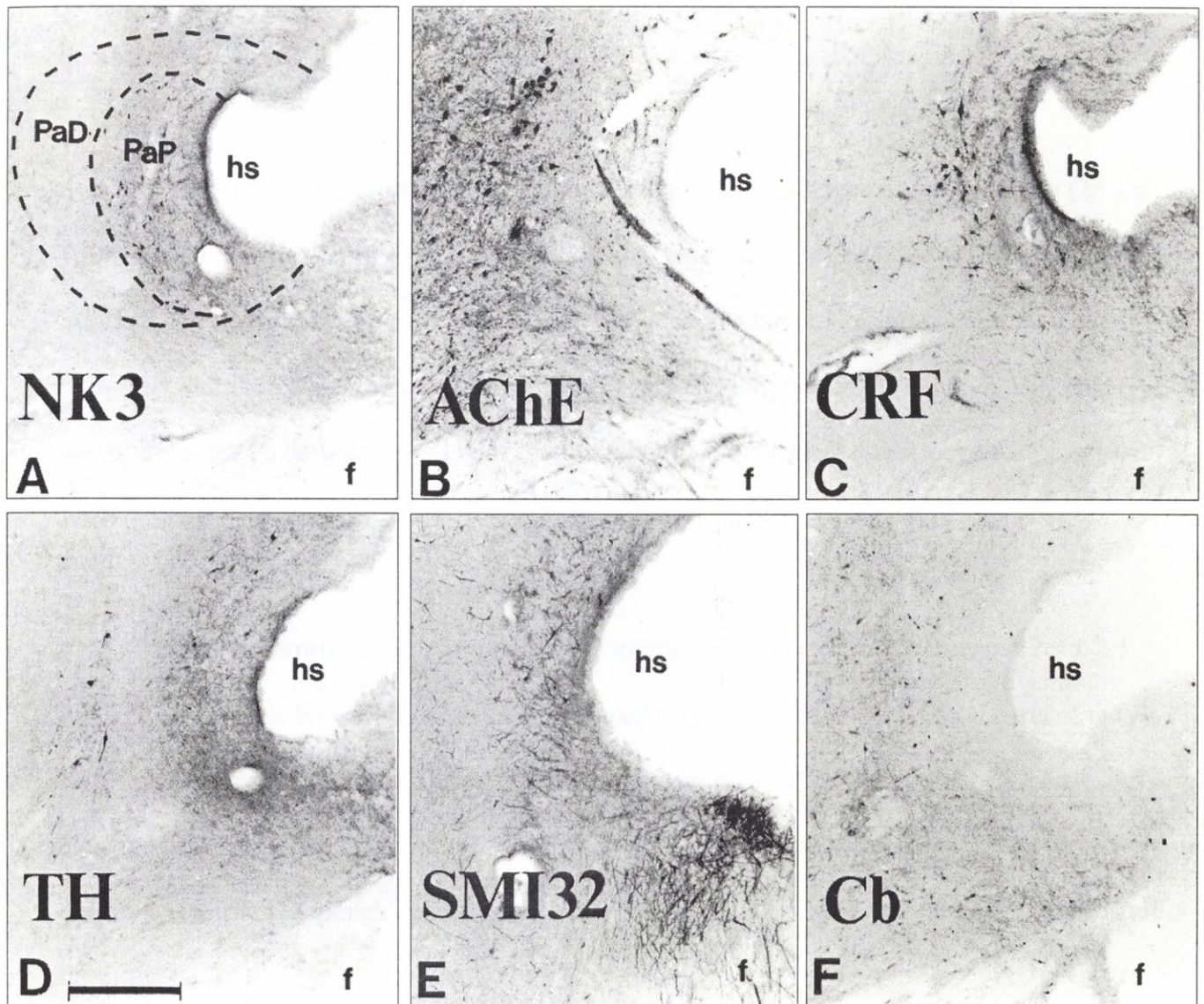


Figure 3. Immuno/enzyme histochemistry of the human Pa above the descending column of the fornix in adjacent coronal sections labeled for histochemical markers as indicated. In each photomicrograph the third ventricle is to the right. Subnuclear boundaries have been indicated by a dashed line in the NK3 immunoreacted section. All remaining sections have similar subnuclear boundaries. Note the SMI32 positive cells and fibers concentrated between the fornix and the ventricular wall in E. Scale bar indicates 0.5 mm for all photomicrographs.

(Fig. 4F). Finally, calbindin-immunoreactive cells were also present in the most anteroventral tip of the Pa.

Vasopressin immunoreactivity. Immunostaining for vasopressin revealed large ($25.1 \pm 4 \mu\text{m}$ somal diameter, $N=100$) cells (Fig. 9A) densely packed and segregated in the ventrolateral quadrant of Pa, avoiding the periventricular area and the dorsolateral quadrant (Fig. 8B), but uniformly distributed and more dispersed through the posterior parts of the nucleus. The very rostral tip of the Pa harbored a group of smaller (about $17.9 \pm 3.3 \mu\text{m}$ diameter somata, $N=50$) AVP positive neurons.

Oxytocin immunoreactivity. All oxytocin immunoreactive cells were large ($22.9 \pm 2.1 \mu\text{m}$ somal diameter, $N=100$) bipolar, spindle shaped cells (Fig. 9B). In the ventral parts of the Pa, these neurons were seen primarily in the dorsolateral quadrant, avoiding the periventricular area and the ventrolateral quadrant (Fig. 8A), while posterior to the fornix the neurons were uniformly distributed through the nucleus. No OXY-positive cells were present in the very rostral tip of the Pa.

Neurophysine immunoreactivity. Neurophysine immunoreactivity revealed heterogeneous population of magnocellular neurons ($23.1 \pm 4.3 \mu\text{m}$ somal diameter, $N=100$) comprised of spindle shaped cells dispersed through the dorsolateral Pa and somewhat larger round shaped neurons packed in the ventrolateral Pa (Fig. 8C). Posterior to the fornix these neurons were intermixed and distributed throughout the Pa. The NPH positive cells were largely avoiding the periventricular area.

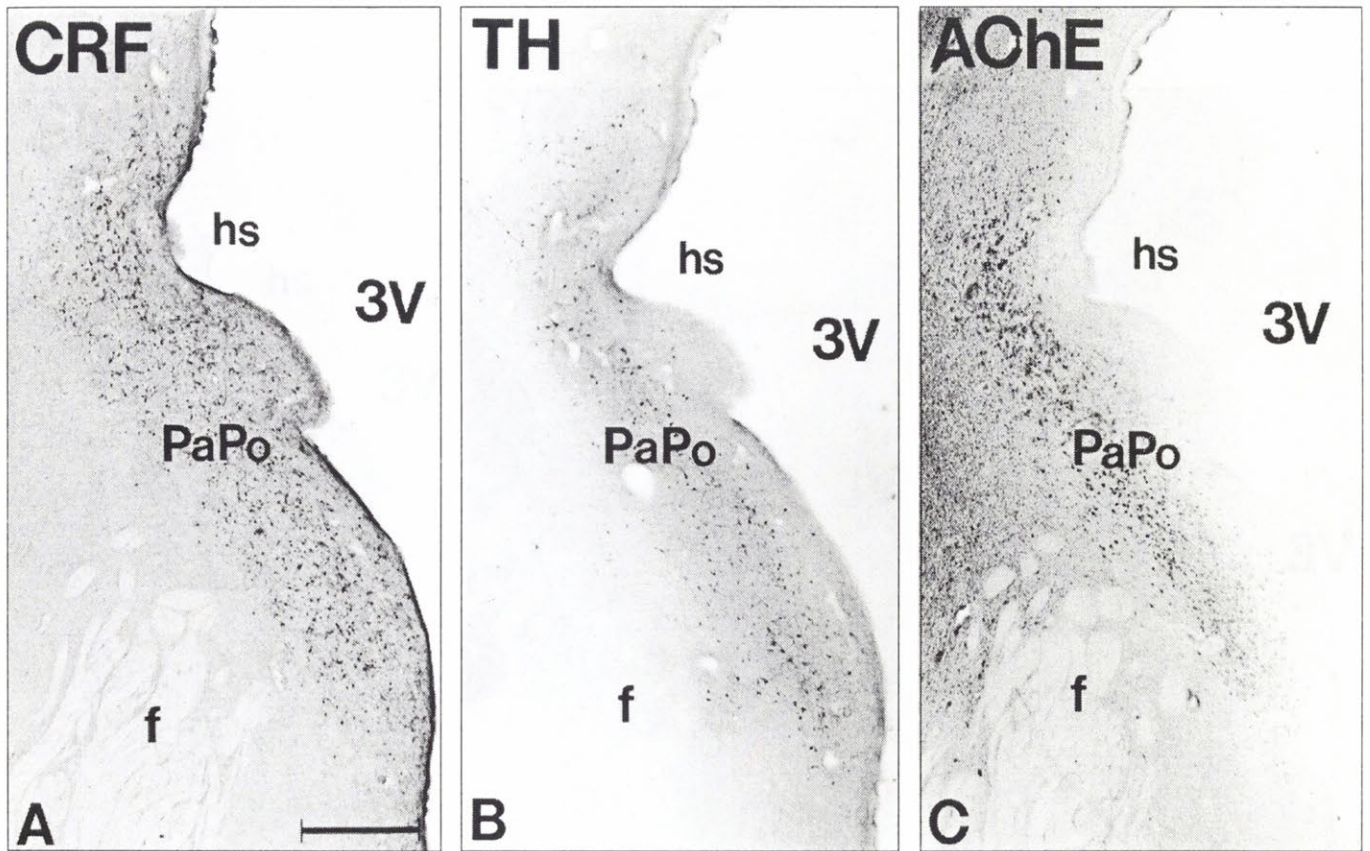
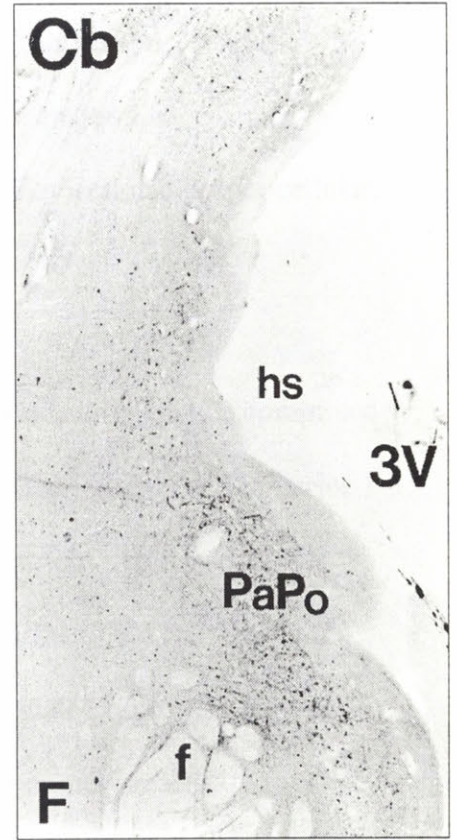
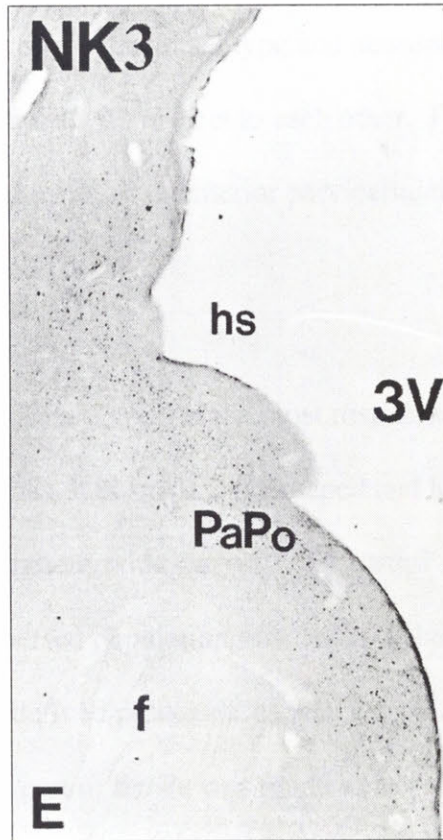
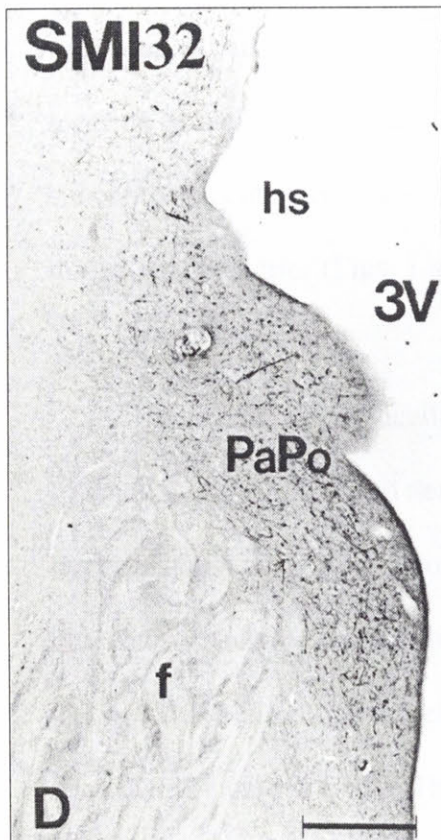


Figure 4. Immuno/enzymehistochemistry of the posterior human Pa (PaPo) in adjacent coronal sections labeled for the six markers used in the present study. In each photomicrograph the third ventricle is to the right. Scale bar indicates 1 mm for all photomicrographs.



Organization of the subnuclei in the human Pa

The comparative analysis of adjacent, sequentially stained sections revealed that the cells immunoreactive for different substances are not randomly dispersed throughout the Pa, but segregated into rather distinct anatomical subcompartments with reasonably well-defined boundaries. In identifying the cytoarchitectonic boundaries of the Pa subcompartments, we also took into account the relative density of each cell type and neuropil (Figs. 6 and 7) and the location of their main concentrations with respect to each other. Five anatomical subcompartments were identified as follows: anterior parvicellular, parvicellular, magnocellular, dorsal, and posterior (Figs. 1 and 11).

The anterior parvicellular Pa (PaAP) is the most rostral subnucleus (Fig. 1A) comprised of small and medium sized neurons. It is small, oval-shaped and located in the ventral anterior hypothalamus near, but not contiguous with, the wall of the third ventricle. This subnucleus characteristically contains a dispersed population of small, bipolar AChE-, AVP-, NPH- and TH-positive neurons, with well-defined processes, as well as some small Cb-positive cells and few SMI32-positive fibers. This part of the Pa was found to have no immunoreactivity for CRF and NK3.

The parvicellular Pa (PaP) lies along the wall of the third ventricle ventrally and above the descending column of the fornix (Figs. 2 and 3). This subcompartment predominantly contains small cells (Figs. 6C and 7C) and is characterized by the presence of prominent populations of small CRF-, NK3- and SMI32-positive neurons and SMI32-positive fibers, and by the absence of TH and Cb immunoreactivity. This compartment also contains numerous small faintly-stained and occasional large AChE-positive neurons, but generally avoided by AVP, OXY and NPH positive cells.

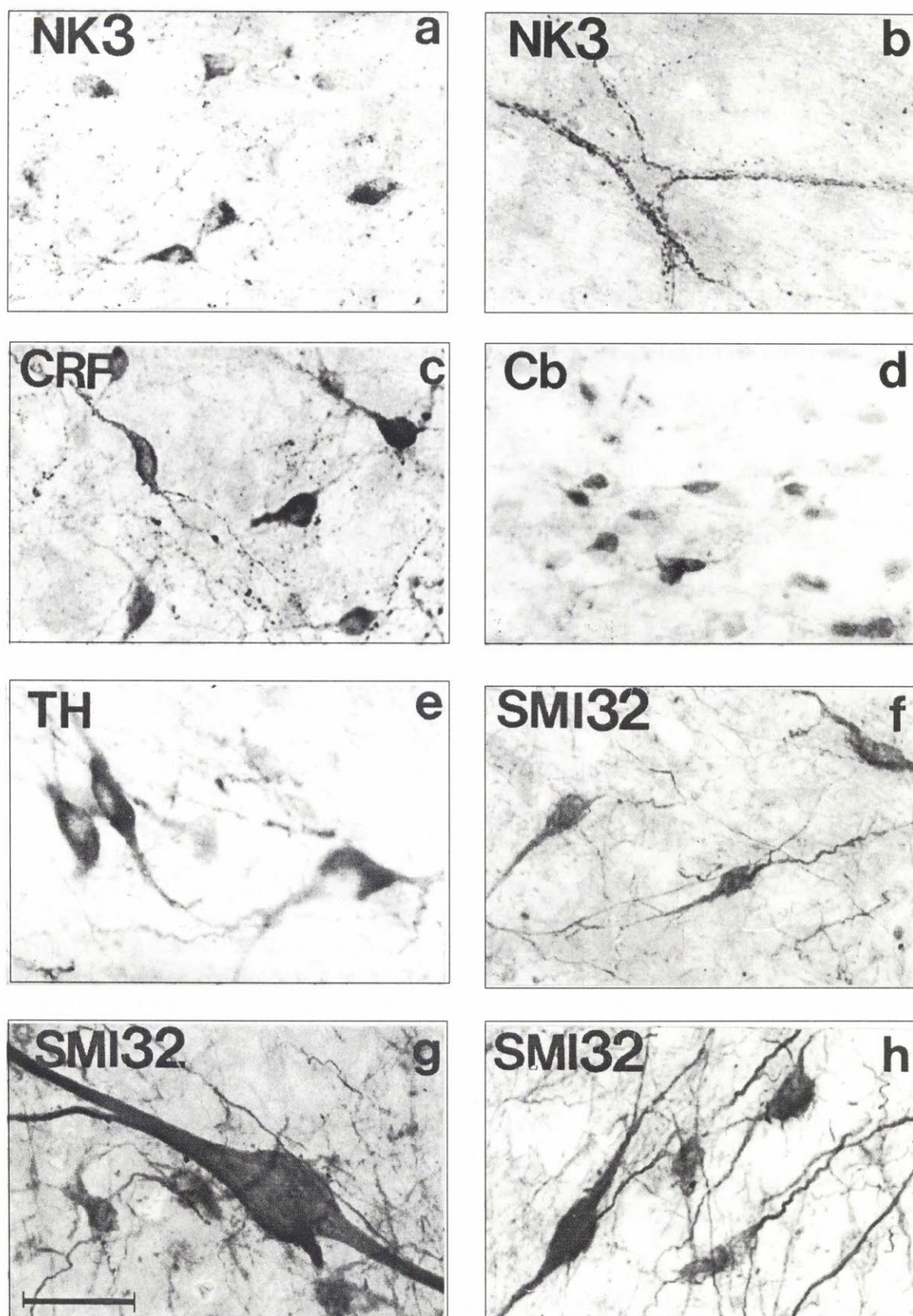


Figure 5. Somata and proximal dendrites of Pa neurons immunoreactive for six immunohistochemical markers as indicated. Note the small somata of neuromedin K and calbindin immunoreactive neurons and large somata of the SMI32 immunoreactive neurons. Scale bars indicate 50 μ m.

The oval-shaped magnocellular Pa (PaM) occupies the ventrolateral quadrant of Pa densely packed large multipolar neurons (Figs. 1, 6A and 7A) and is the most conspicuous subnucleus. In terms of topography, the magnocellular Pa is a posterior continuation of the anterior parvicellular Pa, although it is easily distinguishable from the latter by the size and density of its cells. More posteriorly, the magnocellular Pa assumes a progressively more dorsal position, while bordering the parvicellular Pa laterally and the dorsal Pa ventrally until its caudal boundary reaches the level of the hypothalamic sulcus (Fig. 11). This PaM contains only a few large to medium-sized TH-positive cells (Fig. 2D), but a considerable number of small Cb-positive neurons (Fig. 2F). The PaM is deficient of SMI32-positive cells and devoid of any CRF or NK3 immunoreactivity (Fig. 2). The PaM is densely packed with large AVP-, NPH- and darkly stained AChE-positive neurons, but also few OXY-immunoreactive cells (Fig. 9).

The dorsal Pa (PaD) lies above the PaM in the dorso-lateral quadrant of the Pa (Figs. 2 and 11) and is characterized by numerous large dispersed cells, as well as small neurons (Figs. 1; 6B and 7B). This subnucleus contains dispersed populations of large bipolar TH- and OXY-positive cells and small Cb-positive neurons, but very few AVP immunoreactive cells (Figs. 2 and 9). Large NPH- and AChE-positive cells that are found in the magnocellular Pa are also numerous in the dorsal Pa, although they are distributed more diffusely in the latter, and this feature differentiates these two subnuclei in NPH- (Fig. 9C) and AChE staining (Fig. 6B). The dorsal Pa also contains a large number of small faintly stained AChE-positive cells and a few SMI32 positive fibers. This subnucleus contains no NK3-, CRF- or SMI32-positive cells and thus can be differentiated from the parvicellular Pa which contain an abundance of these substances (Fig 2).

The posterior Pa subnucleus (PaPo) occupies the most posterior part of the Pa, encompassing the hypothalamic sulcus caudal to the descending column of the fornix (Figs.1, 4

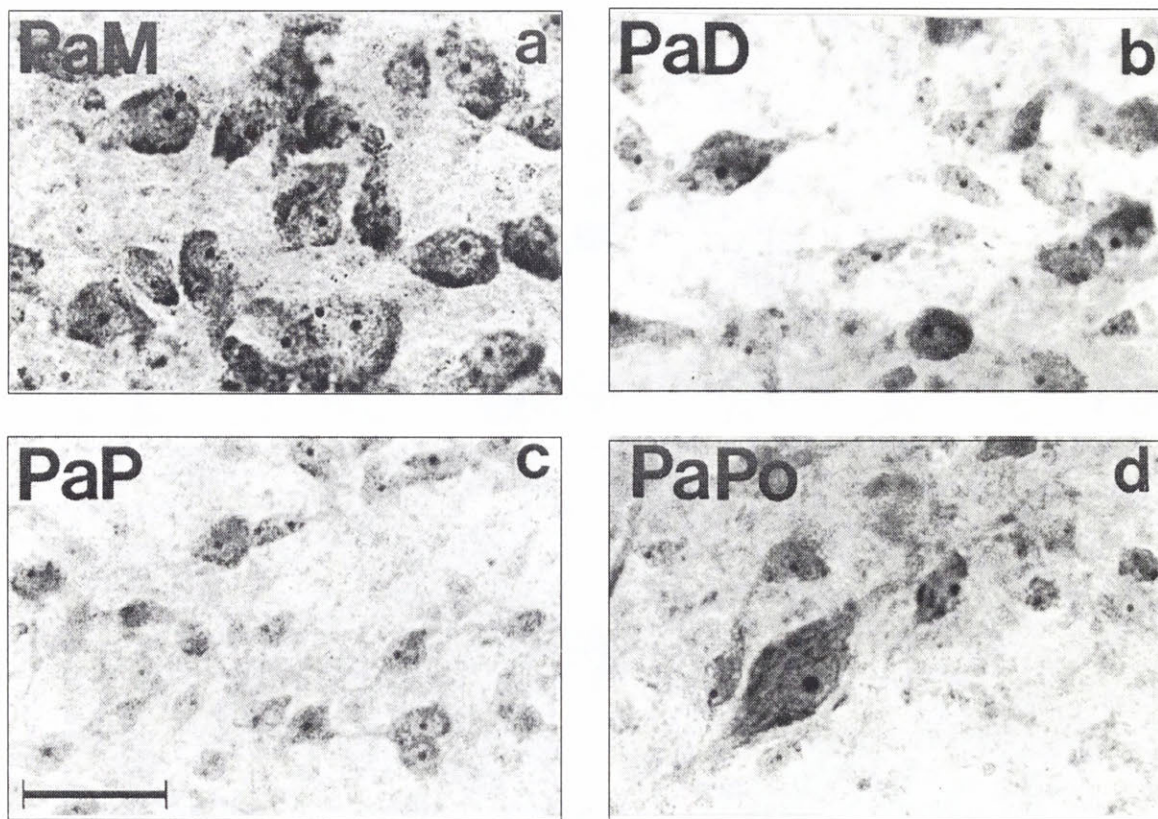


Figure 6. Cytoarchitecture of neuronal types in the different subcompartments of the human Pa as revealed by AChE staining. A) Large densely packed multipolar neurons found in the PaM; B) Large moderately stained spindle shaped neurons characteristic of PaD; C) The PaP typically contains numerous small faintly stained neurons; D) Markedly large darkly-stained spindle-shaped neurons found individually in the PaPo. The scale bar indicates 50 μ m.

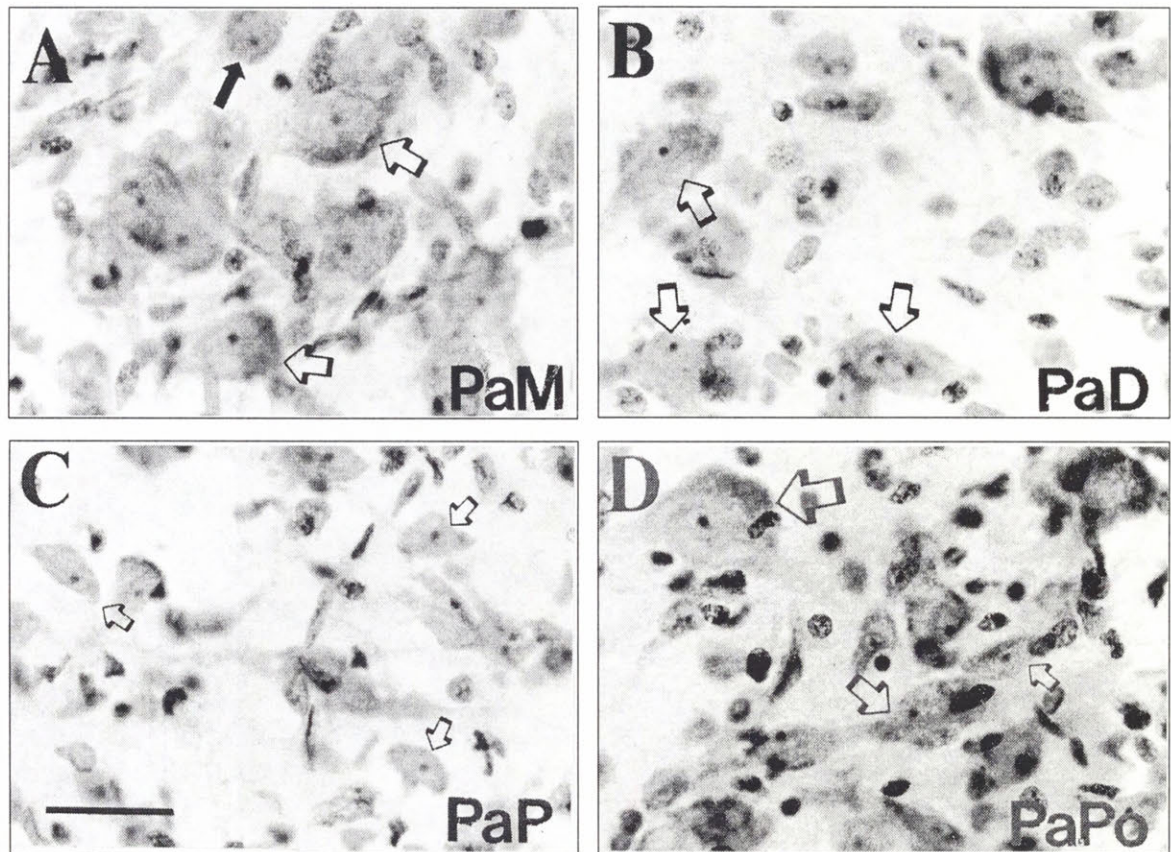


Figure 7. Cytoarchitecture of neuronal types in the different subcompartments of the human Pa as revealed by Cresyl Violet staining. A) PaM is comprised of mostly large, densely packed multipolar neurons (arrows); B) Large spindle shaped neurons (arrows) and small cells scattered through PaD; C) Small neurons (arrows) prevalent in PaP; D) PaC harbors the amalgam of large multipolar neurons (large arrow), large spindle shaped cells (medium size arrow) and small neurons (small arrow). The scale bar indicates 50 μm .

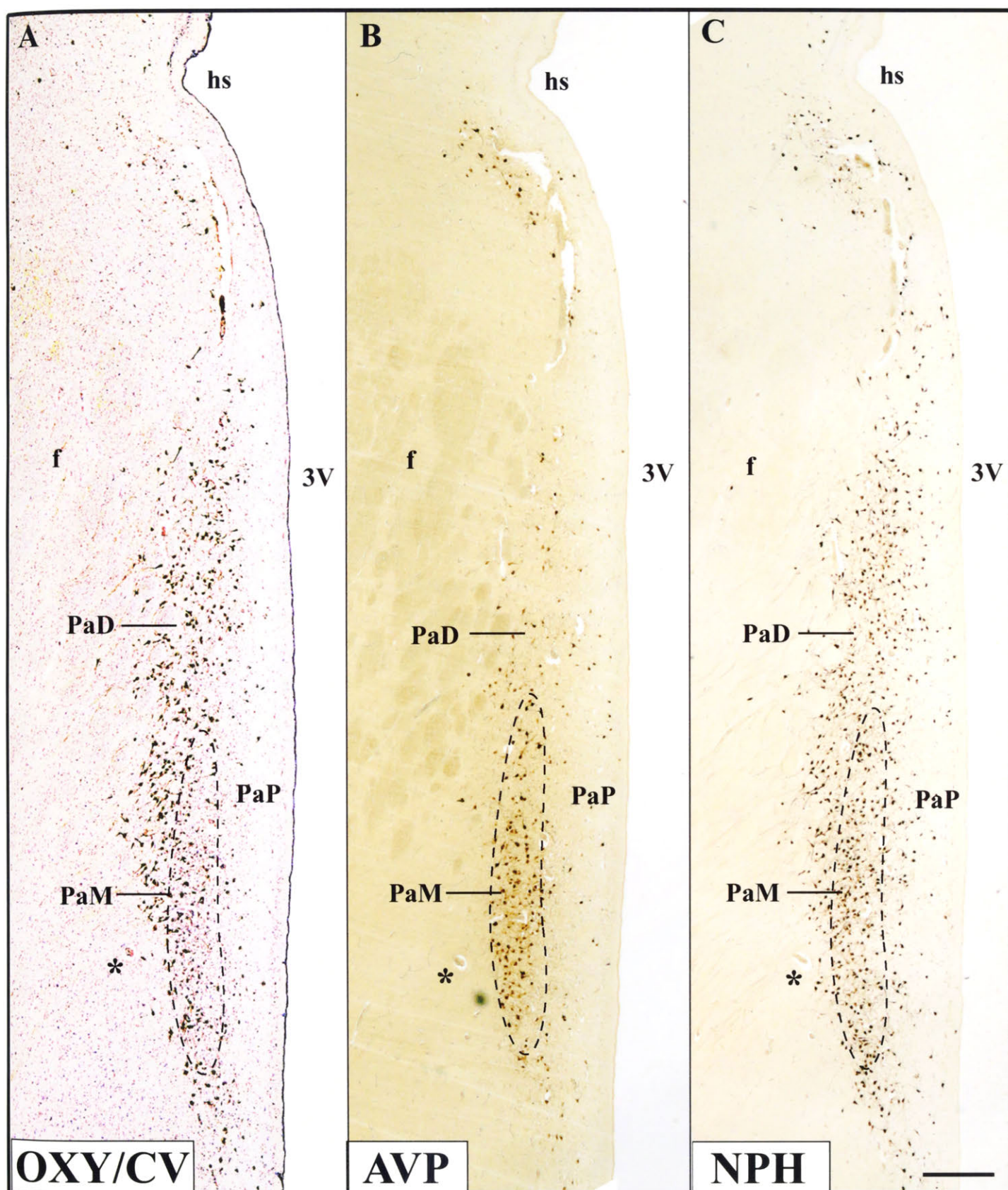


Figure 8 Immunohistochemistry of the human Pa in adjacent coronal sections labeled for OXY, AVP and NPH. In each photomicrograph the third ventricle is to the right. The OXY stained section is counterstained with Cresyl Violet. Subnuclear boundaries have been indicated for PaM by a dashed line. The asterisk indicates the same blood vessel in adjacent brain sections. All remaining sections have similar subnuclear boundaries. Scale bar indicates 0.5 mm for all photomicrographs.

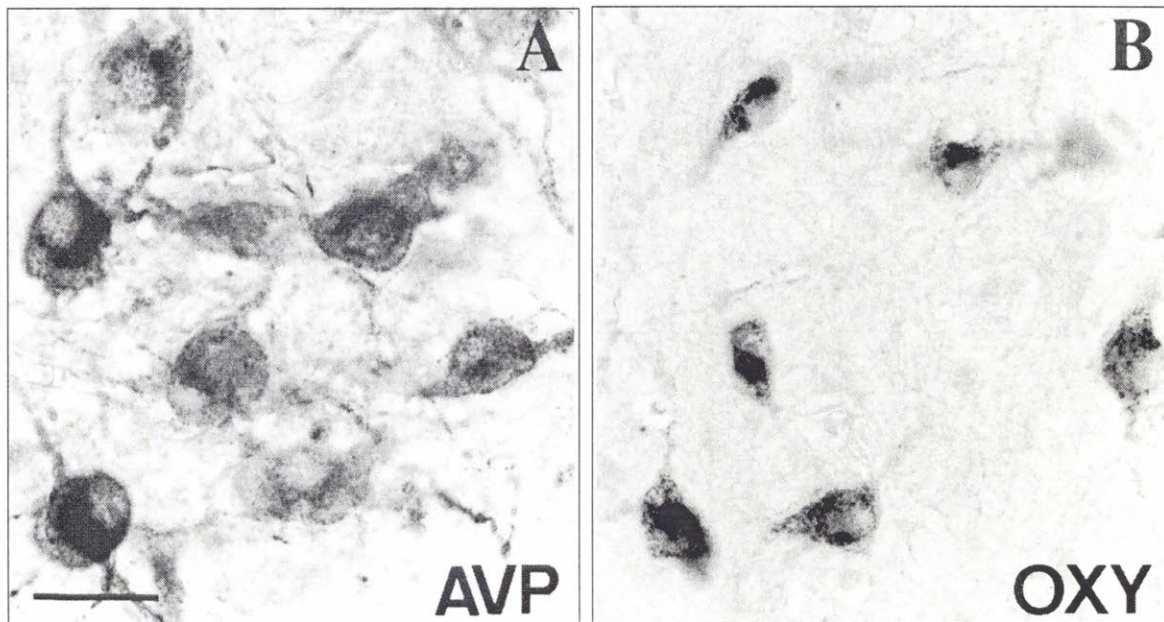


Figure 9. Somata and proximal dendrites of Pa neurons immunoreactive for OXY and AVP. Note the characteristic spindle shape of OXY immunoreactive neurons. Scale bars indicate 50 μ m.

and 11). This subnucleus is comprised of large bipolar and multipolar cells, but also numerous small neurons (Figs. 6D and 7D). The chemoarchitectonic features of the posterior Pa include the presence of dispersed and intermingled CRF-, NK3-, SMI32-, TH- and Cb-immunoreactive neurons (Fig.4). The distributions of the magnocellular AVP-, OXY- and NPH-immunoreactive cells in the PaPo overlaps completely. The posterior Pa also harbors a large number of magnocellular AChE-positive cells. These cells are spindle-shaped and dispersed, in contrast to the densely-packed large AChE-positive neurons found in the magnocellular Pa (Fig. 6D). This part of Pa also contains numerous small AChE-positive neurons and a few large multipolar AChE-positive cells. In some brains an appendix of small round cluster of cells was seen attached to the PaPo laterally.

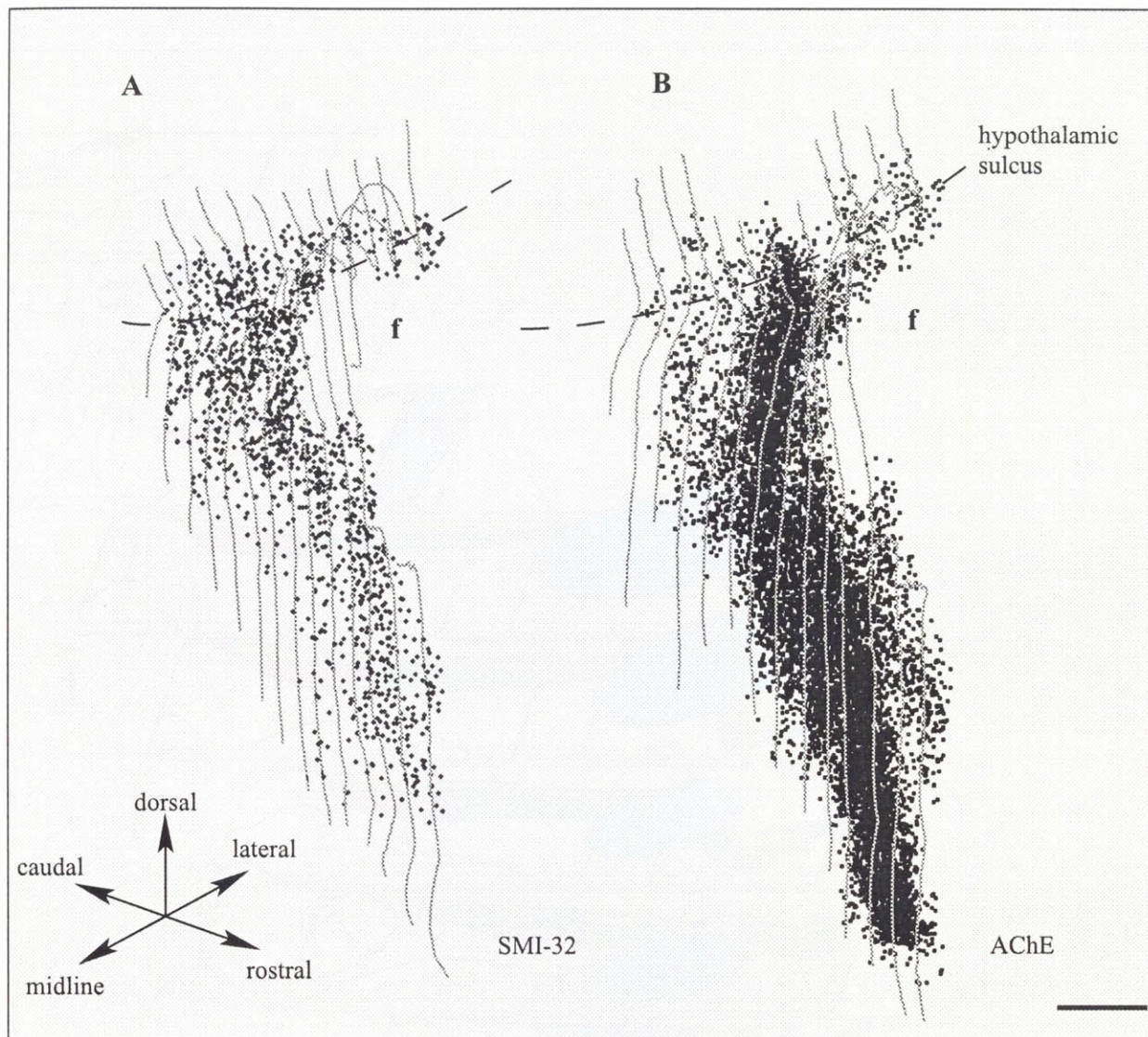


Figure 10. Two Magellan 3.1 generated 3-dimensional reconstructions based on the cell plots of all neurofilament immunoreactive (SMI32+) (A) and all AChE positive (B) neurons, respectively. Note the concentration of AChE positive neurons in the ventrolateral quadrant of the nucleus (PaM). Scale bar for both reconstructions in the transverse plane is 1 mm.

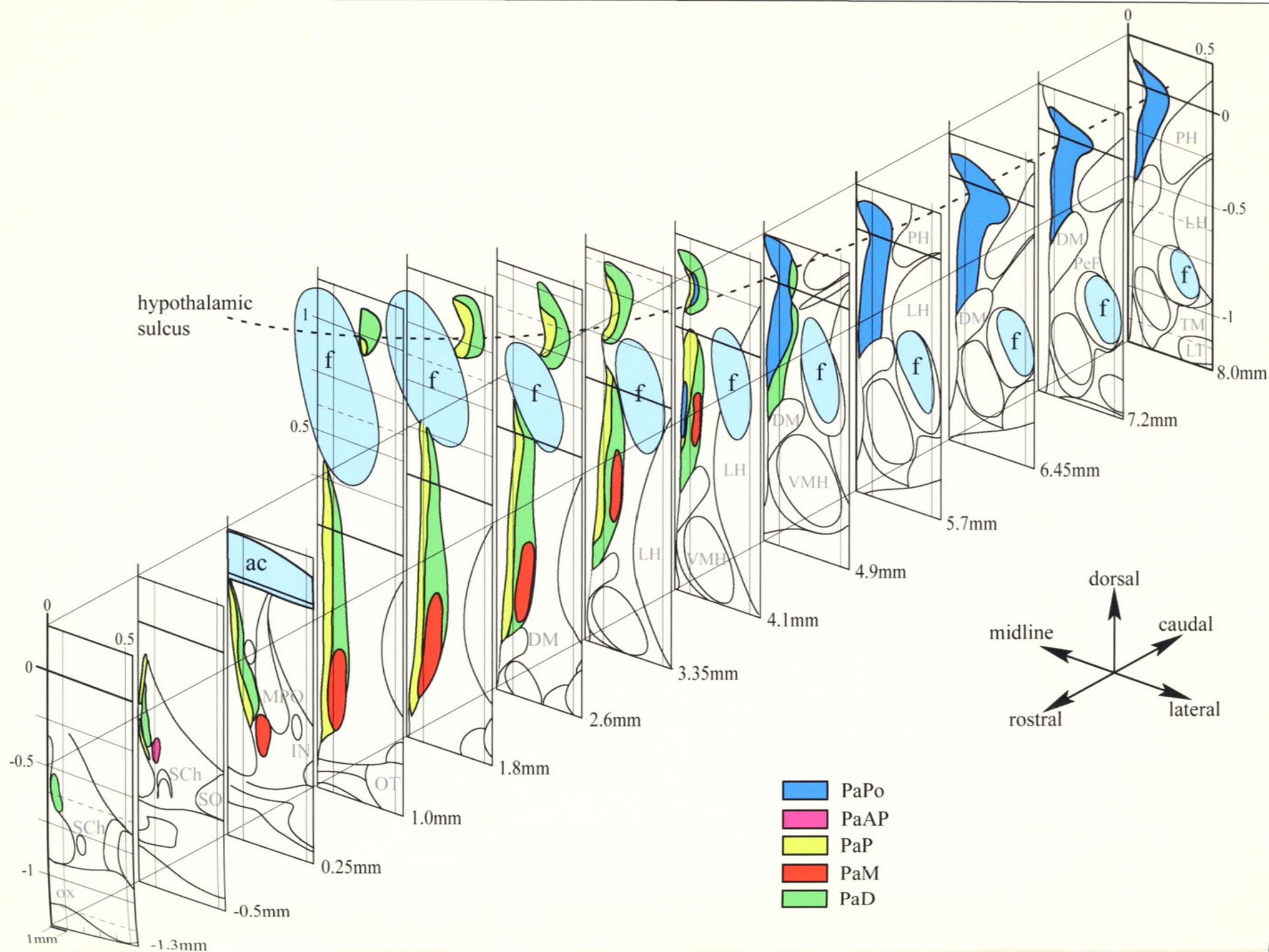


Figure 11 A model of the human Pa showing the subnuclei delineations based on the Magellan 3.1 generated plots of six histochemical markers (AChE; SMI32; Cb; TH; NK3; CRF) and verified with the distribution of AVP, OXY and NPH. Individual subnuclei are illustrated by different colours. The stereotaxic coordinates were borrowed from (Mai et al., 1997). The third ventricle wall lies to the right..

DISCUSSION

The present findings show that the human paraventricular nucleus can be subdivided into five substantially distinct subnuclei on the basis of cell density, cytoarchitecture and chemoarchitecture (Fig. 11). This work provides a basis for comparing the structural organization of the subnuclei in the human Pa with that described for the rat and other experimental animals, where these subdivisions have been ascribed specific functions. The suggested subdivision of the human Pa is simpler and less striking than the intricate and conspicuous subdivision of the nucleus in the rat. This causes some difficulties in establishing anatomical homologues between the species. Nevertheless, the observation that the human Pa features reasonably distinct compartmental neurochemical organization suggests that its parts subserve different functions. The division of the human Pa into five chemoarchitectonic subnuclei, as described in this study, significantly alters the subdivision of the nucleus described in earlier cytoarchitectonic studies (Brockhaus, 1942; Morton, 1969). Wherever possible we retained the original names of the subnuclei, but it needs to be understood that the subnuclear boundaries described in this study substantially differ from the boundaries originally proposed on the basis of cytoarchitecture (Brockhaus, 1942). The 3-dimensional reconstructions of the nucleus reveal the topographic position of the entire Pa as well as its subcompartments in relation to prominent anatomical landmarks including the fornix, the hypothalamic sulcus and the wall of the third ventricle and the anterior commissure (Fig. 11).

The identification of the PaM by clustering of the AChE and AVP positive magnocellular neurons in the present study is in agreement with the earlier reports that distinguished the ventrolateral quadrant of the human Pa by clustering of large AVP neurons (Saper, 1990). The lateral and anterior magnocellular components of the rat (Paxinos and Watson, 1986) and mouse (Paxinos and Franklin, 1997) Pa are also distinguished by strong

AChE labeling. In the human, OXY- and AVP-containing cells were thought to be dispersed throughout the entire Pa (Dierickx and Vandesande, 1977; Mai et al., 1997), unlike in the rat Pa, where these large neurons are segregated into distinct lateral, medial and anterior magnocellular subcompartments (Swaab et al., 1975; Rhodes et al., 1981). Although, in the rat, smaller neurons containing these hormones are found in other parts of the nucleus (Vandesande and Dierckx, 1975; Swanson and Simmons, 1989). Due to the key functional role of these cells in the hypothalamo-hypophyseal pathway and their significance in regulation of autonomic output, the overlap in distribution of these cells in the human Pa may be regarded as a stumbling block in the parcelation of the Pa into discrete subnuclei. On the other hand, Swanson (1991) emphasized that even in the rat, subnuclei are incompletely segregated; in other words, some cells characteristic of one subnucleus can be found within other subnuclei. A fundamental question is whether the magnocellular subnuclei of the human Pa (PaM and PaD) correspond to the anterior, lateral and medial magnocellular subnuclei of the rat Pa. Supporting the functional similarities, Morton (1969) found a dramatic decrease in the number of magnocellular neurons in the ventral, but not caudal, Pa in human patients after hypophysectomy.

The present study demonstrated the difference in the distribution of the AVP and OXY in the human Pa (Fig. 9), consistent with the Rhodes and colleagues (1981) description of AVP and OXY distribution in the rat Pa. This study described the lateral magnocellular subnucleus as formed by the core of vasopressin cells with the rim of oxytocin cells, while depicted the medial magnocellular Pa and the posterior Pa as comprised primarily of oxytocin neurons (Rhodes et al., 1981). On the other hand the intercompartmental overlap of the magnocellular cells in the human Pa is comparatively greater than in the rat. It seems likely, that factors related to the interspecies differences could have contributed to this. For example, the pronounced dorso-ventral neurogenic gradients followed by the large neurons in the developing human Pa

contributes to the significant dorsoventral extension of the human Pa along the ventricular wall (Mai et al., 1997). The large cells of rat Pa, in contrast, follow a more horizontal neurogenic gradient and, during post-mitotic migration, travel a comparatively short distance (Altman and Bayer, 1986).

Acetylcholinesterase staining was found useful in earlier studies of the human Pa (Saper and German, 1987; Spencer et al., 1985), but the failure to co-localize AChE-positive Pa neurons with catecholamines dampened the interest of researchers in enzyme expression within the nucleus. The present study demonstrated AChE staining as a relatively simple method of revealing the boundaries of the Pa subcompartments in human (Figs. 2B and 6). Furthermore, the present study confirmed the suggestion of Saper and Chelimsky (1984) that short postmortem delay (less than 12 hours) and a short fixation period (3 days) are important elements in obtaining optimal AChE staining intensity.

The identification of the PaP in the present study, supports earlier chemoarchitectonic reports describing a medial aggregation of somatostatin positive neurons and fibers (Bouras et al., 1987; Najimi et al., 1989), growth hormone-releasing hormone fibers (Bloch et al., 1984) and luteinizing hormone-releasing factor positive neurons (Barry, 1977) in this area.

The present findings confirm earlier reports on the distribution of CRF-containing neurons in the human Pa (Pelletier et al., 1983; Mouri et al., 1984; Takahashi et al., 1989) and demonstrate an exclusively parvicellular population of CRF-positive cells that are distinct from the populations of OXY- or AVP- secreting magnocellular Pa neurons. The present study also describes the segregation of CRF immunoreactive neurons in the PaP subcompartment of the nucleus, thus supporting the view of Pelletier et al. (1983), who found the distribution of CRF in the human Pa to be similar to the arrangement of CRF neurons in the rat Pa. In the rat CRF-immunoreactive neurons are largely confined to the medial parvicellular subcompartment of the

Pa. However, under specific conditions, the peptide is also expressed in posterior and lateral parvicellular parts of the nucleus (Swanson and Simmons, 1989; Swanson et al., 1986).

On the other hand, the present findings differ from conclusions of Raadsheer et al. (1993) who found a dispersed distribution of CRF neurons in the human Pa. In the present study, although confined to the PaP, CRF-positive neurons were present throughout most of the rostrocaudal extent of the Pa. By contrast, Raadsheer et al. (1993) found no CRF reactivity in the nucleus ventral to the fornix in all but one of 13 brains. These discrepancies may be attributed to the greater sensitivity of the free floating immunohistochemical technique and to a short postmortem delay preceding tissue processing in both the present study (less than 12h) and the study of Pelletier et al. (1983) (6h). On the other hand, Raadsheer et al. (1993) used paraffin embedded tissue and a 24h postmortem period. Bearing in mind that in human Pa the general CRF content is significantly higher than in the rat, the pattern of CRF distribution is similar in the human and rat Pa, with the peptide segregated medially in the anterior part of the nucleus and widely dispersed through the caudal Pa. The CRF is widely implicated in stress responses, metabolic regulation and food intake. Recent studies found increases in the number of CRF-positive neurons in the human Pa with aging (Raadsheer et al., 1994). Another report showed co-localization of CRF with nitric oxide synthase in a subgroup of cells in the human Pa and suggested the possible involvement of these neurons in schizophrenia and depression (Bernstein et al., 1998).

In the present study, PaP was also characterized by the segregated population of small NK3-like immunoreactive cells. The present findings describe, for the first time, the distribution of NK3 receptors in the human hypothalamus. NK3 is a member of a G-protein coupled family of receptors that mediate the effects of the tachykinins. Despite the earlier suggestion that NK3 is not expressed in the human brain (Dietl and Palacios, 1990), recent studies have characterized

the human NK3 receptor in the brain and provide evidence for species homologues of the receptor (Buell et al., 1992; for review see Maggi, 1995). Neurokinin receptor antagonists are available and potentially useful in the treatment of pain and emesis (Longmore et al., 1997). Analysis of neuromedin K receptor distribution in the rat nucleus of the solitary tract, dorsal motor nucleus of vagus, as well as many regions in the hypothalamus including Pa has lead to suggestions of the involvement of the NK3 receptor in autonomic function (Ding et al., 1997). The intraventricular injection of NH2-senktide, a synthetic peptide highly selective for NK3 receptor binding, is known to inhibit salt appetite (Massi et al., 1988). Furthermore, intraventricular injection of neuromedin K has been shown to increase blood pressure presumably via the release of vasopressin from the hypothalamus. This release is, supposedly, mediated through neuromedin K receptor activation in the Pa and is associated with central stress responses (Polidori et al., 1989, Cilman and Unger, 1995). The medial parvicellular Pa in the rat is characterized by the presence of hormone releasing neurotransmitters, efferent connections to the median eminence and regulation of the hormonal output from the anterior pituitary (Swanson et al., 1983). The intimate morphological relationship of Pa to the ventricular wall has been documented in the mouse (Barry, 1975) and dog (Leontovich, 1969-1970), and associated with chemical signals, Pa receives from the cerebrospinal fluid. Segregation of CRF and NK3-like positive cells in the PaP in the human Pa points to a similarity between the medial parvicellular Pa in the rat and PaP in the human. The laminar organization of PaP and PaD in the Pa ventrally to the fornix is also reflected in the nucleus above the fornix (Fig. 3). This is important as these two extremities of the nucleus are not continuous, supporting the view that the compartmental organization pattern is a consistent and independent feature of these parts of the Pa.

Identification of the PaPo in the present study is in agreement with previous cytoarchitectonic descriptions of that part of the nucleus (Brochhaus, 1942; Morton, 1969; Hartwig and Wahren, 1982; Braak and Braak, 1992). Like those earlier studies, we found that the cellular composition of PaPo is distinct from that of PaD or PaM and, in contrast to those areas, PaPo contains a specific subset of distinct large neurons (Figs. 5g and 6d) and a large number of small cells as well (Figs. 6d and 7D). Chemoarchitectonically, the PaPo is an amalgam of features found in PaP and PaD. With the exception of SMI32, which revealed large cells in PaPo, but only medium sized cells in the PaP, all chemoarchitectonic markers depicted similar cell types in PaPo as in these more anterior parts of the nucleus. In the rat Pa, the posterior subnuclei presumably influence the activity of autonomic centers in the brainstem and spinal cord and their neurotransmitter content includes dopamine, CRF, AVP or OXY (Saper et al., 1976; Swanson, 1977; Swanson et al., 1981; Swanson and Kuypers, 1980; Armstrong et al., 1980; Sawchenko and Swanson, 1983; Luiten et al., 1985; Cechetto and Saper, 1988). Consistent with this, the present study found abundant CRF and TH (synthetic enzyme that makes tyrosine into L-DOPA) immunoreactivity in the human PaPo. As noted above, the hypothalamic sulcus is a good landmark for the PaPo. Interestingly, Penfield (1929), and more recently Ropper (1993), documented a syndrome of “autonomic storm” characterized by episodes of acute tachycardia, hypertension, hyperthermia, skin vasodilation, shivering, tachypnoea, lacrimation, and pupillary changes in those patients with either a tumor at the level of the foramen of Monro or lesions near the third ventricle. The topographical position of the described tumors correspond to the position of the PaPo, suggesting a possible role of the subnucleus in manifestation of the syndrome and in the regulation of the autonomic nervous system. The current findings suggest similarities between the PaPo in the human and posterior subnuclei in the rat Pa.

Aside from the possible autonomic function of PaPo, there is substantial evidence for the involvement of PaPo with the hypothalamo-hypophyseal pathway, suggested by the presence of large OXY and AVP neurons and neurophysin (NPH)-positive fibers traveling from the area of PaPo in a ventro-lateral direction (Mai et al., 1997). The topographical position of the PaPo, dorso-caudally at the level of the hypothalamic sulcus, corresponds to the site of phylogenetic origin of the Pa (Mai et al., 1997). In contrast, in the rat and many other vertebrates, Pa and the supraoptic nucleus begin as an anlage located in the medial preoptic area. It is not unreasonable to suggest that the morphology of PaPo in the human reflects closer anatomical cohesion between the neuro-endocrine and autonomic relays that are distinctly segregated in the rat Pa.

The present study describes, for the first time, the distribution of non-phosphorylated neurofilament positive neurons in the human Pa as revealed by immunoreactivity for the SMI32 antibody. Previously, the SMI32 antibody has been successfully used as an anatomical marker in the cortex and thalamus in the human (Hof et al., 1995) and in the hypothalamus of the monkey (Petrides, Paxinos, Huang and Pandya, 2000). In the human Pa, small and medium sized SMI32-positive cells and fibers are segregated in the PaP, close to the ventricular wall. Small and large SMI32-immunoreactive neurons are also found to be numerous throughout the posterior Pa. Hof (1992) suggested that the large size of SMI32-positive neurons found in the monkey and human cortex reflects the large distances to their neuronal targets. If this is the case, then the small SMI32-positive neurons identified by this study in the human Pa are possibly restricted to short distance connections, while the large cells send their axons to distant targets. This feature underpins the distinction between the PaPo and the other subcompartments of the nucleus.

The present findings describing the distribution of Cb- and TH-positive neurons in the human Pa complement earlier studies of the distribution of these substances in the nucleus

(Spencer et al., 1985; Li et al., 1988; Sanghera et al., 1995). Our findings largely support the previous report (Sanghera et al., 1995) on the topographic overlap between the Cb- and the TH-positive cells in the human Pa. In contrast to the earlier report, we found apparent differences in cell size between these neuronal populations (Figs. 5d and 5e). This suggests that Cb and TH may be possessed by different subsets of neurons in the human Pa. Furthermore, in the present study TH neurons were present in fewer numbers in the PaM than in the PaD, while Cb-positive cells were robustly expressed in both subdivisions of the nucleus. This observation further supports the distinction between the PaM and PaD. In the rat Pa, Cb positive cells, which are believed to also contain vasopressin and possibly NADPH-diaphorase, are found primarily in the dorsal cap, posterior Pa, medial magnocellular Pa, and in the area surrounding the lateral magnocellular Pa (Alonso et al., 1992; Arai et al., 1993). This distribution is consistent with the present findings from human Pa, where numerous Cb positive neurons are found throughout the magnocellular subcompartments (PaM and PaD) (Fig. 2F) and the PaPo (Fig. 4F).

The present study described the topographical position of the human Pa subnuclei in relation to prominent anatomical hypothalamic landmarks (Fig. 11) including the fornix, the wall of the third ventricle, the anterior commissure and the hypothalamic sulcus. This association may prove useful for identification of the Pa subnuclei in studies that utilize non invasive imaging techniques (Mai et al., 1997). Moreover, present findings will also assist in assessing the consequences of unavoidable injuries arising from vascular or traumatic lesions or complications related to surgery in the region of the third ventricle (Bruce, 1992).

The pathological changes in the human Pa accompanying such principal homeostatic disorders as diabetes, AIDS, depression and Prader-Willi syndrome (Saper and German, 1987; Purba, 1993; Swaab et al., 1993; Guldenaar and Swaab, 1995; Purba et al., 1996; Swaab, 1997; Gabreels et al., 1998, Bernstein et al., 1998; Braverman et al., 1965; Bergeron et al., 1991) are

of great clinical importance because the associated chemo- and cytoarchitectonic alterations may point at the neural mechanisms underlying these illnesses. Also, age-related changes in the neuronal populations of the Pa are of notable potential therapeutic significance, although never well studied. A recent study found a dramatic increase in number of CRF neurons in the human Pa with aging (Raadsheer et al., 1994). The present findings will be useful in assessing the subnuclei-specific chemo- and cytoarchitectonic changes in Pa in pathologies and aging. This in turn may shed more light on the functional specialization of Pa subcompartments in human.

CONCLUSIONS

In this study cyto- and chemoarchitecture was used to comprehensively describe for the first time the subnuclei of the human Pa. Chemoarchitecture was used as *Rosetta Stone* to establish homologues of these subnuclei to those of the rat. The present study also revealed for the first time the presence of NK3 receptors and SMI32-positive neurons and fibers in the human Pa. In the rat, the Pa subnuclei are considered as vital homeostatic relays for the regulation and integration of neuroendocrine and autonomic output. It is likely that jointly the human PaM and PaD, as described in the present study, are homologous to the anterior, medial and lateral magnocellular Pa of the rat. The PaP as described in the present study corresponds to the medial parvicellular subnucleus of the rat Pa, while the PaPo as described in this study is a likely homologue of the posterior subnuclei of the rat Pa. Despite noticeable similarities in the general pattern of chemical distribution between the human and the rat Pa, there are apparent inter-species differences in internal construction of the nucleus that are difficult to circumvent in establishing further homologies.

CHAPTER 3

Distribution of the Neurokinin B Receptor in the Human and Rat Hypothalamus

This chapter describes, for the first time, the distribution of the neurokinin B receptor (NK3) in the human hypothalamus. It also specifies details of NK3 distribution in the rat hypothalamus. The distributions of the receptor in the hypothalami of the two species is then compared and discussed in relation to the hypertensive effect of neurokinin B.

Neurokinin B (NKB), also known as neuromedin K, is a member of the tachykinin (literally - fast acting) family of small, structurally related peptides which share a similar carboxy-terminal sequence (Phe-X-Gly-Leu-MetNH₂) (Erspamer, 1981). Other well known peptides of this family include substance P (SP) and neurokinin A (NKA). In mammals, the tachykinins including NKB are widely distributed and are involved in a variety of physiological functions (Ronnekleiv et al., 1984; Mai et al., 1986; Marksteiner et al., 1992; Helke et al., 1990; Culman, 1995; Longmore et al., 1997). Thus, in the rat and guinea pig tachykinin-containing pathways within the brain contribute to central cardiovascular, autonomic, and neuroendocrine regulation (Jensen, 1991; Marksteiner et al., 1992; Culman, 1995; Nalivaiko et al., 1997; Danzer et al., 1999). For example, injection of NKB peptide into the 3rd ventricle increases blood pressure (Polidori et al., 1989, Takano et al., 1990).

Molecular evidence suggests that the physiological effects of tachykinins are mediated via a specific G-protein-coupled family of receptors, namely, NK1 (moderately selective for SP), NK2 (moderately selective for NKA), and NK3 (moderately selective for NKB) (Helke et al., 1990; Nakanishi, 1991; Maggi, 1995). It has been shown, that the hypertensive effect of

intracerebroventricular injection of NKB peptide is mediated by Neurokinin B receptors (NK3) in the rat hypothalamus (Polidori et al., 1989, Takano et al., 1990; Ding et al., 1999). Because the hypothalamus contains pivotal autonomic and neuroendocrine relays regulating homeostasis and cardiovascular function, it is important to understand the role of NKB in these relays. An important step in such understanding is to reveal the regional distribution of NK3 receptors in the hypothalamus. The regional distribution of NK3 has been examined in the rat and other species using autoradiography (Dietl and Palacios, 1991), *in situ* hybridisation (Buell et al., 1992), and immunohistochemistry (Ding et al., 1996). The most comprehensive description of NK3 distribution in the rat central nervous system was, however, not particularly concerned with details of NK3 distribution in the hypothalamus (Ding et al., 1996). On the other hand, readily available tachykinin agonists and antagonists and their therapeutic potential (Massi et al., 1988; Longmore et al., 1997; Chalwa et al., 1997; Gao and Peet, 1999) accentuate the need to reveal the regional distribution of neurokinin receptors in the human hypothalamus.

The distributions of substance P and the NK1 receptor have been described in the human brain including hypothalamus (Bouras et al., 1986; Mai, et al., 1986; Dietl and Palacios, 1991). However, the observation that only negligible levels of NK3 receptor exist in the human brain and human hypothalamus (Dietl and Palacios, 1991) temporarily dampened enthusiasm about the therapeutic potential of the NK3 agonist (Massi et al., 1988) and antagonists (Longmore et al., 1997; Gao and Peet, 1999). Nevertheless, more recent reports described substantial presence of the NKB peptide and mRNA and the NK3 receptor mRNA in the human brain and particularly in the human hypothalamus, although these studies did not reveal the regional distribution of the receptor (Buell et al., 1992; Chawla, et al., 1997; Danzer et al., 1999). The present study used a novel NK3 receptor antibody (Ding et al., 1996) to reveal the regional

distribution of NK3 in the human hypothalamus and to compare it with the distribution of the receptor in the rat hypothalamus, where the structure/function associations are better studied.

MATERIALS and METHODS

Three adult Wistar rats (two male, one female) were anaesthetised with ketamine (3mg/100g body weight) and perfused with normal saline followed by cold 4% paraformaldehyde in 0.1 M phosphate buffer (pH 7.4). The brains were removed and cryoprotected with (30%) sucrose solution. Three human hypothalami were also used in this study. The human tissue was obtained at necropsy from two male donors (30 and 69 years old) and one female patient (67 y/o) with no recorded history of neurologic or psychiatric illness. The postmortem intervals were 3, 9, and 12 hours, respectively. The hypothalamus was dissected at autopsy and immersed in a fixative containing 4% paraformaldehyde in 0.1 M PB (pH 7.4). The tissue was then placed in 0.1M PB containing 30% sucrose. After the tissue sank, it was frozen at -70°C and cut into serial 50 μm coronal sections with cryotome.

Histology

The sections of the rat brain and human hypothalami were immunohistochemically reacted for the Neurokinin B receptor using an NK3 receptor antibody (kindly donated by Dr. R. Shigemoto). In addition, every second and third section were stained for AChE and Nissl substance, respectively, according to the protocol used by Paxinos and Watson (1986) for the accurate identification of hypothalamic anatomy. The nuclei were identified using atlases of the human (Mai, Assheuer, and Paxinos, 1997) and rat brain (Paxinos and Watson, 1998). The anti-NK3 antibody used in this study is directed against the C-terminal binding portion of NK3 (Ding et al., 1996) encoded by the RsaI fragment of prTKR3 (Shigemoto et al., 1990) (amino acid residues 388-452). The sequences of cDNA and the protein from the rat and the human NK3 (the human protein is missing 10 amino acids in the mid-molecule compared to the rat) were obtained from the www-based PubMed Entrez nucleotide query and PubMed Entrez Genetic bank and when compared, revealed 89% similarity of the whole molecule and of the

carboxyl terminal binding portion of NK3 in these species. The homology of the gene and molecule were also reported by an earlier study (Buell et al., 1992). The specificity of the anti-NK3 antibody was tested by preadsorption with an excess amount of trpE-NK3 fusion protein, and by replacing the primary antibody with normal IgG in the rat (Ding et al., 1996).

Considering the similarity between the C-terminal portion of the rat and human NK3 molecule, the present study confined the antibody specificity test to processing control sections of the human and rat hypothalamic tissue with normal secondary IgG instead of the primary anti-NK3 antibody (Figure 5).

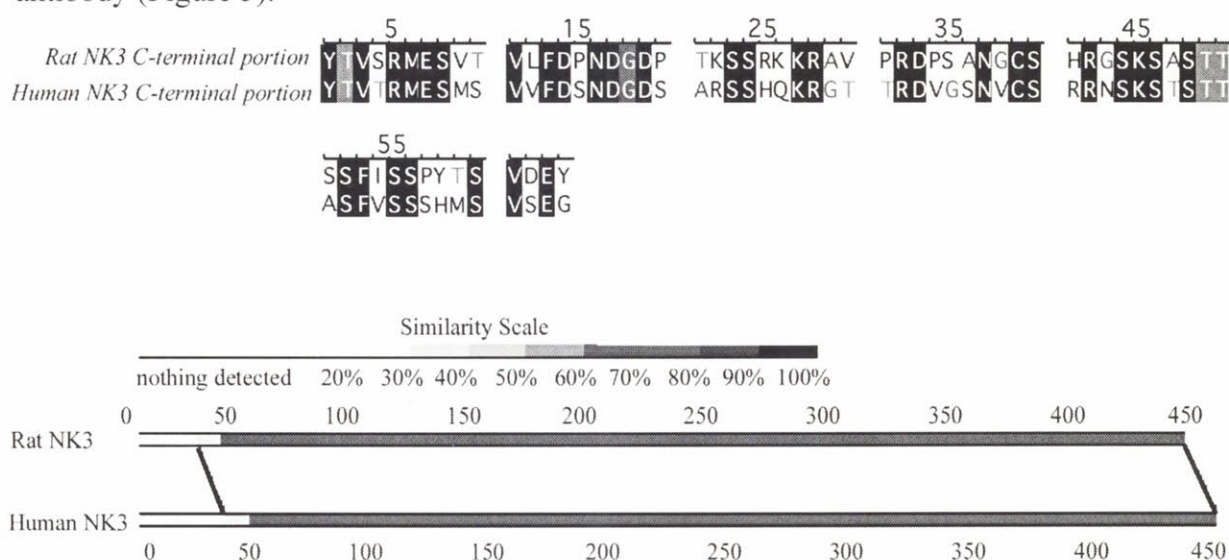


Figure 1. The diagram of nucleotide sequence comparison between the rat and human NK3 receptor demonstrates similarity of the carboxyl-terminal portion (top) and the entire NK3 molecule (bottom) in the two species. The diagram was created with an aid of the PubMed Entrez nucleotide query database (<http://www.ncbi.nlm.nih.gov/htbin-post/Entrez/query/>).

Immunohistochemical procedure. Free-floating sections for immunohistochemistry were incubated with primary antibody in PBH [normal horse serum (2%), Triton X-100 (0.2%) and bovine serum albumin (0.1%, Sigma B-8894) in PB]. The incubation was performed with gentle agitation on an orbital mixer at 4°C for 32 hours. The anti-Neurokinin B Receptor [Rabbit IgG, Ding et al., (1996)] antibody was diluted at 1:5000 for the rat and 1:1000 for

human tissue. Control sections of human and rat hypothalamus were incubated in PBH solution without the primary antibody. The secondary antibody (anti-rabbit IgG (Goat Biotin-SP-conjugated AffiniPure, Jackson ImmunoResearch Laboratories) was diluted at 1: 200 with PBH. Sections were incubated in PBH diluted ExtrAvidin (Sigma E-2886) 1:1,000 in scintillation glass vials on an orbital mixer at room temperature for 1 hour, and washed in 0.1M Tris buffer (pH 7.4) containing 0.004% nickel ammonium sulfate. The final DAB (3,3'-diaminobenzidine) reaction was nickel-enhanced and used a glucose oxidase reaction to generate peroxide. Sections were then mounted on gelatinized slides and cover-slipped. During light microscopic examination, the outlines of NK3 antibody-labeled somata were measured automatically by the DOS based application of the Magellan 3.1 software (Halasz and Tork, 1989) on a microscope driven by an IBM compatible computer.

RESULTS

In the human hypothalamus the highest levels of NK3 immunoreactivity were observed in the paraventricular hypothalamic nucleus (Pa), where, as mentioned in Chapter 1, the NK3

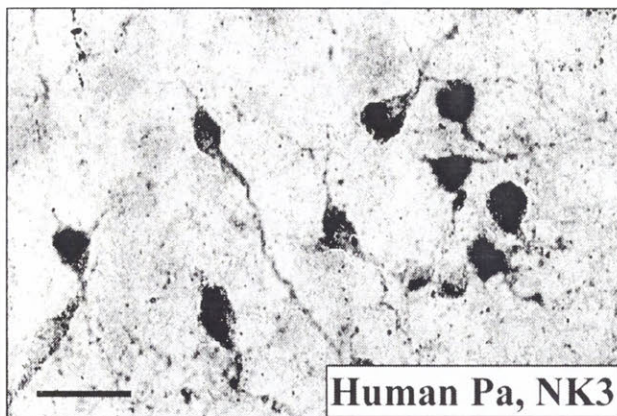


Figure 2 This microphotograph demonstrates small NK3 positive neurons found in the human PaP and PaPo. (scale bar = 25 μ m)

immunoreactivity primarily labeled small bipolar cells (approximately $16.7 \pm 3.3 \mu\text{m}$ diameter somata, N=100) (Figure 2). The NK3 immunoreactive cells were differentially distributed within the nucleus. Thus, the NK3⁺ neurons were found in the parvicellular (Figure 4 B and C) and posterior (Figure 5 A) subnuclei of the human Pa. There was no

NK3-like immunoreactivity observed in the anterior parvicellular, dorsal or magnocellular subnuclei of the Pa. Individual medium sized neurons ($21.8 \pm 3.3 \mu\text{m}$ diameter, N=20) were seen in close proximity to the ventricular wall in the Pa, posterior to the descending column of the fornix, and in fibers located in a narrow layer along the wall of the 3rd ventricle (3V).

Another distinct population of NK3 immunoreactive cells in the human

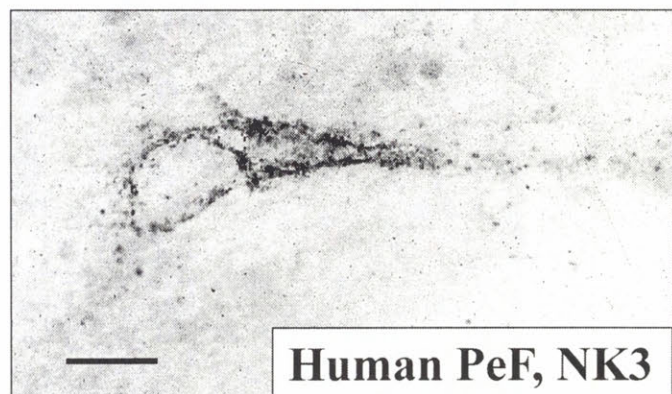


Figure 3 This microphotograph shows large NK3 positive neurons from the human PeF. scale bar=25 μ m

hypothalamus was found in the perifornical nucleus (PeF). These large ($19.2 \pm 4.1 \mu\text{m}$ diameter, N=20) multipolar neurons (Figure 3) were circumferentially arranged around the column of the fornix, but the majority of labeled cells were segregated on the medial side of the fornix (Figure 7).

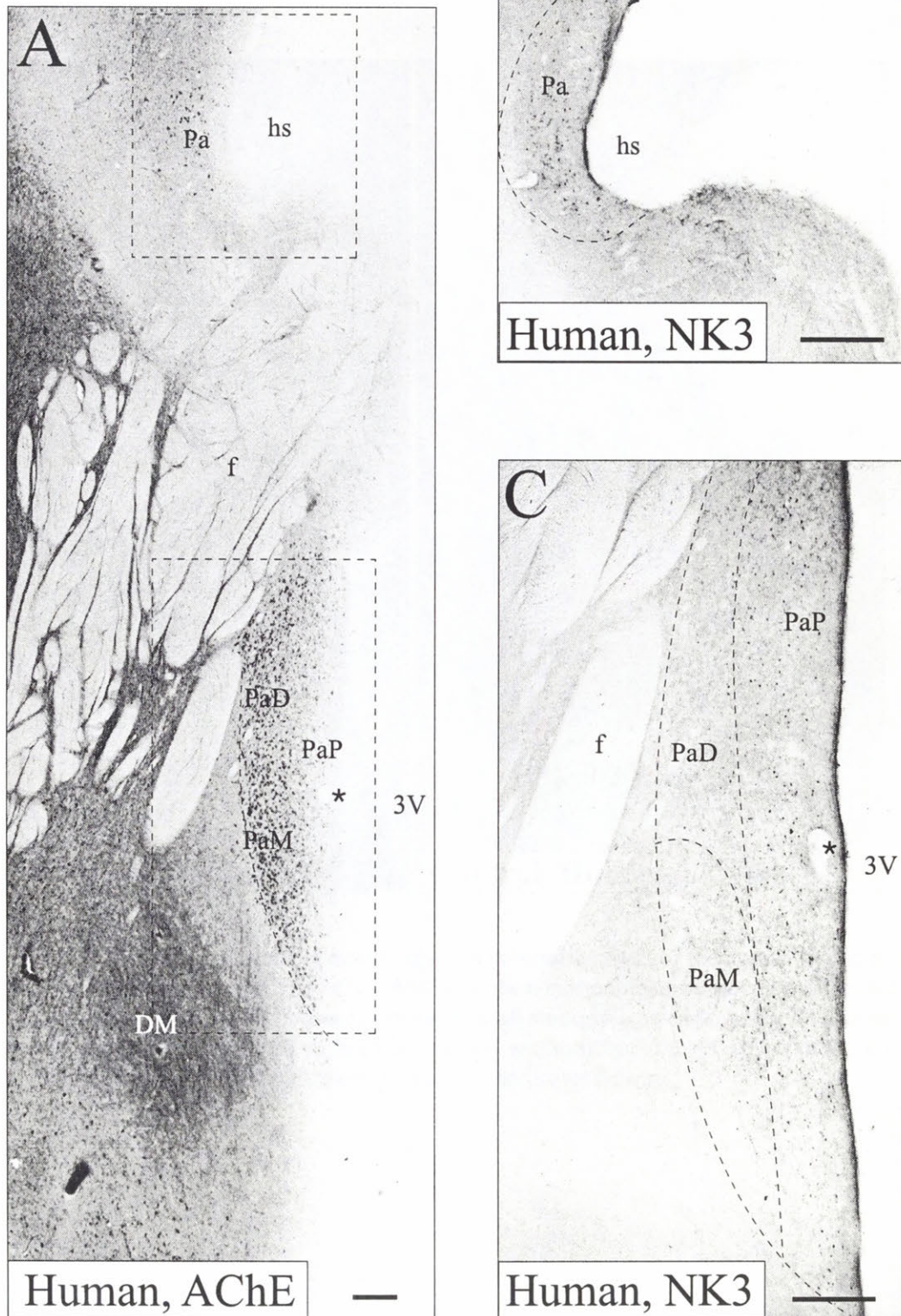


Figure 4. Photographs of adjacent sections from the human hypothalamus. (A) Stained for AChE to demonstrate the topographical boundaries of the Pa subnuclei and surrounding structures. Areas indicated by dashed rectangles in (A) correspond to areas above (B) and below the fornix (C) in the section immediately adjacent to (A) and stained for NK3 to show the distribution of NK3 positive cells with respect to the Pa subnuclei. Arterisk indicates the same blood vessel in (A) and (C). Scale bar indicates 0.5mm.

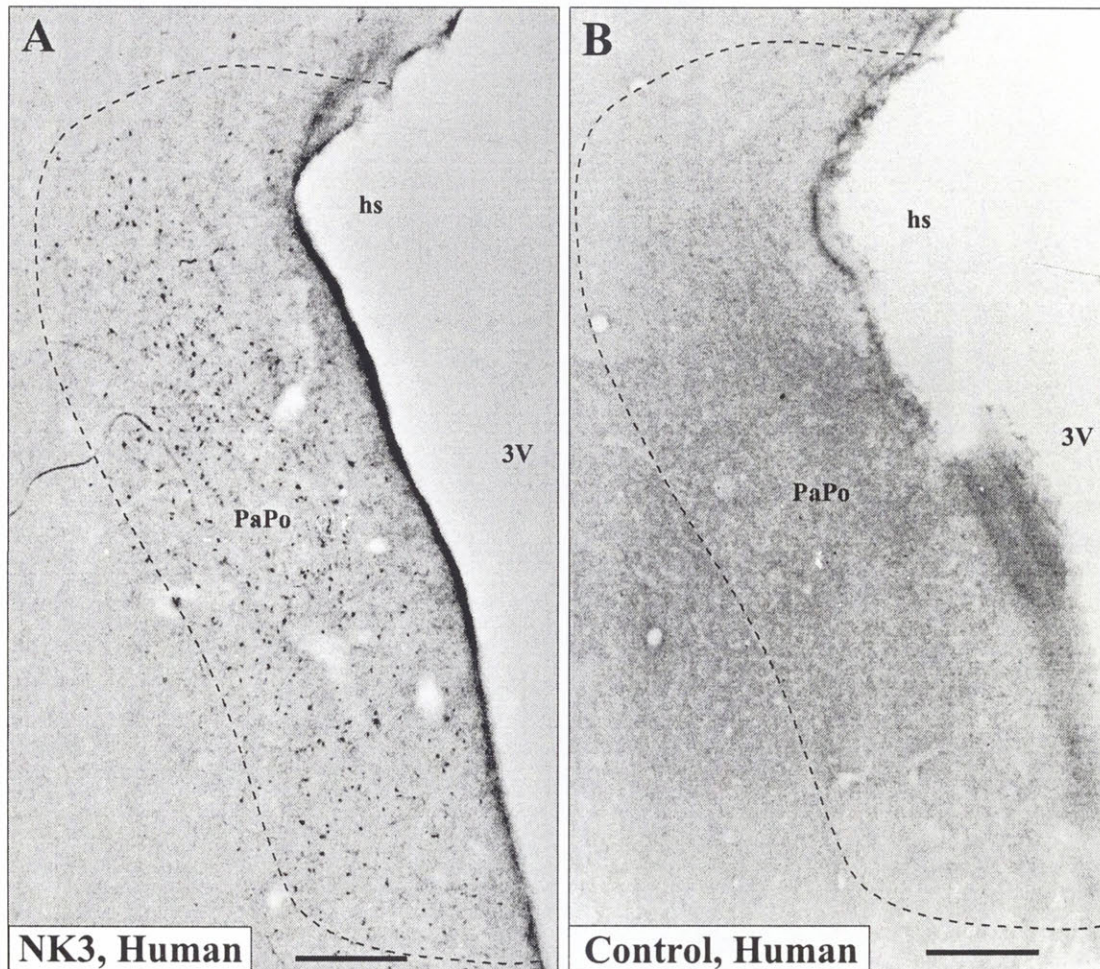


Figure 5. Photomicrographs of nearly adjacent coronal sections of the human hypothalamus through the area of the posterior Pa (PaPo). A) The section immunohistochemically processed with a primary antibody against NK3 showed numerous small strongly labeled neurons. B) The section immunohistochemically processed without the primary antibody but with an excess of the secondary IgG showed no specific observable staining. Scale bar indicates 0.5mm.

In the rat, strong NK3 immunoreactivity was present in the Pa. The strongest NK3 immunoreactivity was found in the large multipolar neurons of the lateral magnocellular Pa

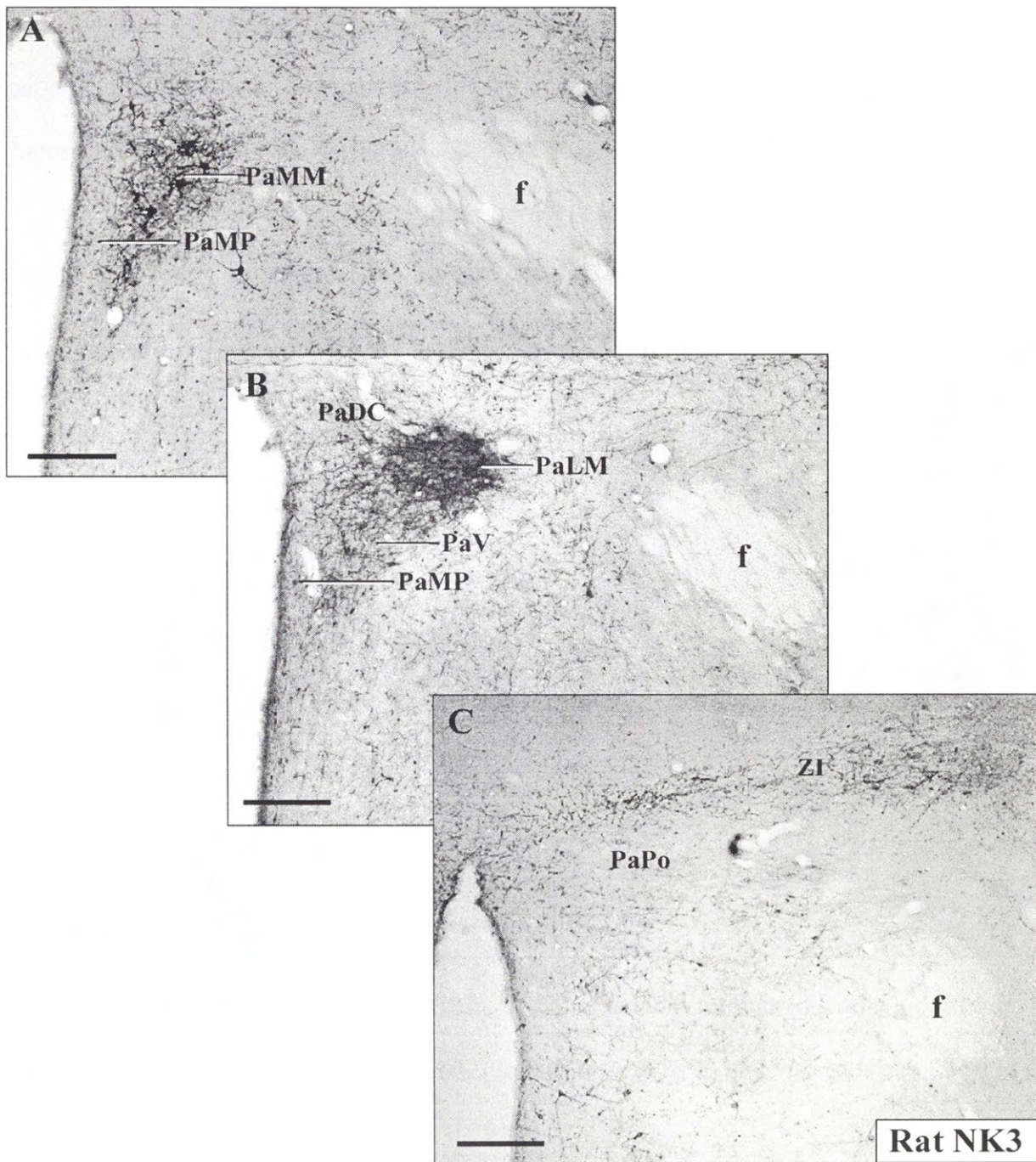


Figure 6. Microphotographs of the coronal sections from three rostro-caudal levels of the rat Pa (A, B, and C respectively) showing differential distribution of the NK3 receptor immunoreactivity in Pa subnuclei. scale bar=0.5 mm

(Figure 6 B), and in large cells of the medial magnocellular Pa (Figure 6A). Some immunoreactive fibers and occasional large immunoreactive neurons were seen in the ventral parvicellular Pa subnucleus (Figure 6B). The dorsal cap, posterior, medial and anterior parvicellular Pa subnuclei contained no NK3 immunoreactivity. The large neurons of the supraoptic nucleus also showed strong NK3 immunoreactivity.

The perifornical nucleus PeF of the rat also contained many large NK3 positive cells and fibers aggregated medial to the fornix similar to what was observed in the human

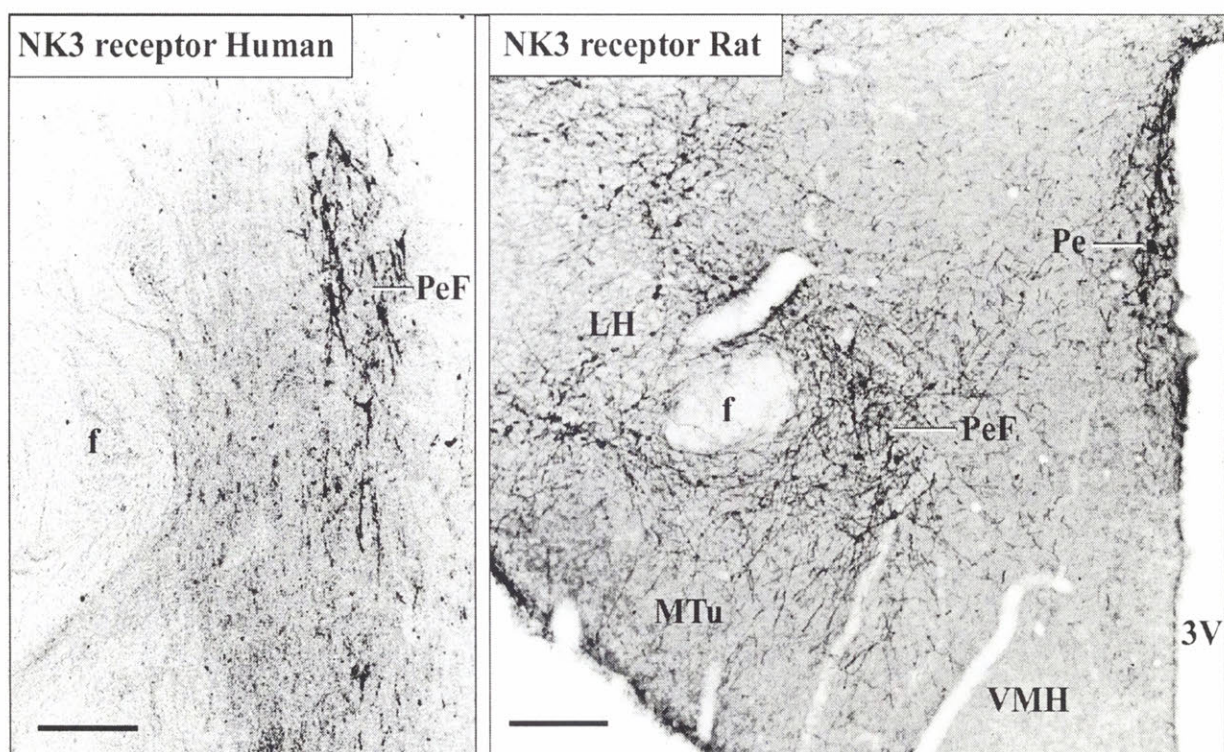


Figure 7. Photomicrographs of corresponding coronal sections through tuberal regions of the rat and human hypothalamus show strong NK3 immunoreactivity in large neurons and fibers of the PeF in both species. Scale bar indicates 0.75mm.

(Figure 7). Although these neurons and fibers were seen encompassing the dorso- and ventromedial boundaries of LH, no labeled neuropil was present in the actual domain of the LH.

Also, NK3 immunoreactivity was strong in numerous neuronal fibers and medium sized cells in the periventricular nucleus (Pe) of the rat hypothalamus (Figure 7).

DISCUSSION

This study described the distribution of the Neurokinin B receptor (NK3) in the hypothalamus of the rat and, for the first time, in the hypothalamus of the human. Immunohistochemistry revealed significantly more NK3 receptors in the human hypothalamus than previously reported with the autoradiographic technique (Dietl and Palacios, 1991). Comparing the localization of NK3 immunoreactivity of the hypothalami of rats and humans revealed a significant degree of similarity in the distribution of the receptor, though the two species are phylogenetically distant. These similarities suggest the phylogenetic conservation of the circuitry underlying physiological effects of neurokinin B in the hypothalamus. Further, the interspecies similarities in the distribution of NK3 can be considered evidence of structural homology between the hypothalami of the most common experimental animal and the human.

In the present study, consistent with a previous report in the rat (Ding et al., 1996), the highest levels of NK3 were seen in the paraventricular nucleus (Pa). The present report further specified the location of the receptor within the rat Pa and showed that NK3 is mostly confined to large neurons of the medial and lateral magnocellular subcompartments of the Pa but also found in the ventral parvicellular Pa.

The Pa in the rat is a major motor relay for the regulation of homeostatic responses (Swanson and Sawchenko, 1983). Stimulation of Pa or NK3 receptors in conscious rats induces cardiovascular, behavioural and endocrine responses (Culman et al., 1995). The cardiovascular responses include increase in blood pressure and heart rate, mesenteric and renal vasoconstriction and are associated with increased sympathoadrenal activity (Culman et al., 1995). The present study found high levels of NK3 in the lateral magnocellular Pa, a subnucleus comprised of large vasopressin containing cells (Schrarrer and Schrarrer, 1940; Vandesande and Dierckx, 1975; Swanson and Kuypers, 1980). This finding is consistent with previous reports

which associated the hypertensive effect of NKB in the hypothalamus with the release of vasopressin (Polidori et al., 1989, Takano et al., 1990; Ding et al., 1996; Ding et al., 1999). The NK3 positive neurons of the medial magnocellular Pa found in the present study are known to contain oxytocin (Schrarrer and Schrarrer, 1940; Vandesande and Dierckx, 1975; Swanson and Kuypers, 1980). There is no direct evidence currently available on possible NKB mediation of oxytocin metabolism in PaMM and it would be interesting to see the condition under which such interaction occurs and its immediate physiological effect. The variety of physiological effects induced by NKB (Culman et al., 1995) certainly suggests the possibility of such an interaction.

The present study also describes NK3 immunoreactive neurons in the ventral parvocellular subnucleus of the rat Pa, which is thought to send direct projections to autonomic centers in the spinal cord and brainstem (Swanson, 1977; Swanson and Kuypers, 1980; Cechetto and Saper, 1988). This finding is consistent with reports of NKB induced increase in sympathoadrenal activity and in other autonomic nervous system mediated functions (Culman et al., 1995). This observation suggests that within the Pa, beside endocrine responses, NK3 may also mediate autonomic feedback, or both, considering that integrated homeostatic feedback is characteristic of Pa (Swanson and Sawchenko, 1983).

According to the present findings in the human Pa, the distribution of NK3 immunoreactive neurons was restricted to the PaP and PaPo subnuclei. Unexpectedly, the cell profile of NK3 immunoreactive neurons in the human Pa is different from what would be expected from the rat homologues of NK3 positive Pa neurons. Indeed, the human VAS and OXY containing neurons in the Pa are reportedly large (Dierckx and Vandesande, 1977; Mai, et al., 1997), like the VAS and OXY containing neurons that comprise medial and lateral magnocellular Pa in the rat. On the other hand, the homology of the NK3 positive neurons in the

posterior Pa of the human and the ventral parvocellular Pa in the rat is consistent with Pa subnuclei homologies established in Chapter 1 and further suggests the possibility of autonomic specialization of this cell group in human. In the rat Pa some small neurons were also reported to express VAS under certain conditions (Swanson and Kuypers, 1980; Swanson and Sawchenko, 1983). Similar observation was reported in the human parvocellular Pa neurons (Raadsheer et al., 1993) suggesting a possible mechanism of NKB mediated VAS release in the human Pa and also indicating further integration of the autonomic and endocrine components in humans Pa.

The present study shows similarities in the distribution of NK3 in the human and rat PeF with regard to both the topography and type of cells. The segregation of labeled cells on the medial side of the fornix is consistent with the anatomical boundaries of the perifornical nucleus in both species (Wahren, 1959; Grünthal, 1952; Paxinos and Watson, 1986). In addition, the caudomedial eccentricity of the PeF seen in rat can also be seen in the human consistent with the original description of PeF's "caudomedial center of gravity" (Wahren, 1959). In the rat hypothalamus, the PeF is considered a pressor site because of the dramatic increase in heart rate and blood pressure reported following the stimulation of the rat PeF (Allen and Cechetto, 1992). In the rat, some cells of PeF contain vasopressin and can, therefore, participate in the mechanism of NKB induced hypertension (Ding et al., 1999). Consistent with the notion of intrahypothalamic autonomic and endocrine integration, the cells of PeF were also shown to project directly to the spinal cord, implying importance of these neurons for regulation of the autonomic nervous system (Cechetto and Saper, 1988). In another important development the neurons of the perifornical nucleus were recently shown to contain orexin and melanin-concentrating hormone, the molecules directly implicated in regulation of feeding and arousal (Sakurai et al., 1998; Broberger et al., 1998; Elias et al., 1998). This findings taken in

consideration with the present results further point to the significance of PeF in the regulation of homeostasis and also raise questions about possible involvement of the neuromedin K containing circuitry in regulation of feeding and arousal. Importantly, the present findings reveal chemoarchitectonic evidence of a homology between the PeF in the rat and in the human.

Given the significance of Pa and PeF in the central integration of endocrine and autonomic responses, it is conceivable that the Neurokinin B receptor plays a role in the hypothalamic regulation of these functions in the human Pa and PeF. The similarity in the distribution of NK3 in the rat and human hypothalamus reinforces the notion of the homology of the entire intrahypothalamic NKB related circuitry.

MATERIALS and METHODS

Three adult monkeys (*Macacca mulata*), one female and two males, were anaesthetised with injections of ketamine (30 mg/kg of body weight delivered intramuscular) and atropine (0.82 ml delivered subcutaneously). The animals were perfused with normal saline followed by cold 4% paraformaldehyde in 0.1 M phosphate buffer (pH 7.4). The brains of the monkeys were removed and cryoprotected with (30%) sucrose solution. The brains of three rats were also obtained according to the procedure described in chapter 3. The procurement and processing of human tissue (five brains altogether - three males and two female) has already been described in chapter 2. The hypothalami of all three species were cut coronally on a cryostat at a thickness of 50 μ m. The enzyme- and immunohistochemical procedures used in this experiment were the same as previously described in chapter 2. In this particular study, the sections were alternately stained for Nissl substance, reacted for AChE and immunoreacted for identification of non-phosphorylated neurofilament protein (SMI32) and calbindin-D28k (Cb). The guidelines for the delineation of the rat and monkey MPO subnuclei and MPA were recent neuroanatomical atlases of the rat (Paxinos and Watson, 1998), monkey (Paxinos, Huang and Toga, 2000), as well as a chemoarchitectonic atlas of the rat (Paxinos et al., 1999). The outlines of labeled somata were measured by the Magellan 3.1 software. The reconstruction of MPO (Figure 7) was not based on cell plots like described in chapter 2 but on the outlines of the subnuclei boundaries revealed by chemical markers for SMI32, AChE, Cb and Nissl substance. The individual drawings for each section from all four histochemical markers were displayed in a sequential mode to create and compiled using Adobe Illustrator 8.0 for three-dimensional view of MPO. Correct alignment of the sections was obtained by reference to outlines of the sections. The

stereotaxic grid (Mai et al., 1997) was aligned in according to the position of anatomical landmarks including fornix, anterior commissure, hypothalamic sulcus and the wall of the third ventricle (Figure 7). The subnuclear boundaries revealed by the markers were averaged. Rotation of the image was performed with the *Shear* computation program (Adobe Illustrator 8.0) for 45° to the sagittal axis of midline in the rostro-lateral direction.

RESULTS

The human MPO is an “inverted comma” shaped structure indented laterally by the lateral hypothalamic area (LH) and bulging medially towards the Pa (Figures 1 and 7). The nucleus is embedded into the medial preoptic area (MPA) staying shy of the suprachiasmatic nucleus ventrally or the anterior commissure dorsally. The rostral tip of the nucleus extends to the most rostral hypothalamic levels, where it occupies the area between the suprachiasmatic (SCh) and supraoptic (SO) nuclei. Caudally, the nucleus is delimited by a bundle of axons arching from Pa towards SO. The dorsolateral tip of MPO borders the bed nucleus of the stria terminalis.

Three compartments of the human MPO can be identified on the basis of cytoarchitecture (Figure 7). Given the homologies of at least two of these structures with the components of the rat MPO, the decision had to be made whether the rat nomenclature will be applied to the human, in spite of being topographically inappropriate. On balance the decision was made to retain the rat nomenclature to make the species homologues immediately accessible, rather than follow topographically correct nomenclature. This approach follows the precedent of calling the ventral lateral geniculate nucleus in primates - ventral, although it is really dorsal to the dorsal lateral geniculate nucleus (Paxinos, Huang and Toga, 2000). The medial MPO (MPOM) (located dorsally) is shaped as a lower canine tooth and characterized by a prominent dense population of large ($21.1 \pm 3.5 \mu\text{m}$ somal diameter, N=50) cells (Figures 1 and 2). The round lateral MPO (MPOL) (located ventrally) contains mostly small ($13.5 \pm 1.2 \mu\text{m}$ diameter, N=50) dispersed cells (Figures 1 and 2). The exact boundaries of the MPOL could only be identified by chemoarchitectonic criteria (described below) (Figure 3). Embedded into the ventrolateral surface of MPOL is a small, but prominent, tightly packed tubular group of

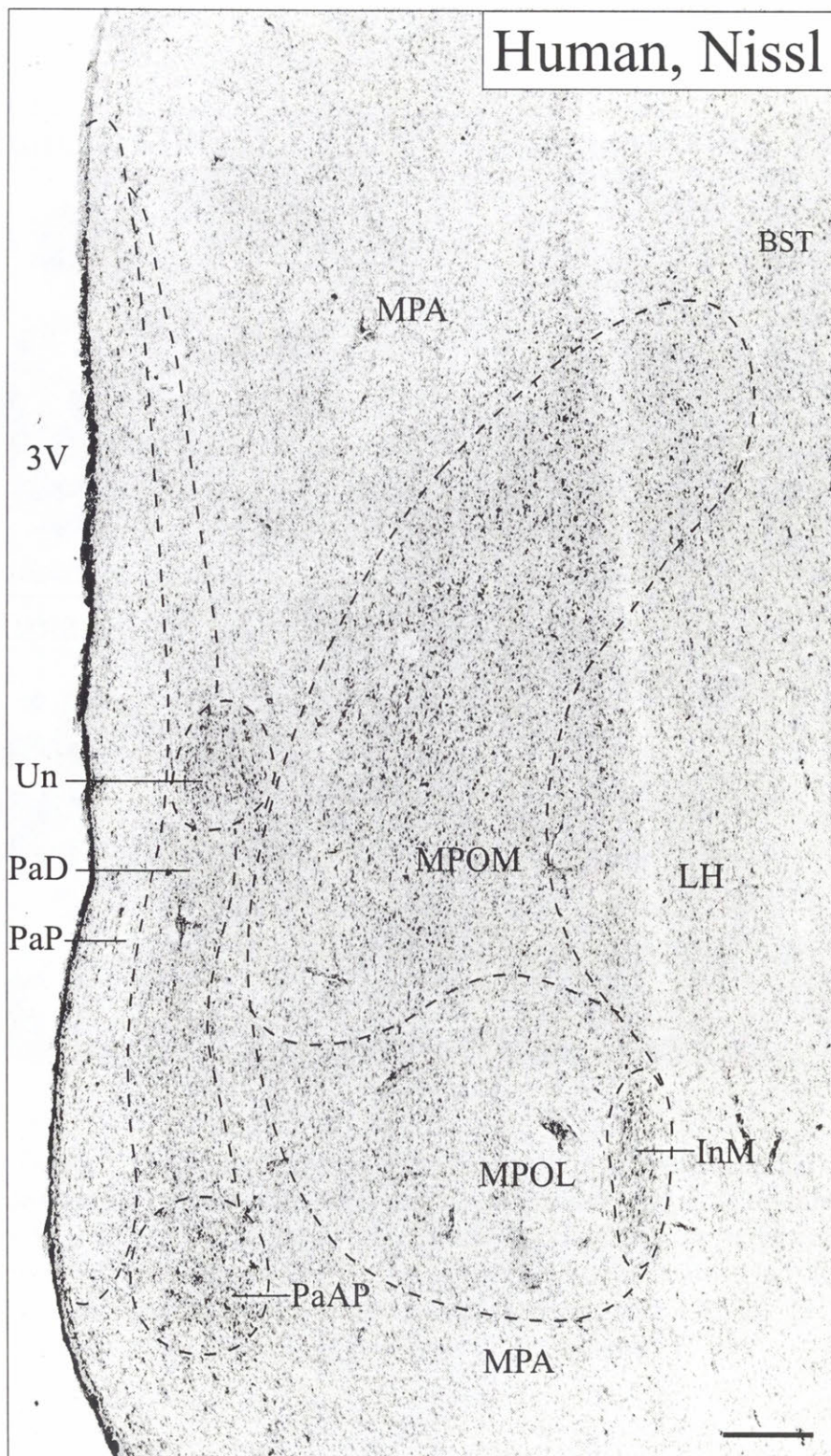


Figure 1. Photomicrographs of a coronal section through the rostral human hypothalamus showing the cytoarchitectonic organization of the human MPO and associated cell groups. Note distinct compact populations of large cells distinguishing MPOM and InM. Scale bar indicates 0.5 mm.

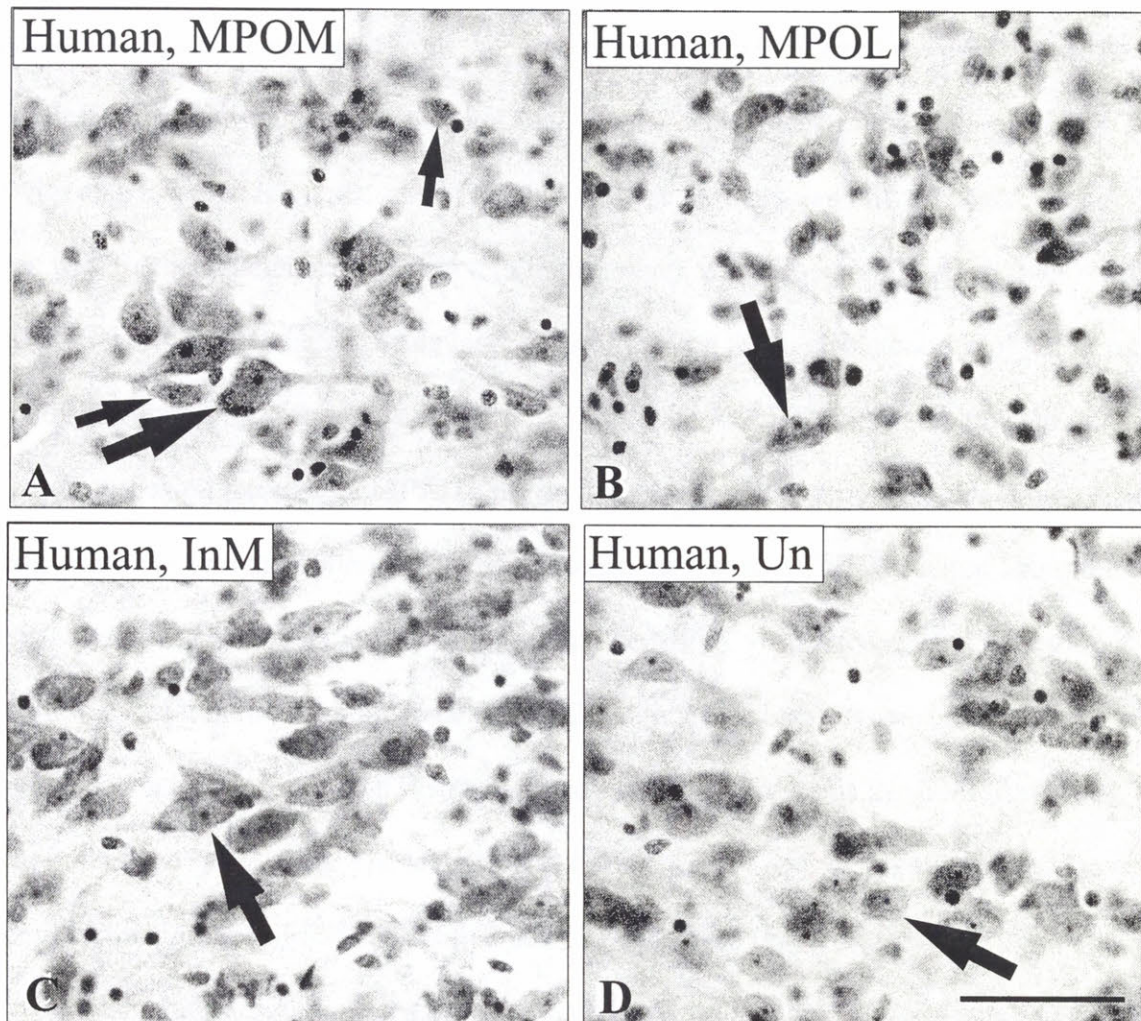


Figure 2. High magnification photomicrographs showing neuronal types in different subcompartments of the human MPO and associated cell groups, as revealed by Nissl substance. A) MPOM is comprised of mostly large, densely packed neurons (large arrow), but also contains some small cells (small arrows); B) Small dispersed bipolar neurons (arrow) characterise MPOL; C) Large tightly packed spindle shaped neurons (arrow) form InM; D) Un is comprised of small tightly packed round neurons (arrow). The scale bar indicates 50 μ m.

large cells ($20.9 \pm 4.2 \mu\text{m}$ diameter, $N=50$) termed the intermediate nucleus (InM) (Brockhaus, 1942; Braak and Braak, 1987; Saper, 1990) (Figures 1 and 2).

Reactivity for AChE was differentially distributed throughout the human anterior hypothalamic region. Thus, apart from the large neurons seen in SO and the dorsal and anterior parvicellular paraventricular subnuclei (PaD and PaAP), which were noted in Chapter 1, AChE reactivity also revealed large neurons of MPOM (Figure 3). Dorsolaterally, this group of cells merges with the bed nucleus of the stria terminalis, which was also strongly labeled by AChE. The MPOL was weakly labeled, while large cells of InM on the ventrolateral tip of MPO were clearly distinguished by strong AChE reactivity. Moderate AChE staining was present in a few small cells dispersed throughout MPA. In the monkey MPO and anterior hypothalamus, AChE staining was weak and did not reveal any cell groups. In the rat AChE was silent about the borders of MPO except for a clear statement about the MPOC – an utterly negative region.

In the rostral human hypothalamus, SMI32 immunoreactivity revealed a prominent round group of small cells and numerous fibers confined to MPOL (Figure 3). No SMI32 staining was present in the InM or MPOM. The lateral MPO of the monkey and rat hypothalamus also harbored distinct groups of SMI32 positive neurons and fibers (Figure 6).

In the human, Cb immunoreactivity revealed a prominent collection of small to medium sized neurons primarily confined to MPOM (Figure 4). These neurons occupied the area between SCh and SO in the most anterior hypothalamic area, defining the rostral extent of MPOM (Figure 5).

Poor Cb neuropil immunoreactivity and the lack of Cb-positive cells defined the boundaries of a round group of small cells intruding onto the anterodorsal Pa, which has previously been termed the uncinate nucleus (Braak and Braak, 1992) (Figure 4). The

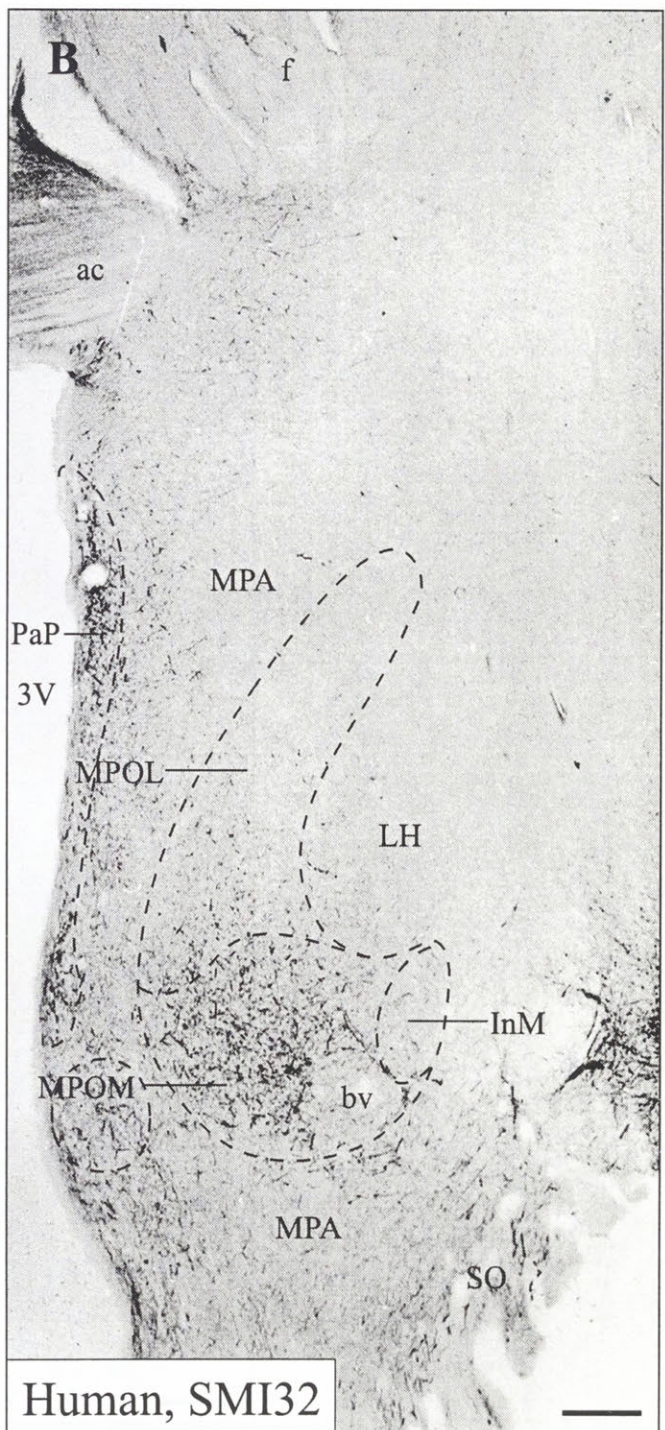
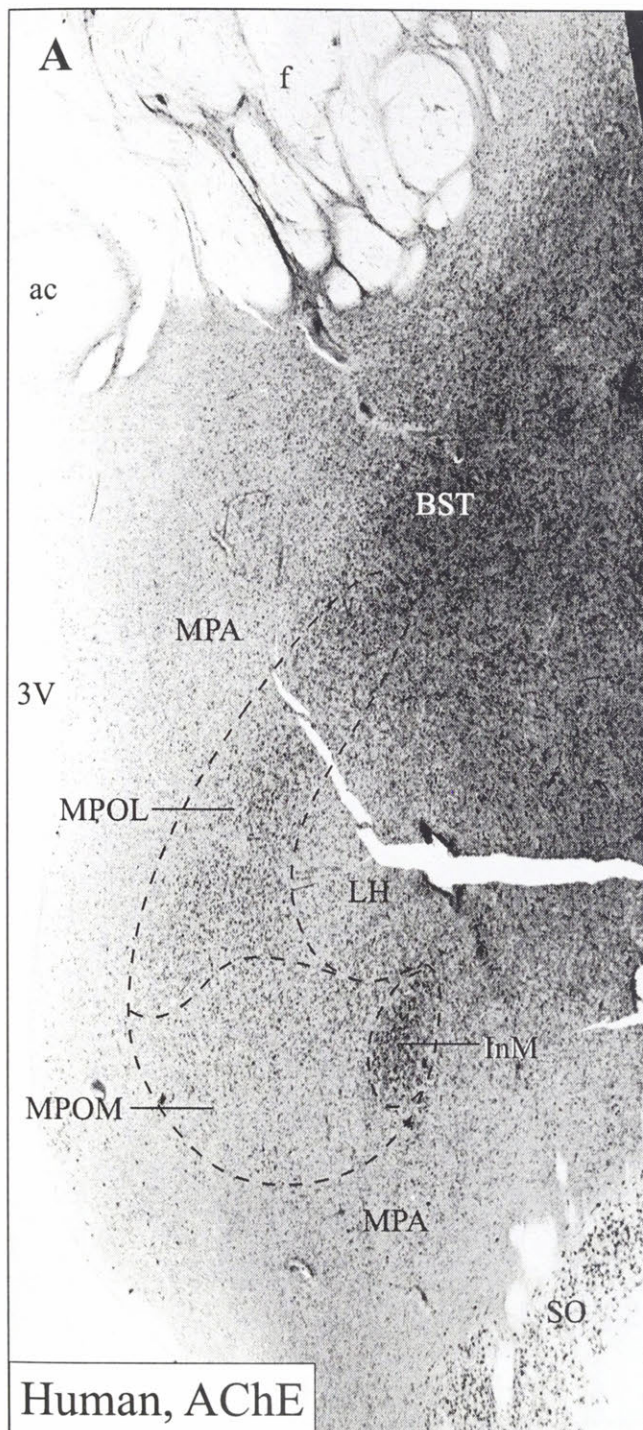


Figure 3. Photomicrographs of virtually adjacent coronal sections through the human anterior hypothalamus processed enzymatically and immunohistochemically for A) AChE and B) SMI32 showing complimentary distribution of these substances and revealing the three constituent subnuclei of the MPO. Scale bar indicates 0.5 mm.

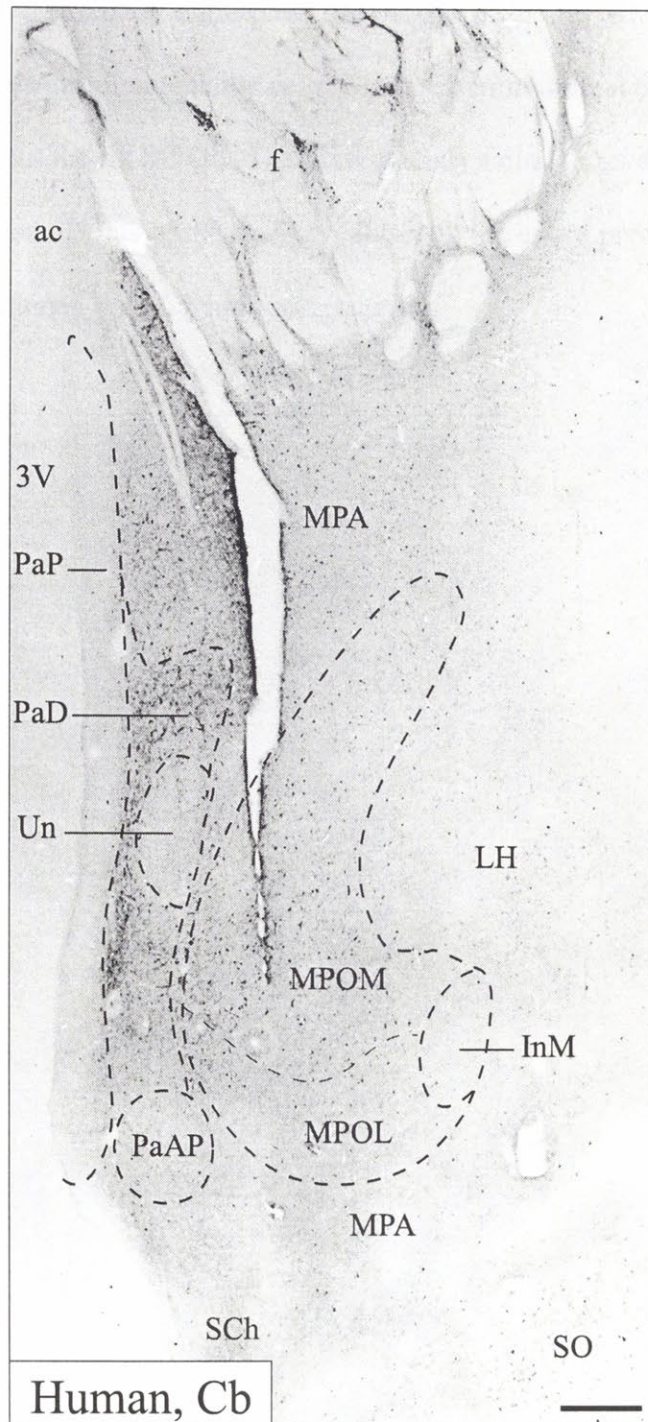


Figure 4. Photomicrograph of a coronal section through the same level of the human anterior hypothalamus as sections in Figure 3 processed immunohistochemically for calbindin. Note how MPOM harbours a dispersed population of large immunoreactive neurons not seen in MPOL or InM. Few small positive cells are seen throughout MPA. Also note distinctly negative Un within abutting laterally the other wise immunoreactive PaD. Scale bar indicates 0.5 mm.

boundaries of the negative Un were made obvious by Cb positive cells of the PaD, which were described in Chapter 1. The lateral boundary of Un is delimited by Cb positive cells of MPOM. In the rat, the central (sexually dimorphic) subnucleus of the rat MPO was harboring a tight group of strongly Cb-immunoreactive cells. Many Cb immunoreactive neurons were also dispersed throughout the rat MPOL. The present study failed to reveal Cb immunoreactive cells in the anterior hypothalamus of the monkey, although the entire preoptic area of the hypothalamus contained light Cb immunoreactivity.

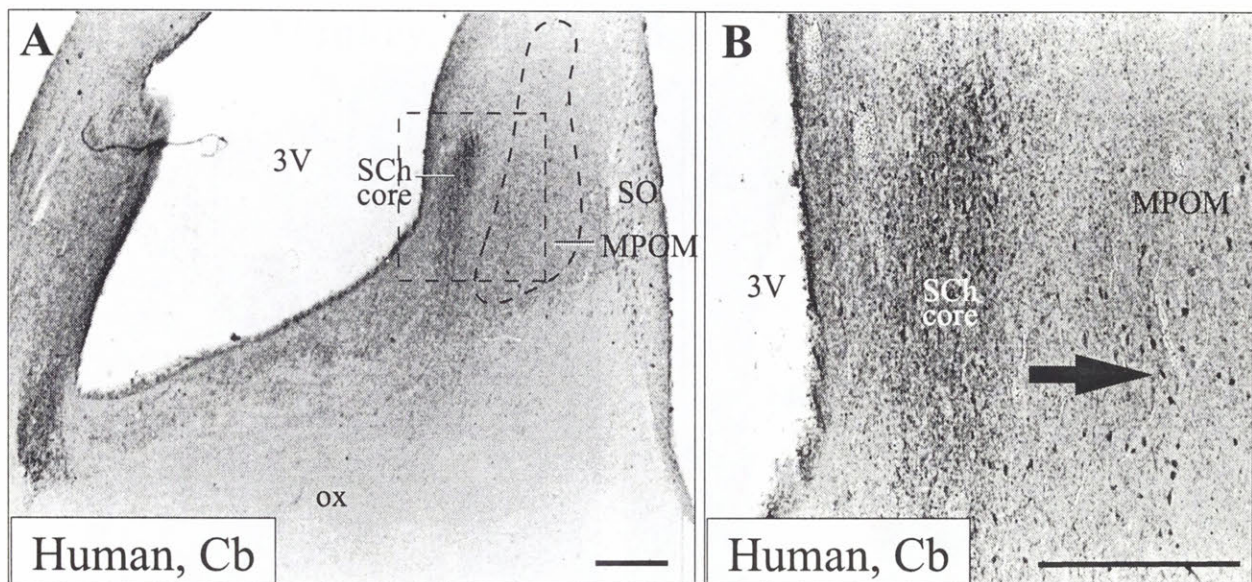


Figure 5. Photomicrographs of a coronal section through the most anterior level of the human hypothalamus processed immunohistochemically for calbindin. Area indicated by rectangle in A) is shown at higher magnification in B). Note large immunoreactive neurons (arrow) characteristic of MPOM. Also note distinct labeling of small cells and pericaria in the core of Sch. Scale bar indicates 1mm.

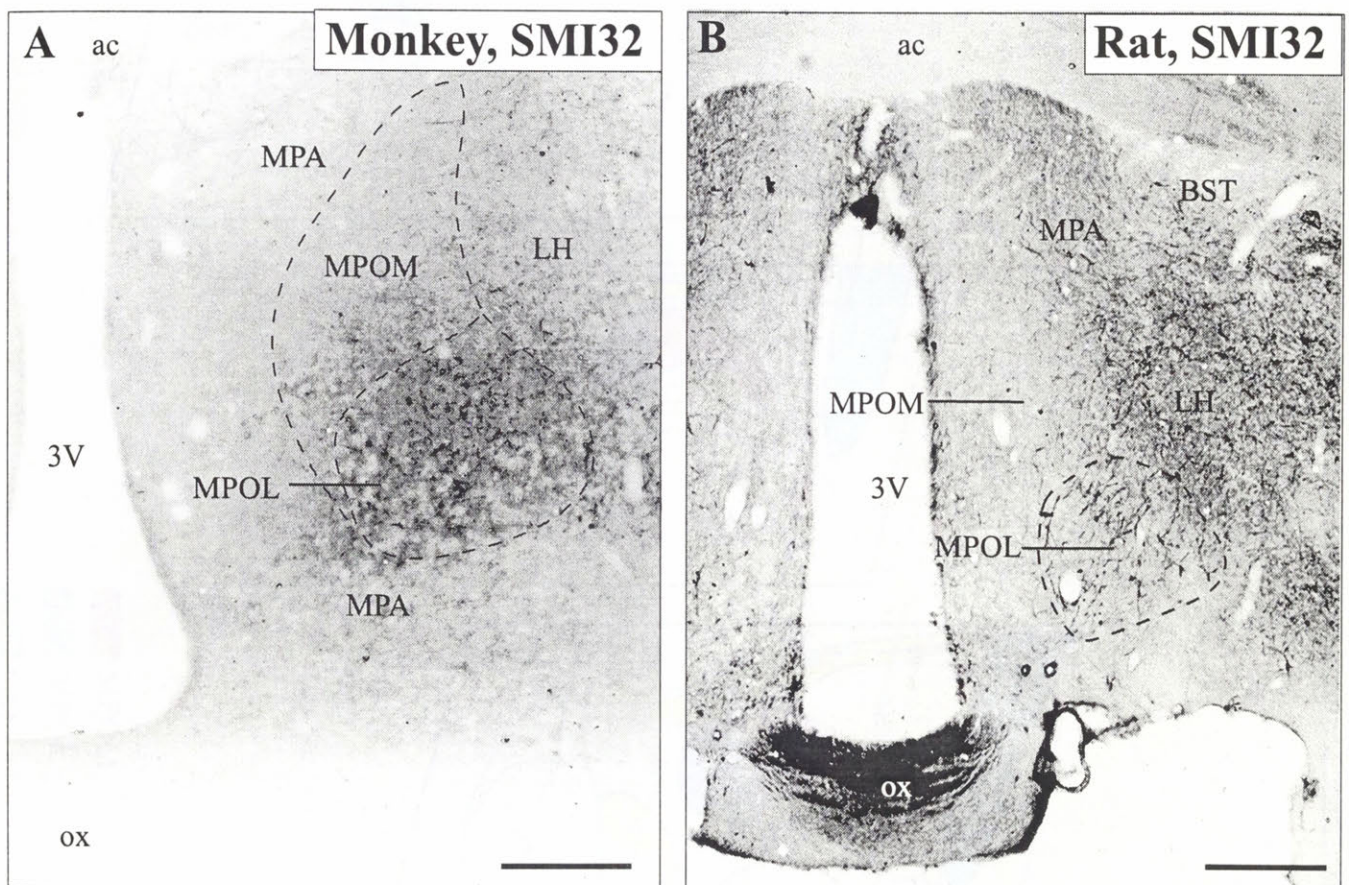


Figure 6. Photomicrographs of the coronal sections from an anterior hypothalamus of the monkey (A) and rat (B) processed immunohistochemically with antibody to SMI32. In both species the lateral subnucleus of the medial preoptic nucleus (MPOL) contains SMI32 immunoreactive neuropil, while the medial MPO (MPOM) is SMI32 negative. Scale bar indicates 1mm (A) 0.5mm (B).

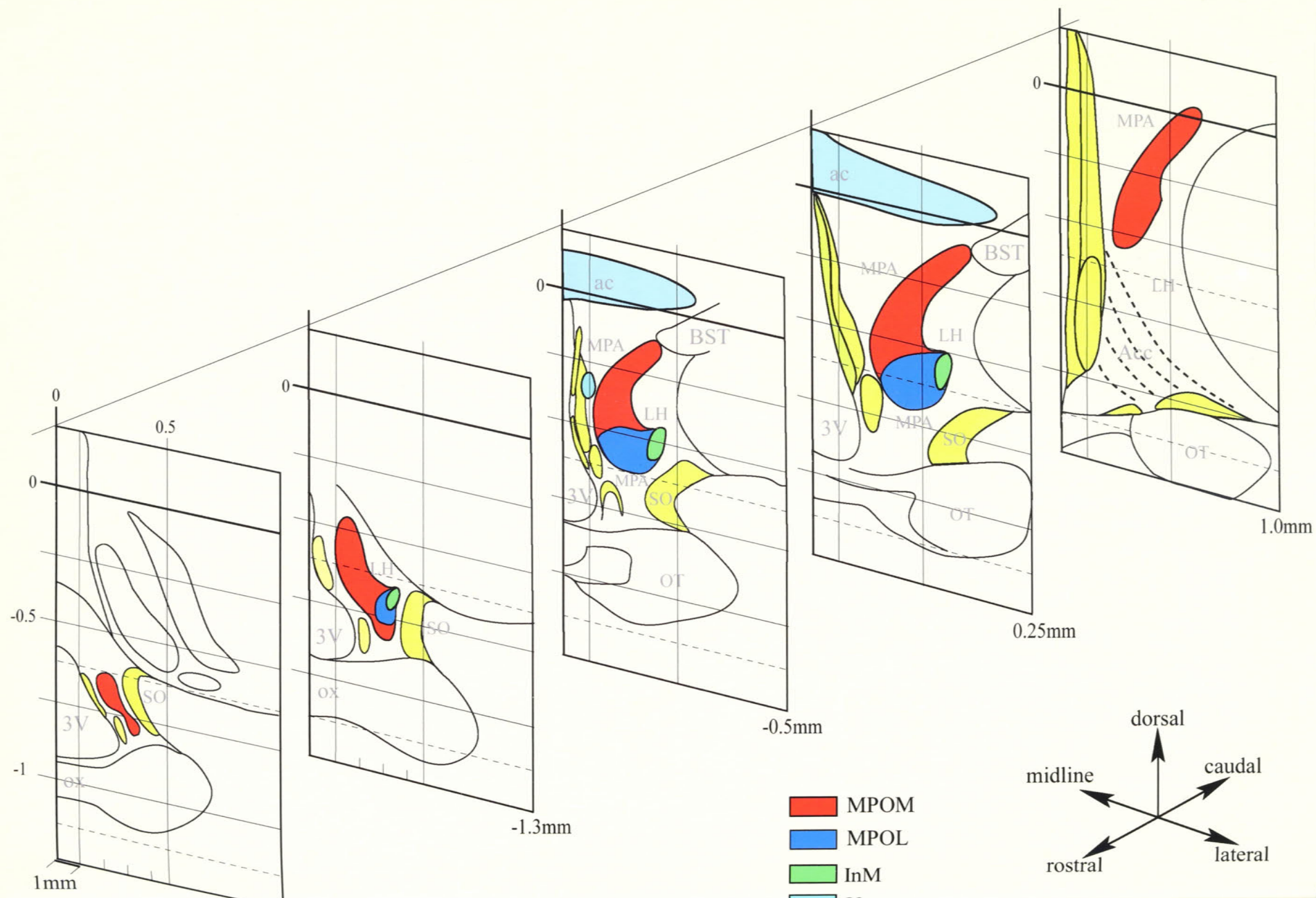


Figure 7 A model of the human MPO showing the subnuclei delineations based on the Magellan 3.1 generated plots of three histochemical markers (AChE; SMI32; Cb). Individual subnuclei are illustrated by different colours. The stereotaxic coordinates were borrowed from (Mai et al., 1997). The third ventricle wall lies to the right..

DISCUSSION

The present study used chemoarchitecture to demonstrate for the first time comprehensively the organization and the boundaries of the medial preoptic nucleus in the human hypothalamus. When the organization of the human MPO was compared to the organization of this nucleus in the monkey and rat substantial similarities became apparent, thus facilitating accurate identification of the subnuclei homologues. The issue of homologies between the sexually dimorphic cell groups in the human and rat has not been resolved in this study. For one, the present study is silent about sexual dimorphism. It was, however, possible to identify the nuclei which others called sexually dimorphic and to establish for the first time their unique chemoarchitecture.

In the present study SMI32 immunoreactivity and AChE staining complimented each other in revealing whole sale the boundaries of the human MPO. The topography and cytoarchitecture of the human MPOM and MPOL revealed by chemoarchitecture in this study generally corresponds to the human hypothalamic nuclei originally described as the prothalamic centralis magnocellularis and parvicellularis, respectively (Brockhaus, 1942). Their renaming in the present study is due to their correspondence with the subnuclei of the rat MPO. Despite some differences, the general topography of the human MPO is very similar to that of the rat MPO. The present findings, however, differ substantially from most common accounts of human MPO boundaries (Clark, 1938; Nauta and Haymaker, 1969; Pavlovits and Zaborszky, 1979) which tend to be exuberant consuming the entire MPA.

In this study the differential distribution of SMI32 and AChE within MPO demonstrated at least three constituent subnuclei of MPO in the human. The cyto- and chemoarchitecture of the human MPOM and MPOL revealed by this study suggest homology

with their namesake, in the rat (Simerly et al., 1984) and monkey (Paxinos, Huang and Toga, 2000). Studies in the rat and guinea pig have shown that MPOL and MPOM differ with respect to their afferent and efferent connections and neurotransmitter content, suggesting a functional difference between the subnuclei (Simerly et al., 1986; Simerly and Swanson, 1988; Rizvi et al., 1992). Although both subnuclei are associated with autonomic and cardiovascular regulation the MPOL is characterized by a more direct effector pathway to the PAG, while MPOM is strongly affiliated with intrahypothalamic autonomic motorelays (Simerly and Swanson, 1988; Rizvi et al., 1992). Both subnuclei were also suggested to be endocrine and behavioral regulatory relays (Simerly and Swanson, 1988). In addition the ventro-lateral position of the MPOL in the human suggests at least topographic similarity with the area recently implicated in the regulation of sleep in the rat (Sherin, et al., 1996). Thus, the differentiation between MPOL and MPOM in the human, indicated by present findings, is likely to have not only structural but also functional relevance.

To discuss further the present results it is necessary to address the confusion in terminology for small cell groups in the human anterior hypothalamus. Firstly, Brockhaus (1942) identified a small group of large cells located ventrolaterally in the anterior hypothalamus and referred to it as intermediate nucleus (InM). Later, Swaab and Fliers (1985) found this cell group to be sexually dimorphic and referred to it as the sexually dimorphic nucleus (SDN). In subsequent study Allen and coworkers (1989) disputed the sexual dimorphism of the cell group addressed by Swaab and Fliers (1985) and renamed it the interstitial nucleus of the anterior hypothalamus 1 (INAH1). That study also identified three more small cell groups in the anterior hypothalamus INAN2, INAH3, INAH4, of which INAH2 and INAH3 were found to be sexually dimorphic. Later descriptions by Saper (1990)

and Braak and Braak (1992) discarded the name INAH1/SDN and returned to the original term, intermediate nucleus. Concurrently, Le Vay (1991), despite admitted ambiguity in defining nuclear boundaries, supported the distinction of INAH3 and INAH4, while failing to replicate the findings of Allen and coworkers regarding sexual dimorphism of so called INAH2. In contrast, Braak and Braak (1992) seemingly referred to both INAH3 and INAH4 collectively as the uncinate nucleus (Un). A recent comparative cytoarchitectonic study in the monkey (Byne, 1998) instead of resolving the confusion added to it by considering the monkey homologue of INAH3 and INAH4 to be the rostral segments of the bed nucleus of stria terminalis. Most of this confusion may have been due to hitherto ill defined boundaries of MPO in cytoarchitectonic material as well as from poor understanding of subcompartmental boundaries of the human MPO.

The present study showed high AChE reactivity exclusively marking most of the cells in the intermediate nucleus (InM) identified by Brockhaus (1942). Resent interest in this cell group has been motivated by its apparent sexual dimorphism. Thus, InM was reported to be more than two times larger in adult males (Swaab and Fliers, 1985) than in females. The nucleus was also reported to contain some thyrotropin-releasing hormone, serotonin and GABA mRNA (Fliers et al., 1994; Swaab et al, 1993; Gao and Moor, 1996). Despite the prominence of InM as a structure, the exact boundaries of the nucleus are poorly differentiated in cytoarchitectonic material, which has been an important shortcoming for the morphometric evaluation of the cell group. This shortcoming, also could have been the reason for conflicting volumetric (Swaab and Fliers, 1985; Allen et al., 1989; LeVay, 1991) and morphometric (Hofman and Swaab, 1988) results with regards to gender and age related changes in the cell group. Clear differentiation of the InM neurons from the surrounding cells, as provided by

relatively simple AChE histochemistry, can offer a more rigorous test of its putative sexual dimorphism and its age related (Swaab, 1992) morphometric changes. Regardless of its alleged sexual dimorphism InM is a prominent feature in this part of the hypothalamus and because it flanks the lateral border of MPOL it is a landmark for this subnucleus.

The present study failed to elucidate any cyto- or chemoarchitectonic evidence of the so-called interstitial nucleus of the anterior hypothalamus 2 (INAH-2) (Allen et al., 1989). This failure is, nevertheless, consistent with the failure of others (Saper, 1990; Braak and Braak, 1992; Young and Stanton, 1994) to find this nucleus. Further, one of the original studies of the human hypothalamus by Herald Brockhaus (1942), known for its staggering consideration of cytoarchitectonic variations, did not depict a cell group resembling in location INAH2.

The present study describes the uncinate nucleus (Un), identified as a tight group of medium sized neurons invading the lateral boundary of the antero-dorsal Pa and bordered laterally by MPOM. The present description of the location of this nucleus is consistent with the original description of the cell group (Braak and Braak, 1992). The boundaries of Un are also confirmed in the present study by the light Cb immunoreactivity and lack of Cb positive cells, which are otherwise abundant in the surrounding Pa and MPOM. This finding and lack of other chemo- or cytoarchitectonic evidence of distinction between INAH4 and INAH3 leads to the conclusion that Un in this study corresponds collectively to INAH4 and INAH3 (Allen et al., 1989; Le Vay, 1991) and to Un as originally described by Braak and Braak (1992). It is also likely, that Young and Stanton (1994) referred to Un as INAH3, while mistaking dorsal Pa for INAH4, which is possible in an absence of reliable chemoarchitectonic markers. On the other hand, it is not inconceivable, that Allen et al., (1989) mistook part of the MPOM for a separate nucleus they referred to as INAH3. Indeed, in the present study MPOM is characterized

cytoarchitectonically by large neurons corresponding to the description of INAH3 as by Allen and coworkers (1989).

In the present study neither InM no Un can be christened as a homologue of the famous MPOC in the rat. but does not contradict the claim of InM sexual dimorphism (Swaab and Fliers, 1985). Indeed, sexual dimorphism has been reported in numerous hypothalamic cell groups and in the anterior commissure (Hofman et al., 1988; Allen and Swaab, 1990). It is important to acknowledge that the phenomenon of sexual dimorphism in the hypothalamic cell groups does not necessarily underlay the differences in sexual behavior, but may reflect general physiological and endocrine differences between sexes.

The sexually dimorphic InM is thus a structural item of unknown function characteristic of the human MPO. Because MPO, on the other hand, has been directly implicated in regulation of sexual behavior in the rat the homology of the MPO subnuclei organization, between species described in this study may facilitate further understanding of sexual behavior in the human.

CHAPTER 5

Topography of the Human and Monkey Dorsomedial Hypothalamic Nucleus

This chapter describes, for the first time with confidence, the boundaries and the topography of the human dorsomedial hypothalamic nucleus (DM) using chemoarchitectonic and comparative criteria. The human and monkey DM display a remarkable degree of similarity in chemoarchitecture and topography strongly implying a high degree of homology between these species.

The dorsomedial hypothalamic nucleus (DM) is thought to play an important role in the regulation of autonomic (Saper et al., 1976; Ricardo and Koh, 1978; Ter Horst and Luiten, 1986; Thompson et al., 1996) and endocrine (Bernardis, 1975; Luiten et al., 1987; Thompson et al., 1996) responses underlying homeostatic control (for review see Bernardis and Bellinger, 1998). Thus, physiological studies, primarily in the rat, strongly implicate DM in regulation of cardiovascular control and stress (Soltis and DiMicco 1990; DiMicco et al., 1996; Soltis et al., 1998), thermoregulation (Kobayashi et al., 1999), food intake and metabolism (Bernardis and Goldman, 1972; Dalton et al., 1981; Greenwood and Dimicco, 1995; Zaia et al., 1997; Elmquist et al, 1998).

Projections of the DM are also suggestive of the involvement of the nucleus in the autonomic control. Thus, direct reciprocal connections of DM with the spinal cord, solitary nucleus and parabrachial nucleus advocate a role for DM in direct mediation of autonomic nervous system activity. Intrahypothalamic connections of the DM suggest an integrative

function of the nucleus in the hypothalamus and include major reciprocal connections with the key autonomic and homeostatic control centers such as the lateral hypothalamus (LH) and ventromedial hypothalamic nucleus (VMH), and a massive efferent pathway to the periventricular hypothalamic zone and particularly to the pivotal autonomic motor relay – the posterior paraventricular hypothalamic nucleus (Pa) (Conrad and Pfaff, 1976; Saper et al., 1976; Luiten and Room, 1980; Ter Horst and Luiten, 1986; Ter Horst and Luiten, 1987; Luiten et al., 1987; Thompson et al., 1996; Thompson and Swanson, 1998). The afferent projections are also suggestive of a role for DM in the regulation of homeostasis. Thus, major afferents to the DM originate in the accumbens nucleus, lateral septal nucleus, parabrachial area (Kita and Oomura, 1982) and suprachiasmatic nucleus (Hoorneman and Buijs, 1982; Buijs et al., 1993). Consequently, in mediating homeostatic responses, DM can relay both emotional and physiological signals.

In the rat, the investigation of the DM was facilitated by a clear anatomical manifestation of the nucleus. Indeed, DM in the rat is a relatively large group of small and medium sized neurons aggregated into at least two subnuclei – the cell dense dorsal and the cell poor ventral compartments (Krieg, 1932). Bleier and Byne (1985) identified a compact part of the nucleus and Paxinos and colleagues (1999) showed that this compact part is conspicuous by its complete lack of Cr immunoreactivity in an otherwise positive nucleus. Among neuroactive substances suggested for the mediation of DM function, are gamma-aminobutyric acid (GABA) (Soltis and Dimicco, 1990; Okamura et al., 1990; Soltis and Dimicco, 1992; Soltis et al., 1998), neuropeptide Y (NPY) (Chronwall et al., 1985; Kesterton et al., 1997), dopamine (Ruggiero et al., 1984) and serotonin (Beaudet and Descarries, 1979). However, apart from GABA, there is no scientific evidence suggesting

that any of the above mentioned substances can produce any potent physiological or behavioral effects within the DM.

In contrast to the rat, the human DM is very vaguely defined cytoarchitectonically, because the nucleus greatly resembles the surrounding hypothalamic tissue, apart from its compact part, which is not seen in every brains. It is not surprising therefore that the human DM boundaries significantly differ from author to author. Thus, the boundaries of the dorsomedial hypothalamic nucleus as described by Wahren (1959) greatly exceed those set on the cell group by Brockhaus (1942), while Dai and colleagues accounted only for the posterior part of DM (Dai et al., 1998). Other studies, using cytoarchitectonic or lipofuscin preparations, provided only approximate boundaries or were not committed to exact boundaries of DM (Saper, 1990; Braak and Braak, 1992). Until now, there have been no reports of distinguishing histochemical markers for the DM in humans. Fiber networks immunoreactive for vasopressin (AVP) and vasoactive intestinal polypeptide reported in the rat DM (Hoorneman and Buijs, 1982) were also observed in the area of DM in the adult human (Dai et al., 1997). However, these fibers were not confined to DM in the human but also occupied the surrounding areas, thereby failing to provide convincing evidence of DM boundaries. A study using Dil in the human found that the intrahypothalamic projections of DM were similar to those of the rat, indicating analogous function of the DM in both species (Dai et al., 1998). However, the lack of a comprehensive method of identifying DM boundaries hinders effective interpretation of their results.

The aim of the present study was (a) to establish unambiguously the borders of the DM in the human and monkey using chemo- and cytoarchitecture and (b) to compare structural organization of the nucleus in primates with that in the rat.

MATERIALS and METHODS

The present chemo- and cytoarchitectonic analysis was based on five adult human and three monkey brains. The source and characteristics of the tissue used was the same as described in chapter 4. Out of all the available sections, this study analysed sections reacted for AChE, Calbindin and for Nissl substance. Other details of the procedures used in this study have already been described in chapter 2.

RESULTS

The boundaries of the dorsomedial nucleus in the human and monkey were revealed by strong AChE enzyme-reactivity (Figures 1 and 2). In both primates, as well as in the rat (Paxinos and Watson, 1998), DM was a rectangular-shaped and obliquely oriented cell group. In the human and monkey, DM was positioned ventral to the paraventricular nucleus (Pa) throughout most of the rostrocaudal extent of the latter (Figures 1 and 2) from the level of anterior commissure rostrally to the most caudal PaPo. The medial boundary of DM is separated from the wall of the 3rd ventricle by a thin cell-poor zone in the human (Figure 1) and monkey (Figure 2), as is the case in the rat (Paxinos and Watson, 1994). Laterally, the nucleus is flanked by various structures throughout its rostrocaudal extent. Thus, at rostral levels it is bordered by the NPH-containing (Mai et al., 1997) fiber bundle streaming between PaM and SO, more caudally it is flanked by the descending column of the fornix and the perifornical nucleus, and finally, posterior to the fornix, the lateral surface of DM is encompassed by the cells of the posterior hypothalamus (Figures 1 and 2).

Cytoarchitectonically, DM in the human and monkey is comprised of small (approximately 10-15 μ m diameter somata) neurons (Figure 3A and B). In both the human and the monkey DM some neurons formed a small, round, compact group situated anteriorly in the nucleus (not shown). In the monkey, however, this compact DM subnucleus was much more prominent than in the human, where the variation in cell density was only slight. At the most posterior levels the human DM was encircled by a thin cell-poor area (Figure 3A and B).

The AChE reactivity marked neuropil, but not somata, in both the human and monkey DM. In the monkey DM, differential distribution of AChE reactivity distinguished between an AChE negative compact DM and an AChE positive diffuse DM (Figure 2A), but this feature was not present in the human DM (Figure 1). Dorsally, the human DM was separated from Pa

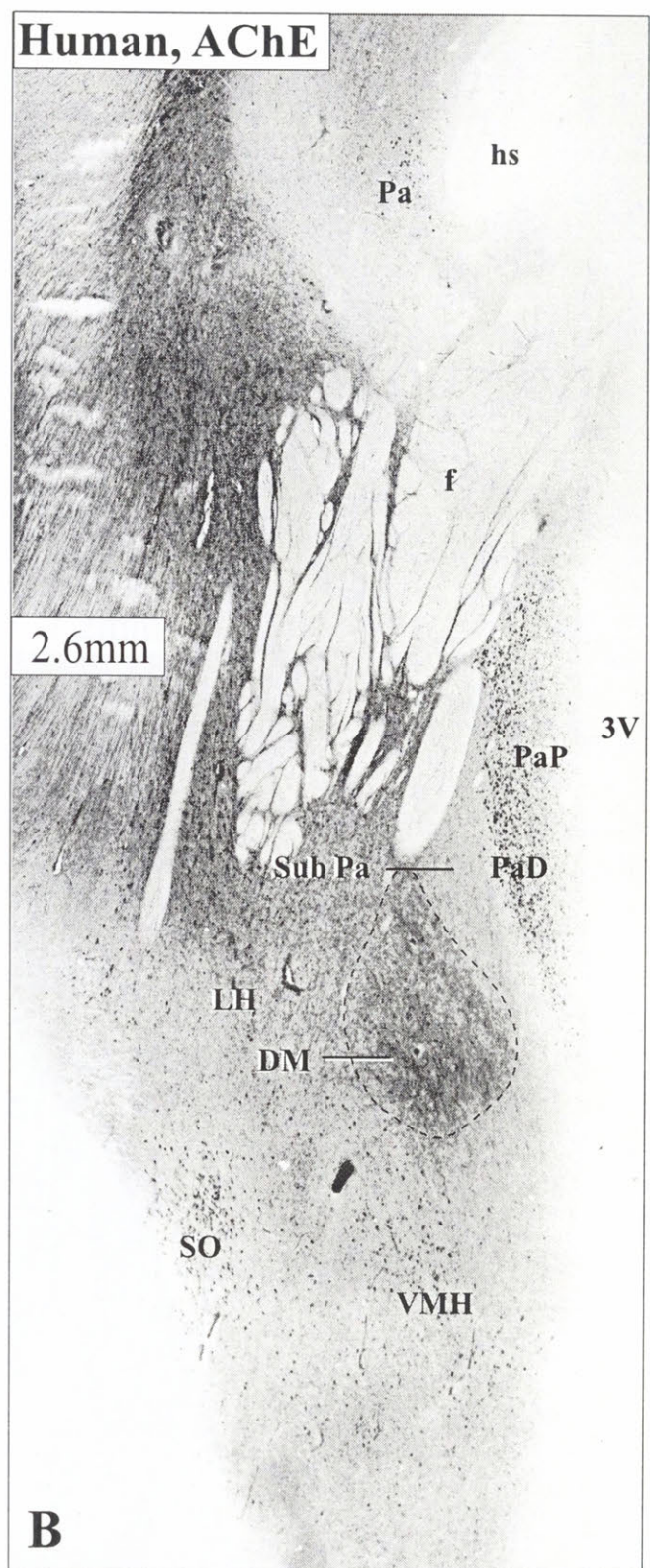
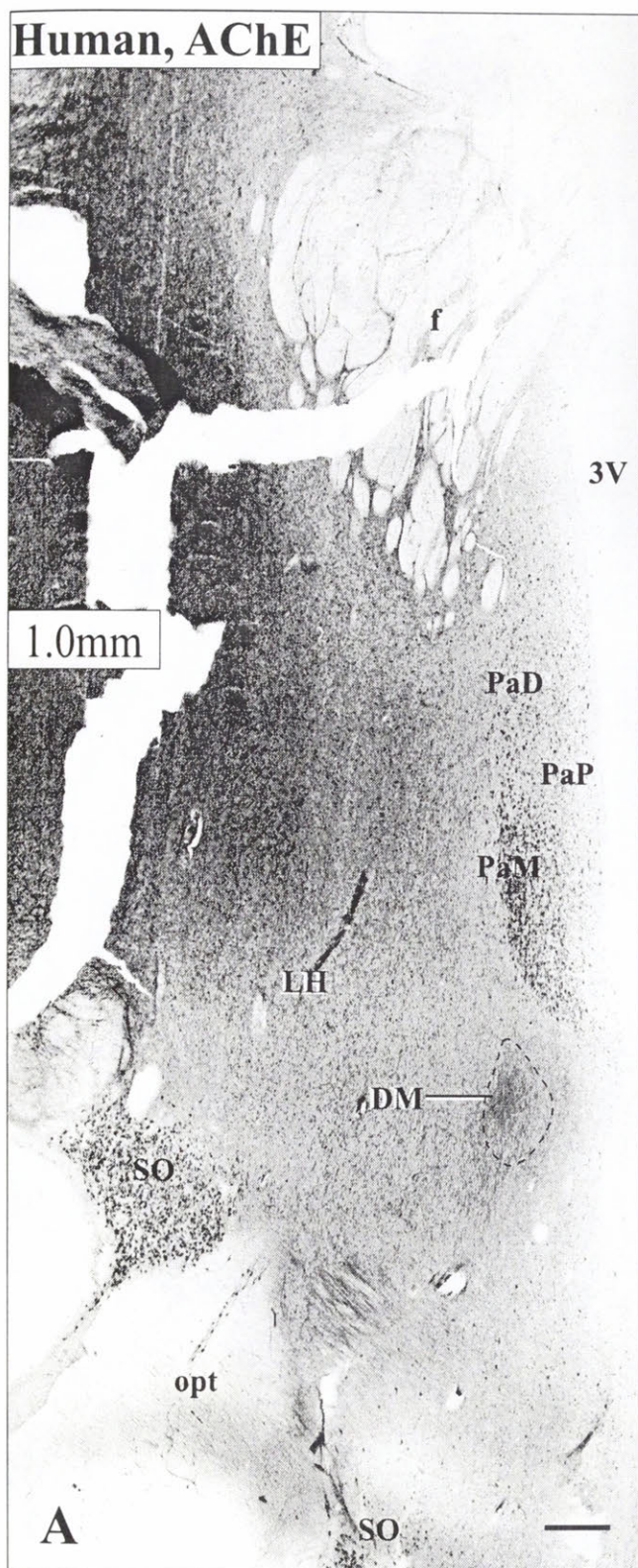
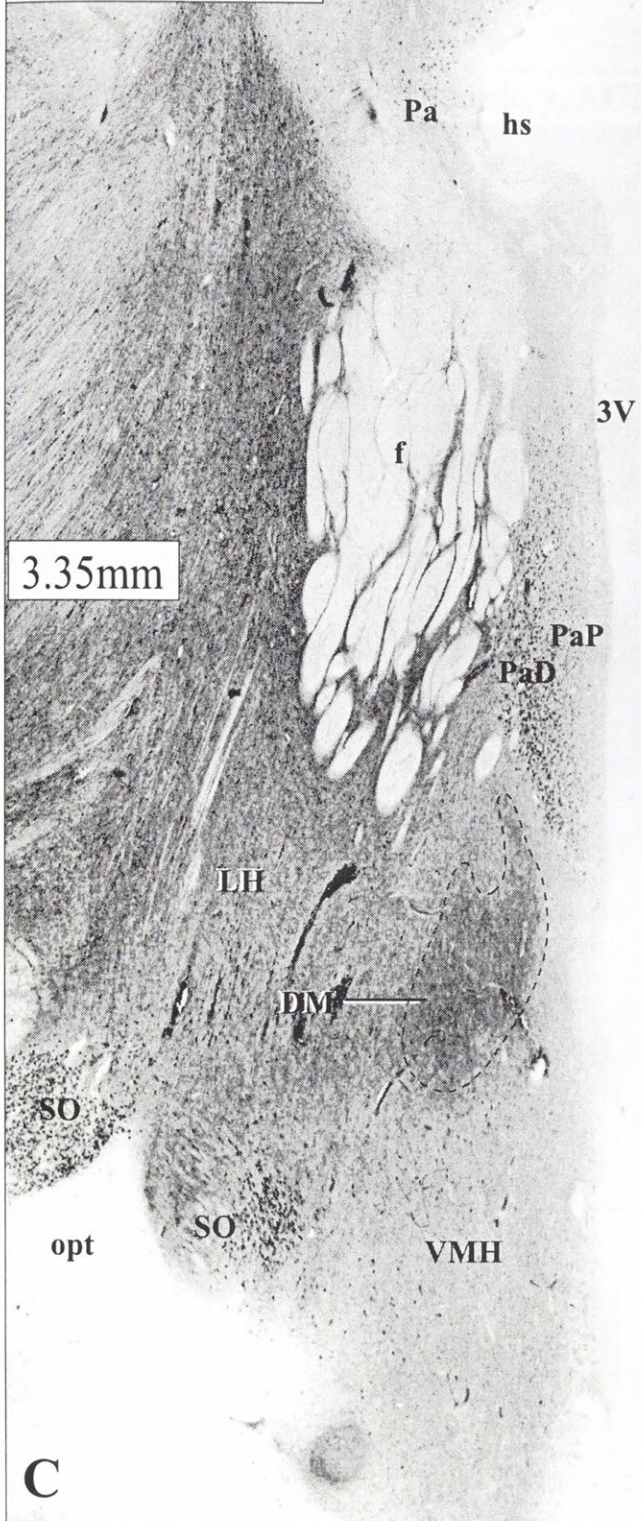
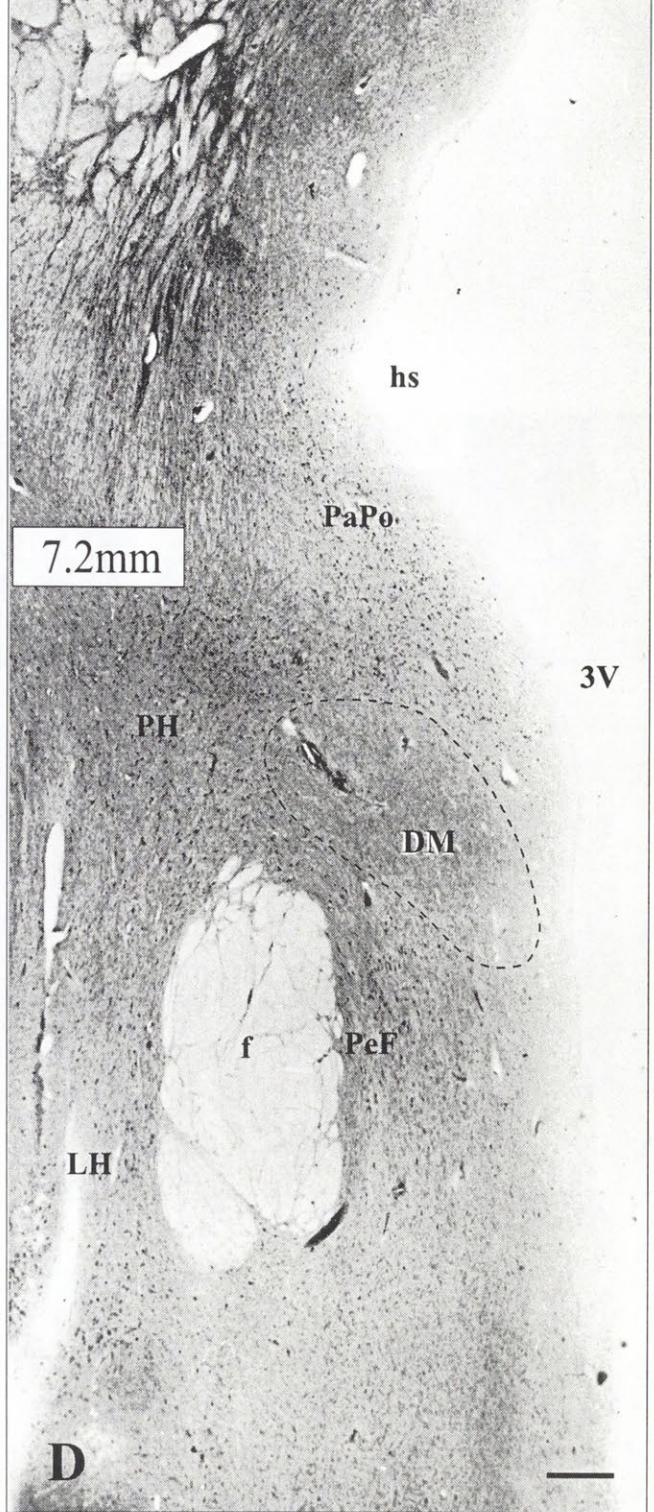


Figure 1. Photomicrographs of a series of consecutive coronal sections stained with acetylcholinesterase demonstrating the boundaries of the DM at four rostro-caudal levels of the human hypothalamus. Stereotaxic coordinates are indicated on the left side of photomicrographs. Note the area between DM and Pa labelled in (B) as Sub Pa by homology with the rat Sub Pa. Scale bar indicates 1mm.

Human, AChE



Human, AChE



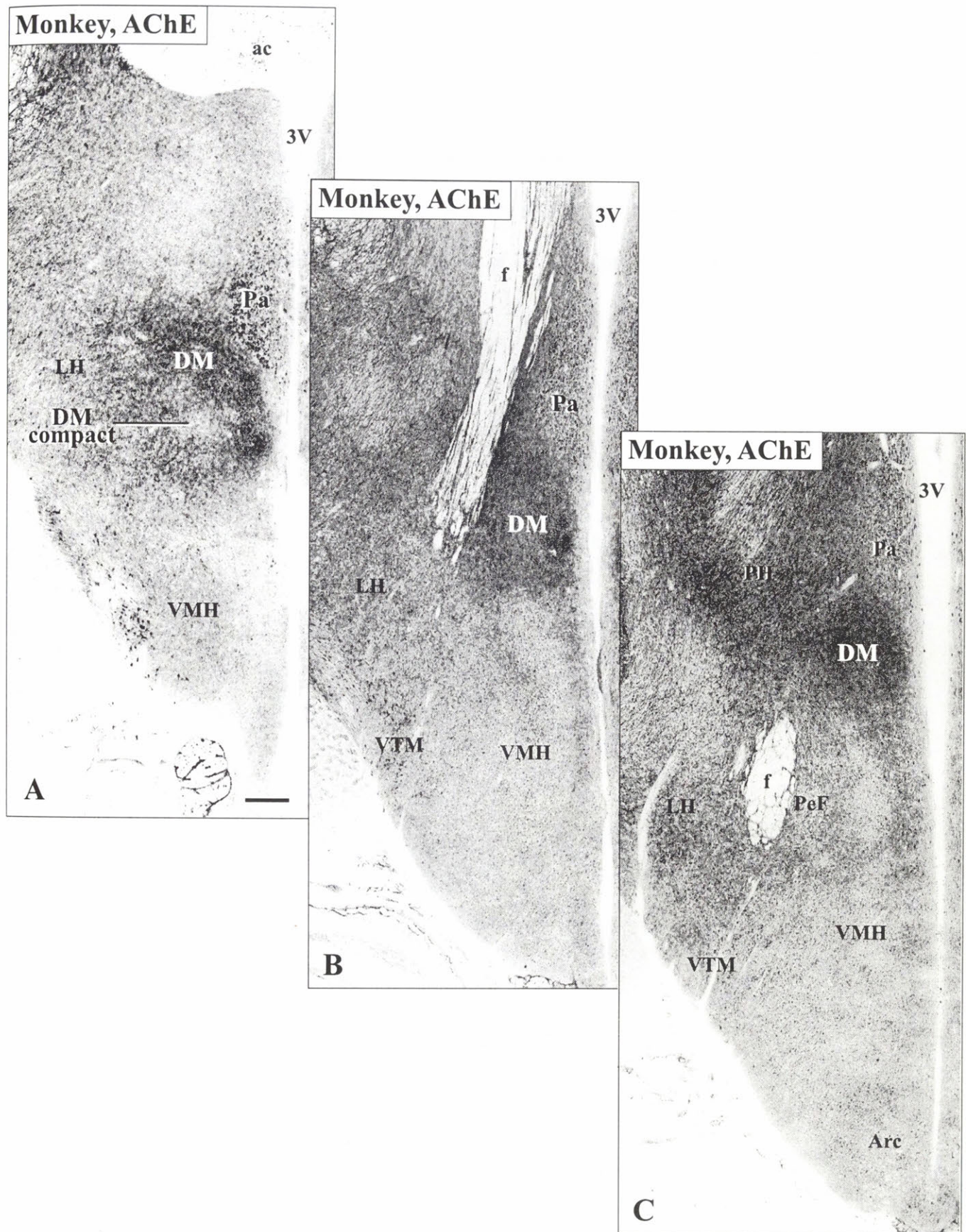


Figure 2. Photomicrographs of coronal sections stained with acetylcholinesterase of the monkey hypothalamus demonstrating the boundaries of the DM at three rostro-caudal levels. Note the absence of the Sub Pa area between DM and Pa. Also note an AChE negative compact DM prominent in the monkey (A) but not in the human (Figure 1). Scale bar indicates 1mm.

by an AChE negative, cell-poor area identified as the Sub-Paraventricular zone (Sub Pa). In contrast, the monkey DM was closely adjacent to Pa.

In the human and monkey, Cr immunoreactivity marked large neurons in the LH and posterior hypothalamus. No Cr reactivity was detected in DM (Figure 3C). Because topographically PH encompasses the posterior part of DM, this pattern of negative staining clearly reveals the boundaries of DM.

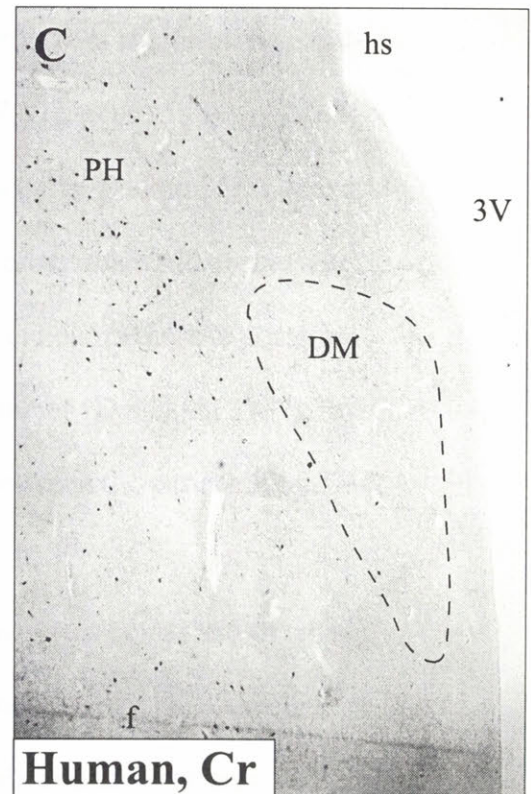
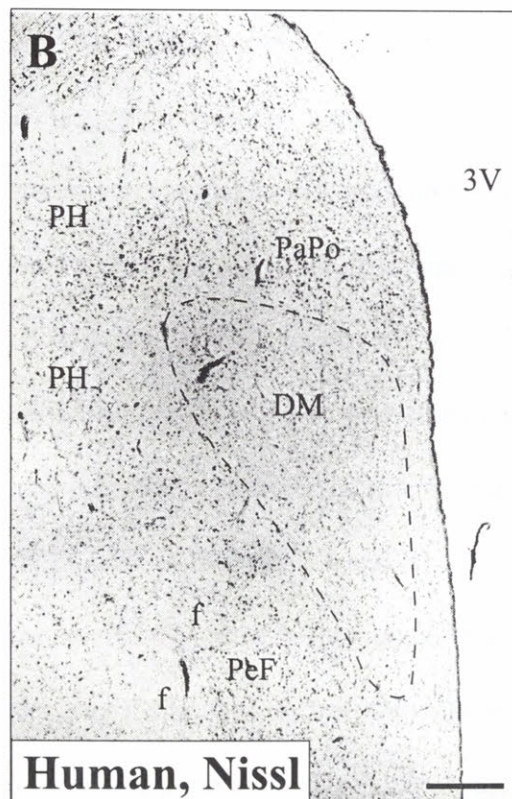
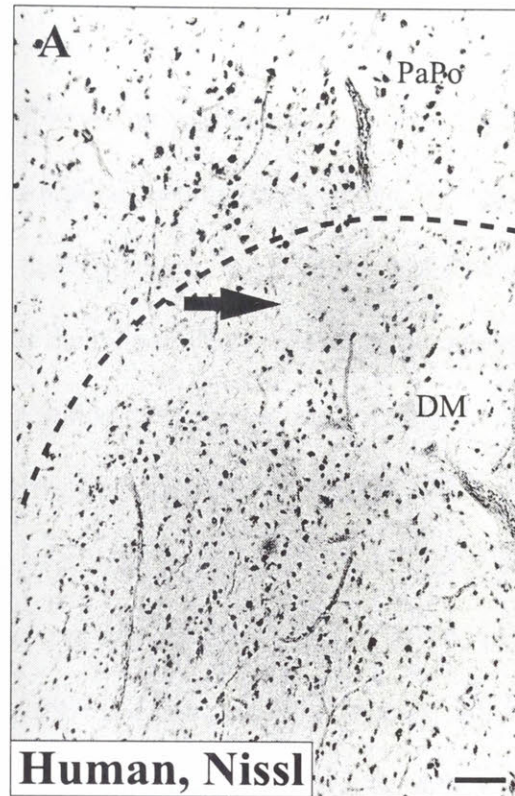


Figure 3. Photomicrographs of coronal sections through the human hypothalamus demonstrating the presence of DM. A) In the section stained for Nissl substance the DM is seen as a population of small (~10-15 μ m) neurons, separated from the magnocellular PaPo by a cell poor zone (arrow). Scale bar indicates 100 μ m. B) and C) The boundaries of posterior DM are shown at low magnification in closely positioned sections stained for (B) Nissl substance and (C) for Cr. C) Note how Cr negativity differentiates DM from the surrounding PH which, in contrast contains numerous large Cr positive neurons. Scale bar indicates 0.5mm.

DISCUSSION

In the present study, positive AChE enzyme-reactivity revealed unambiguously the boundaries of the dorsomedial nucleus (DM) in the human and monkey hypothalamus. Both the human and monkey DM demonstrate similarities in nuclear shape, topography, cytoarchitecture and chemoarchitecture, thereby suggesting homology of DM in these species.

The topographic boundaries of the human DM revealed in the present study by AChE reactivity most appropriately correspond to the boundaries of paired nuclei parvicellularis oralis and parvicellularis dorsomedialis of Brockhaus (1942) and are also in agreement with the previous suggestion of a close topographical relationship between the DM and the fornix (Dai et al., 1997). The present findings, however, differ from recent descriptions of DM borders (Dai et al., 1997; Dai et al., 1998) primarily with respect to the rostral extent of the nucleus. Thus, in the present study, the rostral boundary of DM is depicted at the level of the anterior commissure, unlike in other recent studies, where only the posterior part of DM is apparently considered (Dai et al., 1997; Dai et al., 1998). Also, it is clear from our comparative data that nowhere along the rostrocaudal extent of DM does it border the tuberomammillary nucleus (here called the ventral tuberomammillary nucleus) as recently suggested (Dai et al., 1997). In contrast to another recent claim that the posterior boundary of DM gradually merges with the posterior hypothalamus (Dai et al., 1997), the present findings found a distinct cytoarchitectonic boundary between the parvicellular DM and magnocellular PH and PaPo (Figure 3A and B).

Cytoarchitectonically, DM in the human and monkey was comprised of small neurons not quite reaching the wall of 3V medially and elsewhere wedged between the postero-ventral surface of the paraventricular nucleus, the fornix and the ventromedial hypothalamic nucleus (Figures 1 and 2). Consistent with previous observations (Saper, 1990;

Braak and Braak, 1992) the boundaries of the human DM are ambiguous in cytoarchitectonic preparations. The exception, observed in this study, is the postero-dorsal border of the nucleus where the parvicellular DM is separated from the magnocellular Pa and PH by a cell-poor area (Figure 3A and B). The topography and shape of the human and monkey DM strongly resembles that of the rat DM.

Apart from striking similarities the human and monkey DM, the present study also demonstrated some differences. Thus, the Sub Pa was evident in the human, but not in the monkey hypothalamus (Figure 1B). The present depiction of the Sub Pa zone in the human is consistent with an earlier study which identified this area in the human by virtue of dense vasopressin and vasoactive intestinal polypeptide positive fibers (Dai et al., 1997). In the rat, the cell poor SubPa is thought to play a role in relaying inhibitory pathways to the Pa (Boubaba et al., 1996) one of which is thought to originate in the suprachiasmatic nucleus (Watts, 1991).

On the other hand, the compact DM was less prominent in the human than in the monkey, where this subdivision was also distinguished by negative AChE reactivity. In the rat, the compact, ventral and dorsal DM subdivisions are more prominent than in the monkey and obvious even in cytoarchitectonic preparations (Paxinos and Watson, 1994). Further, Paxinos et al. (1999) found high NADPH levels in the ventral, but not in the dorsal, DM in the rat, providing a chemoarchitectonic criterion for the subdivision. In the human, differences in projections between the dispersed (ventral) and compact (dorsal) DM have been suggested by a postmortem tracing study (Dai, et al., 1998). Nevertheless, the significance of the subdivision is unclear, and in the light of present findings it can be said that the distinction between the subnuclei declines from rat to monkey to human.

Apart from cytoarchitectonic discrepancies, the human and monkey DM also differed from the rat DM in chemoarchitecture. Thus, chemoarchitectural features of the human and monkey DM are similar with respect to AChE reactivity and lack of Cr immunoreactivity, but differ with that for the rat DM, which contains Cr positive neurons and no AChE reactivity.

The AChE staining, nevertheless, provides a relatively simple method of depicting the boundaries of the DM in the human brain, and one which is easily applicable to most postmortem material. The details of this procedure that ensure the best outcome of the AChE reaction were discussed by Saper and German (1986) and in Chapter 1. This finding would facilitate further investigation of this cell group in the human brain.

CHAPTER 6

Human Hypothalamus in Fetal and Perinatal Periods

The hypothalamus is a structural maze of neural relays that integrate fundamental autonomic, endocrine and behavioral responses into an elegant strategy regulating homeostasis and reproduction. These relays are organized into cyto- and chemoarchitectonically distinct nuclei, which also differ with respect to their affiliations and functions. This organization in turn, is to a great extent determined by the differentiation patterns of the hypothalamic nuclei in development (Spatz, 1949; Kühlenbeck and Haymaker, 1949; Grünthal, 1952; Kahle, 1956; Diepen, 1962; Christ, 1969; Keyser, 1979, 1983; Altman and Bayer, 1986). In the rat, learning about these developmental patterns contributed greatly to the understanding of the structural organization of the hypothalamus and also benefited the multi-disciplinary research concerned with affiliations and physiology of the hypothalamic nuclei (Ströer, 1956; Coggeshall, 1964; Hyypä, 1969; Ifft, 1972; Altman and Bayer, 1986; also see Swanson, 1987). For example, the longitudinal subdivision of the hypothalamus into the *midline*, *core* and *lateral* zones was originally depicted in a cytoarchitectonic study of the adult brain (Crosby and Woodburne, 1940), but later, convincingly confirmed in the neurogenic pattern of the developing hypothalamic nuclei (Altman and Bayer, 1986). Further, in the rat this structuro-developmental scheme was validated by chemoarchitectonic and functional evidence (Swanson, 1987). For example, the neurons of the *lateral zone* are generated early in gestation (Altman and Bayer, 1986) and structures formed by these neurons are generally associated with arousal, and autonomic responses in feeding and reproduction, while their connections are dominated by the medial forebrain bundle and the fornix. The second wave of neurogenesis involves neurons of the nuclei of the hypothalamic *core* characterized by limbic afferents from the amygdala and

septum and major intrahypothalamic connections; functionally, these cell groups are thought to mediate autonomic responses in the regulation of homeostasis. The last to be generated are the neurons of the *midline zone*, a zone considered critical for the regulation of biological rhythms, neuroendocrine output and integrated autonomic responses, and which is directly connected with the retina, pituitary and autonomic centers in the brainstem and spinal cord. Clearly, in the rat, the distinct developmental pattern of major hypothalamic nuclei is intimately linked to the structure and function of the hypothalamus.

As in the case of the rat, the human hypothalamus is also strongly implicated in the control of homeostatic responses including regulation of the endocrine and autonomic nervous system, cardiovascular function, thermoregulation, metabolism, and sleep. Neuroactive substances (e.g. VAS, OXY, TH, thyrotropin-releasing hormone, galanin and CRF) associated with hypothalamic function in the rat are also present in the human (Dierickx and Vandesande, 1977; Pelletier et al., 1983; Spencer et al., 1985; Borson-Chazot et al., 1986; Gai et al., 1990; Fliers et al., 1994). Importantly, the human hypothalamus was implicated in homeostatic and developmental disorders including the Sudden Infant Death Syndrome, Prader-Willi syndrome, disturbances in sleep and temperature regulation, diabetes and obesity (Swaab et al., 1993; Swaab, 1997).

Absence of connectional studies, limited functional evidence and difficulty in obtaining adequate quality human brain tissue hindered the correlation of functional attributes with structural elements. Tritiated thymidine autoradiography, used to determine the time of origin of neurons of hypothalamic nuclei in experimental animals (Altman and Bayer, 1986) cannot be used in the human. Further, cell groups in the adult human hypothalamus are less obvious than in those of the rat and are difficult to differentiate. This structural ambiguity may have

been the major reason for confusion in the terminology of the human hypothalamus and posed significant obstacles for comparative studies.

These obstacles were partly overcome by consideration of developing human material where the boundaries of cell groups are better defined than in the adult (His, 1893; LeGros Clark, 1936), and by comparing chemoarchitectonic organization of the developing or adult human hypothalamus with the better studied rat hypothalamus. The former approach, however, was limited to cytoarchitectonic criteria and was not concerned with the dynamics of fetal nuclear differentiation. Human fetal material has at times been considered cursorily in studies focusing either on the adult brain and early embryonic brain material - where cell groups are not yet formed (Gilbert, 1935; Diepen, 1948; Spatz, 1949; Kahle, 1956; Kühlenbek, 1959; Diepen, 1962; Richter, 1965). More recent chemoarchitectonic studies of the human fetal hypothalamus reported on the development of the hypophyseal portal plasma system (Trandafir et al., 1988), CRF containing circuitry (Bugnon et al., 1982), growth hormone releasing hormone (GRH) neurons (Bloch et al., 1984), somatostatin (Ackland et al., 1983), oxytocin and vasopressin (Burford and Robinson, 1982) and neurophysin (Mai et al., 1997). These studies, while very useful in differentiating the developmental dynamics for particular neuronal circuits, were not concerned with the structural development of hypothalamic nuclei. Combining the developmental and chemoarchitectonic approaches into a comprehensive chemoarchitectonic study of the human hypothalamus in fetal development should provide insight into the structural organization in the human hypothalamus.

The present study used as markers of hypothalamic nuclei the antibodies to calbindin (Cb), calretinin (Cr), parvalbumin (Pv), neuropeptide Y (NPY), neurophysin (NPH), as well as substances that exposed some aspects of the synaptogenesis such as GAP43 and SYN. In addition, an antibody directed against a cell surface membrane glycoconjugate, 3-fucosyl-N-

acetyl-lactosamine (FAL or CD15) was used because of its capacity to reveal general topography of the fetal hypothalamus and glial cells including radial glia. In the present study, a nucleus was considered as having attained a level of differentiation by the extent to which it met criteria of similarity with its perinatal form in topography, subnuclear composition, and chemoarchitecture. Identification of human fetal hypothalamic nuclei is expected to facilitate the establishment of nuclear homologies between the rat and the human.

MATERIALS AND METHODS

This study used 31 fetal and 2 postnatal human brains, ranging in development from 9 weeks of gestation (w.g.) to 3 weeks after birth. The aborted fetuses were collected and examined by the departments of Pathology and Neuropathology, H. Heine University, Düsseldorf, between 1989–1998, in accordance with the local Ethical Committee protocols. Procedures for collecting the fetal tissue strictly conformed to the ethical guidelines of the Helsinki Declaration regarding informed consent (British Medical Council, 1964). (Human Experimentation. Code of ethics of the World Medical Association and statement on responsibility in investigations on human subjects. *Br. Med. J.* 2: 177-180. The gestational age of the fetus was initially determined from the last reported menstruation, crown to rump length, and fronto-occipital length (Hinrichsen, 1990, Moore, 1996). The fetal age estimates were further verified by the depth of the matrix layer, body and brain weight. More detailed characteristics of the tissue was previously reported (Mai, et al., 1997).

The postmortem delay for the fetal tissue ranged between 2 hours and 3 days. The brains were extracted from the skull, and fixed in 10% formalin. The brains were then postfixed for 3-5 days in Bouin's solution, dehydrated and embedded in paraffin. All brains were then cut into serial 20 µm thick serial sections and mounted on sequentially marked glass slides. Every 5th section was chosen for the immunohistochemical and histochemical staining. The immunohistochemical procedure used in this study was described previously (Mai, et al., 1993).

Immunohistochemistry

Deparaffinized sections were incubated in 3% H₂O₂ in anhydrous methanol for 30 min to block the endogenous peroxidase activity. After rehydration and rinsing in phosphate-buffered saline (PB), sections were preincubated with non-immune serum diluted 1:100 in

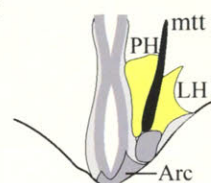
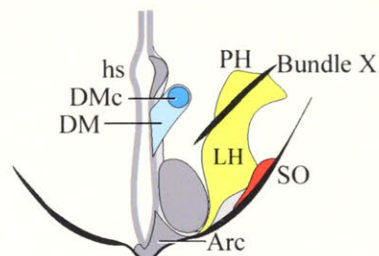
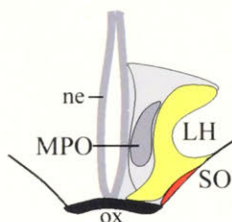
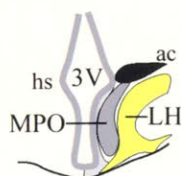
PBTA [phosphate-buffered containing 2% bovine serum albumin (Sigma, Deisenhofen, FRG) and 1% Triton X-100 (Serva, Heidelberg, FRG)] for 1 hour, followed by the primary antibodies diluted as shown in table 1. All antibodies were applied overnight in PBTA at room temperature. Species-specific secondary antibodies conjugated to horseradish peroxidase (Dakopatts, Hamburg, FRG) were applied for 2 hours at room temperature diluted 1:50 to 1:100 in PBTA. The final DAB (3'-3 diaminobenzidine) reaction used 0.3% H₂O₂ solution in PB.

Substances	Type and dilution of the antibody.	Immunized species and source/specificity test .
Neurophysin RB41 (NPH)	Polyclonal; 1:300	Rabbit; (Sofroniev et al., 1981)
Calbindin-D 28K (Cb)	Polyclonal; 1:400	Sheep; (Mai et al., 1991)
Calretinin (Cr)	Monoclonal; 1:500	Mouse; Swant, Bellinzona, CH
Neuropeptide Y (NPY)	Polyclonal; 1:300	Rabbit; (Gaspar et al., 1987)
Parvalbumin (Pv)	Polyclonal; 1:400	Sheep; from P.C. Emson , (Celio & Heizman, 1981)
Synaptophysin (SYN)	Monoclonal; 1:100	Mouse; Boeringer Mannheim
Growth associated protein GAP43	Monoclonal; 1:2000	Mouse; Sigma; Deisenhofen, D
3-fucosyl-N-acetyl-lactosamine-epitop (FAL)	Monoclonal; 1:100	Mouse; (Mai et al., 1991)

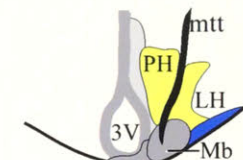
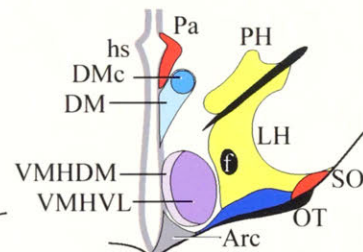
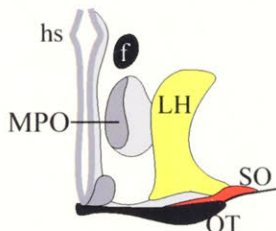
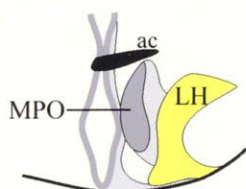
Table 1. The antibodies used for the present study.

Sections reacted with vasopressin antibody, referred to in Figure 14, were available but were not analyzed in this study except for this mention. The description of the anti-AVP antibody can be found in chapter 2.

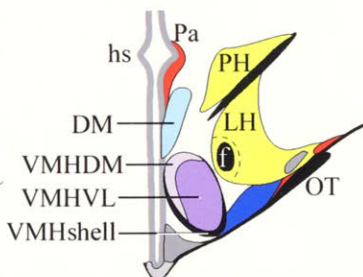
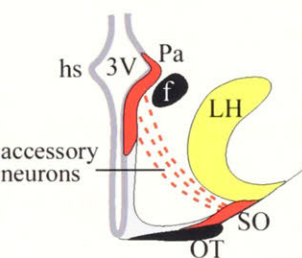
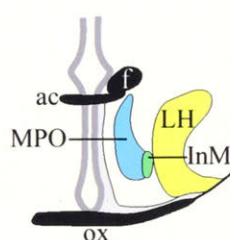
9-10 w.g.



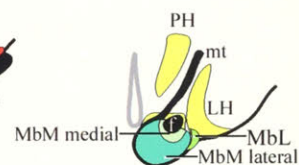
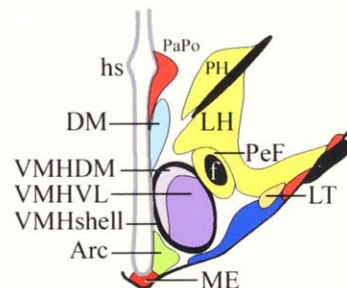
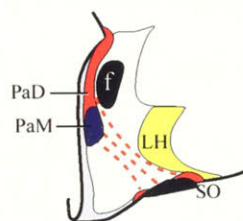
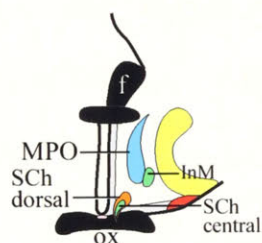
11-14 w.g.



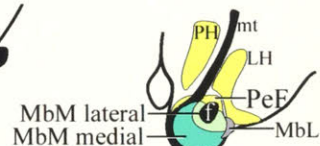
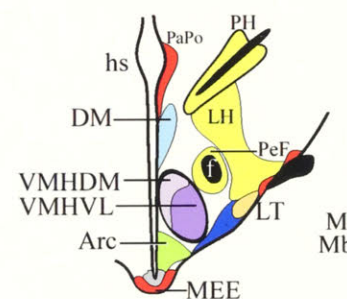
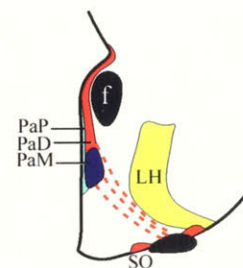
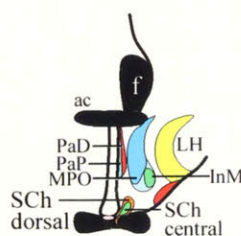
15-17 w.g.



18-23 w.g.



24-32 w.g.



34 w.g.
to birth

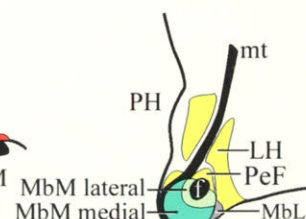
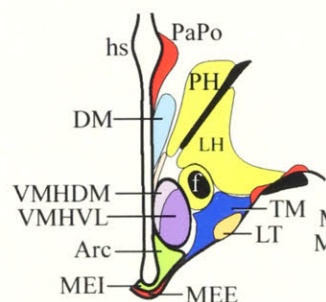
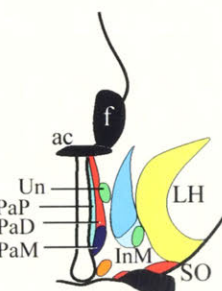
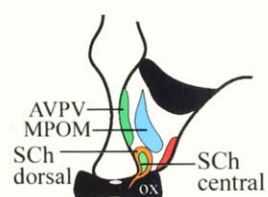


Figure 1. Diagram showing the organization of major cell groups in the developing human hypothalamus depicted at landmark stages of fetal differentiation. Grayscale represents hypothalamic structural entities revealed by cytoarchitecture of the neuroepithelial primordia and transient chemoarchitectonic labeling. Color coding indicates an advanced stage of structural differentiation of a cell group. Please note that these diagrams are not to scale.

RESULTS

Although staging for embryonic human brain development is available (O'Rahilly and Muller, 1994), a clear staging system for the human fetal period has not been established yet. The age, fetal length (crown to rump length – CRL) and fetal brain length (fronto-occipital length – FOL) were used to provide guidelines for morphologic stages; however, morphology, not size, should be the principal criterion for staging (O'Rahilly and Muller, 1994). In the present study, the development of the fetal human hypothalamus is presented in stages designated according to the major morphological changes observed in the hypothalamus. The fetal development of the hypothalamus is described in relation to obstetric trimesters, of which the first is divided into two morphogenetic periods, the second into three morphogenetic periods while the third trimester comprises only one morphogenetic stage.

Weeks 9-11 of gestation (first trimester, early post-embryonic period, n=2, CRL: 45-50mm, FOL: 24-25mm). The fetal hypothalamus at this stage showed only minimal signs of nuclear differentiation, but contained a clear division into three longitudinal zones. These zones were well differentiated in cresyl violet stained sections (Figure 2A), but were also visible by respect to the distribution of GAP43 (Figure 4A) and parvalbumin (Pv) (Figure 3A) immunoreactivity. A considerable part (circa 20%) of the developing hypothalamus lay anterior to the optic chiasm, effectively forming a true transient preoptic hypothalamic area. The well-defined hypothalamic sulcus indicated the dorsal hypothalamic boundary, while the subthalamic nucleus marked the lateral hypothalamic border.

Characterizing the lateral zone, strong GAP43 immunoreactivity revealed clear boundaries for the lateral hypothalamic area (LH) (Figure 4A). The LH occupied most of the

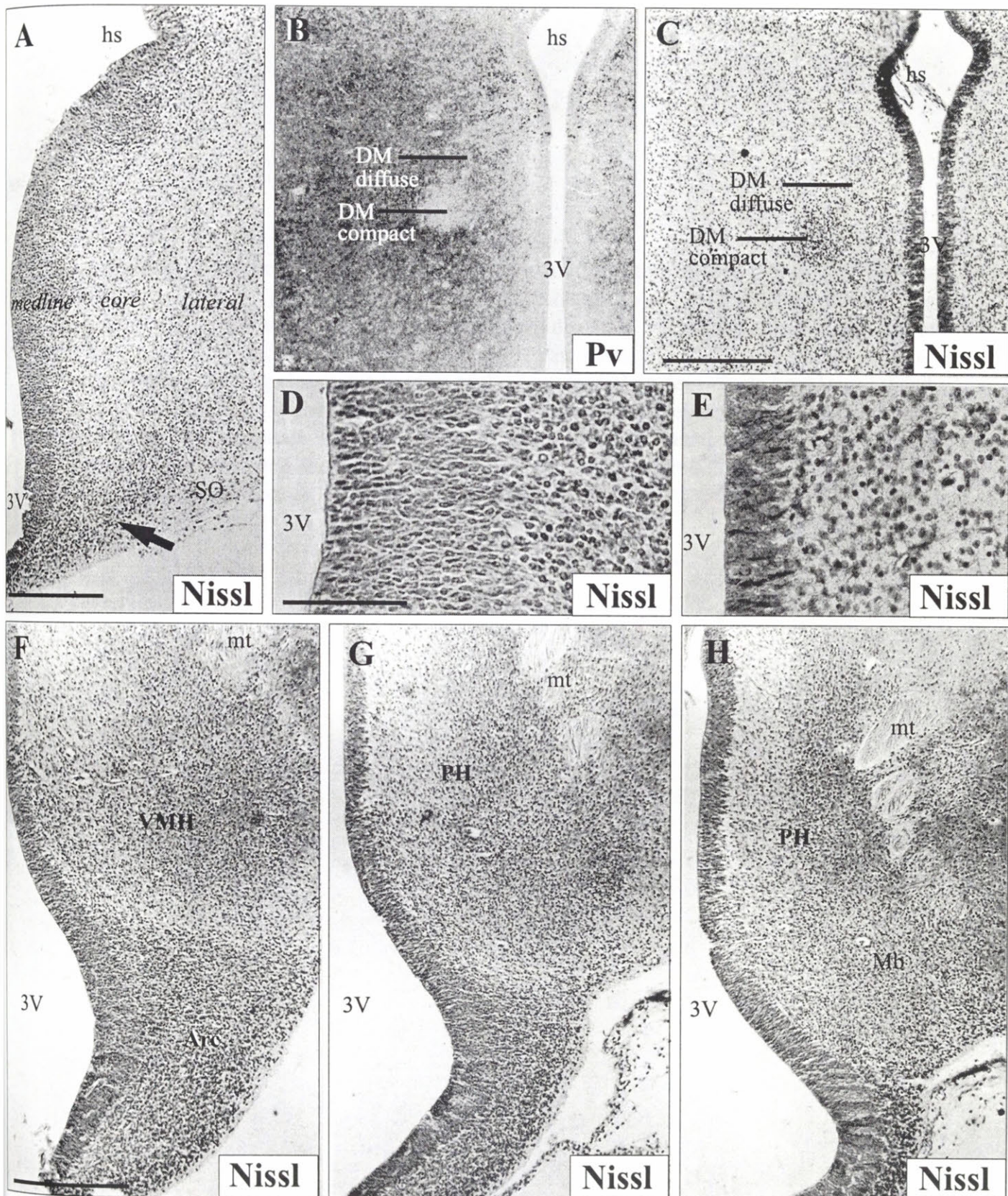


Figure 2. Photomicrographs of coronal sections at different rostrocaudal levels of the human fetal hypothalamus at 10 w.g. A) Section of the rostral hypothalamus stained for Nissl substance reveals the *midline*, *core*, and *lateral* zones by the differences in cell densities. Ventrally a narrow extension of the *lateral* zone reaches towards the midline (arrow). Scale bar=1mm. B) and (C) are adjacent sections stained for Pv and Nissl displaying clearly the borders of the dorsomedial nucleus. Scale bar=1mm D) and E) demonstrate the difference in the thickness of the germinal neuroepithelium between the anterior (D) and the tuberal (E) hypothalamus. Clearly seen preponderance of the mantle layer over the exhausted matrix layer (for original work see Kühlenbeck, 1948; Kahle 1956) Scale bar=0.25mm. F), G) and H) depict Nissl stained sections spaced through the posterior hypothalamus. Scale bar=1mm.

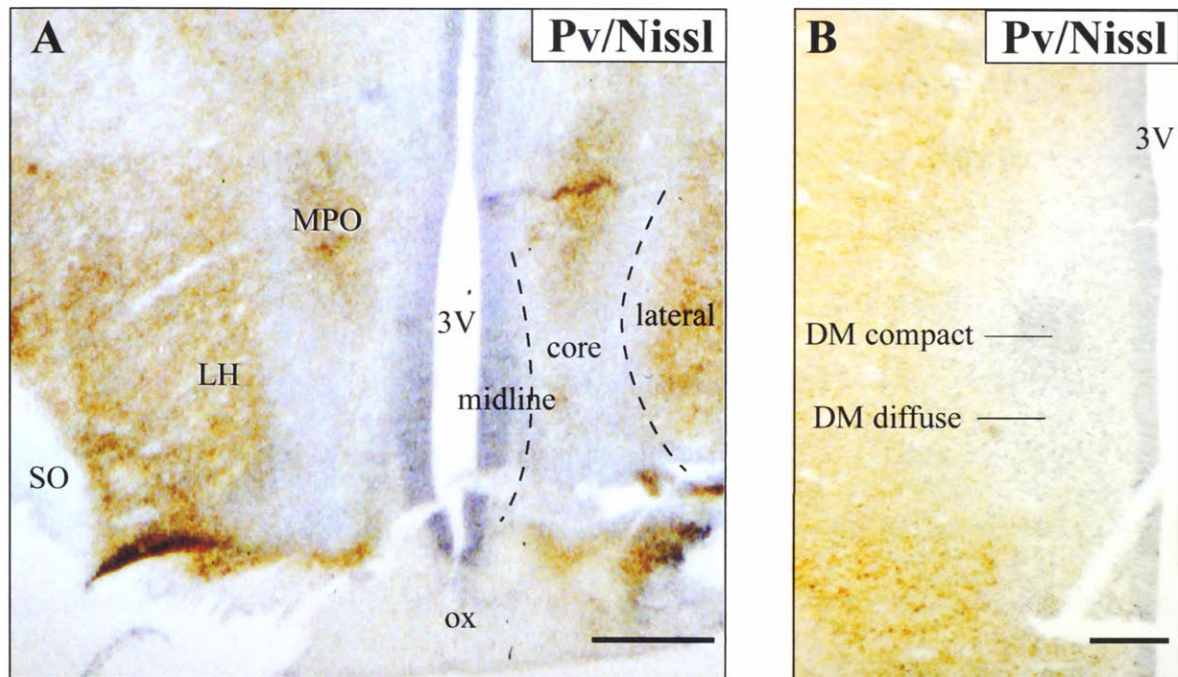


Figure 3. Photomicrographs of coronal sections from the 9 w.g. fetal hypothalamus processed immunohistochemically for parvalbumin (Pv) and counterstained for Nissl substance. A) The domain of MPO revealed by Pv immunoreactivity, which is also seen in LH. Demarcated by the dashed line on the right are: *the midline* longitudinal zone primarily comprised at this stage of a thick layer of neuroepithelial cells; *the core* zone where neurons are beginning to group into nuclei, and the *lateral zone* represented by the lateral hypothalamic area. Scale bar indicates 0.5mm. B) High magnification photomicrograph of the putative DM subnuclei revealed by lack of immunoreactivity for Pv and dense aggregation of Nissl substance counterstained cells in compact DM. Scale bar indicates 0.2mm.

diencephalon below the hypothalamic sulcus, apart from the well defined lens-shaped subthalamic nucleus (not shown). Immunoreactivity for GAP43 also revealed a more dorsal hypothalamic region, which was tentatively assigned to the posterior hypothalamus (PH) and which was separated from LH by a bundle x (Fasciculus x (of Forel)), also well-defined at this age (Figure 4A). This tract has also been known as *fibrae Hypothalamico-pallidares* (Wahren, 1959) or *fasciculus lenticularis* (Asu Christ, 1951). Posteriorly in the hypothalamus, the PH was positioned medial to LH and separated from it by a prominent mammillo-thalamic tract (mt) (Figure 2G and H). The Pv immunoreactivity also strongly labeled LH (Figure 3A). At anterior and posterior levels, there was a Pv negative region ventral to LH. At anterior levels, this ventral region was occupied by the cell sparse supraoptic nucleus (SO) (Figure 3A), which was identifiable by neurophysin (NPH) immunoreactivity (in agreement with Mai et al., 1997). At posterior levels, this Pv negative region was larger and contained numerous small cells revealed in Cresyl Violet (CV) counterstained sections. This group of neurons was lining the ventral pial surface of the posterior hypothalamus comprising the premature ventral tuberomammillary nucleus (VTM).

The *core* zone of the hypothalamus was characterized by a greater cell density than the *lateral* zone (Figure 2A). Within the *core*, particularly dense cell aggregations demarcated domains of forming nuclei. Thus, in the tuberal hypothalamic region, the dorsomedial nucleus (DM) was a well-defined, oval-shaped, ventromedially to dorsolaterally oriented structure bordering the third ventricle neuroepithelium (Figure 2C). In contrast to the adjoining area, DM contained no Pv immunoreactivity and this defined the boundaries of the nucleus (Figure 2B and 3B). Staining with Nissl substance revealed two constituent parts of DM: a compact round group of cells in its lateral part and dispersed cells in its medial part (Figure 3B). Ventral to the DM, the ventromedial hypothalamic nucleus (VMH) was represented by a poorly differentiated

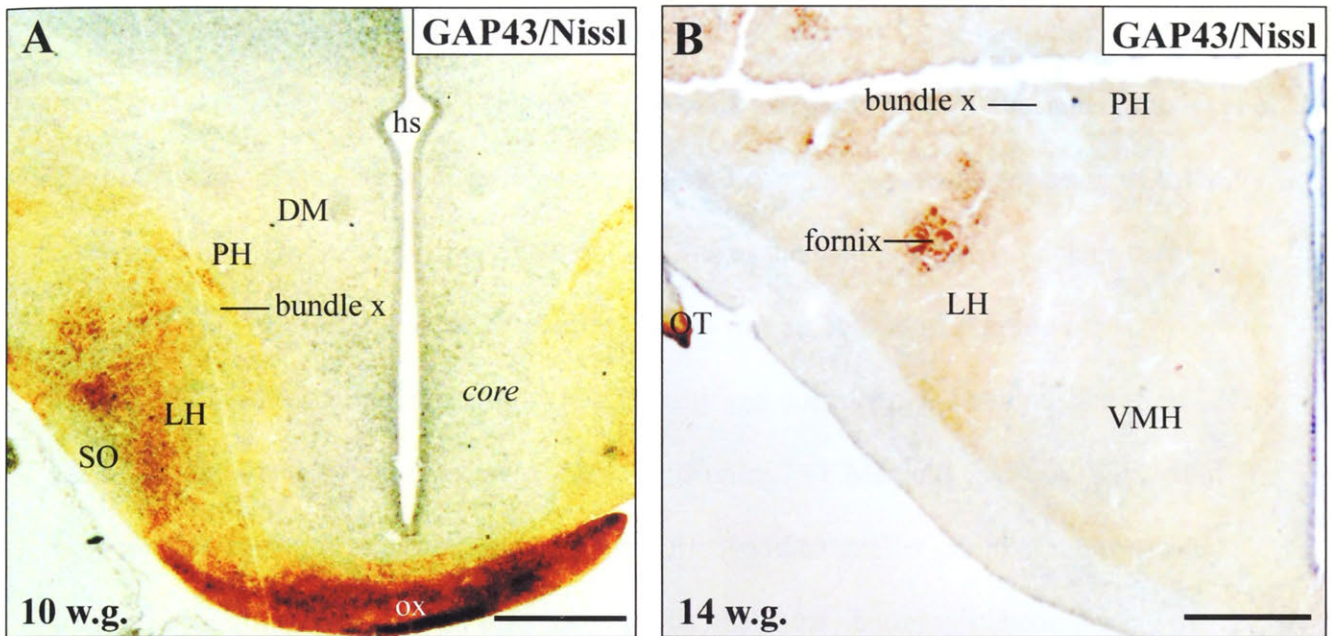


Figure 4. Photomicrograph depicting GAP43 immunoreactivity in the tuberal hypothalamic region at consecutive fetal ages. A) Prominent GAP43 labeling demarcates the lateral hypothalamus, the first hypothalamic cell group to attain observable features of structural differentiation. Coinciding with this is the strong GAP43 labeling of the optic chiasm. Also Note the GAP43 positive bundle x. B) GAP43 positive fornix is deep within the boundaries of the lateral hypothalamus. Scale bar indicates 0.5mm.

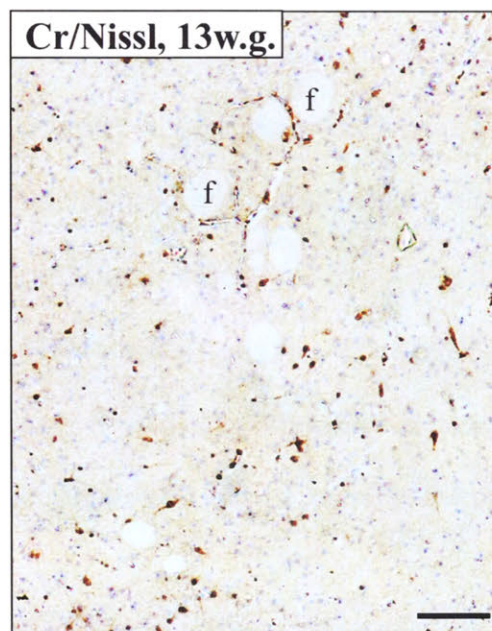


Figure 5. Photomicrograph depicting the first appearance of fascicles of the postcommissural fornix coinciding with the initial appearance of Cr positive neurons in the surrounding lateral hypothalamus. Scale bar indicates 0.25mm

collection of small cells distinguishable from the rest of the *core* by its marginally greater cell density and rounded appearance (Figure 2F). Rostrally in the hypothalamus, and at the level of the optic chiasm, the *core* zone harbored an inverted comma shaped condensation of cells showing strong Pv immunoreactivity and identified as the medial preoptic nucleus (MPO) (Figure 3A). The medial mammillary body (MbM) was an oval-shaped group of undifferentiated cells encompassed by LH laterally and dorsally and distinguished from LH by the higher cell density and negative Pv staining (Figure 7A). Medially and ventrally, MbM was bordered by thick periventricular neuroepithelium. Another smaller group of neurons was lining the ventral pial surface of the posterior hypothalamus ventral to LH comprising the lateral Mb (MbL) (Figure 7A).

The *midline* hypothalamus at this age was a layer of tightly packed cells in the periventricular neuroepithelium. The neuroepithelial lining was thicker in the anterior hypothalamus (Figure 2A and D) than in the tuberal levels (Figure 2E) and yet thicker again in the ventral caudal hypothalamus (Figure 2H). At the posterior hypothalamic level, the wedge-shaped region between the ventral pial surface and the base of the third ventricle was filled with a thick stratum of undifferentiated proliferating cells constituting the putative arcuate nucleus (Figure 2 F and G). The hypothalamic sulcus was an obvious feature of the ventricular wall (Figure 2 A,B and C). Few NPH positive cells demarcated the supraoptic hypothalamic nucleus (SO) (not shown), as previously described by Mai and colleagues (1997). At this fetal age, a significant part of the hypothalamus was located rostral to the optic chiasm.

Weeks 13-15 of gestation (first trimester, late post-embryonic period, n=3, CRL: 75-90mm, FOL: 35-50mm.). The lateral hypothalamic zone was further differentiated with the appearance of large Cr⁺ neurons in the LH and PH (Figure 5) at 13w.g. Calretinin positive

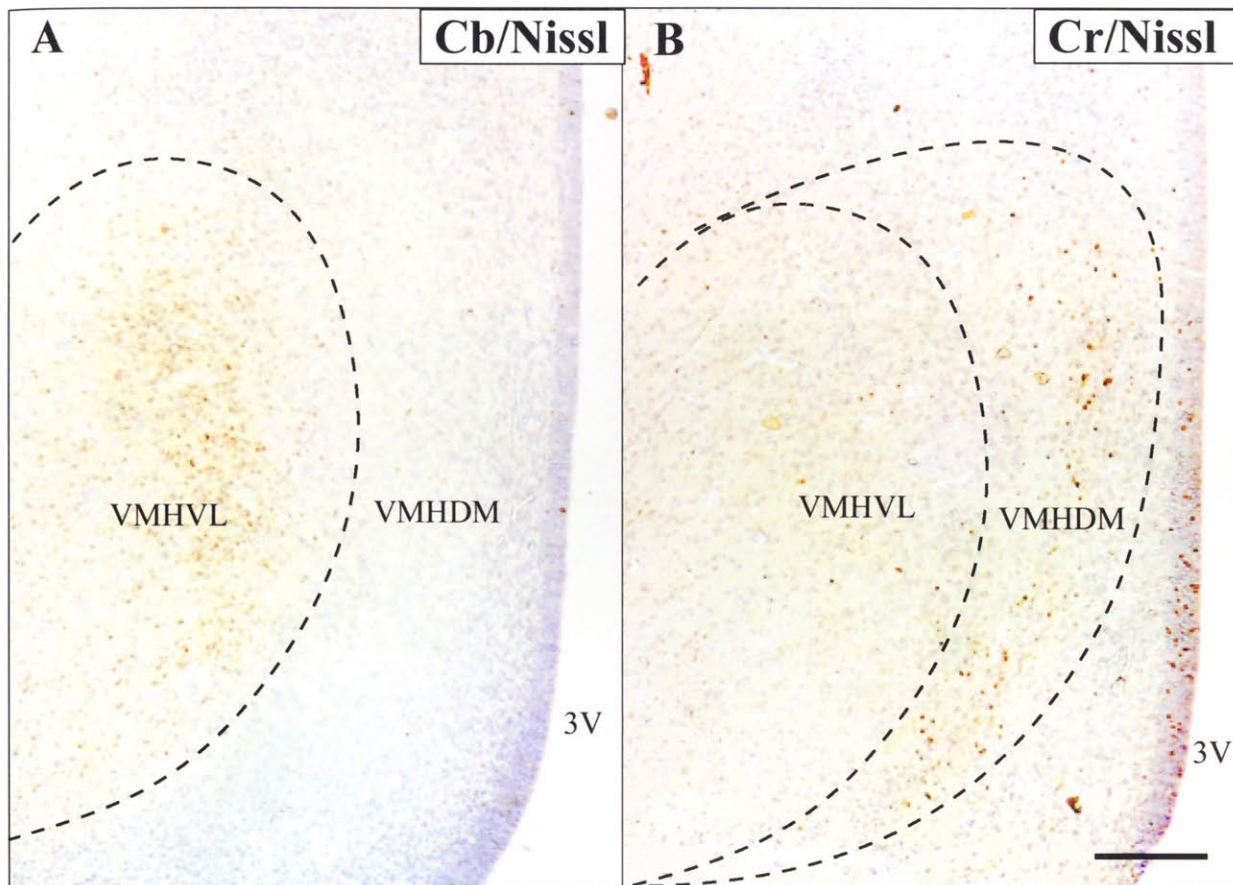


Figure 6. Microphotographs of the adjacent sections from the hypothalamus of the human fetus 13 weeks of gestation reacted immunohistochemically for calbindin (A) and calretinin (B) and counterstained with Nissl substance. Differential distribution of Cb and Cr positive neurons within the ventromedial hypothalamic nucleus reveals two complimentary subnuclei the ventrolateral and teh dorsomedial. Scale bar indicates 0.5mm

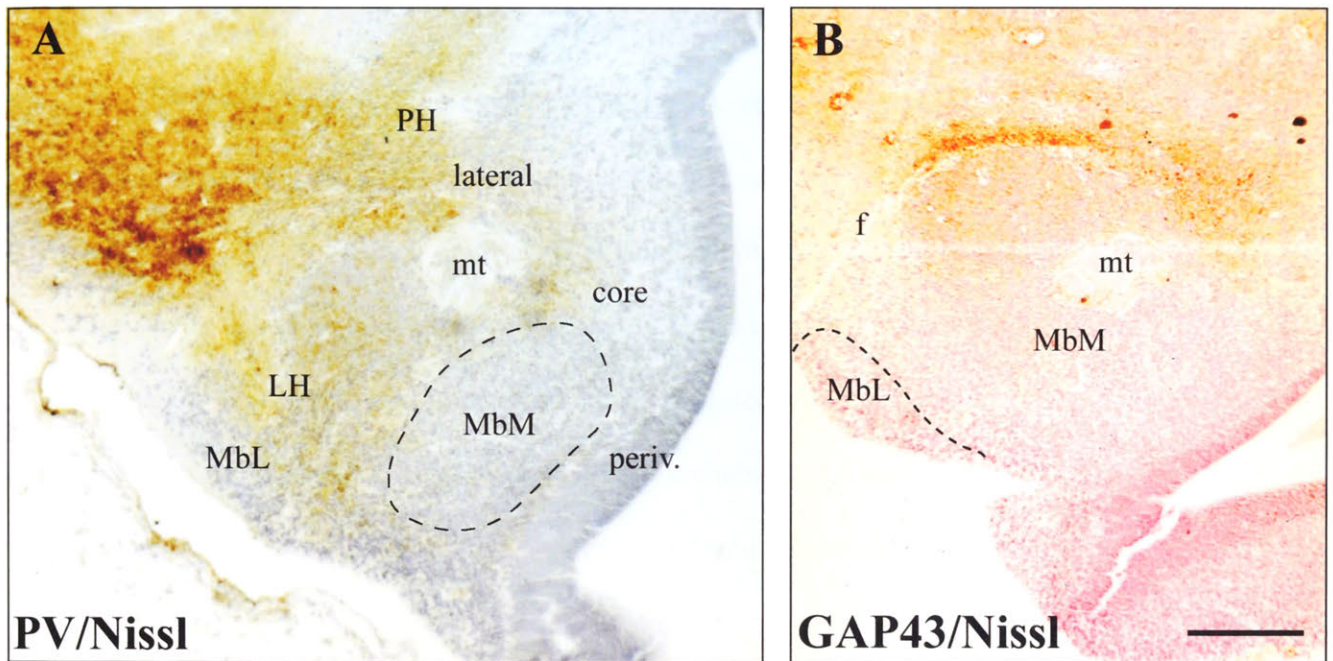


Figure 7. Photomicrographs of coronal sections from caudal hypothalamic levels of (A) 10 w.g. and (B) 13 w.g. fetuses showing structural organization of the mammillary hypothalamic region at early gestational stages. Scale bar indicates 0.5mm.

cells are found in the adult LH – their presence at this developmental stage heralds an early differentiation of the LH. The fornix became visible in the lateral hypothalamus at about 11 w.g. At 14 w.g., GAP43 immunoreactivity became detectable in the fornix for the first time. In the tuberal region, the fornix was deeply embedded in the LH (Figure 4B). Fibers of fornix were also labeled by strong synaptophysin (SYN) immunoreactivity (Figure 8B). Parvalbumin immunoreactivity was not as strong at this stage of gestation as at 9-10 w.g., indicating the transient character of this protein in the hypothalamus.

The main feature of the hypothalamic *core* was the well defined VMH with a clearly differentiated dorsomedial part marked by a population of Cr positive neurons (Figure 6A) and a ventrolateral part occupied by a group of Cb positive cells (Figure 6B). The DM was composed of compact and diffuse parts readily seen in CV sections through the tuberal hypothalamus. Parvalbumin immunoreactivity revealed VTM as a distinct population of large neurons on the ventral surface of the tuberal hypothalamus (Figure 8C and D). The medial Mb was a distinctly round homogeneous collection of small neurons perforated on its lateral side by the terminal fornix (Figure 7B). The dorsal boundary of the Mb was encompassed by a bundle of mt revealed by strong GAP43 immunoreactivity. The lateral Mb was seen on the ventral pial hypothalamic surface adjacent to the medial Mb just below the fornix (Figure 7B).

In the *midline* zone at this stage, the neuroepithelium was substantially thinner than at 10 w.g., suggesting the slowing of neuroepithelial proliferation. FAL⁺ radial glial fibers were visible in an arc-shaped band extending from the ventral third of the ventricular surface in a ventrolateral direction. These fibers could be followed most of the way to, but did not quite reach, the ventral hypothalamic pial surface (Figure 8A). Below the hypothalamic sulcus, alongside the ventricular surface, there was a small compact group of cells visible in CV material which was tentatively identified as the *anlage* of the paraventricular nucleus (Pa).

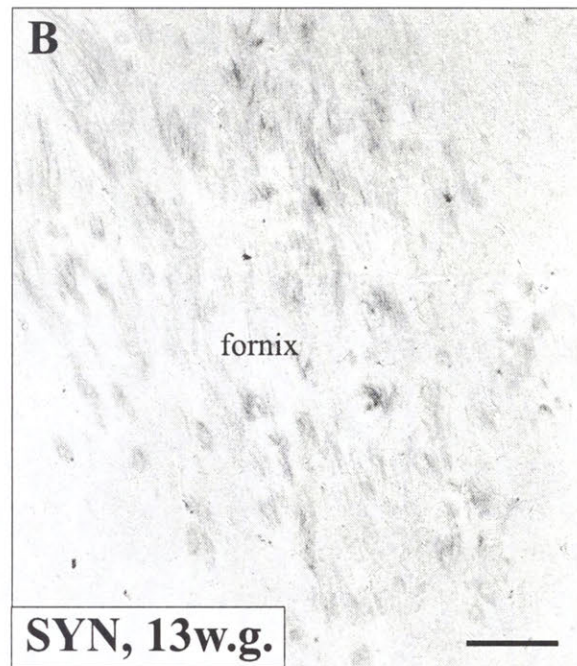
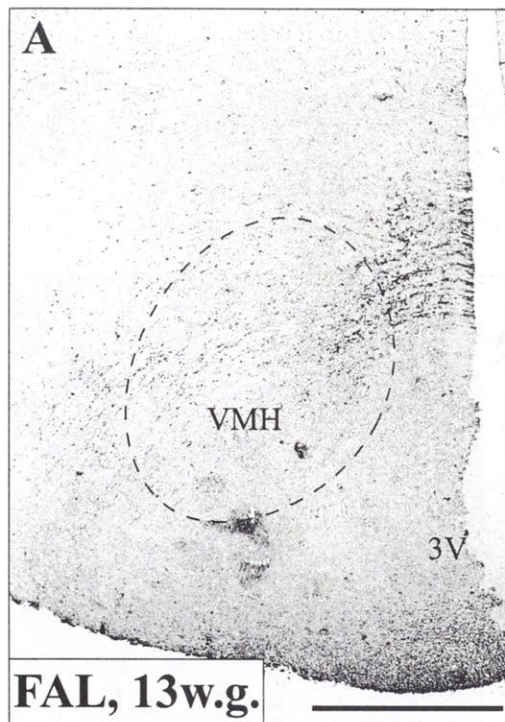


Figure 8. Photomicrographs of a series of coronal sections from the tubera levels of a 13 w.g. fetal hypothalamus demonstrating FAL immunoreactive radial glial fibers arching from the periventricular epithelium through the area occupied by VMH (A), synaptophysin immunoreactive fibers of fornix (B). Scale bar indicates 1mm (A) 0.25mm (B).

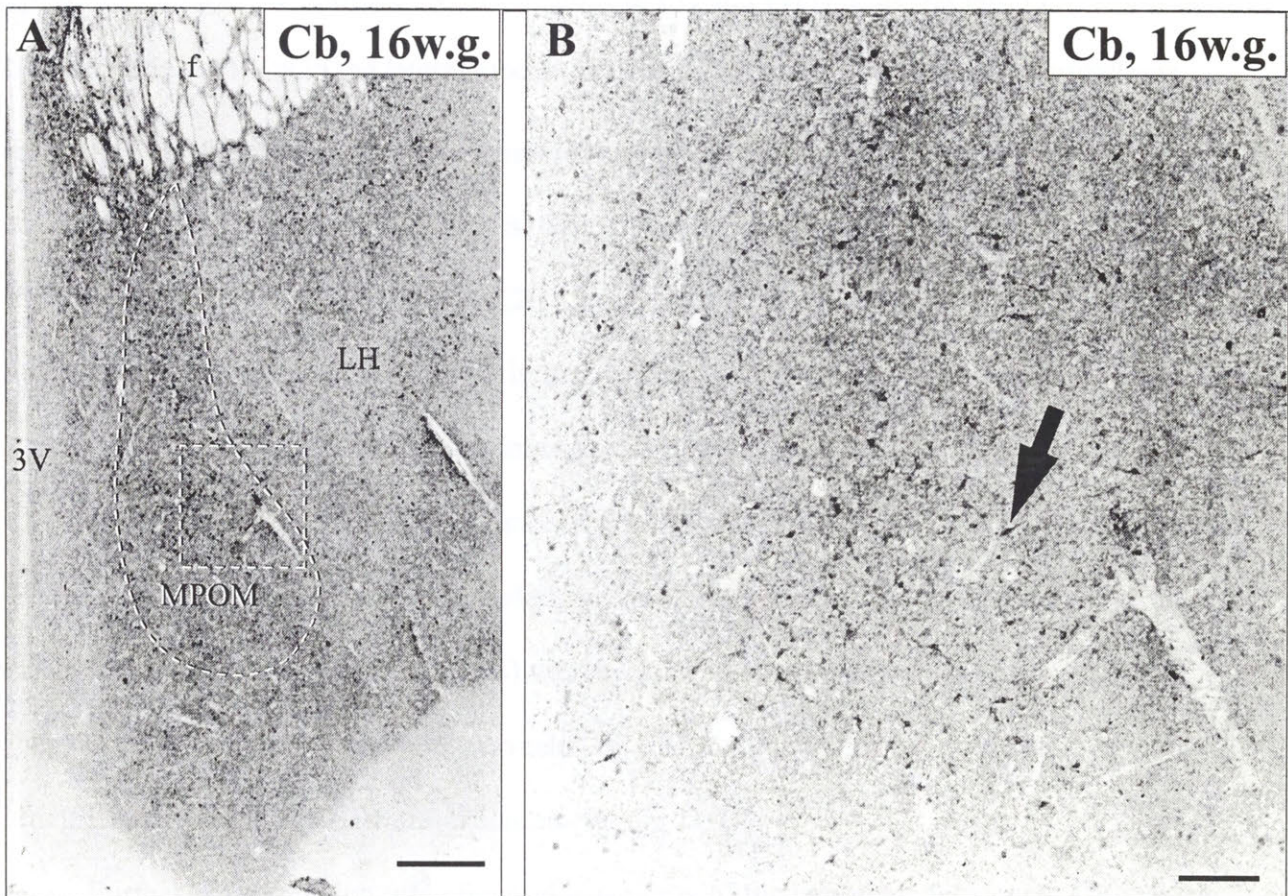


Figure 9. Photomicrographs of the coronal sections from the anterior hypothalamic levels demonstrating (A) two populations of Cb immunoreactive cells in MPO and in LH. Scale bar indicates 1mm. Area identified by rectangle in (A) is shown at higher magnification in (B) to demonstrate Cb immunoreactive neurons in MPO. Scale bar indicates 0.25mm.

Some of the laterally positioned cells of this anlage were NPH⁺. The SO had manifestly more NPH⁺ cells than in the previous stage (not shown; see Mai et al., 1997).

Week 16-17 of gestation (second trimester, early period, n=3; CRL: 100-130mm; FOL: 50-65mm). Further differentiation of the lateral hypothalamic zone was marked by the initial appearance of large Cb immunoreactive neurons in LH and PH (Figure 9A and 11). The lack of Cr immunoreactivity in the lateral tuberal nucleus (LTu) made this structure conspicuous within the LH, which itself contained numerous large Cr⁺ cells (Figure 20). In GAP43 stained sections, LTu was also visible for the first time as a patch of negative staining within the otherwise immunoreactive LH (Figure 12C). Counterstaining for CV revealed LTu as a tightly packed group of small neurons. GAP43 immunoreactivity was also expressed in the fornix, still located fully within the lateral hypothalamus at this stage (Figure 12C). Continuous maturation of the fornix was marked by the appearance of FAL immunoreactivity (not shown). Within the LH, at this stage, the fornix was surrounded by Cr and Cb positive neurons (Figure 17A). The periventricular fiber bundle (Figure 11B) was revealed by strong GAP43 immunoreactivity. Fibers of the medial forebrain bundle revealed by Cb, immunoreactivity could be seen in the area of LH as well as in the ventral thalamus (Figure 11A).

Further differentiation was observed in the *core* of the hypothalamus where CV stained sections revealed the well defined intermediate nucleus (InM, sexually dimorphic nucleus) (Figure 10) within the anterior hypothalamic region. This nucleus was embedded medially into a inverted comma shaped MPO whose continuous maturation was marked by numerous medium sized Cb immunoreactive neurons (Figure 9). In the tuberal hypothalamus, a distinct GAP43⁺ fiber bundle was girthing VMH ventrolaterally (Figure 12 A and B) effectively forming the shell of the nucleus. The mammillary complex was well-differentiated in CV

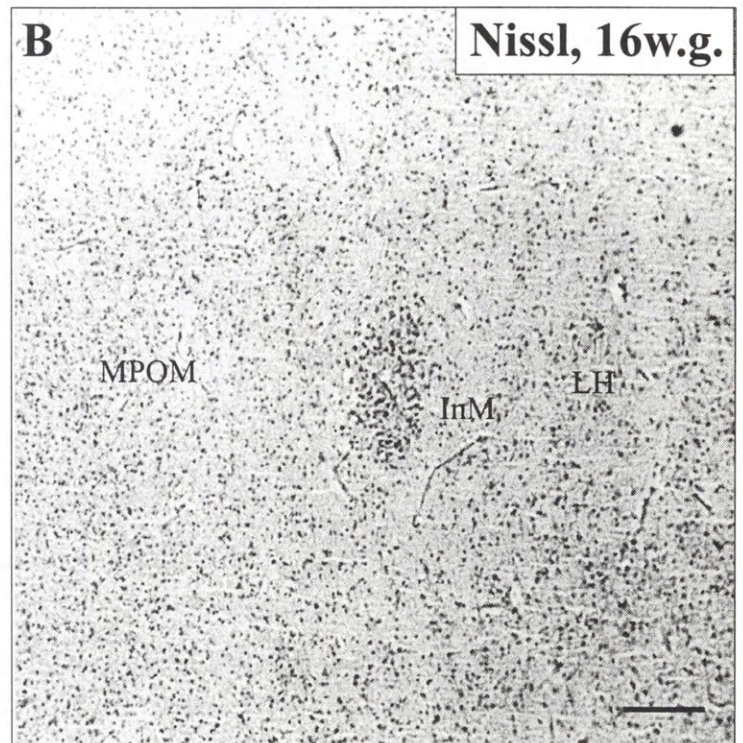
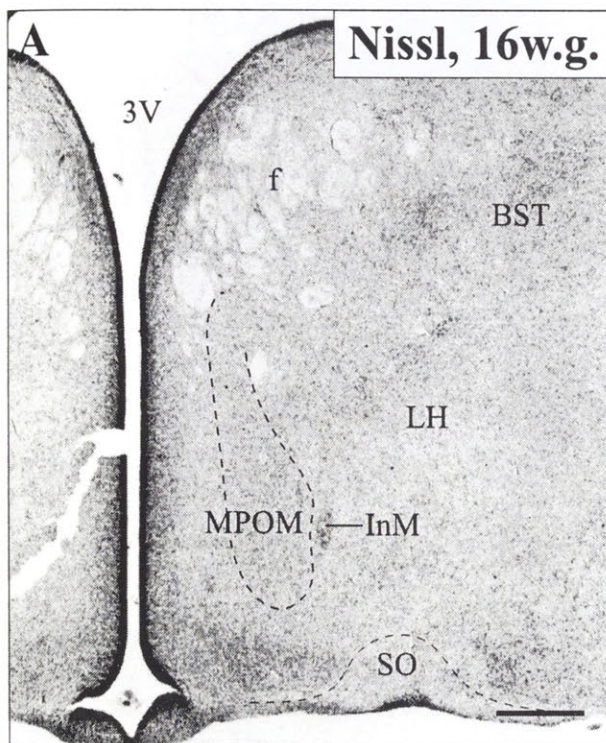


Figure 10. Photomicrographs of a coronal sections from the anterior hypothalamic levels stained for Nissl substance showing intermediate nucleus identified by a compact group of medium size cells also shown at higher magnification in (B). Note a tightly packed group of neurons in SO surrounded by a cell poor area (A). Scale bar indicates 1mm in (A) and 0.25 mm in (B).

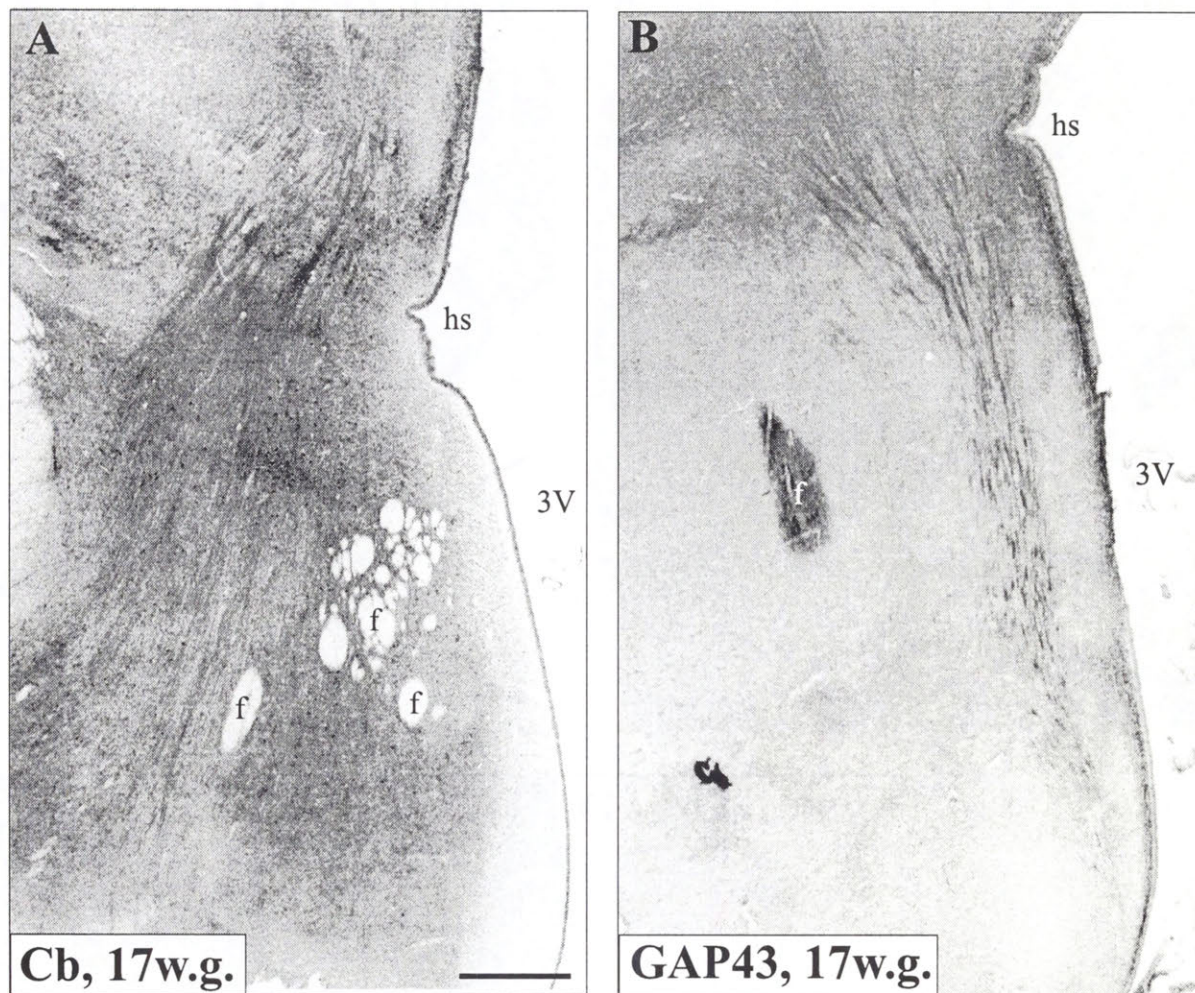


Figure 11. Photomicrographs of the coronal sections from the hypothalamus of 16w.g. fetus showing prominent fiber bundles revealed by Cb (A) and GAP43 (B) immunoreactivity. Scale bar indicates 1mm.

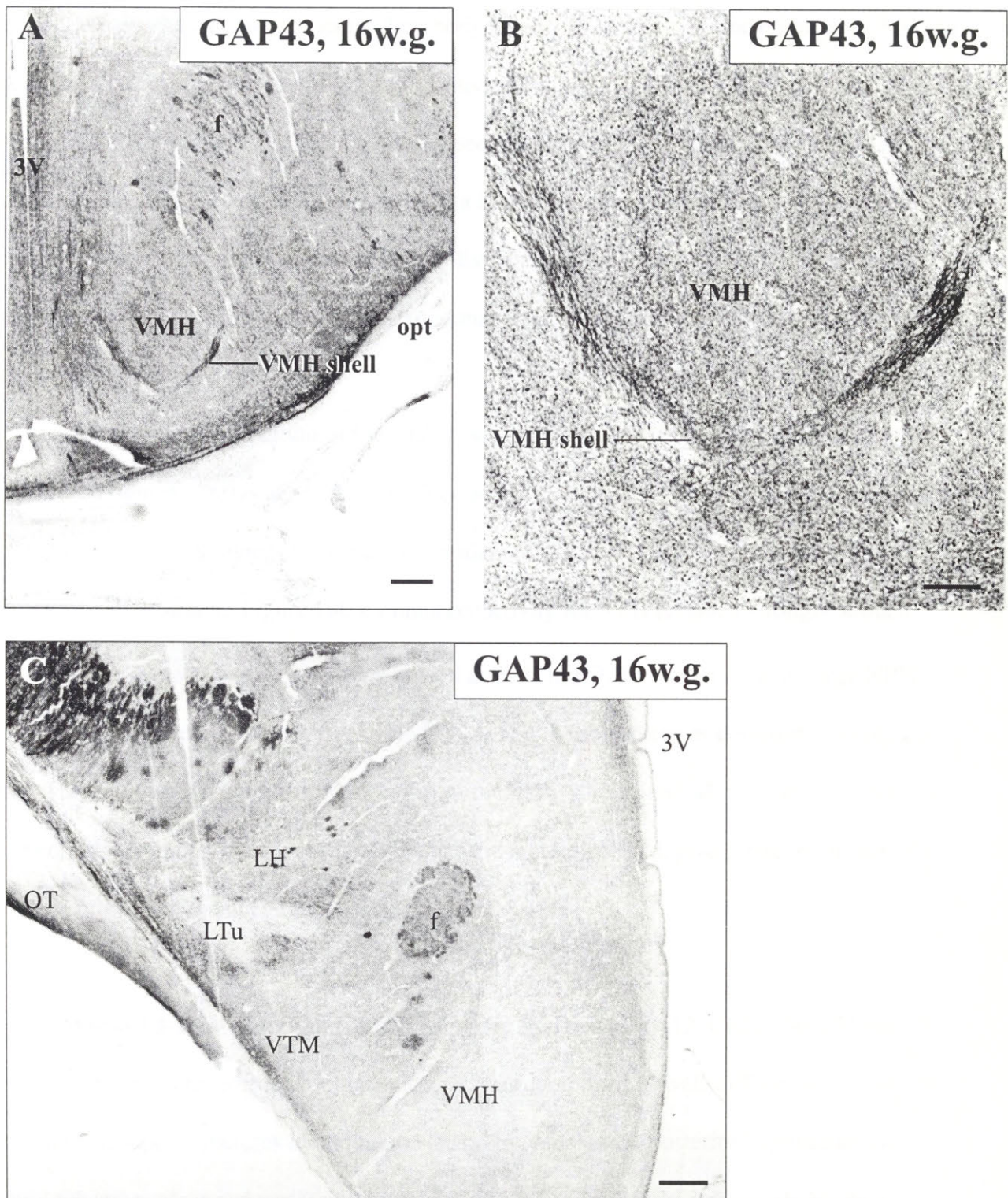


Figure 12 Photomicrographs of the coronal sections from posterior levels of 16 w.g. fetal hypothalamus. Sections are processed immunohistochemically for identification of GAP43. A) demonstrate the shell of the VMH revealed as a GAP43 immunoreactive fiber bundle encompassing the nucleus ventrally. The fiber bundle of VMH shell is shown at higher magnification in (B). At more posterior levels distinctly negative GAP43 immunoreactivity in (C) reveals the boundaries of the lateral tuberal nucleus within the lateral hypothalamus. The topography of the fetal human LTu is similar to that of the rat terete nucleus. Note that at more posterior levels the shell of VMH is not evident. Scale bar 0.5mm in (A) and (C), 50 μ m in (B).

staining and was comprised of two parts; a larger, spherical, medial mammillary body and a smaller, kidney-shaped, lateral mammillary body (Figure 13 A and C). The entire complex was encompassed dorsally by a rim of GAP43 positivity (Figure 13B). The triangle-shaped supramammillary nucleus (SUM) was readily seen in CV stained sections dorsal to the mammillary bodies (Figure 13A). It contained a large number of small compactly clustered cells. The supramammillary nucleus was also distinguished by its negative staining in GAP43 preparations (Figure 13B). Note that the supramammillary nucleus cannot be seen in the adult human hypothalamus.

The thin neuroepithelium of the *midline* was still tightly packed, but contained only a few mitotic figures. At this age, FAL immunoreactivity revealed what appears to be radial glial cells (Mai et al., 1998) along the dorsal ventricular surface, with peripheral processes extending towards the pial surface (Figure 18C). Immunoreactivity for NPH revealed strongly stained, large spindle-shaped accessory neurons as well as cells in SO. Pa was filled with large NPH⁺ neurons, which revealed a greater ventro-rostral extent to the nucleus as compared to younger ages. The neurons of the posterior Pa (PaPo) were tightly packed and adjacent to the surface of the ventricle. At more anterior levels, Pa cells were more dispersed, giving rise to the dorsal subcompartment of the nucleus (PaD) (not shown).

Weeks 18-23 of gestation (second trimester, mid period, n=12, CRL: 150-170mm; FOC: 75-80mm). The lateral hypothalamic zone was comprised of well-differentiated, yet, still intimately grouped structures including the lateral hypothalamus, posterior hypothalamus, lateral tuberal nucleus and perifornical nucleus. The LTu was clearly distinguishable as a compact group of small Cb immunoreactive cells (Figure 20). The circumferential arrangement of Cb positive neurons around the fornix indicated the differentiation of the PeF and defined its

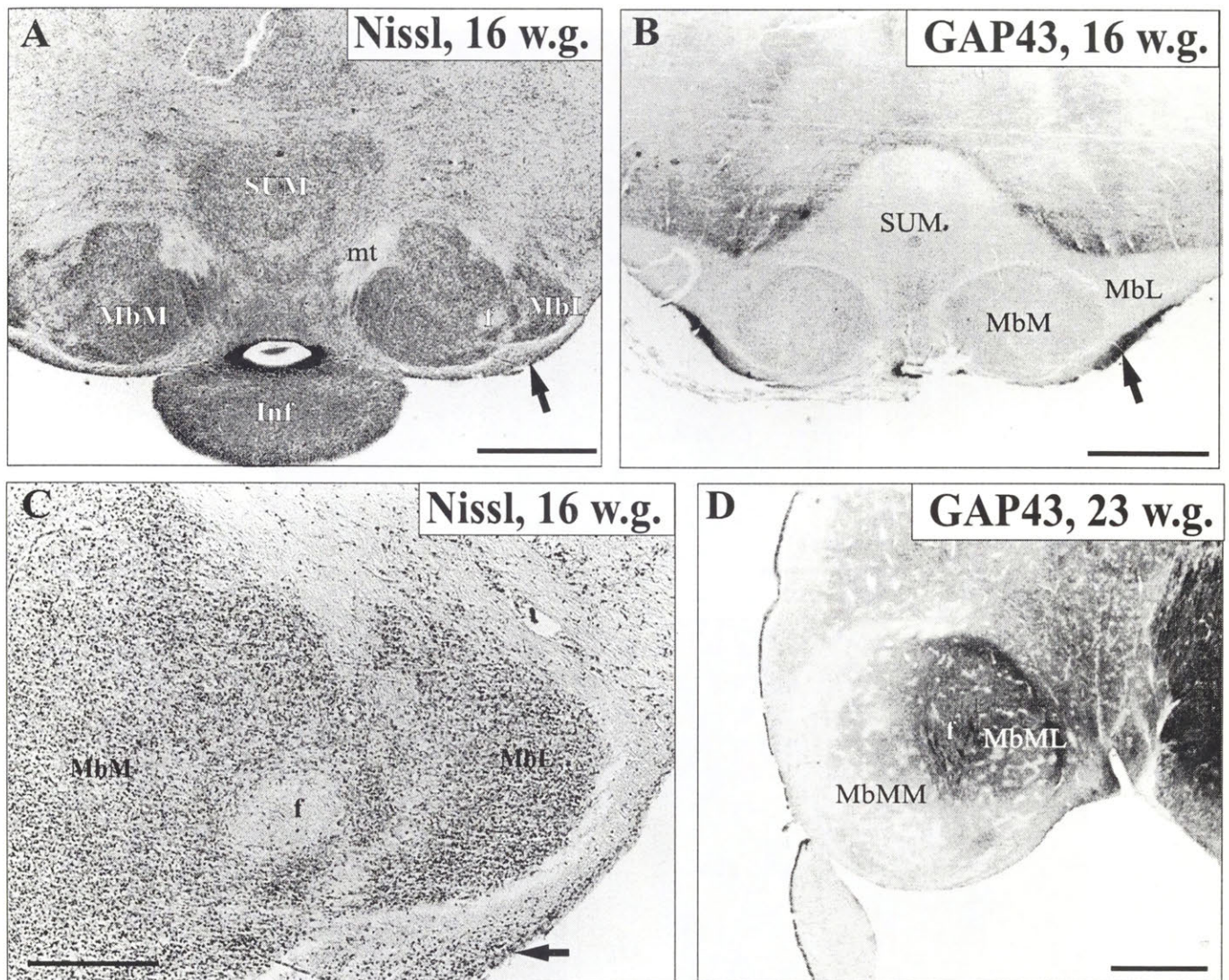


Figure 13. Photomicrographs of coronal sections through the mammillary body demonstrating organization of the mammillary region at 16 w.g. (A, B, C) and at 23 w.g. (D). Arrow points at transient group of cells that may correspond to the ventral Mb in the rat (Altman and Bayer, 1986). This cell group was evident only in one brain at 16w.g. scale bar indicates 1 mm (A,B,D) and 0.5 mm (C).

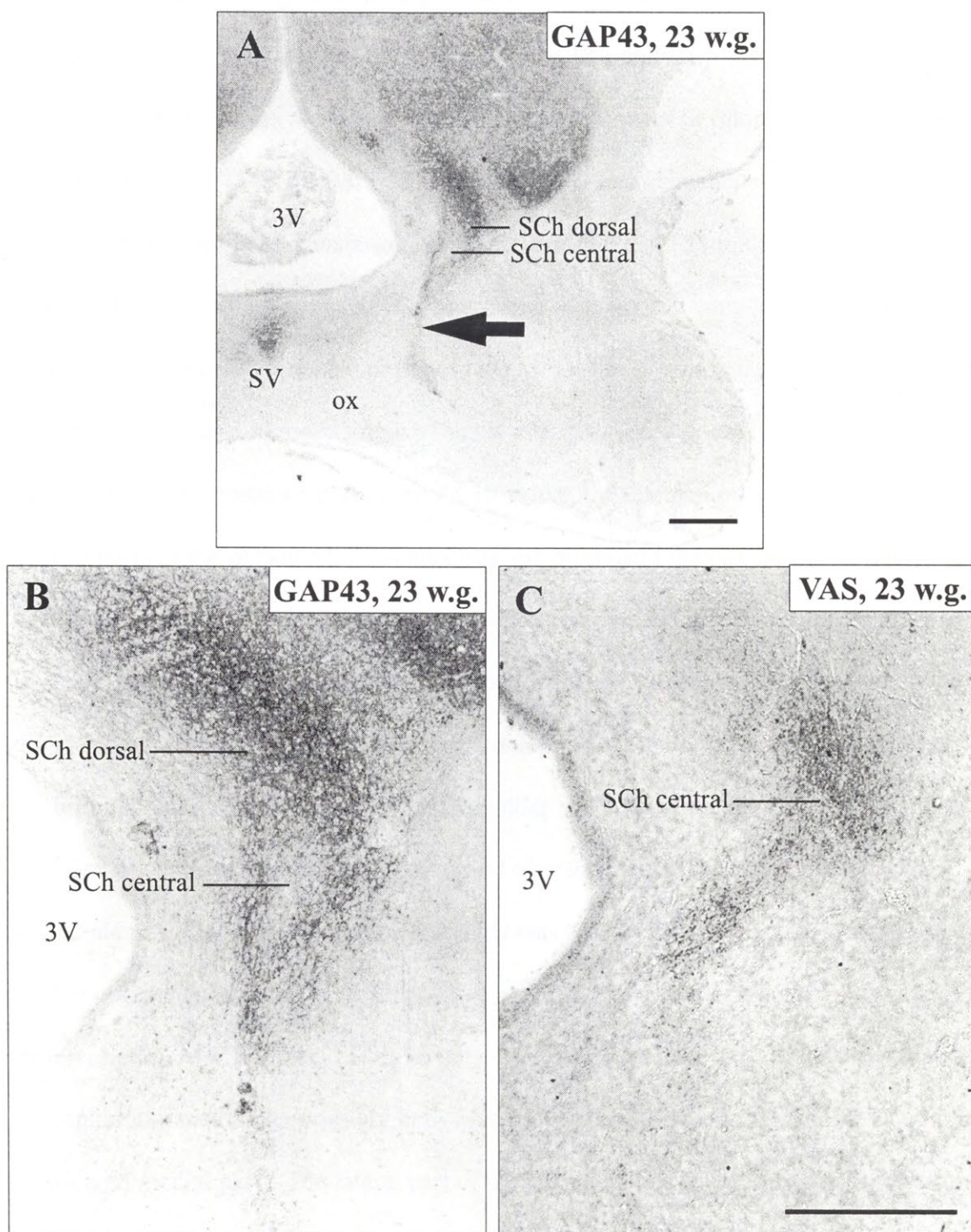


Figure 14. Photomicrographs of the coronal sections of the 21 w.g. human fetal hypothalamus revealing compartmental organisation of the suprachiasmatic nucleus. Scale bar indicates 0.5mm

boundaries (Figure 17E). The Cr immunoreactivity was present in numerous large (~ 20 μ m diameter) multipolar and spindle-shaped neurons in LH (Figure 17C), PH and VTM, but was absent from the LTu (Figure 20). Large neurons in PH, but not in LH, showed FAL immunoreactivity at 19 weeks of gestation (Figure 18A and B).

In contrast to the previous stages and also subsequent development, the structures of the hypothalamic *core* (MPO, InM, DM and VMH) were best demarcated by clear boundaries in sections stained for Nissl substance. Numerous mid-sized (~15 μ m diameter) Cr positive cells were readily detectable in the MPO, demarcating this inverted comma shaped nucleus. The Cb immunoreactive cells were also present in the MPO. The dorsomedial nucleus was prominent in Nissl sections as a rounded group of small cells positioned dorsally in the hypothalamic *core* just ventral to the posterior part of the Pa. However, the distinction between the compact and diffuse parts of the dorsomedial nucleus was less prominent than in the earlier ages and even undetectable in some brains, prompting the omission of nuclear subdivision from the Figure 1. In sections stained for Nissl substance, the cells of VMH were divided between a more compact dorso-medial and a more dispersed ventro-lateral part. Consistent with previous stages, Cr and Cb immunoreactive cells were differentially distributed in the nucleus. The CV staining revealed the large neurons of VTM dispersed over the ventral surface of the tuberal hypothalamus. The GAP43 immunoreactivity was equally distributed throughout the *core*. The VTM contained numerous large Cr positive neurons. However, this feature did not permit differentiation of VTM from the more dorsolateral LH, which also contained this type of cell. The spherical, medial mammillary body was well differentiated in CV stained sections into lateral and medial parts. The lateral part of the medial mammillary body contained strong GAP43 immunoreactivity associated with the bundle of the fornix which was deeply embedded in this part of Mb, with fornical fibers distributed throughout this nuclear subdivision (Figure

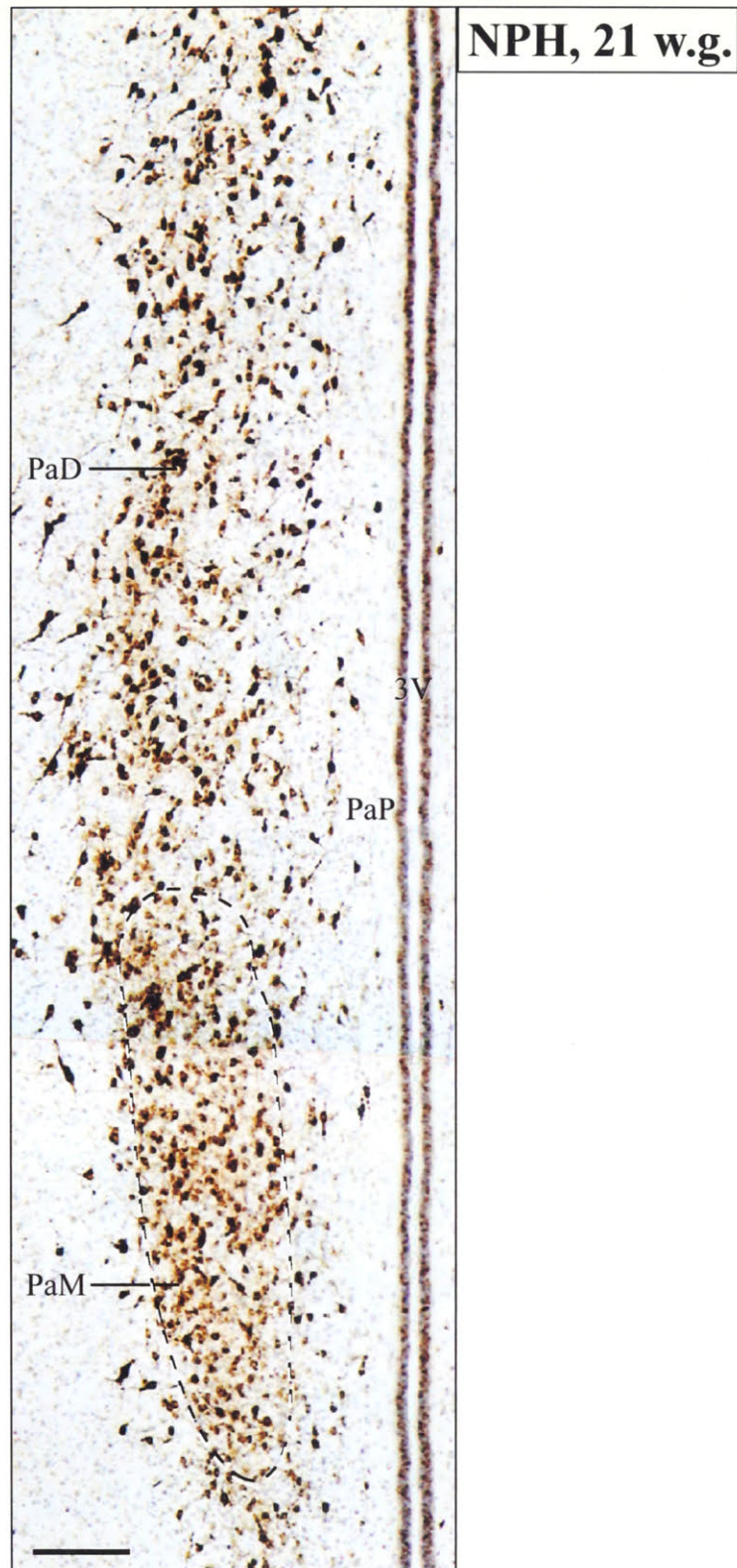


Figure 15. Photomicrograph of a coronal section through the Pa of the 18 w.g. hypothalamus stained for NPH and counterstained for Nissl substance. Note the morphologically mature NPH positive neurons of PaD and, although NPH positive but morphologically immature neurons forming the core of the PaM. Also note a prominent periventricular lamina of undifferentiated NPH negative small cells forming PaP. These findings indicate that neurons of PaD differentiate before neurons of PaM and well before neurons of PaP, consistent with findings from the developing rat Pa (Altman and Bayer, 1989). Scale bar indicates 1mm.

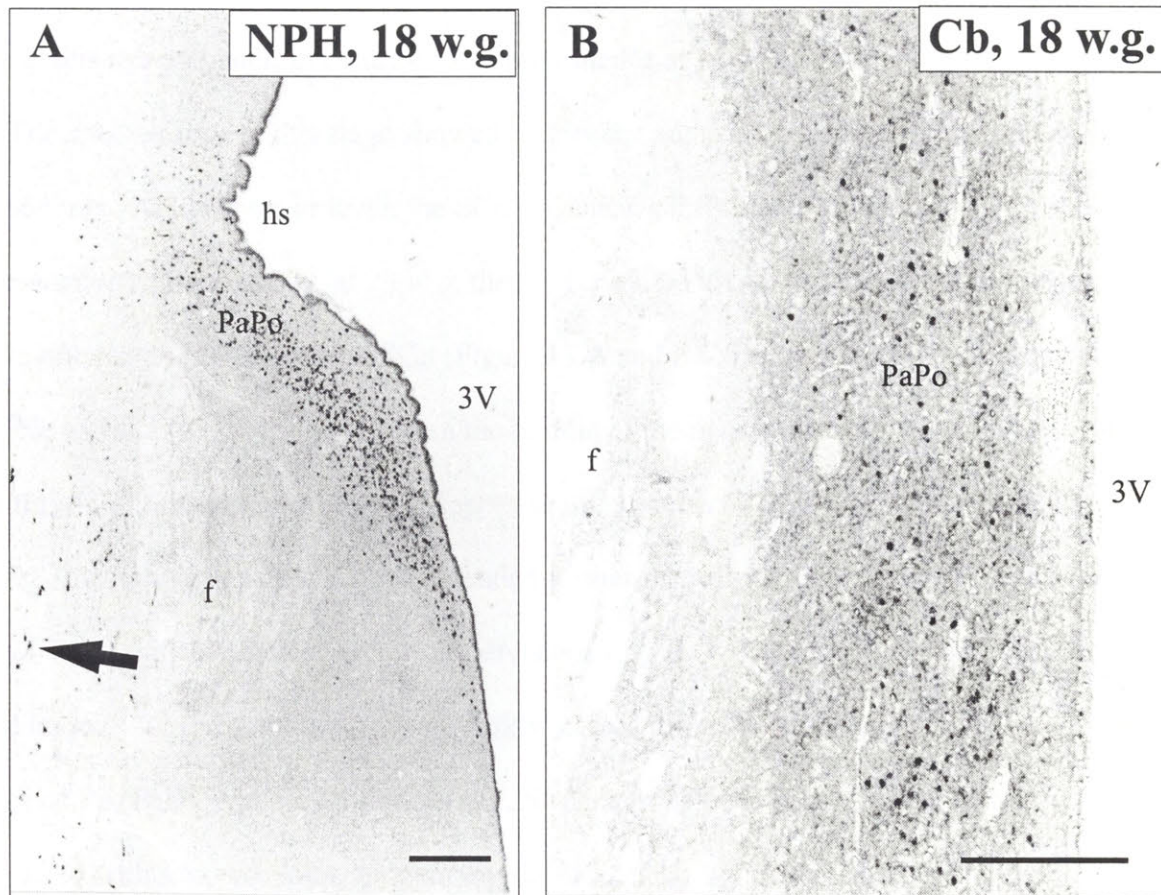


Figure 16. Photomicrographs of PaPo at 18 w.g. demonstrating the advanced stage of PaPo differentiation with respect to NPH immunoreactivity (A) and the first appearance of Cb positive neurons in the subnucleus (B). Please note the scattered morphologically mature NPH positive accessory neurons indicated by arrow in (A). Scale bar indicates 250 μm.

13D). The medial part of the medial mammillary body was positively stained for FAL and contained nascent mammillo-thalamic tract fibers. The lateral mammillary body was not obvious at this age and later, in contrast to its prominence at 16 w.g.

The *midline* zone at this stage showed its greatest advances in structural maturation of its components. At the anterior level, the SCh was clearly differentiated by GAP43 immunoreactivity. Importantly, at 23 w.g. the SCh could be divided into a GAP43+ dorsal compartment and a GAP43- central SCh (Figure 14 A and B). The retinohypothalamic tract was visible as GAP43+ fibres issued from the middle of the optic tract to the SCh (Figure 14C). The central SCh contained prominent vasopressin immunoreactivity (see also Mai et al., 1997).

At 18 w.g., the paraventricular nucleus extended further rostrally than earlier and, for the first time at 21 w.g., evinced distinct subnuclear divisions (Figure 15). Specifically, NPH staining revealed large (~ 22 µm somata diameter) darkly stained differentiated neurons with processes in the dorsal Pa (PaD), while further ventrally, NPH neurons were less morphologically differentiated with few processes, moderately stained and tightly clustered revealing the magnocellular Pa (PaM) (Figure 15). The part of the Pa immediately adjacent to the 3V – the parvicellular Pa (PaP) - was made distinct by paucity of NPH immunoreactivity. Also at this age, the PaPo maintains the expression of numerous NPH+ cells, while revealing for the first time in gestation, small (~15 µm diameter) Cb+ cells (Figure 16). For the first time in gestation, immunoreactivity for Cb was strong in fibers traversing the Arc from the ventricular surface towards (but not quite reaching) the pial surface of the hypothalamus, and in small cells aggregated near the ventricular surface (Figure 19). Importantly, for the first time in gestation, small (~10 µm diameter) NPY positive neurons were present in the Arc, indicating the emergence of a distinctively adult feature in this structure (Figure 23C). As for the previous age, FAL immunoreactivity continued to be strong in presumptive radial glia along the

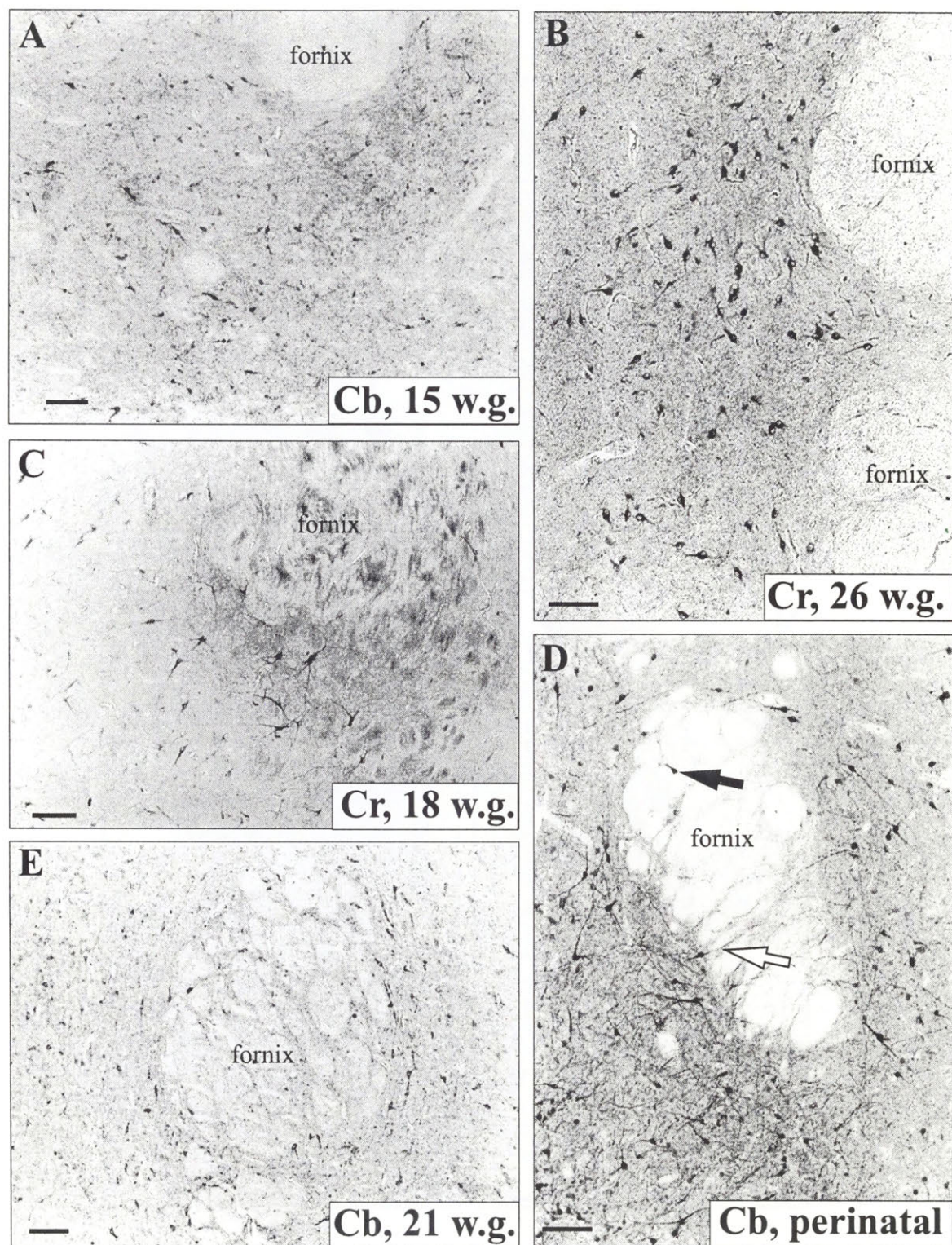


Figure 17. Photomicrographs of coronal sections through the posterior hypothalamic levels showing perifornical nucleus at different stages of fetal development as revealed by calretinin (Cr) and calbindin (Cb immunoreactivity). Black arrow in D points at a neuron inside the fornix bundle, while white arrow points at a neuronal process extending into the fornix bundle. Scale bars indicate 50 μ m.

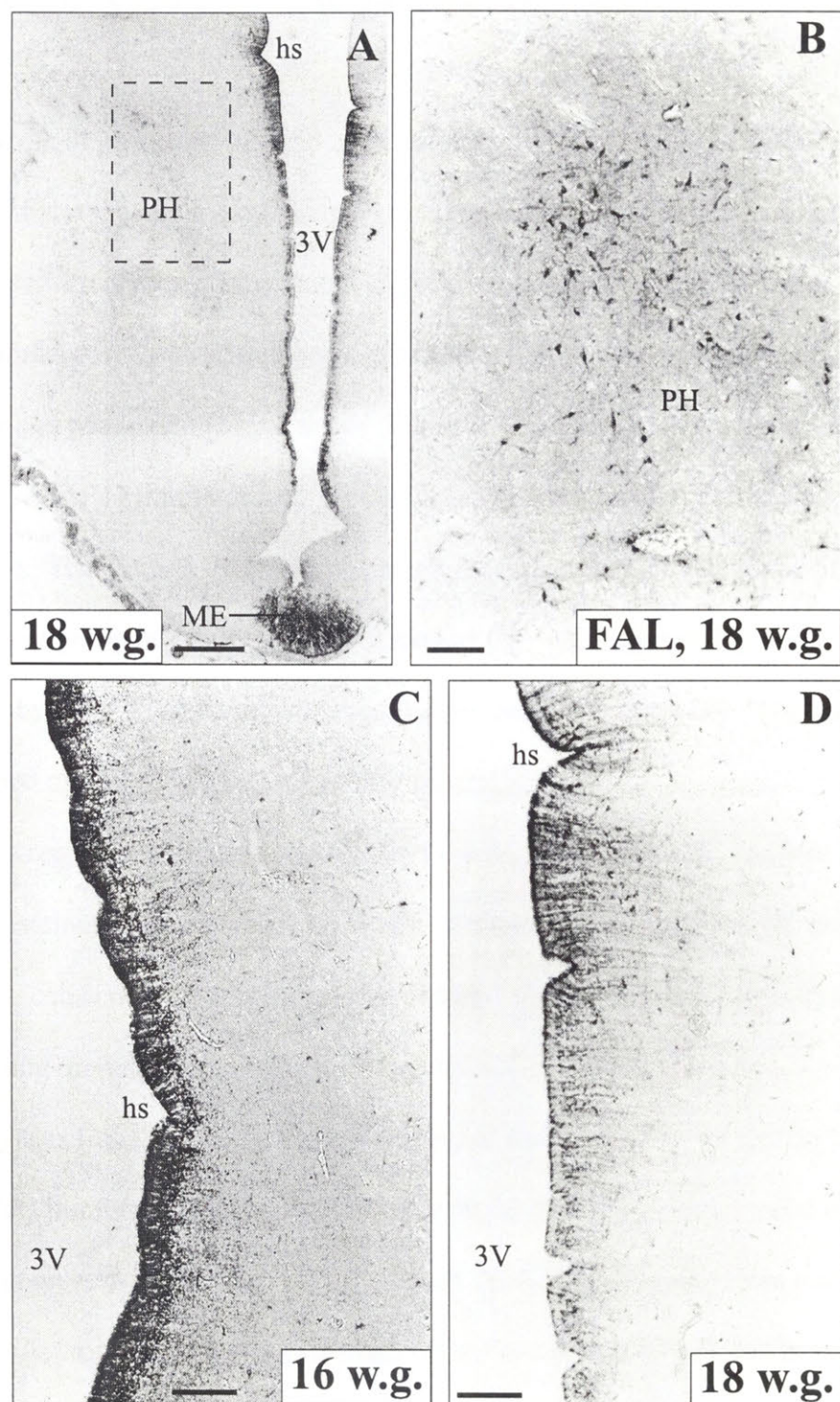


Figure 18. Photomicrographs of coronal sections through the posterior levels of the hypothalamus showing the distribution of FAL immunoreactivity at 16 and 18 w.g. Area indicated by rectangle in A is shown at higher magnification in B. Scale bars indicate 250 μm in A and 50 μm in B, C and D.

ventricular surface, but also was particularly strong in the median eminence (ME), thereby defining this region for the first time in gestation (Figure 18A and C).

Week 24 -32 of gestation (second trimester, late period, n=5, CRL: 250-350mm, FOC: 125-150mm). By this stage, the hypothalamus has taken on an adult-like appearance, with clearly differentiated structures. In the lateral hypothalamic zone, the PeF was well differentiated, with large (~20 to 25µm diameter) Cb and Cr immunoreactive neurons arranged around the fornix and positioned medial to LH (Figure 17B). The fornix contained strong FAL immunoreactivity. GAP43 immunoreactivity was less intense in the LH at this stage than earlier in gestation. The LH and PH contained many magnocellular Cb and Cr positive cells. The tightly clustered group of small (~12 µm diameter) Cb+ cells comprising the LTu was distinctly marked by the cell poor shell surrounding the nucleus (Figure 20). Topographically LTu was positioned medial to LH in the posterior tuberal region.

In the *core* region, the principal nuclei (MPO, InM, DM and VMH) had less striking boundaries in CV staining than in the previous age. However, in immunoreacted material the morphology of the cells could be readily studied. Thus, Cr and Cb positive cells in the VMH and MPO had strong immunoreactivity and clearly defined processes. GAP43 immunoreactivity was found in the neuropil of the lateral part of the medial mammillary body and PH, while SYN immunoreactivity was present in the medial part of the medial mammillary body. FAL immunoreactivity was strongly present in the fibers of fornix, optic tract and ME.

In the *midline* zone, tightly grouped small Cb stained cells were present in the central SCh, completing the characteristic chemoarchitectonic adult features of the nucleus. At this age, the compartmental organization of the Pa was at its most obvious. Large, morphologically mature NPH positive neurons were compactly grouped in the ventrolateral quadrant of Pa

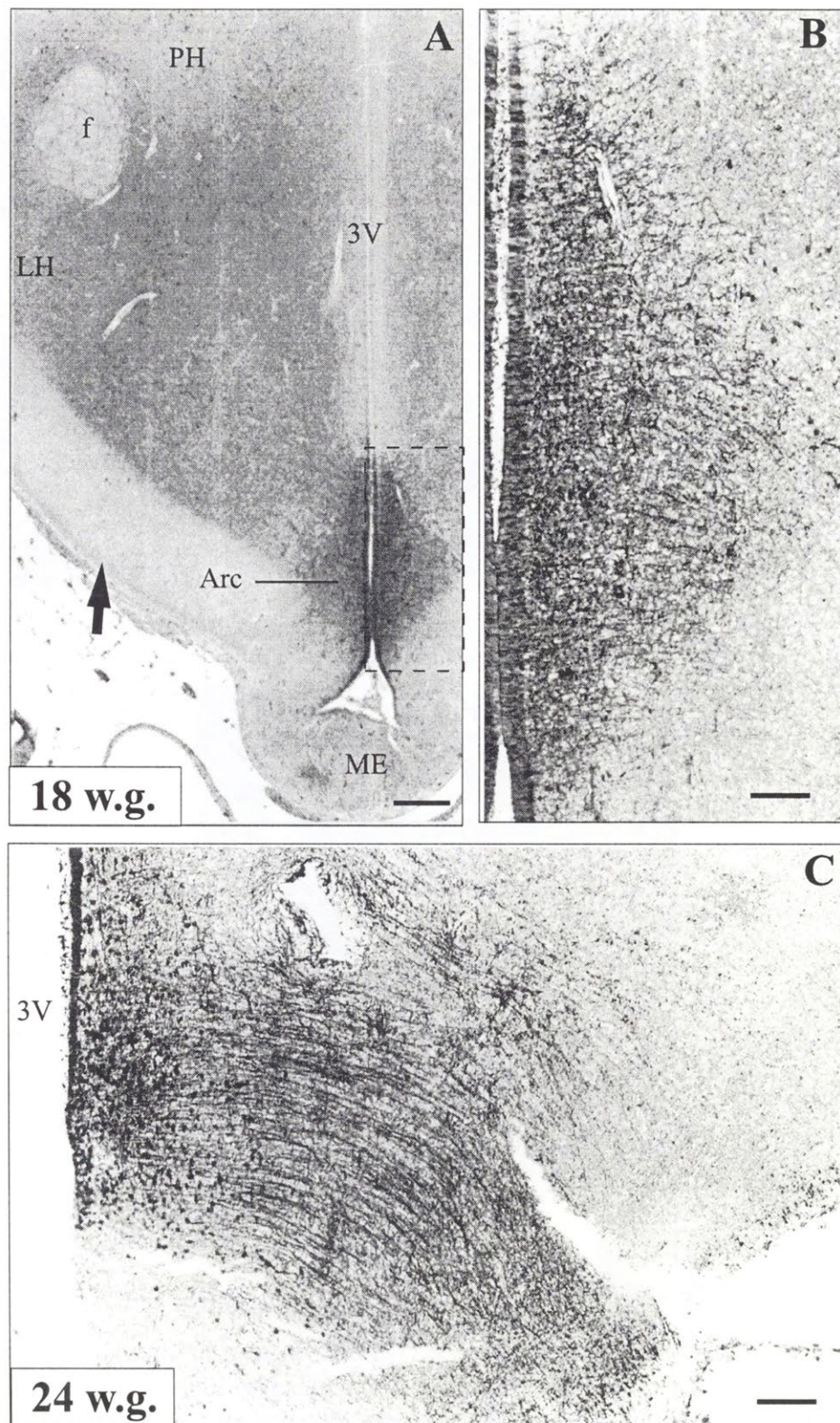


Figure 19. Photomicrographs of coronal sections through the fetal hypothalamus at 18 (A and B) and 24 (C) w.g. showing Cb positive radial glial fibers in Arc. At 18 w.g. (A) and (B) the fibers do not quite reach the pial surface while at 24 w.g. they can be seen extending the entire distance to the ventral pial surface. The negative area indicated by arrow is found a number of brains and may be an artifact. Scale bar indicates 250 μ m in (A) and 50 μ m in (B) and (C).

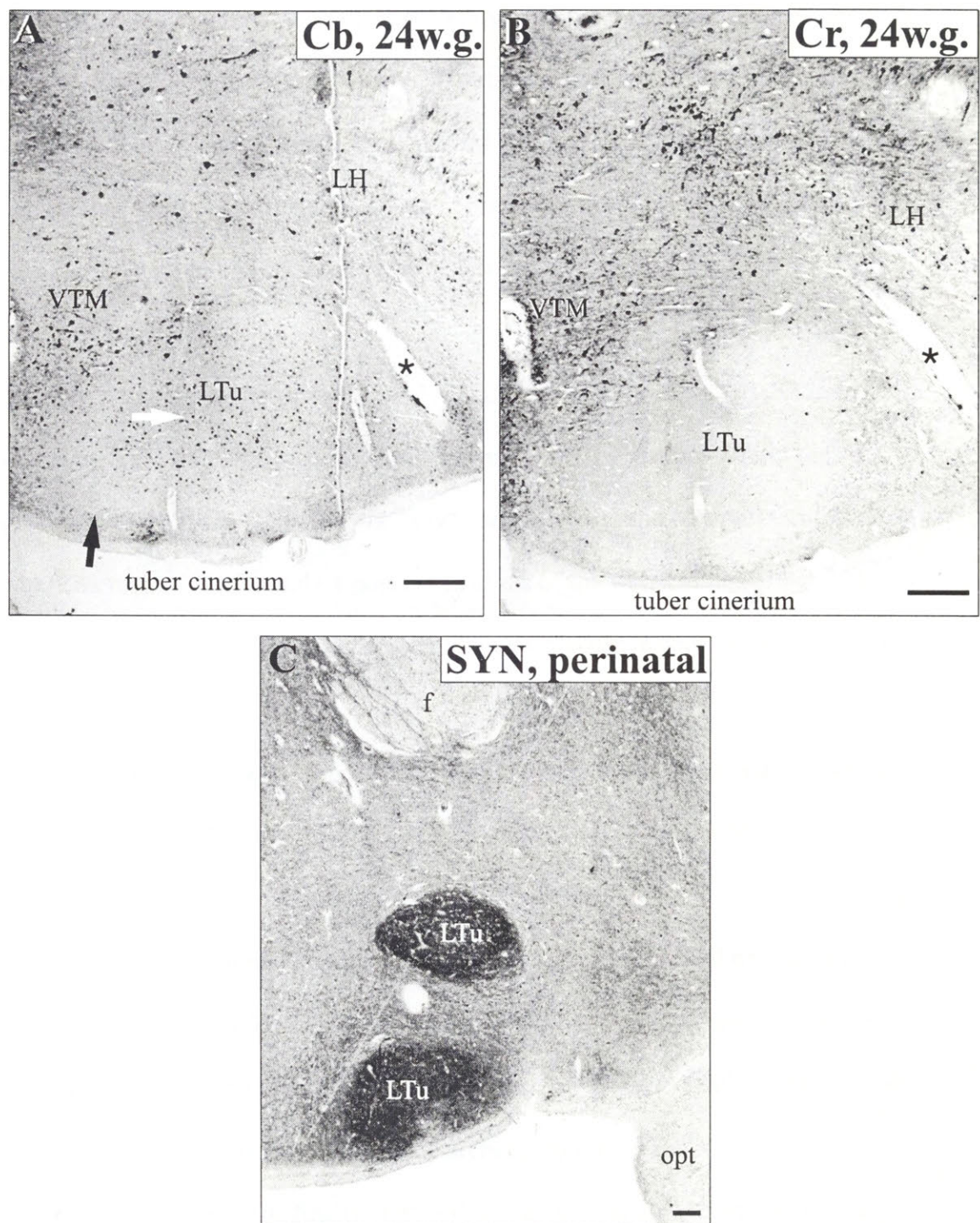


Figure 20. Photomicrographs of coronal sections from the posterior hypothalamic levels shows the lateral tuberal nucleus revealed by Cb positive cells in (A), by Cr negativity within LH which otherwise contains numerous positive neurons (B) and synaptophysin immunoreactivity in (C). The LTu is often split in two segments. Arrow in (A) points at a cell poor area encompassing LTu. Scale bar indicates 100µm.

(PaM), but dispersed in the PaD and PaPo. At the same time, PaP was almost totally devoid of NPH positive neurons, although many small cells were visible there in CV counter-stained sections. At 26 w.g. small (10 to 15 μm diameter) Cb stained cells were present throughout Pa, with the exception of PaP. Calbindin staining remained intense in small cells in Arc while the associated Cb immunoreactive fiber bundle appeared broader and reached from the ventricular neuroepithelium to the ventral pial surface (Figure 19C).

Week 36 to newborn (third trimester, n=3, CRL: 325-400mm FOC:150-200mm). For the first time, strong SYN immunoreactivity in LTu demarcated the nucleus within the surrounding VTM (Figure 20C). The LTu was comprised of two round components found within the tuber cinereum. The Cb and Cr positive neurons of the well-circumscribed PeF nucleus were seen to extend dendrites into the fornix. Few Cb positive cells were seen inside the bundle of fornix (Figure 17D).

In the *core* region, DM was now poorly defined but still visible in CV-stained sections as a group of medium to small size cells positioned between Pa and VMH. VMH was still clearly distinguishable in cresyl violet, Cb and Cr stained sections.

In the *midline* hypothalamus, SCh readily revealed its compartmental organization in Cb stained material (see Chapter 3). Strong FAL staining was present in magnocellular neurons of SO and Pa (Figure 22). The NPH immunoreactivity revealed the organization of Pa and also labeled the hypothalamo-hypophyseal fiber bundle arching from the PaM towards SO and further ventro-medially where it was finally confined to the external component of the median eminence (ME) (Figure 21A and 23A). In the perinatal hypothalamus the synaptophysin immunoreactivity labeled PaM and also a small but prominent uncinate nucleus (Un) (Braak and Braak, 1992) embedded within the lateral surface of PaD (Figure 21). The nucleus was

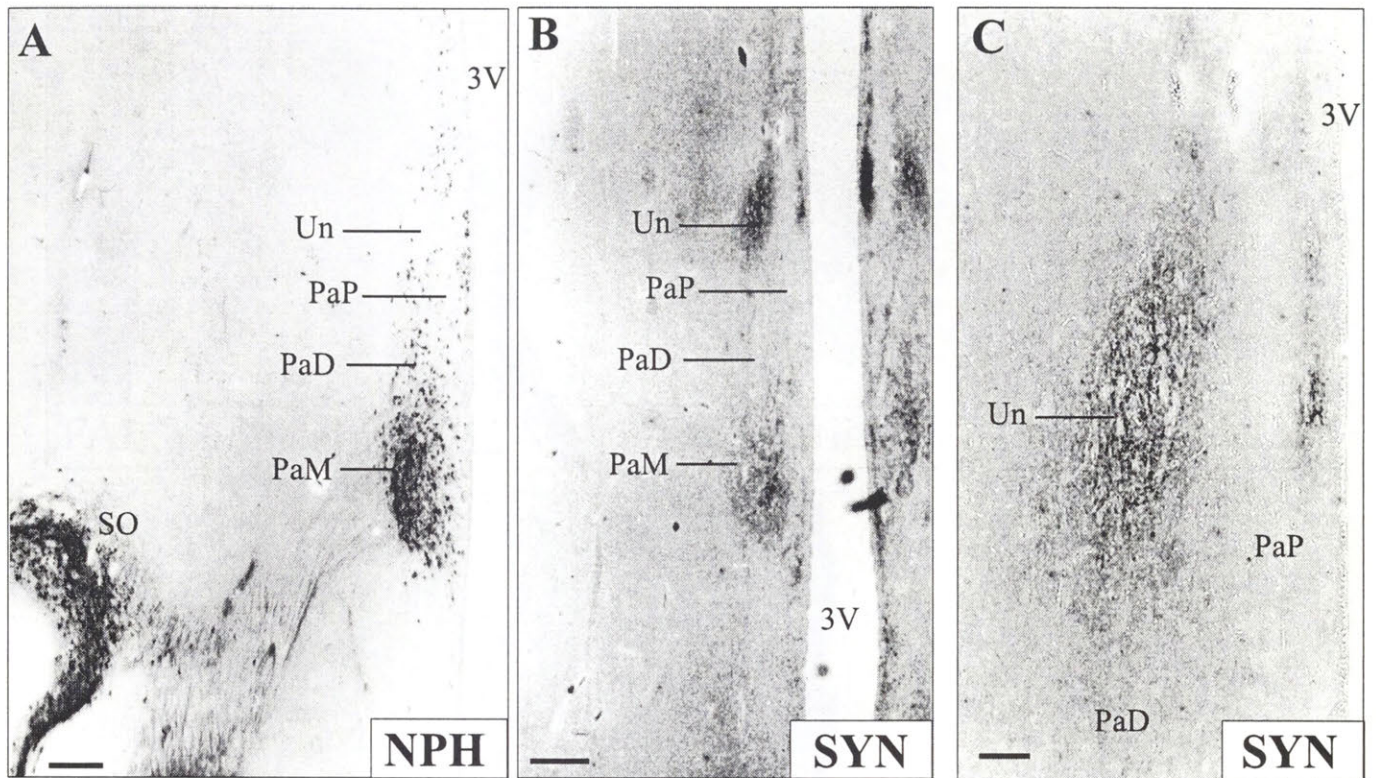


Figure 21 Photomicrographs of nearly adjacent coronal sections from the perinatal hypothalamus showing complimentary distribution of neurophysin (A) and synaptophysin (B). Synaptophysin immunoreactivity revealed uncinate nucleus intimately overlapping Pa. The area of the uncinate nucleus is shown at higher magnification in C. Scale bar indicates 0.5mm in (A) and (B), and 50 μ m in (C).

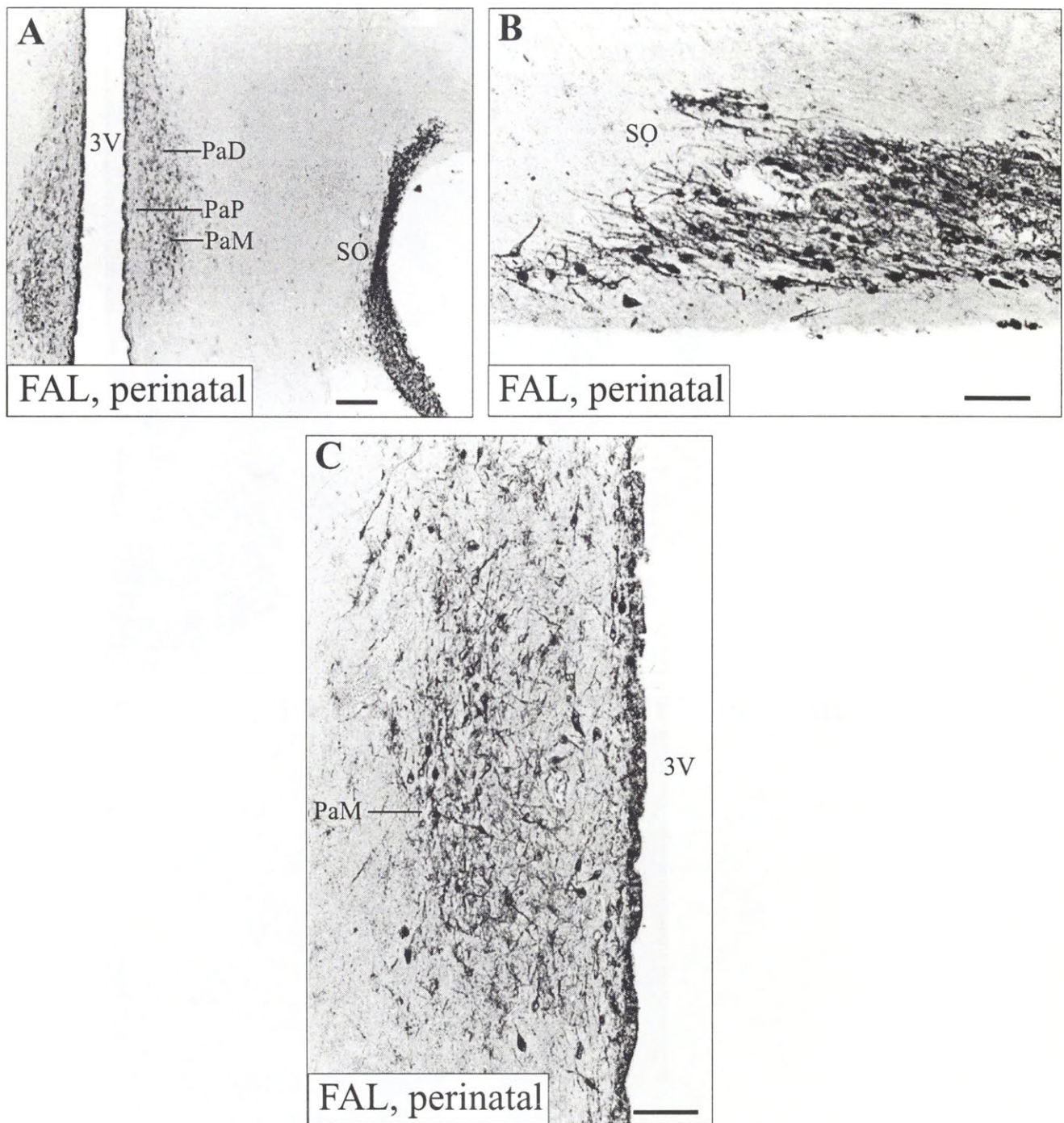


Figure 22 Photomicrographs of the coronal sections through the anterior level of perinatal hypothalamus demonstrating the distribution of FAL immunoreactivity in Pa (A) and (C) and SO (A) and (B). The area of the Pa in (A) is shown at higher magnification in (C). Note that FAL immunoreactivity is shown in numerous magnocellular neurons and fibers of SO but only some magnocellular neurons are immunoreactive in Pa (C). Scale bar indicates 0.5mm for (A) and 50 μ m for (B) and (C).

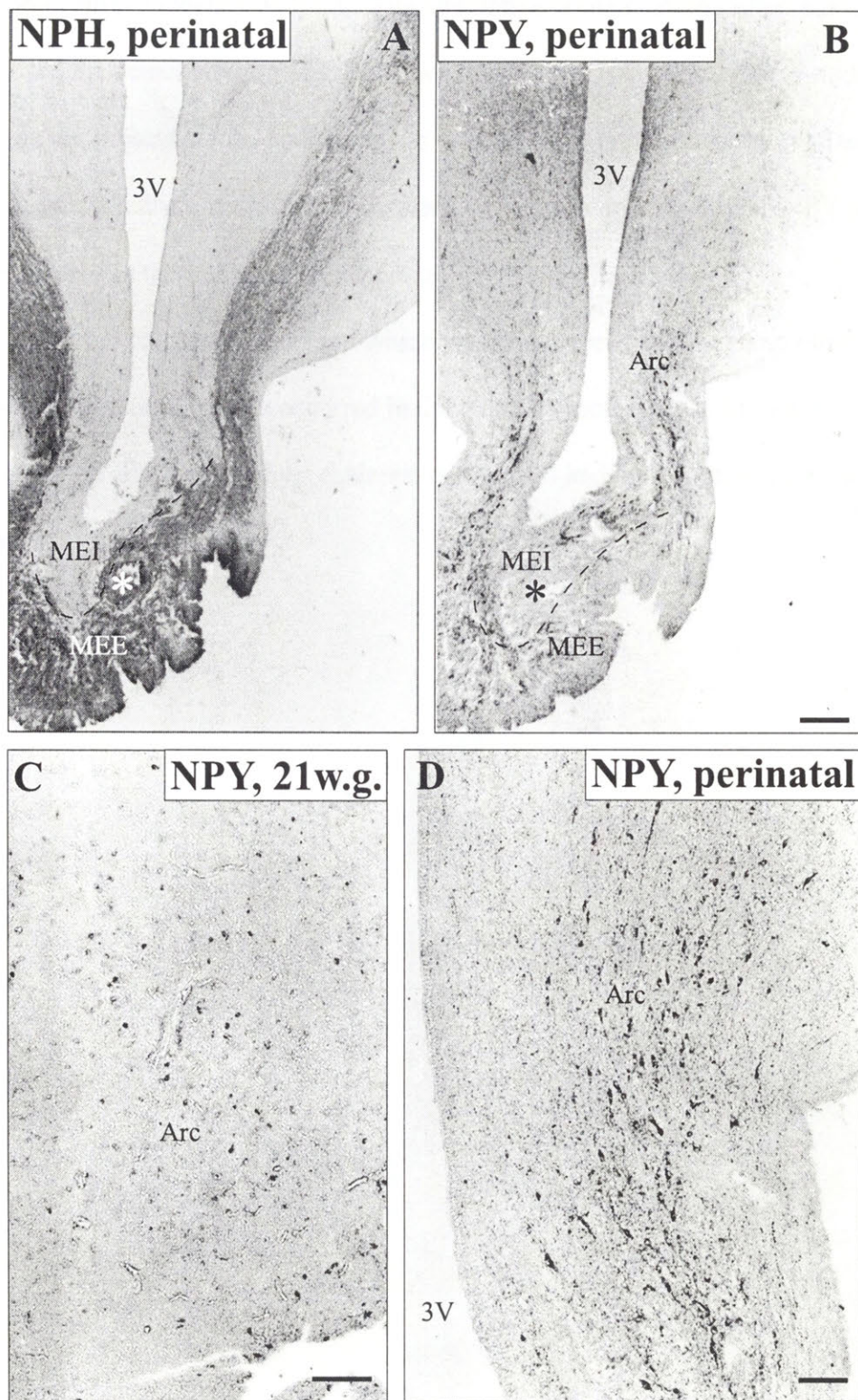


Figure 23 Photomicrographs of coronal sections through the human hypothalamus demonstrating differential distribution of NPH positive fibers and neuropeptide Y positive cells and fibers (A) and (B). This immunoreactivity reveals internal and external components of the median eminence in adjacent sections of perinatal human hypothalamus. Asterisks indicate the same blood vessel. C) First appearance of NPY-positive neurons in arcuate nucleus at 21 w.g. D) Area of arcuate nucleus in (B) at higher magnification demonstrating a population of morphologically developed NPY positive neurons. Scale bar indicates 0.5mm in (A) and (B) and 50 μ m in (C) and (D).

comprised of two unequal round parts but the name was retained due to the obvious topographic correspondence with Un. The alternative nomenclature (Allen et al, 1989) presupposed the demonstration of at least two dorsally positioned interstitial nuclei (3 and 4) not seen in the present study. In the arcuate nucleus NPY immunoreactivity revealed numerous morphologically mature ventro-medially oriented neurons and fibers. The NPY positive fibers were segregated in the internal component of ME (Figure 23B and D).

Up to the oldest age examined which was three weeks postnatal, no other significant observable structural changes occurred in the human hypothalamus. In fact, by the immediate postnatal period all the major hypothalamic cell groups had largely attained an adult like appearance.

DISCUSSION

The present experiment revealed the cyto- and chemoarchitecture of hypothalamic nuclei during fetal development. Human fetal hypothalamic nuclei are more evident than those of the adult in cytoarchitectonic preparations and even more so in chemoarchitectonic material. The findings of the present study have two major implications. Firstly, the resulting anatomical scheme of the developing human hypothalamus provides for a better understanding of the complex structural organization of the adult human hypothalamus. Secondly, the structural resolution of the human hypothalamus achieved by the present study provides new evidence for homologies with the thoroughly delineated and functionally studied rat hypothalamus. It is indeed possible to suggest human structural homologues for most of the nuclei, subnuclei and areas described in the rat. The transient pattern of hypothalamic nuclear organization observed during human fetal development provides additional evidence of similarities between species, similarities that might have remained concealed if not for the developmental approach.

Hypothalamic development is considered to be initiated with cell proliferation in the ventricular germinal zone adjacent to the wall of the 3V, followed by formation of neuroblasts or post-mitotic cell populations external to the germinal layer during the second half of gestation in the rat (Keyser, 1979; 1983; Altman and Bayer, 1986), in the middle of gestation in the cat (Wyss and Sripanidkulchai, 1985) and in the first quarter of gestation in the rhesus monkey (Keyser, 1979; van Eerdenburg and Rakic, 1994). Scarce reports on human fetal chemoarchitecture (Bugnon et al., 1982; Burford and Robinson, 1982; Ackland et al., 1983; Bloch et al., 1984; Mai et al., 1997) and cytoarchitecture (Clark, 1938; Gouldsmit et al., 1992) suggest early hypothalamic neurogenesis (circa 9-10 w.g.). Postmitotic cells, possibly guided by adhesion molecules (Mai et al., 1998), aggregate into either compact cell groups termed nuclei, or into more dispersed populations termed areas, but the mechanism of such aggregation

is still largely unclear. The onset of myelination marks the final stage of neuronal differentiation, also characterized by the formation of connections between different cell groups within and outside the hypothalamus.

It must be acknowledged that the developing human hypothalamus undergoes extensive elongation along both dorsoventral and rostrocaudal axes (Grünthal, 1952), unlike the rat hypothalamus which elongates principally in the rostrocaudal direction (Altman and Bayer, 1986). It is important to bear this aspect of fetal growth in mind when studying the organization of hypothalamic cell groups through ontogeny and phylogeny. Also, it is important to acknowledge the significance of the neuromere based structural subdivision of the embryonic hypothalamus into *regio preoptica*, *regio supraoptica*, *regio postoptica* and *regio mammillaris* (Keyser, 1979; 1983), although by the developmental period considered here (9w.g. to postnatal) those subdivisions are no longer clearly manifested. In the present study, the topography and chemoarchitecture of differentiating hypothalamic cell groups was instead consistent with three parental post-mitotic *anlagen* arranged longitudinally into *lateral*, *core* and *midline* hypothalamic zones (Altman and Bayer, 1986).

Lateral and Posterior Hypothalamus

In the present study the earliest observable structural differentiation of the hypothalamus involved the *lateral hypothalamic zone* which gives rise to the lateral hypothalamus (LH), posterior hypothalamus (PH), lateral tuberal nucleus (LTu) and perifornical nucleus (PeF).

In the rat, the lateral hypothalamic area is reportedly implicated in autonomic responses associated with cardiovascular regulation (Spencer et al., 1988; Allen and Cechetto, 1992; Cechetto and Chen, 1992), thirst, food intake and metabolism (Swanson and Mogenson, 1981;

Arase et al., 1987; Yoshimatsu et al., 1988). The projections of LH neurons, particularly from the tuberal hypothalamic region, have been followed to the parabrachial nucleus and spinal cord (Kohler et al, 1984; Cechetto and Saper, 1988). Regional differences in chemoarchitecture and connections have facilitated the distinction between preoptic, anterior, posterior and magnocellular lateral hypothalamic areas in the rat (Saper, 1985; Paxinos and Watson, 1986). In the human adult, the lateral hypothalamus occupies an area between the descending column of the fornix medially and the basal nucleus of Meynert and the fiber bundle of the ansa lenticularis laterally (Clark, 1938; Wahren, 1959; Diepen, 1962). Early studies, while distinguishing between rostral and caudal LH in the human, based their conclusions mainly on topography (Brockhaus, 1942; Feremutsch, 1952). More recent reports suggested some chemoarchitectonic similarities between LH in the rat and human (Saper, 1985; 1990), although the lateral hypothalamus in the human is viewed as a more homogeneous structure than in the rat.

In the present study, the structural differentiation of LH and PH was apparent already at 9 w.g., when these structures were marked by strong immunoreactivity for GAP43, a nerve terminal membrane phosphoprotein associated with the development and restructuring of axonal connections (Skene et.al., 1986). In the rat brain, the expression of GAP43 has been shown to coincide with the formation of axonal end-arbors, the beginning of synaptogenesis, and the period when synaptic organization can be modified by ongoing patterns of activity (Jacobson et.al., 1986; Dani et al., 1991). The present study suggests that within the hypothalamus synaptogenesis is well underway in the lateral and posterior hypothalamic areas as early as 10 w.g. In addition, GAP43 immunoreactivity clearly revealed, at 13 w.g., the otherwise ill-defined bundle x, which separates LH ventrally from PH dorsomedially.

Following the emergence of GAP43, another significant event in the differentiation of the lateral and posterior hypothalamic areas was the appearance of large Cr and Cb immunoreactive neurons at 13 and 16 w.g. respectively, and their persistence into the postnatal period. Little attention has been paid in the literature to these neurons (Sanghera, et al., 1995), while the present study revealed them to be an early permanent and prominent characteristic of the lateral and posterior hypothalamus. The mature morphological appearance of these neurons is reached by approximately 16 w.g. (Figure 20) when they liberally spread far laterally, abutting the *pallidum* and dorsally mingling with the zona incerta.

The present findings are consistent with reports from the rat (Altman and Bayer, 1986) that suggest early neuronal differentiation and synaptogenesis in the lateral hypothalamic zone. Consistent with the present results in the human fetus, the first appearance of Cb immunoreactivity in the developing rat hypothalamus was reported at Day 14 of gestation in the infundibular recess and the posterior hypothalamus (Enderlin et al., 1987), suggesting further similarities between the developing lateral hypothalamus in the rat and human. Additionally, in the present study, as well as in the rat (Enderlin et al., 1987) the adult pattern of Cb immunoreactivity was reached before birth and the same type of cells that were Cb immunoreactive in development were also positive in the adult hypothalamus. This, of course, is suggestive, but does not constitute proof that they were the same cells.

The present study showed distinct chemoarchitectonic differences between the constituent structures of the *lateral hypothalamic zone*. For example, cells in PH, but not LH, showed distinct FAL immunoreactivity from 18 w.g. until birth. Further, the area LH contained Cr and Cb positive neurons and GAP43 immunoreactivity early in fetal gestation, unlike the adjacent tuberomammillary nucleus, which acquired Cb positive neurons only late in gestation.

Finally, Chapter 2 showed abundant NK3 immunoreactivity in the PeF neurons, thus distinguishing this structure from the surrounding NK3 negative LH.

Perifornical Nucleus

In the rat, PeF has been implicated in cardiovascular regulation (Allen and Cechetto, 1992), while projections of PeF have been followed to the spinal cord (Cechetto and Saper, 1988). The distinction between PeF and LH in the rat has been demonstrated by chemoarchitectonic (Cechetto and Saper, 1988) and functional studies (Allen and Cechetto, 1992). The adult human perifornical nucleus was mainly defined on topographic criteria (Wahren, 1959; Brockhause, 1942) because cytoarchitectonically it largely resembles surrounding structures.

According to the present findings, PeF is formed as a result of passive displacement of LH neurons medially. During gestation, the neurons of lateral hypothalamus, which develop early, are progressively displaced laterally by the successive waves of neurons of the *midline* and *core* zones that develop later. In contrast to the LH neurons, the neurons of the PeF that originate from the lateral hypothalamic zone remain anchored in the perifornical position, possibly by virtue of their dendrites invading the fornical bundle. Indeed, the exchange of fibers between the perifornical nucleus and the fornix has long been suspected in different species including human (Gurdjian, 1927; Rioch, 1929; Papez and Aronson, 1934; Kühlenbeck and Haymaker, 1949; Wahren, 1959) and cells have been described inside the fornix itself (*nucleus interfornicatu* of Greving and Gagel). Consistent with these earlier reports, the present study describes Cb positive cells among the fibers of the fornix as well as circumferentially arranged around the fornix from 16 w.g. The fornix is first seen embedded within the boundaries of LH at 13 w.g. At 16 w.g., it is located medially in LH and at this stage the large Cb and Cr

containing neurons of PeF acquire a circumferential orientation around the fornix. By 20 w.g. the fornix and PeF were located on the medial boundary of LH and at the age of 23 w.g. a well differentiated PeF was seen medial to LH in the tuberal region. Further, such a mechanism of PeF differentiation would explain the greater proximity of PeF to the midline at caudal levels, which may be the consequence of the smaller cell mass of the *core* and *midline* zones in those regions. Thus, the present study suggests that the mechanism of the structural differentiation of the human PeF depends on its intimate relationship with the fornix and reinforces the distinction of PeF from the lateral hypothalamic area in the human.

Lateral Tuberal Nucleus

In the present study, LTu was seen to differentiate as a distinct parvicellular part of the lateral hypothalamic area. First evidence of LTu is seen at 15 w.g. to 18 w.g. At this age the nucleus is located within the ventrolateral part of LH, marked by GAP43 negativity within the otherwise GAP43 positive LH. This continues until LTu differentiates as a compact group of small Cb positive (but Cr negative) neurons embedded between LH and the tuberomammillary nucleus, both of which contain large Cr and Cb positive cells. The lateral tuberal nuclei were thought to occur only in primates and usually consist of two cell groups forming the tuber cinereum (Atlas and Ingram, 1937; LeGros Clark, 1938; Ingram, 1940), although Morgan (1930) described a possible LTu homologue in the dog. The LTu corresponds to the tuberal nucleus of Malone (1910) and has been described as the lateral tuberal nucleus in humans (Diepen, 1962; Nauta and Haymaker, 1969). Intrigued by pathological studies, Ingram (1940) once described LTu, together with the paraventricular and supraoptic nuclei, as the “only nuclei of consequence” in the hypothalamus. Despite great expectations, the functional significance of LTu remains unclear, although there are suggestions of a functional role of LTu in

thermoregulation, food intake and energy balance (Kremer et.al., 1990; Swaab, 1992). Thus, changes in morphometric parameters of LTu have been reported in various homeostatic disorders (see Swaab, 1992), Huntington's disease (Kremer et.al., 1990), and depression (Horn et al., 1988). Later studies identified CRF receptors, somatostatin, muscarinic cholinergic receptors, and NMDA receptors in LTu (Kremer, 1992). However, comprehensive experimental research into the function and affiliations of the LTu is held back by the lack of a rodent homologue of the nucleus.

Paxinos and Watson (1986) described the terete nucleus on the basis of Timm's staining in the rat hypothalamus, while Saper (1990) suggested that the terete nucleus in the rat may be homologous to LTu in the human. Like LTu, the terete nucleus is also a small group of

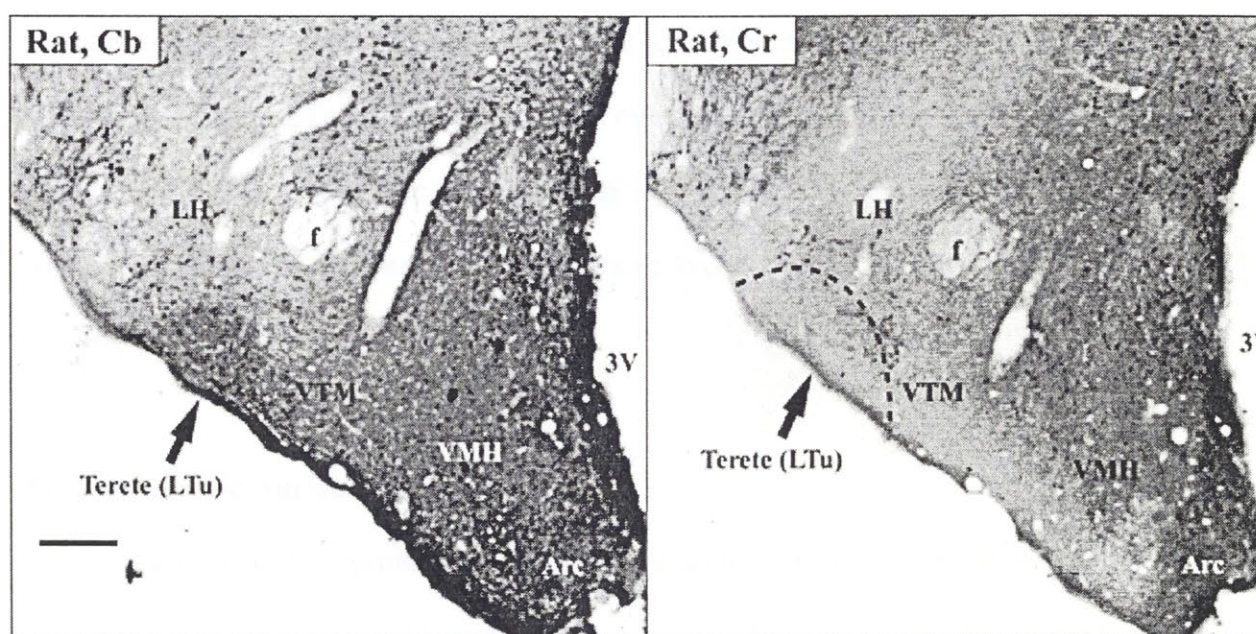


Figure 24. Photomicrographs of adjacent sections of the rat hypothalamus stained for calbindin and calretinin. The terete nucleus (arrows) shows topography and chemoarchitecture similar to that of the primates LTu. Like LTu, the terete nucleus is comprised of small tightly packed cells. Scale bar indicates 1mm.

parvocellular neurons positioned on the ventrolateral margin of the tuberal hypothalamus. The present study found an abundance of Cb, and lack of Cr, immunoreactive cells in both the LTu

and terete (Figure 24), thus providing some chemoarchitectonic evidence for homology between the nucleus in the rat and human as proposed by Saper (1990).

In the present study, the perinatal LTu was strongly labeled with synaptophysin immunoreactivity. Synaptophysin (SYN) is an abundant integral membrane glycoprotein, characteristic of presynaptic vesicles of mature neurons. It has been suggested that SYN can be involved in the late stages of synaptic vesicle formation and exocytosis. The distribution of SYN has been described in the brain and hypothalamus of mature and developing rodents (Laemle et al., et al, 1991; Tixier-Vidal et al., 1992). The present study provides the first description of SYN distribution in the developing human hypothalamus. Immunostaining for GAP43 and SYN allowed the present study to augment the criteria of structural differentiation to include the maturation of synaptic vesicles. Thus, SYN immunoreactivity found in the fornix at 13w.g. and in the LTu perinatally heralds a milestone in the maturation of these structures. To be more confident about the proposed homology between the terete and the LTu it would be comforting if these nuclei were also demonstrated to concur with respect to SYN and Timm's staining.

Medial Preoptic Nucleus

The *core of the hypothalamus* consists of a heterogeneous collection of nuclei positioned between the *lateral* hypothalamus and the *midline* structures. Major nuclei of the hypothalamic core include the medial preoptic nucleus (MPO), ventromedial nucleus (VMH), dorsomedial nucleus (DM), supramammillary nucleus (SUM) and the mammillary body (Mb).

In the present study, similarities in topography and time of differentiation, suggested a topographical affinity of the medial MPO (MPOM) and the intermediate (or sexually dimorphic) nucleus. The inverted comma shaped MPO was first identified at 10 w.g. by

transient Pv immunoreactivity. By 16 w.g., the MPO was harboring a population of Cb immunoreactive neurons. At the same gestational period, the intermediate nucleus (InM) was depicted in the rostral anterior hypothalamus, topographically overlapping the lateral portion of the Cb positive MPO. Because the medial MPO (MPOM) in the adult is characterized by Cb immunoreactive neurons, it is suggested that at 16 w.g. most of the nucleus is represented by MPOM and at this stage the InM is embedded in the lateral surface of MPOM. This is an important point, because until now one of the main arguments against the homology of the human InM and the rat central MPO (MPOC) has been the location of the InM within the lateral MPO in the human, heterologous to the more medial position of the rat MPOC, within the MPOM. It is proposed that the MPOM, with its constituent InM, is displaced medially by the subsequent development of a MPOL (see Figure 25 below).

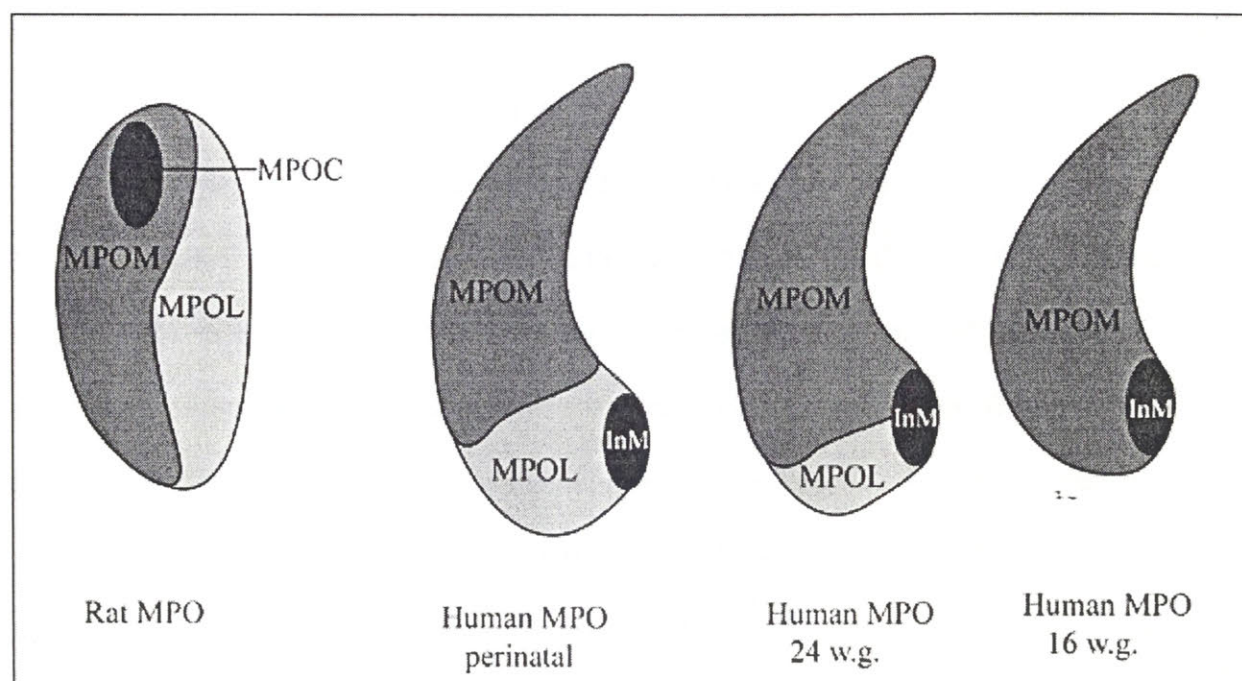


Figure 25. Schematic diagram showing topographic relationship between the MPO subnuclei in the adult rat and in the human fetus at different stages of gestation. The diagrams are not to scale.

Originally described by Brockhaus (1942) the InM is known to be sexually dimorphic (Swaab and Fliers, 1985; see Chapter 3). The sexual dimorphism of InM, however, has been shown to occur as late as 2-4 years postnatal, presumably due to selective cell death in females (Hofman and Swaab, 1989). Thus, it is unlikely that InM plays any important role in sexual differentiation at such an early developmental stage as 16 w.g. Further, the function of InM is not clear, but current evidence from experiments in the rat suggests that this cell group may have some other function apart from regulating the endocrine aspects of sexual behavior (Turkenburg et al., 1988; De Jonge et al., 1989). The present study showed that the InM abuts MPOM early in development, coming one step closer to establishing a homology with MPOC in the rat (Fliers et al., 1994; Gao and Moore, 1996). Further, the present study showed that the perinatal uncinate nucleus is topographically associated with the PaD rather than with MPO, thus evicting the Un from the list of probable candidates for the human homologue to the rat MPOC, in contrast to the suggestion of Allen et al (1989).

The topographic position and shape of the MPOM in the present study corresponds to the posterodorsal preoptic area described in the rat by Altman and Bayer (1986) (denoted as MPO in other nomenclature: Gorski et al, 1978; Paxinos and Watson, 1998) providing additional evidence of homology between the nuclei in the rat and human. Thus, in both species, MPOM assumes the form of a lower canine shaped nucleus, whose dorsolateral tip merges with the bed nucleus of the stria terminalis (Altman and Bayer, 1986). However, despite the topographical proximity of the MPO and the BST, these structures were shown to be derived from different neuroepithelial origins, namely the third and lateral ventricles, respectively (Altman and Bayer, 1986). The present results demonstrate that the structural organization of the MPO complex in the human fetus strongly resembles the fetal rat MPO; these results establish a greater degree of homology between the adult rat and human MPO.

Ventromedial Hypothalamic Nucleus

In the present study, the ventromedial hypothalamic nucleus was first detected at 10 w.g. as a round aggregation of postmitotic neurons in a ventromedial position within the hypothalamus. By 13 w.g., VMH contained a well differentiated dorsomedial part (VMHDM) characterized by a prominent population of Cb immunoreactive neurons and a bigger ventrolateral part (VMHVL) harboring Cr-positive cells. This complimentary distribution of Cr and Cb positive neurons also differentiates ventrolateral and dorsomedial subnuclei in the adult human VMH and was recently reported in the VMH of the rat (Paxinos et al., 1998; Brager et al., 2000). In the rat, the VMHVL and VMHDM are distinguished by their cytoarchitecture (Gurdjian, 1927) and have substantial differences with respect to their connections (Saper et al., 1976; Canteras, et al., 1994) and physiology (Simerly et al., 1990). Moreover, the neurons of the VMH subnuclei in the rat also differ in the timing of neurogenesis (Altman and Bayer, 1986). The present findings provide chemoarchitectonic evidence of the early distinction between these subnuclei in the human fetal VMH. However, the similarity in the timing of the subnuclear differentiation supports the consideration of the VMH as a consolidated whole.

At 13 w.g., FAL immunoreactive radial glial fibers (Mai et al., 1998) arch from the ventricular wall towards the VMH. The place of origin of radial glia in the middle of the sub-sulcal ventricular wall suggests the neuroepithelial site of origin of VMH. This area on the periventricular neuroepithelium corresponds to the medial boundary of the dorsomedial hypothalamic nucleus at 10 w.g., suggesting similar *anlage* for VMH and DM. These findings are also consistent with the original report of Altman and Bayer (1986) on the neuroepithelial origin of the VMH and DM in the rat. These ontogenetic and topographic similarities are consistent with the comparable connectivity and functional associations of the two nuclei (Luiten and Room, 1980; Luiten et al., 1987; Thompson et al., 1996).

In the present study the VMH was encompassed at 16 w.g. by a bundle of GAP43 positive fibers which effectively formed a shell reminiscent of the cell poor shell seen in the rat. In the rat and cat a body of evidence points to the shell of the VMH as a target for amygdalo-hypothalamic projections carried via the stria terminalis and associated with emotion-driven learning (Millhouse, 1973; Conrad and Pfaff, 1976; De Olmos and Carrer, 1978; Krettek and Price, 1978; Post and Mai, 1980; Kita and Oomura, 1982). The present study reports chemoarchitectonic evidence for a VMH shell in the human fetus and tentatively suggests an additional structural homology between the rat and the fetal human VMH. However, it must be noted that neither the adult rat nor adult human VMH demonstrate GAP43 immunoreactivity, suggesting that these synapses are not as labile in the adult. Thus, the present results, when compared with the description of VMH neurogenesis in the rat (Altman and Bayer, 1986), suggest a similar pattern of structural differentiation of VMH in the rat and human.

Ventral Tuberomammillary Nucleus

The ventral tuberomammillary nucleus featured in the tuberal hypothalamic region from 13 w.g. It was characterized by an accumulation of transiently Pv-positive cells on the ventral surface of the tuberal hypothalamus. Recent delineations of the nucleus in the human either considered the entire lateral and ventral hypothalamus together (Braak and Braak, 1992) or omitted the exact boundaries of the nucleus because of cytoarchitectonic similarities with the lateral hypothalamus (Saper, 1990). The first issue to resolve in the present study was whether to use the term tuberomammillary (TM) or ventral tuberomammillary (VTM). In the rat, there are two tuberomammillary nuclei - the ventral and the dorsal. No dorsal nucleus was found in the human (abutting 3V as seen in the rat, Paxinos and Watson, 1998), while the position of the human tuberomammillary nucleus resembles that of the rat VTM, thus prompting the presently

adopted term. The nucleus is differentiated by 23 w.g., with the appearance of dispersed spindle shaped large Cb-positive neurons. In its posterolateral part, the VTM borders the mammillary body, while PeF forms the dorsal boundary of the nucleus. The lateral boundary of VTM is formed by LH, which has a striated appearance. Medially VTM borders the ventrolateral boundary of the VMH. The present findings will help to resolve the ambiguity concerning boundaries of the human VTM, which may have hindered the interpretation of recent connectivity studies of human hypothalamus (Dai et al., 1997; Dai et al., 1999). The topography and cytoarchitecture of the VTM in the present study corresponds to the characteristics of the tuberal magnocellular nucleus (Altman and Bayer, 1986) described in the developing rat hypothalamus. The neuroepithelium of the rat caudal mammillary recess was suggested as the origin of VTM neurons (Altman and Bayer, 1986).

In the present study, despite the early appearance of transient Pv immunoreactivity in VTM, the differentiation of this nucleus is likely to occur relatively late in gestation, as heralded by the appearance of magnocellular Cb immunoreactive cells. In the rat, VTM is also characterized by late differentiation and neurogenesis in contrast to the structures of the *lateral zone*, which develop early (Altman and Bayer, 1986). Also in the rat, the neurons of the VTM were reported to bind estrogen (Pfaff and Keiner, 1973) and contain estrogen receptors (Simerly et al., 1990), while the projections of the nucleus extend widely to the periventricular hypothalamus, zona incerta, rostral thalamus, septum and amygdala, generally resembling projections of the VMHVL (Canteras, et al., 1994). In light of differences in the timing of differentiation, chemoarchitecture and topography of the two structures in the fetus, the present study did not find evidence in the human fetus to support the view that the VTM is a lateral component of VMH (Canteras, et al., 1994).

Dorsomedial Nucleus

In the present experiment, the 9 and 10 w.g. hypothalamus contained a clearly defined DM positioned just ventral to the hypothalamic sulcus and composed of a compact part and a diffuse part. The bigger, diffuse part was positioned more medially near the ventricular wall and contained dispersed small immature cells. The smaller compact part was composed of small tightly packed cells and positioned more laterally surrounded by the diffuse DM. This organization persisted in the 13 w.g. fetus, but by the 23rd w.g. the differentiated DM is a well defined but largely homogenous cell group demonstrating poor distinction between the compact and diffuse compartments.

In the rat, DM originates from the same neuroepithelial *anlage* as VMH (Altman and Bayer, 1986) and in the adult rat it is structurally comprised of a cell dense compact part, conspicuous ventral part and poorly defined dorsal part (Krieg, 1932; Paxinos and Watson, 1998). Despite the clear cytoarchitectonic boundaries of DM found in the early human fetus, the nucleus is never as prominent as in the adult rat, pointing at an interspecies difference in hypothalamic organization. Aside from the relative size of the nucleus, there is an inverse progression of subnuclear complexity with advancing age in the two species. Thus, the most complex structural appearance of the nucleus is found early in gestation in the human, but postnatally in the rat (Altman and Bayer, 1986). This means that the rat DM becomes more differentiated into subnuclei with advancing age, but the human DM becomes less differentiated into subnuclei with advancing age. Further, even at its most complex phase in the human (fetal 10-13w.g.) the nucleus is not as complex as in the perinatal rat.

Mammillary body

The present study found two distinct cell populations comprising the mammillary body: a larger medial and a smaller lateral mammillary nucleus. These were identifiable already at 10 w.g. The MbM was a dispersed collection of neurons occupying most of the core of the caudal hypothalamus, while MbL lined the hypothalamic pial surface ventral to LH. At 13 w.g. MbM assumed a round form tightly wrapped dorsally (and later at 16 w.g. dorsomedially) by mammillothalamic tract. At the same gestational age, the fornix reached the lateral boundary of MbM, while the droplet-shaped MbL was a lateral neighbor to MbM. This structural pattern of the mammillary complex was most clearly differentiated at 16 w.g. At 26 w.g., MbM was subdivisible into a bigger medial part and a smaller lateral part penetrated by the fibers of the fornix. After 23 w.g., MbL was not as prominent as at 16 w.g., but was still distinguishable in Nissl preparations. With respect to the medial and lateral Mb the structural pattern of differentiation reported by the present study in the human corresponds to the developmental pattern described for these cell groups in the rat (Altman and Bayer, 1986). On the other hand, Altman and Bayer (1986) reported that the neurons in the rat MbL had earlier birth dates than those of MbM, while in the present study the nuclei differentiated at the same time.

In the rat, Mb has a complex subnuclear organization. The medial Mb is comprised of three subnuclei; the median, the dorsal, the medial and the lateral (Paxinos and Watson, 1998). The neurons of the lateral Mb are thought to be generated earlier than the neurons of the larger medial Mb. Topographically organized projections of the Mb reach the anterior thalamic nuclei via the mammillothalamic tract (Seki and Zyo, 1984), and dorsal and ventral tegmental nuclei via the mammillotegmental tract (Cruce, 1977). The poor development of the mammillotegmental tract in the human is possibly associated with poor development of the

lateral Mb as seen in the adult human (Saper, 1990).

Supramammillary nucleus

In the present study, at 16 w.g., a well defined group of small cells identified as the supramammillary nucleus was seen within the mammillary hypothalamus. Earlier in gestation, the cells of this nucleus were probably dispersed throughout the posterior levels of the hypothalamus ventral to the PH, medial to the mamillothalamic bundle, and lateral to the caudal 3V neuroepithelial primordium. However, in the absence of cyto- or chemoarchitectonic clues, this speculation is based only on topographic considerations. It is surprising that SUM is not present in fetuses older than 18 w.g. nor in the adult human, suggesting a rudimentary role of this cell group or a rudimentary significance of grouping for these cells in the human. The observed human fetal SUM corresponds to the rat SUM with respect to both topography and cytoarchitecture (Altman and Bayer, 1986), suggesting homology of the structures. The neurons of the rat SUM contain calretinin, calbindin, VIP, substance P, CCK and glutamate (Kiss et al, 1997). In the present study, neither Cr or Cb immunoreactivity was detected in SUM neurons at 16 w.g. nor in the topographically corresponding area at later gestational stages. In the rat, the function of SUM is unclear, although extensive reciprocal affiliations with the raphe nucleus, septal nuclei and dentate gyrus suggested that SUM may provide a relay in memory function of the brainstem-diencephalo-septo/hippocampal systems (Vertes and Kocsis, 1997; Borhegyi and Freund, 1998; Leranth et al., 1999). Otherwise, the connections of SUM neurons were shown to resemble the connections of the lateral hypothalamus, and mammillary body (Swanson and Cowan, 1979; Saper et al., 1979; Haglund et al., 1984). Some importance of SUM neurons in the regulation of metabolism was recently suggested by the demonstration of the altered function of SUM

neurons in genetically obese mice (Huang and Wang., 1998), but this direction of research is itself at the embryonic stage.

Paraventricular and Supraoptic Nuclei

The midline hypothalamus is comprised of structures differentiating in direct proximity to the ventricular wall and includes the suprachiasmatic nucleus (SCh), the arcuate nucleus (Arc), the paraventricular nucleus (Pa) and the supraoptic nucleus (SO). In the present study, during early stages of fetal development (i.e. 9-10 w.g.) the premordia of the midline structures were concealed in a thick periventricular neuroepithelium and the structures became evident only late in gestation.

The fetal development of the paraventricular and supraoptic hypothalamic nuclei has been previously studied using NPH chemoarchitecture in the human (Mai et al., 1997); therefore, this discussion considers only aspects of Pa and SO development which have not already been described. In the present study, the Pa and SO are considered jointly because of the apparently common neurogenetic *anlage* shared by the majority of the large neurons comprising the nuclei (Choy and Watkins, 1979; Altman and Bayer, 1986; van Eerdenburg and Rakic, 1993; Mai et al., 1997).

The present findings are consistent with previous reports of a dorsal-to-ventral gradient of Pa development reported in the rat (Choy and Watkins, 1979; Altman and Bayer, 1986), monkey (van Eerdenburg and Rakic, 1993) and human (Mai et al., 1997). On the other hand, the developmental gradient of the rat Pa is also characterized by a prominent lateral-to-medial horizontal vector (Altman and Bayer, 1986). Compared with the rat, the human Pa extends significantly more dorsoventrally and significantly less mediolaterally. This latter mediolateral

neurogenetic and differentiation gradient is of significance because it apparently underlies the subnuclear differentiation of the Pa (Altman and Bayer, 1986).

In the present study the onset of differentiation for the caudal part of the Pa (PaPo) and SO occurs as early as 10 w.g., and by 18 w.g. PaPo resembles its postnatal morphology and topography. From 16 to 18 w.g., a more anterior portion of the nucleus – the dorsal Pa (PaD) - undergoes structural differentiation to reach its adult-like appearance. At the same gestational age of 18 w.g. the densely packed, but yet morphologically immature, magnocellular neurons of PaM begin to form that subnucleus ventral to PaD. The neurons of PaM reach their postnatal morphological appearance by 23 w.g. From 23 w.g., the PaM, PaD and PaPo demonstrate a prominent population of small Cb positive neurons, also found in the postnatal and adult Pa. These findings are consistent with findings in the developing rat Pa where neurons of the medial magnocellular and posterior subnuclei develop before the neurons of the lateral magnocellular Pa, which contain vasopressin (Rhodes, et al., 1981; Swanson and Sawchenko, 1983; Altman and Bayer, 1986). This finding provides additional evidence (to that already described in Chapter 2) of homology between PaM in the human and PaLM in the rat, PaD in the human and PaMM in the rat, and PaPo in both species. This evidence also points to a similar dorso-ventral gradient of differentiation of the developing Pa in both rat and human.

In the fetal Pa the magnocellular neurons are more confined to the limits of the subnuclei (as shown in chapter 2) than in the adult. Thus, from 18 w.g. a population of parvicellular neurons is forming PaP and there are only fewer stray magnocellular neurons mingling with them compared with the adult PaP. The PaP reaches its perinatal appearance by 26 w.g., extending rostrally to the level of the optic chiasm. These findings point to a similar latero-medial gradient of differentiation in the rat (Altman and Bayer, 1986) and the human Pa. Gouldsmit and colleagues (1992) reported that the number of neurons in the adult human Pa is

reached by 26 w.g. The present study showed that the adult-like subnuclear organization of Pa can be seen at 26 w.g. Interestingly, starting from 26 w.g. and also in older brains, the magnocellular Pa and SO neurons featured strong FAL immunoreactivity.

Considering the spatial differences between Pa in the rat and human the present findings demonstrate a remarkable similarity in the developmental pattern of the nucleus in these phylogenetically distant species. With respect to the human Pa development, the present results suggest that the large Pa cells differentiate early in gestation following the pattern of SO and accessory cells, while the parvicellular PaP cells form into a subnucleus late in gestation, similar to other midline structures.

Arcuate nucleus

In the present study, the arcuate nucleus (Arc) was concealed before 13 w.g. within the funnel of tightly packed periventricular primordium between the floor of the posterior third ventricle and ventral hypothalamic surface (Figure 2 F,G,H). From 18 w.g. the Arc harbors a prominent Cb immunoreactive fiber bundle reaching from the ventricular surface to the ventral pial surface of the hypothalamus. By 26 w.g. this bundle occupies the entire area of Arc and persists into the perinatal period. In the rat, postmitotic Arc neurons migrate ventrolaterally from the ventral third ventricular neuroepithelium (Altman and Bayer, 1986). There is no definitive evidence that would characterize Cb immunoreactivity as a marker of radial glial fibers, and, of course, the morphological analysis of these fibers would require electron microscopy. However, based entirely on topography, it is tempting to speculate that these fibers belong to radial glia.

The earliest NPY immunoreactivity in Arc neurons was seen at 21 wg. Between this age and birth, these NPY positive neurons increase in number and differentiate

morphologically, extending their axons into the median eminence; some NPY positive cell bodies are also found in the median eminence. These cells and fibers are topographically located directly dorsal to the NPH positive neurohaemal pathway from the SO and Pa. Conclusive experimental evidence from the rat and mouse indicate that the NPY producing neurons in Arc are a critical part of the hypothalamic neuronal network regulating eating behavior and energy expenditure (Stephens, et al, 1995; also for reviews see Leibowitz, 1991; Frankish et al., 1995). In the rat, these NPY producing neurons were shown to project to the parvocellular and dorsal Pa (Baker and Herkenham, 1995) and to the internal component of the median eminence (Chronwall et al., 1985; also see Simerly, 1995) and so influence autonomic and endocrine activity. The present findings are consistent with previous reports on the peptide distribution in the adult human Arc (Adrian, 1985) and, in addition, indicate relatively late morphological differentiation of the NPY positive cells in Arc. Considering the pivotal role of these NPY neurons in regulation of feeding behavior and related fluctuations of energy expenditure, the late maturation may indicate that in earlier gestational periods fetal metabolism is regulated by a different system to that in the adult.

In the rat, Arc is positioned in the doorway to the infundibulum and provides major projections to the median eminence. It constitutes a pivotal component of the tuberoinfundibular system which apparently regulates output from the anterior pituitary (Lechlan, et al., 1982). Apart from the already mentioned pathway to Pa, other projections of Arc neurons were traced to the ventromedial hypothalamic nucleus, parabrachial nucleus and spinal cord, suggesting that Arc may play a role in regulation of the autonomic function (Swanson and Kuypers, 1980; Cechetto and Saper, 1988; Moga et al., 1990, also see Saper, 1995). Chemoarchitectonically Arc is arguably the most diverse cell group in the brain with respect to neuroactive substances in the rat (Simerly, 1995). In the adult human, Christ (1951)

made a profound observation of the close relationship between the cerebrospinal fluid in 3V and the Arc. He revealed that Arc as well as the infundibulum itself lack the inner layer of glial fibers which separate ependyma from the neurons of the hypothalamus and, thus, formed an anatomical basis for the idea of diffusion exchange of molecules between the neurohypophysis and the brain. Examples of molecules using this pathway may include the *obese* gene product leptin (Stephens, et al, 1995). Neuroactive substances found in the rat Arc, including neurokinin B, somatostatin, neurotensin, luteinizing hormone-releasing hormone (LHRH) and catecholamines, are also reported in the neurons of the human Arc (Spencer et al., 1985; Schwanzel-Fukuda et al., 1989; Swaab, 1993; Chawla, et al., 1997). Morphological changes in Arc including hypertrophy of neurons containing increased amounts of Neurokinin B have been documented in women suffering from postpartum hypopituitarism, hypogonadal men and malnourished patients (Rance, 1992). In Kallman syndrome, LHRH containing neurons apparently fail to migrate from the olfactory placode to the brain and are thereby absent from Arc in the adult (Schwanzel-Fukuda et al., 1989; Swaab, 1993).

The present study described the distribution of NPY and NPH in the median eminence of the perinatal human. The complimentary distribution of these markers allowed for the distinction between the external and internal segments of the median eminence. This distinction is consistent with the organization of ME in the rat (Wiegand and Price, 1980). Thus, internal ME is associated with the pathways and output regulation of the anterior pituitary, while the external ME harbors a direct pathway to the posterior pituitary.

Suprachiasmatic Nucleus

Chemoarchitecture revealed the boundaries of the SCh in the fetal hypothalamus far earlier than cytoarchitecture. None the less the nucleus was nowhere to be found until 23 w.g.

when it was revealed by GAP43 immunoreactivity to be made up of two subnuclei: a GAP43 positive dorsal SCh that was connected by a GAP43 positive fiber bundle with the optic tract and the AVP immunoreactive central SCh. This, of course, does not mean that the nucleus was not differentiated at all before 23 w.g. but rather, that the present study simply did not recognize the nucleus in its early cytoarchitectonic appearance. These findings are also consistent with reports showing that levels of AVP and NPH are not found in the SCh early in fetal development but instead develop quite rapidly in the perinatal period (Reppert, 1992). Later in gestation the central SCh also contained numerous Cb positive cells while the dorsal subnucleus harbored many NPH positive neurons (Mai et al., 1997). This structural and chemoarchitectonic organization is consistent with organization of SCh found in the adult (Mai et al., 1991).

The present findings indicate the late differentiation of SCh consistent with that of other nuclei of *midline* zone. In the rat SCh neurons are generated late in gestation, last of hypothalamic nuclei (Altman and Bayer, 1986), while in the monkey SCh neurogenesis was reported early in gestation (van Eerdenburg and Rakic, 1993). Also, apart from the late appearance of Cb positive neurons in the central SCh the present study found no difference in timing of SCh subnuclear differentiation. Altman and Bayer (1986) on the other hand showed evidence of two consecutive waves of neurogenesis of ventromedial and dorsomedial SCh. Subnuclear organization of the human SCh has been comprehensively shown with chemoarchitecture (Mai et al., 1991).

CONCLUSION

In the present study the use of chemoarchitecture in human fetal development permitted a more confident identification of nuclear organization compared to that which would be afforded with cytoarchitecture. Nuclear organization in the fetal hypothalamus is more distinct than in the adult. De Clark (1938) originally made this observation on the basis of cytoarchitecture. The present chapter extended this approach to demonstrate in a comprehensive way that chemoarchitecture is advantageous in revealing the hypothalamic nuclei during development.

Confidence in identification of nuclear boundaries in the human hypothalamus allows for a more confident establishment of homologues with the rat. An indication of usefulness of this approach is that structures that were thought to be long lost in the human brain can be seen during development (like SUM) and structures that were thought to be heterologous are found to be homologous (like LTu and MPO).

CHAPTER 7

General Discussion/Conclusions

The general discussion presented here is concerned with general issues relevant to this thesis. The reader will find relevant specific discussions at the end of each chapter.

The work reported in this thesis shows that the human hypothalamus is significantly more homologous to the hypothalamus of the rat than previously thought. First, four of the five subnuclei identified in the Pa of the human were found to be homologous with subnuclei of the rat Pa, thus advancing the resolution of homology to the subcompartmental organization of this nucleus. Second, the present study may have solved the mystery of non existence of a lateral tuberal nucleus in the rat by presenting evidence in favor of the notion that the rat terete nucleus is homologous to the primate lateral tuberal nucleus. Third, the present study showed homology in the neurokinin B related hypothalamic network in the rat and human by revealing the similarities of the neurokinin B receptor distribution between the species. Fourth, the present study showed analogous developmental patterns in the rat and human hypothalami with respect to nuclear differentiation (for example three parental longitudinal zones each associated with specific nuclei are evident in the development of both species). Fifth, the present study showed transient homologues of cell groups that are prominent in the adult rat, but are seen only in the fetal human (e.g. SUM).

The combination of chemoarchitecture and development has proven a powerful paradigm for establishing hypothalamic nuclear homologues. Previously hypothalamic development was also used to reveal organization of the human hypothalamus but mainly with cytoarchitecture (Gilbert, 1935; Clark, 1938; Kahle, 1956; Richter, 1965). There were also occasional reports on fetal development of individual chemical substances (Bugnon et al., 1982; Burford and Robinson, 1982; Ackland et al., 1983; Bloch et al., 1984; Trandafir et al.,

1988; Mai et al., 1997), but no systematic chemoarchitectonic study of the nuclear differentiation.

In the present thesis chemoarchitecture has been utilized in two ways; one related to the presence of the neuroactive substance itself and another related to the structural boundaries this substance reveals. The first approach infers homology on the basis of similar neuroactive content of the putative homologue across species. For example, vasopressin and oxytocin in chapter 2 and neurokinin B receptor in chapter 3 were used to establish homologies. The second approach infers homology on the basis of unambiguous borders at times revealed by the distribution of these neuroactive substances.

At times homologous nuclei in different species do not correspond fully in their chemical profile. For example no one would dispute the homology of the basal nucleus in the rat and human established on the basis of cyto- and chemoarchitecture. Yet with respect to some substances, including calbindin, these cells have opposite profiles in the rat and human. In the present study AChE positive cells were found in the human MPOM and, thus, helped to reveal the subnucleus with confidence, but these cells are not featured in the rat MPOM. However, in the present study, chemoarchitecture granted confidence about the borders of this subnucleus revealing proportions and position which correspond to the homologous structure in the rat.

The topography of some human hypothalamic nuclei has hitherto been as stable as shifting sand dunes and their rat homologues a mystery. The present thesis used chemoarchitecture and development to anchor some of these nuclei and to propose their homologues. The structural plan presented in this thesis permits a better understanding of the human hypothalamus than hitherto possible and harmonizes the organization of some of the major nuclei with that of the rat. This work may prove of value to scientists/clinicians, who,

after developing initial physiological prototypes in the rat, may wish to undertake diagnosis, pathological studies and therapeutic interventions in the human.

LITERATURE CITED

- Abe, J., H. Okamura, T. Kitamura, Y. Ibata, N. Minamino, H. Matsuo, W.K. Paull (1988) Immunocytochemical demonstration of dynorphin (PH-8P)-like immunoreactive elements in the human hypothalamus. *J. Comp. Neurol.* 276: 508-513
- Ackland, J., S. Ratter, G.L. Bourne, L.H. Rees (1983) Characterization of immunoreactive somatostatin in human fetal hypothalamic tissue. *Regul. Pept.* 5: 95-101
- Adrian, T.E., J.M. Allen, S.R. Bloom, M.A. Ghatei, M.N. Rossor, G.W. Roberts, T.J. Crow, K. Tatemoto and J.M. Polak (1983) Neuropeptide Y distribution in human brain. *Nature* 306: 584-586
- Alam, M.N., R. Szymusiak, and D. McGinty (1995) Local preoptic /anterior hypothalamic warming alters spontaneous and evoked neuronal activity in the magnocellular basal forebrain. *Brain Res.* 696: 221-230
- Allen, G.V. and Cechetto (1992) Functional and anatomical organization of cardiovascular pressor and depressor sites in the lateral hypothalamic area: I. Descending projections. *J. Comp. Neurol.* 315 : 313-332
- Allen, L.S., M. Hines, J.E. Shrine, R.A. Gorski (1989) Two Sexually Dimorphic Cell Groups in the Human Brain. *J. of Neuroscience* 9: 497-506
- Alonzo, J.R., F. Sanchez, R. Arevalo, J. Carretero, J. Aijon, and R. Vazquez (1992) CaBp D-28k and NADPH-diaphorase coexistence in the magnocellular neurosecretory nuclei. *Neuroreport* 3: 249-252.
- Altman, J., and S.A. Bayer (1986) The Development of the Rat Hypothalamus. *Advances in Anatomy Embryology and Cell Biology* 100: Springer-Verlag.
- Antoni, F.A., M. Palkovits, G.B. Makara, E.A. Linton, P.J. Lowry, and J.Z. Kiss (1983) Immunoreactive corticotropin-releasing hormone in the hypothalamoinfundibular tract. *Neuroendocrinology* 36: 415-432
- Antunes, J.L., and E.A. Zimmerman (1978) The hypothalamic magnocellular system of the rhesus monkey: An immunohistochemical study. *J. Comp. Neurol.* 181: 539-566.
- Arai R., D.M. Jacobowitz and D. Shigeyuki (1993) Colocalization of calbindin- $\tilde{D}28k$ with vasopressin in hypothalamic cells of the rat: double-labeling immunofluorescence study. *Brain Res.* 623: 342-345
- Armstrong, W.E. (1995) Hypothalamic Supraoptic and Paraventricular Nuclei. In: G. Paxinos (Edr.), *The Rat Nervous System*, Academic Press, Sydney, pp: 377-390
- Armstrong, W.E., S. Watch, G.I. Hutton and T.H. McNeill (1980) Subnuclei in the rat hypothalamic paraventricular nucleus: a cytoarchitectural horseradish peroxidase and immunohistochemical study. *Neuroscience* 5: 1931-1958
- Atlas, D., and W.R. Ingram (1937): Topography of the Brainstem of the Rhesus monkey with special reference to the Diencephalon. *J. Comp. Neurol.* 66: 263-289
- Babinski, J. (1900) Tumeur du corps pituitaire sans acromegalie et avec arret de developement des organes genitaux. *Rev. Neurol.* 8: 531-533

- Baker, R. A. and M. Herkenham (1995). Arcuate nucleus neurons that project to the hypothalamic paraventricular nucleus: neuropeptidergic identity and consequences of adrenalectomy on mRNA levels in the rat. *J. Comp. Neurol.* 358: 518-530
- Barry, J. (1975) Essai de classification, et technique de Golgi, des diverses catégories de neurones du noyau paraventriculaire chez le souris. *C. R. Soc. Biol.* 145:1088-1091
- Beaudet, A. and L. Descarries (1979) Radioautographic characterization of a serotonin-accumulating nerve cell group in the adult rat hypothalamus. *Brain Res.* 160: 231-243
- Behbehani, M.M., T.M. Da Costa Gomez (1996) Properties of a projection pathway from the medial preoptic nucleus to the midbrain periaqueductal gray of the rat and its role in the regulation of cardiovascular function. *Brain Res.* 740:141-50
- Beitz, A.J. (1982) The organization of afferent projections to the midbrain periaqueductal gray of rat. *Neuroscience* 7: 133-159
- Bergeron, C., K. Kovacs, C. Ezrin, C. Mizzen (1991) Hereditary diabetes insipidus: an immunohistochemical study of the hypothalamus and pituitary gland. *Acta Neuropathol.* 81: 345-348
- Berk M.L., A.B. Butler (1981) Efferent projections of the medial preoptic nucleus and medial hypothalamus in the pigeon. *J Comp Neurol* 203:379-99
- Bernardis L.L. (1975) The dorsomedial hypothalamic nucleus in autonomic and neuroendocrine homeostasis. *Can J Neurol Sci* 2: 45-60
- Bernardis, L.L. and J.K. Goldman (1972) Growth and metabolic changes in weanling rats with lesions in the dorsomedial hypothalamic nuclei. *Brain Res.* 15: 424-429
- Bernardis, L.L. and L.L. Bellinger (1987) The Dorsomedial Hypothalamic Nucleus Revisited: 1986 Update *Brain Res. Rev.* 12:321-381
- Bernardis, L.L. and L.L. Bellinger (1998) The Dorsomedial Hypothalamic Nucleus Revisited: 1998 Update *P.S.E.M.B.* 218: 284-306
- Bernstein, H.G., A. Stanarius, B. Baumann, H. Henning, D. Krell, P. Danos, P. Falkai, B. Bogerts (1998) Nitric oxide synthase-containing neurons in the human hypothalamus: reduced number of immunoreactive cells in the paraventricular nucleus of depressive patients and schizophrenics. *Neuroscience* 83: 867-75
- Blair, R. and W. Byne (1985) Septum and Hypothalamus In: G. Paxinos (Edr.), *The Rat Nervous System, Volume 1, Forebrain and Midbrain*, Academic Press, Sydney, pp: 87-118.
- Bleier, R. (1984) *The hypothalamus of the Rhesus Monkey. A Cytoarchitectonic atlas.* Madison: The university of Wisconsin Press.
- Bloch, B., R.C. Gaillard, P. Brazeau, H.D. Lin, N. Ling (1984). Topographical and ontogenetic study of the neurons producing growth hormone-releasing factor in human hypothalamus. *Regul. Pept.* 8: 21-31
- Borhegyi Z., T.F.Freund (1998) Dual projection from the medial septum to the supramammillary nucleus in the rat. *Brain Res. Bull.* 46:453-9

- Borson-Chazot, F., D. Jordan, M. Fevre-Montange, N. Kopp, J. Tourniaire, J.M. Rouzioux, M. Veisseire, R. Mornex (1986) TRH and LH-RH distribution in discrete nuclei of the human hypothalamus: evidence for a left prominence of TRH. *Brain Res.* 382: 433-436
- Boubaba, C., K. Szabo, and J.G. Tasker (1996) Physiological mapping of local inhibitory inputs to the hypothalamic paraventricular nucleus. *J. Neurosci.* 16:7151-7160
- Bouras, C., P.J. Magistratti, J.H. Morrison and J. Constantinidis (1987) An immunohistochemical study of pro-somatostatin-derived peptides in the human brain. *Neuroscience* 22: 781-800
- Braak, H. and E. Braak (1992) Anatomy of the human hypothalamus (chiasmatic and tuberal regions). *Progress in Brain Res* 93:3-16
- Brager, D.H., Sickel M.J., McCarthy M.M. (2000) Developmental sex differences in calbindin-D (28K) and calretinin immunoreactivity in the neonatal rat hypothalamus. *J Neurobiol.* 42:315-22
- Braverman, L.E., J.P. Mancini and D.M. McGoldrick (1965) Hereditary ideopathic diabetes insipidus. A case report with autopsy findings. *Ann. Intern. Med.* 63: 503-508
- Brockhaus, H. (1942) Beitrag zur normalen Anatomie des Hypothalamus und der Zona incerta beim Menschen. *J. Psychol. Neurol.* 51: 1-51
- Brownstein, M., R.L. Eskay and M. Palkovits (1982). Thyrotropin-releasing hormone in the medial eminence is in processes of paraventricular nucleus neurons. *Neuropeptides* 2: 197-201
- Buell, G., M.F. Schulz, S.J. Arkininstall, K. Maury, M. Missotten, N. Adami, F. Talabot and E. Kawashima (1992) Molecular characterisation, expression and localisation of human neurokinin-3 receptor. *FEBS Letters* 299:90-95
- Bugnon, C., D. Fellmann, J.L. Bresson, M.C. Clavequin (1982) Immunocytochemical study of the ontogenesis of the CRF-containing neuroglandular system in the human hypothalamus. *C R Seances Acad. Sci. III* 294: 491-6
- Buijs, R.M., M.M. Markman, Y.X. Hou and S. Shinn (1993) Projections of the suprachiasmatic nucleus to stress-related areas in the rat hypothalamus: A light and electron microscopical study. *J. Comp. Neurol.* 335: 42-54
- Burford, G.D. and I.C.A.F. Robinson (1982) Oxytocin, vasopressin and neurophysins in the hypothalamo-neurohypophyseal system of the human fetus. *J. Endocr.* 95: 403-408
- Byne, W. (1998) The medial preoptic and anterior hypothalamic regions of the rhesus monkey: cytoarchitectonic comparison with the human and evidence for sexual dimorphism. *Brain Res.* 793: 346-50
- Cajal, S. Ramony (1911): Histologie du systeme nerveux de l'homme et des veretebres, Maloine. Paris II.
- Canteras, N. S., R. B. Simerly and L. W. Swanson (1994) Organization of projections from the ventromedial nucleus of the hypothalamus: A *Phaseolus vulgaris*-leucoagglutinin study in the rat. *J Comp. Neurol.* 348: 41-79
- Carmel P.W. (1980) Surgical syndromes of the hypothalamus. *Clinical Neurosurgery* 27:133-159

- Cechetto, D.F. and C.B. Saper (1988) Neurochemical organization of the hypothalamic projections to the spinal cord in the rat. *J. Comp. Neurol.* 272: 579-604
- Chawla, M.K., M.G. Graciela, S. Young, N.T. McMullen, N.E. Rance (1997) Localization of neurons expressing substance P and neurokinin B gene transcripts in the human hypothalamus and basal forebrain. *J. Comp. Neurol.* 384: 429-442
- Choy, V.J., and W.B. Watkins (1979) Maturation of the hypothalamo-neurohypophyseal system. I. Localization of neurophysin, oxytocin and vasopressin in the hypothalamus and neural lobe of the developing rat brain. *Cell Tissue Res.* 197: 325-336
- Christ, J. (1951) Zur Anatomie des Tuber cinereum beim erwachsenen Menschen D.Z. f. Nervenheilk 165: 340-408
- Chronwall, B. M., D. A. DiMaggio, V. J. Massari, V. M. Pickel, D. A. Ruggiero, T. L. O'Donohue (1985). The anatomy of neuropeptide-Y-containing neurons in rat brain. *Neuroscience* 15: 1159-1181
- Claude, H., and J. Lhermitte (1917) Le syndrome infundibulaire dans un cas de tumeur du Troisième ventricule. *Presse med.* 25: 417-418
- Conrad, L.C.A. and D.W. Pfaff (1976) Efferents from medial basal forebrain and hypothalamus in the rat. I. An autoradiographic study of the medial preoptic area. *J. Comp. Neurol.* 169: 185-220
- Crosby, E.C. and R.T. Woodburne (1940) The comparative anatomy of the preoptic area and the hypothalamus. *Proc. Assoc. Res. Nervous. Mental Dis.* 20: 52-169
- Crosby, E.C. and R.T. Woodburne (1951) The hypothalamotegmental pathways. *J. Comp. Neurol.* 94: 1-32
- Crouch, R.L. (1934) The nuclei configuration of the hypothalamus and subthalamus of Macacus rhesus. *J. Comp. Neurol.* 59: 451-485
- Culman J. and T. Unger (1995) Central tachykinins: mediators of defence reaction and stress reaction. *Can. J. Physiol. Pharmacol.* 73: 885-891
- Cushing, H. (1906) Sexual infantilism with optic atrophy in cases of tumor affecting the hypophysis cerebri. *J. Nerv. & Ment. Dis.* 33: 704-716
- Dai J., D.F. Swaab and R.M. Buijs (1997) Distribution of Vasopressin and Vasoactive Intestinal Polypeptide (VIP) Fibers in the Human Hypothalamus with special emphasis on Suprachiasmatic Nucleus Efferent projections. *J. Comp. Neurol.* 383: 397-414
- Dai J., J. Van Der Vliet, D.F. Swaab and R.M. Buijs (1998) Postmortem Anterograde Tracing of Intrahypothalamic Projections of the Human Dorsomedial Nucleus of the Hypothalamus. *J. Comp. Neurol.* 401: 16-33
- Dalton L.D., R.G. Carpenter, S.P. Grossman (1981) Ingestive behavior in adult rats with dorsomedial hypothalamic lesions. *Physiol Behav* 26: 117-23
- Dani, J.W., Armstrong D.M., Benowitz L. I. (1991) Mapping the development of the rat brain by GAP43 immunocytochemistry. *Neuroscience* 40: 277-287

- Danzer, S.C., R.O. Price, N.T. McMullen, N.E. Rance (1999) Sex steroid modulation of neurokinin B gene expression in the arcuate nucleus of adult male rats. *Brain Res. Mol. Brain Res.* 66: 200-204
- Davison, C., and E.D. Friedman (1937) Poikilothermia with hypothalamic lesions. A clinicopathologic study. *Arch. Neurol. & Psychiat.* 38: 1271-1281
- Davison, C., and N.E. Selby (1935) Hypothermia in cases of hypothalamic lesions. *Arch. Neurol. & Psychiat.* 33: 570-591
- De Jonge, F.H., Louwerse A.L., Ooms M.P., Evers P., Endert E., N.E. Van de Poll (1989) Lesions of the SDN-POA inhibit sexual behavior of male Wistar rats. *Brain Res. Bull.* 23: 483-492
- De Olmos, J. S (1972) The amygdaloid projection field in the rat as studied with the cupric-silver method. In: The Neurobiology of the Amygdala. B. Eleftheriou (Edr.); Plenum Press, New York.
- De Olmos, J. S. and W.R. Ingram (1972) The projection field of the stria terminalis in the rat brain. An experimental study. *J. Comp. Neurol.* 146: 303-334
- De Olmos, J. S. and Carrer (1978) A horseradish peroxidase study of the afferent connections of the medial basal hypothalamus in the rat. *Anat. Res.* 190: 380
- Diepen, R. (1948) Über Lage- und Formänderungen des Hypothalamus und des Infundibulum in Phylogenese und Ontogenese. *Dtsch. Z. f. Nervenheilk.* 159: 340-358
- Diepen, R. (1962) Der Hypothalamus. In: W.v. Möllendorff and W. Bergmann (Eds.), Handbuch der Mikroskopischen Anatomie des Menschen, Vol IV/7, Springer, Berlin, Heidelberg, pp: 1-525.
- Dierickx, K., and F. Vandesande (1977) Immunohistochemical localization of the vasopressinergic and oxytocinergic neurons in the human hypothalamus. *Cell Tissue Res* 184: 15-27
- Dietl, M.M. and J.M. Palacios (1991) Phylogeny of tachykinin receptor localization in the vertebrate central nervous system: apparent absence of neurokinin-2 and neurokinin-3 binding sites in the human brain. *Brain Res.* 539: 211-222
- DiMicco, J.A., E.H. Stotz-Potter, A.J. Monroe, and S.M. Morin (1996) Role of dorsomedial hypothalamus in cardiovascular response to stress. *Clin. Experim. Pharm. Phys.* 23: 171-176
- Ding, Y.Q., B.Z. Lu, Z.L. Guan, D.S. Wang, J.Q. Xu, J.H. Li (1999) Neurokinin B receptor (NK3)-containing neurons in the paraventricular and supraoptic nuclei of the rat hypothalamus synthesize vasopressin and express Fos following intravenous injection of hypertonic saline. *Neuroscience* 91:1077-85
- Ding, Y.Q., R. Shigemoto, M. Takada, H. Ohishi, S. Nakanishi and N. Mizuno (1996) Localization of the neuromedin K receptor (NK3) in the central nervous system of the rat. *J. Comp. Neurol.* 364: 290-310
- Diz D.I., D.M. Jacobowitz (1984) Cardiovascular effects produced by injections of thyrotropin-releasing hormone in specific preoptic and hypothalamic nuclei in the rat. *Peptides* 5:801-808

- Elmqvist, J.K., R.S. Ahima, C.F. Elias, J.S. Flier and C.B. Saper (1998) Leptin activates distinct projections from the dorsomedial and ventromedial hypothalamic nuclei. *Proceedings of the National Academy of Sciences of the United States of America* 95: 741-746
- Enderlin, S., A.W. Norman, M.R. Celio (1987) Ontogeny of the calcium binding protein calbindin D-28k in the rat nervous system. *Anat Embryol (Berl)* 177: 15-28
- Erdheim, J. (1904) Ueber Hypophysenganggeschwulste und Hirncholesteatome. *Sitzungsb. d. k. Akad. d. Wissensch. Math.-naturw. Cl. (Abt.3)*. 113: 537-72.6
- Feremutsch K. (1955) Strukturanalyse des menschlichen Hypothalamus. Karger, Basel.
- Fliers, E., N.W.A.M. Noppen, W.M. Wiersinga, T.J. Visser, and D.F. Swaab (1994) Distribution of Thyrotropin-Releasing Hormone (TRH)-Containing Cells and Fibers in the Human Hypothalamus. *J. Comp. Neurol.* 350: 311-323
- Frankish H.M., S. Dryden, D. Hopkins, Q. Wang, and G. Williams (1995) Neuropeptide Y, the Hypothalamus, and Diabetes: Insights into the Central Control of Metabolism. *Peptides* 16 : 757-771
- Frohlich, A. (1901) Ein Fall von Tumor der Hypophysis cerebri ohne Akromegalie. *Wien. klin. Rundschau*. 15: 883-906
- Fykse, E.M., Takei K., Walch-Solimena C., Geppert M., Jahn R., Camilli P., Sudhof T.C. (1993) Relative properties and localisations of synaptic vesicle protein isoforms: the case of synaptophysins. *J of Neuroscience* 13: 4997-5007
- Gabreels, B.A., D.F. Swaab, D.P. de Kleijn, N.G. Seidah, J.W. Van de Loo, W.J. Van de Ven, G.J. Martens, and F.W. van Leeuwen (1998) Attenuation of the polypeptide 7B2, prohormone convertase PC2, and vasopressin in the hypothalamus of some Prader-Willi patients: indications for a processing defect. *J of Clin. Endocr. Metab.* 83: 591-599
- Gagel, O (1928) Zur topik und feineren histologie der vegetativen kerne dse Zwischenhirns. *Z Anat u entw gesch* 87: 558-584
- Gai, W.P., L.B. Geffen, and W.W. Blessing (1990) Galanin immunnoreactive neurons in the human hypothalamus: Colocalization with vasopressin-containing neurons. *J. Comp. Neurol.* 298: 265-280
- Gao, B. and R.Y. Moore (1996) The sexually dimorphic nucleus of the hypothalamus contains GABA neurons in the rat and man. *Brain Res.* 742: 163-171
- Gao, Z., and N.P. Peet (1999) Resent advances in neurokinin receptor anatagonists. *Curr. Med. Chem.* 6: 375-388
- Geula, C, CR Scharzt, and MM Mesulam (1993) Differential localization of NADPH-diaphorase. *Neurosc*, 54: 461-76
- Gilbert, M.S. (1935) The early development of the human diencephalon. *J. Comp. Neurol.* 62: 81-116
- Gorski, R.A., Gordon J.H., Shriyne J.E., Southam A.M. (1978) Evidence for a morphological sex difference within the medial preoptic area in the rat brain. *Brain Res.* 148: 333-346

- Gouldsmit, E., A. Neijmeijer-Leloux and D.F. Swaab (1992) The human hypothalamo-neurohypophyseal system in relation to development, aging and Alzheimer's disease. In D.F. Swaab, M.A. Hofman, M. Mirmiran, R. Ravid, and F.W. van Leeuwen (Eds.) *Progress in Brain Research* 93, Elsevier, Amsterdam; pp: 237-248.
- Greenwood B. and J.A. DiMicco (1995) Activation of the hypothalamic dorsomedial nucleus stimulates intestinal motility in rats. *Am. J. Physiol.* 268: G514-G521
- Greving R. (1925) Beitrage zur Anatomie des Zwischenhirns und seiner Funktion. I. Der anatomische Aufbau der Zwischenhirnbasis und des anschliessenden Mittelhirngebietes beim Menschen. *Z. Anat. Entw. Gesch.* 75: 597-620
- Greving R. (1928) Die zentralen anteile des vegetativen nervensystems. In v. Mollendorff's Handbuch der mikroskopischen Anatomie des Menschen, Vol 4 pt 1 p 817-1060. Springer-Verlag, Berlin.
- Grünthal E. (1930) Vergleichend anatomische und entwicklungsgeschltliche Untersuchungen uber die Zentren des Hypothalamus der Sauger und des Menschen. *Arch. Psychiatr. Nervenkr.* 90: 216-267
- Grünthal, E. (1952) Untersuchungen zur Ontogenese und über den Bauplan des Gehirns. In: Feremutsch, K. and Grünthal, E. : Beiträge zur Eitwicklungsgeschichte und normalen Anatomie des Gehirns. *Bibl. Psychiatr. Neurol. (Basal)* pp: 5-35
- Guldenaar, S.E. and D.F. Swaab (1995) Estimation of oxytocin mRNA in the human paraventricular nucleus in AIDS by means of quantitative in situ hybridization. *Brain Res.* 700: 107-114
- Gurdjian E.S. (1927) The diencephalon of the albino rat. *J. Comp. Neurol.* 43: 1-114
- Halasz, P., and I. Tork (1989) Imaging of immunohistochemically identified neurons using IBM compatible and Macintosh computers. *Neurosci. Lett. Suppl.* 34: 588
- Hall C.W., M.M.Behbehani (1997) The medial preoptic nucleus of the hypothalamus modulates activity of nitric oxide sensitive neurons in the midbrain periaqueductal gray. *Brain Res.* 765:208-17
- Harding, A.J., J.L.F. Ng, G. Halliday and J. Oliver (1995) Comparison of the number of vasopressin-producing hypothalamic neurons in rats and humans. *J. Neuroendocrinol.* 7: 629-636
- Hartwig, H.G. and W. Wahren (1982) Anatomy of the hypothalamus. In G. Schaltenbrand and A.E. Walker (ed): *Stereotaxy of the Human Brain. Anatomical, Physiological and Clinical Applications.* New York: Georg Thieme Verlag, pp. 87-106.
- Hatton, G.I., U.E.Hutton, E.R.Hoblitzell and W.E.Armstrong (1976) Morphological evidence for two populations of magnocellular elements in the rat paraventricular nucleus. *Brain Res.* 108: 187-193
- Helke, C.J., J.E. Krause, P.W. Mantyh, R. Couture and M.J. Bannon (1990) Diversity in mammalian tachykinin peptidergic neurons: Multiple peptides, receptors and regulatory mechanisms. *FASEB J.* 4: 1606-1615
- Herrick, C.J. (1910) The morphology of the forebrain in Amphibia and Reptilia. *J. Comp.Neurol.* 20: 413 - 547

- His, W. (1893) Vorschläge zur Einteilung des Gehirns. *Arch Anat Entwicklungsgesch* (Leipzig) 17: 172-17
- Hof, P.R., E.A. Nimchinsky, J.H. Morrison. (1995) Neurochemical phenotype of corticocortical connections in the macaque monkey: quantitative analysis of a subset of neurofilament protein-immunoreactive projection neurons in frontal, parietal, temporal, and cingulate cortices. *J.Comp. Neurol.* 362:109-33
- Hofman, M.A., E. Fliers, E. Goudsmit, D.F. Swaab (1988) Morphometric analysis of the suprachiasmatic and paraventricular nuclei in the human brain: sex differences and age dependent changes. *Journal of Anatomy* 160: 127-143
- Hoorneman, E.D.M., and R.M. Buijs (1982) Vasopressin fibers pathways in the rat brain following suprachiasmatic nucleus lesioning *Brain Res.* 243: 235-241
- Horn, E., Lach B., Lapierre Y., Hrdina P. (1988) Hypothalamic pathology in the neuroleptic malignant syndrome. *American Journal of Psychiatry* 145: 617-620
- Huang X.F., H.Wang (1998) Altered c-fos expression in autonomic regulatory centers of genetically obese (ob/ob) mouse brain. *Brain Res.* 799:307-10
- Ingram, W.R. (1940) Nuclear organization and chief connections of the primate hypothalamus. *Res. Publ. Ass. Nerv. Ment. Dis.* 20: 195-244
- Isenschmid, R. and L. Krehl (1912) Über den Einfluss des Gehirns auf die Wärmeregulation. *Arch. f. exp. Path. u. Pharmacol.* 70: 109-147
- Jacobson, R.D, Virag I., Scene J.H. (1986) A protein associated with axon growth, GAP-43, widely distributed and developmentally regulated in rat CNS. *J. of Neuroscience* 6: 1843-1855
- Jenkins, J.S., V.T.Y. Ang, J. Hawthorn, M.N. Rossor and L.L. Iversen (1984) Vasopressin, oxytocin and neurophysins in the human brain and spinal cord. *Brain Res.* 291: 111-117
- Jensen, I, C. Alafaci, J. McCulloch, R.Uddman, L. Edvinsson (1991) Tachykinins (substance P, neurokinin A, neuropeptide K, and neurokinin B) in the cerebral circulation: vasomotor responses in vitro and in situ. *J. Cereb. Blood Flow Metab.* 11: 567-575
- Kahle, W. (1956) Zur Entwicklung des menschlichen Zwischenhirnes. Studien über die Matrixphasen und die örtlichen Reifungsunterschiede im embryonalen menschlichen Gehirn. II. *Mitteilung. Dtsch Z Nervenheilk* 175: 259-318
- Kesterson, R.A., D. Huszar, C.A. Lynch, R.B. Simerly, and R.D. Cone (1997) Induction of neuropeptide gene expression in the dorsal medial hypothalamic nucleus in two models of the Agouti obesity syndrome. *Mol. Endocrinol.* 11: 630-637
- Keyser, A. (1979) Development of the hypothalamus in mammals. In (Eds. P.J. Morgane, J. Panksepp) *Anatomy of the Hypothalamus*. New York and Basel. pp: 65-136
- Keyser, A. (1983) Basic aspects of development and maturation of the brain: embryological contributions to neuroendocrinology. *Psychoneuroendocrinology* 8: 157-181

- Kiss J., A.Csaki, H.Bokor, K.Kocsis, G.Szeiffert (1997) Topographic localization of calretinin, calbindin, VIP, substance P, CCK and metabotropic glutamate receptor immunoreactive neurons in the supramammillary and related areas of the rat. *Neurobiology* 5:361-388
- Kita, H., and Y. Oomura (1982) An HRP study of the afferent connections to rat medial hypothalamic region. *Brain Res. Bull.* 8: 53-62
- Kobayashi A., T. Osaka, Y. Namba, S. Inoue, S. Kimura (1999) CGRP microinjection into the ventromedial or dorsomedial hypothalamic nucleus activates heat production. *Brain Res.* 827: 176-184
- Koiwegami, H. (1938) Beiträge zur Kenntnis der Kerne des Hypothalamus bei Säugetieren. *Arch. f. Psychiatr. (D.)* 107: 742-774
- Korogi, Y., M. Takahashi (1995) Current concepts of imaging in patients with pituitary/hypothalamic dysfunction. *Semin Ultrasound CT MR* 16:270-8
- Koutcherov, I., K. Ashwell and G. Paxinos (1998) Parcellation of the human paraventricular hypothalamic nucleus. *Soc. Neurosci. Abstr.*, Vol. 24, Part 1, p. 119.
- Kremer, H.P.H. (1992) The hypothalamic lateral tuberal nucleus: normal anatomy and changes in neurological disease. In : (Eds) Swaab D.F., Hofman M.A., Mirmiran M., Ravid R., Van Leeuwen F.W. The human hypothalamus in health and disease. *Progress in Brain Res.* 93: 249-261, Elsevier, Amsterdam.
- Kremer, H.P.H., Roos R.A.C., Dingjan G., Marani E., Bots G.T.M. (1990) Atrophy of the hypothalamic lateral tuberal nucleus in Huntington's disease. *J of Neuropathology and Experimental Neurology* 49: 371-382
- Krettek, J.E., and J. L. Price (1978) A description of the amygdaloid complex in the rat and cat with observations on intraamygdaloid axonal connections . *J. Comp. Neurol.* 178: 255-280
- Krettek, J.E., and J. L. Price (1978) Amygdaloid projections to subcortical structures within the basal forebrain and brainstem in the rat and cat. *J. Comp. Neurol.* 178: 225-254
- Krieg W.J.S. (1932) The hypothalamus of the albino rat. *J. Comp. Neurol.* 55: 19-89
- Kühlenbeck H. and Haymaker (1949) The derivatives of the hypothalamus in the human brain; their relation to extrapyramidal and autonomic systems. *The Milit. Surgeon* 105: 26-52
- Kühlenbeck, H. (1954) The human diencephalon. A summary of development, structure, function and pathology. *Confin. Neurol.* 14 (Suppl.): 1 - 230
- Kühlenbeck, H., Haymaker W. (1949) The derivatives of the hypothalamus in the human brain; their relation to the extrapyramidal and autonomic systems. *Military Surgery* 105: 26-52
- Laemle, L.K., Repke K.B., Hawkes R., Rice F.L. (1991) Synaptogenesis in the rat suprachiasmatic nucleus: a light microscopic immunocytochemical survey. *Brain Res.* 544: 108-117
- Lang, L. (1985) Surgical anatomy of the hypothalamus. *Acta Neurochir.* 75: 5-22

- Larsson, K. (1979) Features of the neuroendocrine regulation of masculine sexual behavior. In C. Beyer (ed.) *Endocrine control of sexual behavior*, pp. 77-163. Raven Press, New York.
- Le Vay, S.A. (1991) A difference in hypothalamic structure between heterosexual and homosexual men. *Science* 253: 1034-1037
- LeGros Clark, W.E. (1936) The topography and homologies of the hypothalamic nuclei in man. *J. Anat.*, 70: 203-214.
- LeGros Clark, W.E. (1938) Morphological aspects of the hypothalamus. In: (Eds) Le Gros Clark, W.E., Beattie J., Riddoch G., Dott N.M. *The hypothalamus. Morphological, functional, clinical, and surgical aspects*. Oliver & Boyd, Edinburgh, pp 325-337
- Leibowitz, S.F. (1991) Brain neuropeptide Y: an integrator of endocrine, metabolic and behavioral processes. *Brain Res Bull* 27: 333-337
- Lemire, R.J., Loeser J.D., Leech R.W., Alvord Jr. E.C. (1975) Normal and Abnormal Development of the Human Nervous System. pp 169-196, Harper and Row, London.
- Leontovich, T. A. (1969-1970) The neurons of the magnocellular neurosecretory nuclei of the dog's hypothalamus: A Golgi study. *J. Hirnforsch.* 11: 499-517
- Leranth C., D.Carpi, G.Buzsaki, and J.Kiss (1999) The entorhino-septo-supramammillary nucleus connection in the rat: morphological basis of a feedback mechanism regulating hippocampal theta rhythm. *Neuroscience* 88: 701-718
- Li, Y.W., G.M. Halliday, T.H. Joh, L.B. Geffen, and W.W. Blessing (1988) Tyrosine hydroxylase-containing neurons in the supraoptic and paraventricular nuclei of the adult human. *Brain Res.* 461: 75-86
- Longmore, J., R.G. Hill and R.J. Hargreaves (1997) Neurokinin-receptor antagonists: pharmacological tools and therapeutic drugs. *Can. J. Pharmacol.* 75: 612-621
- Luiten P.G.M. and P. Room (1980) Interrelations between lateral, dorsomedial and ventromedial hypothalamic nuclei in the rat: An HRP study. *Brain Res.* 190: 321-332
- Luiten, P.G.M., G.J. ter Horst and A.B. Steffens, (1985) The course of paraventricular hypothalamic efferents to autonomic structures in medulla and spinal cord. *Brain Res.* 329: 374-378
- Maggi, C.A. (1995) The mammalian tachykinin receptors. *General Pharmac.* 26: 911-44
- Mai, J.K., C. Andressen, and K.W.S. Ashwell (1998) Demarcation of prosencephalic regions by CD15-positive radial glia. *Eur. J. Neurosci.* 10 : 746-751
- Mai, J.K., J. Assheuer, G. Paxinos (1997) *Atlas of the human brain*. Academic Press, San Diego.
- Mai, J.K., O. Kedziora, L. Teckhaus, and M.V. Sofroniew (1991) Evidence for subdivisions in the human suprachiasmatic nucleus. *J. Comp. Neurol.* 305: 508-525
- Mai, J.K., P.H. Stephens, A. Hopf, and A.C. Cuello (1986) Substance P in the human brain. *Neuroscience* 17: 709-739

- Mai, J.K., S. Lensing-Hohn, A.A. Ende and M.V. Safroniew (1997) Developmental organization of neurophysin neurons in the human brain. *J. Comp. Neurol.* 385:477-489
- Malone E. (1910) Über die Kerne des menschlichen Diencephalon. Adh. Königl. Preuß. Akad. Wiss. Berlin.
- Marie, P., and A. Leri (1905) Persistance d'un faisceau intact dans les bandelettes optiques apres atrophie complete des nerfs: Le "faisceau residuaire de la bandelette." Le ganglion optique basal et ses connexions. *Rev. Neurol.* 13 : 493 -503
- Marksteiner, J., G. Sperk, and J.E. Krause (1992) Distribution of neurons expressing neurokinin B in the rat brain: Immunohistochemistry and in situ hybridization. *J. Comp. Neurol.* 317: 341-356
- Massi, M. C. Polidori, L. Gentili, M. Perfumi, G. de Caro, C.A. Maggi (1988) The tachykinin NH₂-senktide, a selective neurokinin B receptor agonist, is a very potent inhibitor of salt appetite in the rat. *Neuroscience Letters* 92: 341-346
- Mauthner, L. (1890) Zur Pathologie und Physiologie des Schlafes, nebst Bemerkungen uber die 'Nona". Wein. Med. Wchnschr. 4: 961-1185
- Millhouse, O.E. (1973) The organization of the ventromedial hypothalamic nucleus. *Brain Res.* 55: 71-87
- Milosevic, A., S. Kanazir, N. Zecevic (1995) Immunocytochemical localisation of growth-associated protein GAP43 in early human development. *Brain Res. Devel. Brain Res.* 84: 282-286
- Morton, A.A. (1969) Quantitative analysis of the normal neuron population of the hypothalamic magnocellular nuclei in man and their projections to the neurohypophysis. *J. Comp. Neurol.* 136: 143-158.
- Mosinger, M. (1950) Anatomie de l'hypothalamus et du sous-thalamus elargi. Schweiz. *Arch. f. Neur.* 65: 135-186
- Mouri, T., T. Suda, N. Sasano, N. Andoh, Y. Takei, M. Takase, A. Sasaki, O. Murakami, K. Yoshinaga (1984) Immunocytochemical identification of CRF in the human hypothalamus. *Tohoku Journal of Experimental Medicine.* 142(4):423-426
- Okamura, H., M. Abitol, J.F. Jukien, S. Dumas, A. Berod, M. Geffard, K. Kitahama, P. Bobillier, I. Mallet, L. Wiklund (1990) Neurons containing messenger RNA encoding glutamal decarboxylaze in rat hypothalamus demonstrated by *in situ* hybridization with special emphasis on cell groups in medial preoptic area, anterior hypothalamic area and dorsomedial hypothalamic nucleus. *Neuroscience* 39: 675-699
- O'Rahilly R. and F. Muller (1994) The embryonic human brain: an atlas of developmental stages. Willey-Liss, New York.
- Ott, I. (1891) The function of the tuber cinerium. *J. Nerv. & Ment. Dis.* 18: 431-432
- Panayotacopoulou, M.T., and D.F. Swaab (1993) Development of tyrosine hydroxylase-immunoreactive neurons in the human paraventricular and supraoptic nuclei. *Dev. Brain Res.* 72: 145-150

- Papez, J.W. and R. Aronson (1934) Thalamic nuclei of *Pithecus* (Macacus) rhesus. *Arch of neur and Psychiat* 32: 1-44
- Paxinos, G, Kus, L, Ashwell, KWS, C. Watson (1999) *Chemoarchitectonic Atlas of the Rat Forbrain*, Academic Press, SD.
- Paxinos, G, Huang, XF and Toga, AW, (2000) *The Rhesus Monkey Brain in Stereotaxic Coordinates*, Academic Press, SD.
- Paxinos, G, Huang, X-F. (1995) *Altas of the Human Brainstem*, Academic Press, San Diego.
- Paxinos, G., and C. Watson (1986) *The Rat Brain in in Stereotaxic Coordinates*, Academic Press, San Diego.
- Paxinos, G., and C. Watson (1994) *The Rat Brain in in Stereotaxic Coordinates*, Academic Press, San Diego.
- Paxinos, G., and K.B.J. Franklin (1997) *The mouse brain in stereotaxic coordinates*. Sydney: Academic Press.
- Pelletier, G., L. Desy, J. Cote, and H. Vaundry (1983) Immunocytochemical localisation of corticotropin-releasing factor-like immunoreactivity in the human hypothalamus. *Neurosci. Lett.* 41: 259-263
- Penfield, W. (1929) Diencephalic autonomic epilepsy. *Arch. Neurol. Psychiatry* 22: 358-374
- Perkins, M.N., N.J. Rothwell, M.J. Stock, and T.W. Stone (1981) Activation of brown adipose tissue thermogenesis by the ventromedial hypothalamus. *Nature* 289: 401-402
- Petrides, M., G. Paxinos, H.F. Huang, R. Morris, D. Pandya (2000) Delineation of the Monkey Cortex on the Basis of the Distribution of a Neurofilament Protein. In G. Paxinos, H.F. Huang, A. Toga (ed): *The Rhesus Monkey Brain in Stereotaxic Coordinates*. San Diego: Academic Press.
- Pfaff, D.W. and M. Keiner (1973) Atlas of estradiol-concentrating cells in the central nervous system of the female rat. *J. Comp. Neurol.* 151: 121-158
- Polidori, C, A. Saija, M. Perfumi, L. Gentili, G. de Caro, G. Costa, M. Massi (1989) The paraventricular nucleus as a site of action for the vasopressin releasing affect of tachykinins. *Pharmacological Research* 21: 141-142
- Polidori, C., A. Saija, M. Perfumi, G. Costa, G. Caro and M. Massi (1989) Vasopressin release induced by intracranial injection of tachykinins is due to activation of central neurokinin-3 receptors. *Neuroscience Lett.* 103: 320-325
- Post, S. and J. K.Mai (1980) Contribution to the amygdaloid projection field in the rat. A quantitative autoradiographic study. *Journal Für Hirnforschung.* 21: 199-225
- Purba, J.S., M.A. Hofman, P. Portegies, D. Troost, D.F. Swaab (1993) Decreased number of oxytocin-immunoreactive neurons in the paraventricular nucleus of the human hypothalamus in AIDS. *Brain* 116: 795-809
- Purba, J.S., W.J. Hoogendijk, M.A. Hofman and D.F. Swaab (1996) Increased number of vasopressin- and oxytocin-expressing neurons in the paraventricular nucleus of the hypothalamus in depression. *Archives of General Psychiatry* 53: 137-143

- Raadsheer, F.C., A.A. Sluiter, R. Ravid, F.J.H. Tilders and D.F. Swaab (1993) Localization of corticotropin-releasing hormone (CRH) neurons in the paraventricular nucleus of the human hypothalamus; age-dependent colocalization with vasopressin. *Brain Res.* 615: 50-62
- Raadsheer, F.C., D.E. Oorschot, W.H. Verwer, F.J.H. Tilders and D.F. Swaab (1994) Age-related increase in the total number of corticotropin-releasing hormone neurons in the human paraventricular nucleus in controls and Alzheimer's disease. *J. Comp. Neurol.* 339: 447-457
- Rance, N.E. (1992) Hormonal influences on morphology and neuropeptide gene expression in the infundibular nucleus of post-menopausal women. In: Swaab, D.F., Hofman M.A., Mirmiran M., Ravid R., Van Leeuwen F.W. (Eds.) *The human hypothalamus in health and disease. Progress in Brain Research*, vol 93. Elsevier, Amsterdam, pp119-132
- Ranson, S.W., C. Fisher, and W.R. Ingram (1937) Hypothalamic regulation of the temperature in the monkey. *Arch. Neurol. & Psychiat.* 38: 445-466
- Ratner, J. (1925) Tumor des Mittelhirns unter dem Bilde einer pluriglandularen Insuffizienz. *Klin. Wchnsch.* 4: 599-600
- Reichlin, S. (1985) The hypothalamus in human disease : Achievements and challenges. *Acta Neurochir.* 75: 3-4
- Rhodes, C.H., J.I. Morell and D.W. Pfaff (1981) Immunohistochemical analysis of magnocellular elements in the rat hypothalamus. *J. Comp. Neurol.* 198:45-64.
- Ricardo J.A. and E.T. Koh (1978) Anatomical evidence of direct projections from the nucleus of the solitary tract to the hypothalamus, amygdala, and other forebrain structures in the rat. *Brain Res.* 153: 1-26
- Richter, E. (1965) *Die Entwicklung des Globus Pallidus und des Corpus Subthalamicum.* Springer, Berlin Heidelberg New York.
- Righetti, R. (1903) Contributo clinico e anatomo-patologico allo studio dei gliomi cerebrali e all'anatomia delle vie ottiche centrali. *Riv. di. pat. nerv.* 8: 241-267
- Rioch D. M. (1929) Studies on the diencephalon of carnivora. I. Nuclear configuration of thalamus, epithalamus and hypothalamus of dog and cat. *J. Comp Neurol.* 49:1-94
- Rizvi T.A., M. Ennis, M.T. Shipley (1992) Reciprocal connections between the medial preoptic area and the midbrain periaqueductal gray in rat: a WGA-HRP and PHA-L study. *J Comp Neurol* 315:1-15
- Roberts, D.W. and J.R. Martin (1977) Effects of lesions in central thermosensitive areas in thermoregulatory response in rats. *Physiol. Behav.* 19: 503-511
- Ronnekleiv, O.K., M.J. Kelly, and R.L. Eskay (1984) Distribution of immunoreactive substance P neurons in the hypothalamus and pituitary of the rhesus monkey. *J. Comp. Neurol.* 224: 51-59
- Ropper, A.H. (1993) Acute autonomic emergencies and autonomic storms. In P.A. Low (ed): *Clinical Autonomic Disorders.* Boston: Little, Brown, pp. 747-760
- Roussy, G., and M. Mossinger (1935) L'hypothalamus chez l'homme et chez le chien. *Rev. Neurol.* 63: 1-35

- Rugierro, D.A., H. Baker, T.H. Joh, and D.J.Reis (1984) Distribution of catecholamine neurons in the hypothalamus and preoptic region of mouse. *J. Comp. Neurol.* 223: 556-582
- Sanghera, M.K., J.L. Zamora and D.C. German (1995) Calbindin-D28k-containing neurons in the human hypothalamus: relationship to dopaminergic neurons. *Neurodegeneration* 4: 375-81
- Saper, C.B. (1990) Hypothalamus. In G. Paxinos (ed): *The Human Nervous System*. Sydney: Academic Press, pp.389-413
- Saper, C. B. (1995) Central Autonomic System. In: G. Paxinos (Edr.), *The Rat Nervous System* , Academic Press, Sydney, pp: 107-135
- Saper, C.B. and A.D. Loewy (1980) Efferent connections of the parabrachial nucleus in the rat. *Brain Res.* 288: 21-31
- Saper, C.B. and D.C. German (1987) Hypothalamic pathology in Alzheimer's disease. *Neurosci. Lett.* 74: 364-370
- Saper, C.B. and T.C. Chelimsky (1984) A cytoarchitectonic and histochemical study of nucleus basalis and associated cell groups in the normal human brain. *Neuroscience* 13: 1023-1037
- Saper, C.B., A.D. Loewy, L.W. Swanson and W.M. Cowan, (1976) Direct hypothalamo-autonomic connections. *Brain Res.* 117: 305-312
- Saper, C.B., C.K. Petito (1982) Correspondence of melanin-pigmented neurons in human brain with A1-A14 catecholamine cell groups. *Brain* 105: 87-102
- Sawchenko, P.E. and L.W. Swanson (1982) Immunohistochemical identification of neurons in the paraventricular nucleus of the hypothalamus that project to the medulla or to the spinal cord in the rat. *J. Comp. Neurol.* 205: 260-272
- Sawchenko, P.E. and L.W. Swanson (1983) The organization of forebrain afferents to the paraventricular and supraoptic nucleus in the rat. *J. Comp. Neurol.* 218: 121-144
- Scharrer, B., and E. Scharrer (1940) Sensory cells within the hypothalamus. In (eds.) Fulton J.F., S.W. Ranson, and A.M. Franz : *The Hypothalamus*. William & Wilkins, Baltimore.
- Scharrer, E. and B. Scharrer (1940) Secretory cells within the hypothalamus. *Proc. Assoc. Res. Nervous and Mental Disorders* 20: 170-194
- Schwanzel-Fukuda, M., D. Bick, D. Pfaff (1989) Luteinizing hormone-releasing hormone (LHRH)-expressing cells do not migrate normally in an inherited hypogonadal (Kallmann) syndrome. *Mol. Brain Res.* 6: 311-326
- Sherin, J.E., P.J. Shiromani, R.W. McCarley, and C.B. Saper (1996) Activation of ventrolateral preoptic neurons during sleep. *Science* 271: 216-219
- Shimada, M., and T. Nahamura. (1973) Time of neurone origin in mouse hypothalamic nuclei. *Experimental Neurology* 41: 163-173
- Simerly, R.B. (1995) Anatomical substrates of hypothalamic integration. In: G. Paxinos (Edr.), *The Rat Nervous System* , Academic Press, Sydney, pp: 353-376

- Simerly, R.B. and L.W. Swanson (1986) The organization of neural inputs to the medial preoptic nucleus in the rat. *J. Comp. Neurol.* 246: 312-342
- Simerly, R.B. and L.W. Swanson (1988) Projections of medial preoptic nucleus: A phaseolus vulgaris leucoagglutinin anterograde tract-tracing study in the rat. *J. Comp. Neurol.* 270: 209-242
- Simerly, R.B., C. Chang, M. Maramatsu, and L.W. Swanson (1990) Distribution of androgen and estrogen receptor mRNA-containing cells in the rat brain: An in situ hybridization study. *J. Comp. Neurol.* 270: 209-242
- Simerly, R.B., L.W. Swanson and R.A. Groski (1984). Demonstration of a sexual dimorphism in the distribution of serotonin immunoreactive fibers in the medial preoptic nucleus of the rat. *J. Comp. Neurol.* 225: 151-166
- Simerly, R.B., R.A. Groski, and L.W. Swanson (1986) Neurotransmitter specificity of cells and fibers in the medial preoptic nucleus: An immunohistochemical study in the rat. *J. Comp. Neurol.* 246: 343-363
- Skene, J.H., R.D. Jacobson, G.J. Snipes, C.B. McGuire, J.J. Norden, J.A. Freeman (1986) A protein induced during nerve growth (GAP43) is a major component of growth-cone membranes. *Science* 233: 783-786
- Soltis, R.P. and J. A. Dimicco (1990) GABA_A and excitatory amino acid receptors in dorsomedial hypothalamus and heart rate in rats. *Am J. Physiol.* 260: R13-20
- Soltis, R.P., J.C. Cook, A.E. Gregg, J.M. Stratton, K.A. Flickinger (1998) EAA receptors in the dorsomedial hypothalamic area mediate the cardiovascular response to activation of the amygdala. *Am. J. Physiol* 275: R624-631
- Spencer, S., C.B. Saper, T. Joh, D.J. Reis, M. Goldstein and J.D. Raese (1985) The distribution of catecholamine-containing neurons in the normal human hypothalamus. *Brain Res.* 328: 73-80
- Stephens, T. W., M. Basinski, P. K. Bristow, J. M. Bue-Valleskey, S. G. Burgett, L. Craft, J. Hale. (1995) The role of neuropeptide Y in antiobesity action of the obese gene product. *Nature* 377: 530-532
- Swaab, D.F. (1997) Prader-Willi syndrome and the hypothalamus. *Acta Paediatr. Suppl* 423: 50-54
- Swaab, D.F. and M.A. Hofman (1988) Sexual differentiation of the human hypothalamus: ontogeny of the sexually dimorphic nucleus of the preoptic area. *Dev. Brain Res.* 44: 314-318
- Swaab, D.F., and E. Fliers (1985) A sexually dimorphic nucleus in the human brain. *Science* 228: 1112-1115
- Swaab, D.F., F. Nijveldt, C.W. Pool (1975) Distribution of oxytocin and vasopressin in the rat supraoptic and paraventricular nucleus. *J. Endocrinol.* 67: 461-462
- Swaab, D.F., M.A. Hofman, P.J. Lucassen, J.S. Purba, F.C. Raadsheer, J.A.P. Van de Nes (1993) Functional neuroanatomy and neuropathology of the human hypothalamus. *Anat. Embryol.* 187: 317-330

- Swanson, L.W and D.M. Simmons (1989) Differential Steroid Hormone and Neural Influences on Peptide mRNA Levels in CRH Cells of the Paraventricular Nucleus: A Hybridization Histochemical Study in the Rat. *J. Comp. Neurol.* 285: 413-435
- Swanson, L.W. (1977) Immunohistochemical evidence for a neurophysin-containing autonomic pathway arising in the paraventricular nucleus of the hypothalamus. *Brain Res.* 128: 346-353
- Swanson, L.W. (1991) Biochemical switching in hypothalamic circuits mediating responses to stress. *Progress in Brain Res.* 87: 181-200
- Swanson, L.W. and H.G.J.M. Kuypers (1980) The paraventricular nucleus of the hypothalamus: Cytoarchitectonic subdivisions and organization of projections to the pituitary, dorsal vagal complex, and spinal cord as demonstrated by retrograde fluorescence double-labeling methods. *J. Comp. Neurol.* 194: 555-570
- Swanson, L.W. and P.E. Sawchenko (1983). Hypothalamic integration: Organization of the paraventricular and supraoptic nuclei. *Annu. Rev. Neurosci.* 6: 269-324
- Swanson, L.W., P.E. Sawchenko and R.W. Lind (1986) Regulation of multiple peptides in CRF parvocellular neurosecretory neurons: implications for the stress response. *Progress in Brain Res.* 68: 169-190
- Swanson, L.W., P.E. Sawchenko, A. Berod, B.K. Hartman, K.B. Helle and D.E. Van Orden, (1981). An immunohistochemical study of the organization of catecholaminergic cells and terminal fields in the paraventricular and supraoptic nuclei of the hypothalamus. *J. Comp. Neurol.* 196: 271-285
- Swanson, L.W., P.E. Sawchenko, J. Rivier, and W.W. Vale (1983) Organization of ovine corticotropin-releasing factor immunoreactive cells and fibers in the rat brain: An immunohistochemical study. *Neuroendocrinol.* 36: 165-186
- Swanson, L.W., P.E. Sawchenko, S.J. Wiegand, and J.L. Price (1980) Separate neurons in the paraventricular nucleus project to the medial eminence and to the medulla or spinal cord. *Brain Res.* 197: 207-212
- Takahashi, K., T. Mouri, T. Yamamoto, K. Itoi, O. Murakami, K. Yoshinaga, and N. Sasano (1989) Corticotropin-releasing hormone in the human hypothalamus. Free-floating immunostaining method. *Endocrinologia Japonica* 36: 272-280
- Ter Horst, G.J. and P.G.M. Luiten (1986) The projections of the Dorsomedial Hypothalamic Nucleus in the Rat. *Brain Research Bulletin* 16: 231-248
- Ter Horst, G.J. and P.G.M. Luiten (1987) Phaseolus vulgaris leucoagglutinin tracing of intrahypothalamic connections of the lateral, ventromedial, dorsomedial and paraventricular hypothalamic nuclei in the rat. *Brain Res. Bull.* 18: 191-203
- Thompson, R.H., and L.W. Swanson (1998) Organization of inputs to the dorsomedial nucleus of the hypothalamus: a reexamination with fluorogold and PHAL in the rat. *Brain Res. Rev.* 27: 89-118
- Thompson, R.H., N.S. Canteras and L.W. Swanson (1996) Organisation of projections from the dorsomedial nucleus of the hypothalamus: A PHA-L study in the rat *J. Comp. Neurol.* 376: 143-173